Simplified *In Vitro* Engineering of Functional Mammalian Neuromuscular Junctions between Embryonic Rat Motor Neurons and Immortalised Human Skeletal Muscle Cells

JASDEEP SAINI

A thesis submitted in partial fulfilment of the requirements of Manchester Metropolitan University for the degree of Doctor of Philosophy

Department of Life Sciences
Manchester Metropolitan University

2019

Acknowledgements

Firstly, thank you to my director of studies Dr Nasser Al-Shanti for the opportunity to pursue my academic career and all the support and guidance throughout this project.

Special thanks to Dr Jamie S McPhee, Prof Hans Degens, Dr Alessandro Faroni, and Dr Adam J Reid for their help and time throughout this project.

Most importantly, thank you to my father (Harnek Singh), mother (Daljit Kaur), and wife (Seema Saini) for their past, present, and future support.

Lastly, thank you to my son Aary Saini for motivating me to pursue excellence in all aspects of my life.

Publications

Original Research Paper

Saini, J., Faroni, A., Abd Al Samid, M., Reid, A. J., Lightfoot, A. P., Mamchaoui, K., Mouly, V., Butler-Browne, G., McPhee, J. S., Degens, H. and Al-Shanti, N. (2019) 'Simplified in vitro engineering of neuromuscular junctions between rat embryonic motoneurons and immortalized human skeletal muscle cells.' Stem Cells Cloning, 12 pp. 1-9.

Review

Saini, J., McPhee, J. S., Al-Dabbagh, S., Stewart, C. E. and Al-Shanti, N. (2016) 'Regenerative function of immune system: Modulation of muscle stem cells.' Ageing Res Rev, 27, May, pp. 67-76.

Contributing Author

Abd Al Samid, M., McPhee, J. S., **Saini, J.,** McKay, T. R., Fitzpatrick, L. M., Mamchaoui, K., Bigot, A., Mouly, V., Butler-Browne, G. and Al-Shanti, N. (2018) 'A functional human motor unit platform engineered from human embryonic stem cells and immortalized skeletal myoblasts.' Stem Cells Cloning, 11 pp. 85-93.

List of abbreviations

± SD	plus/minus standard deviation
α-BTX	α-bungarotoxin
αFF	fast-twitch fatigable motor neurons
αFR	fast-twitch fatigue-resistant motor neurons
αMN(s)	alpha motor neuron(s)
αS	slow-twitch fatigue resistant motor neurons
β-III-tubulin	class III β-tubulin
βMN(s)	beta motor neuron(s)
γMN(s)	gamma motor neuron(s)
AP(s)	action potential(s)
ACh	acetylcholine
AChR(s)	acetylcholine receptor(s)
ADP	adenosine diphosphate
ALS	amyotrophic lateral sclerosis
AR	aspect ratio
ATM	37°C with a 5% CO2 atmosphere
ATP	adenosine triphosphate
BDNF	brain-derived neurotrophic factor
bHLH	basic helix–loop–helix
C25	25-year-old immortalised human myoblasts
C83	83-year-old immortalised human myoblasts
Ca^{2+}	calcium ions
CF	contraction frequency
ChAT	choline acetyltransferase
CMS	congenital myasthenic syndrome
CNS	central nervous system
DAPI	4′,6-Diamidine-2′-phenylindole dihydrochloride
DHPR	dihydropyridine receptor
DM	differentiation media
DMEM	Dulbecco's modified eagle medium
DMSO	Dimethyl sulfoxide

Dok7	docking protein 7
DPBS	Dulbecco’s phosphate buffered saline 1X
DRG(s)	dorsal root ganglion(s)
DS	donkey serum
DSC	disassociated spinal cord
ECM	extracellular matrix
ED	embryonic development day
EGF(s)	epidermal growth factor(s)
EPP	endplate potential
FBS	fetal bovine serum
FGF-7	fibroblast growth factor 7
FGF(s)	fibroblast growth factor(s)
FGFb	basic fibroblast growth factor
FI	fusion index
GABA	γ-aminobutyric acid
GDF-11	growth differentiation factor 11
GDNF	glial-cell-line-derived neurotrophic factor
GFAP	glial fibrillary acidic protein
GM	complete growth media
GS	goat serum
HBSS	Hanks' balanced salt solution
hESC(s)	human embryonic stem cell(s)
HGF(s)	Hepatocyte growth factor(s)
hiPSC(s)	human induced pluripotent stem cell(s)
HMC(s)	hypaxial motor column(s)
HS	horse serum
ICC	immunocytochemistry
IGF-1	insulin-like growth factor 1
IGFBP(s)	insulin-like growth factor-binding protein(s)
IP	inorganic phosphate
K^+	potassium ions
LEMS	Lambert-Eaton myasthenic syndrome
L-Glut	L-glutamic acid
LMC(s)	lateral motor column(s)

LMCl	lateral lateral motor column
LMCm	medial lateral motor column
LRP4	low-density lipoprotein receptor-related protein 4
MA	myotube area
MEP(s)	motor endplate(s)
MMC(s)	medial motor column(s)
MN(s)	motor neuron(s)
MNT(s)	motor neuron terminal(s)
MHC	myosin heavy chain
MRF4	myogenic regulatory factor 4
MRF(s)	myogenic regulatory factor(s)
MG	myasthenia gravis
MuSK	muscle-specific tyrosine kinase
Myf5	myogenic factor 5
Na^+	sodium ions
ND	neurodegenerative
NFH	neurofilament heavy
NGF	nerve growth factor
NM	neuromuscular
NMJ(s)	neuromuscular junction(s)
NT3	neurotrophin 3
NT4	neurotrophin 4
NT5	neurotrophin 5
Pax3	paired box protein 3
Pax7	paired box protein 7
Pen/Strep	penicillin-streptomycin
PGC	preganglionic column
PlGF	placental growth factor
PMC	phrenic motor column
PWB	Prem/Wash buffer
Rapsyn	43 kDa receptor-associated protein of the synapse
RyR	ryanodine receptor
SC(s)	satellite cell(s)
SCE(s)	spinal cord explants

SkM	skeletal muscle
SkMC(s)	skeletal muscle cell(s)
SMA	spinal muscular atrophy
SMN1	survival motor neuron 1
SMN2	survival motor neuron 2
SOD1	superoxide dismutase 1
SR	sarcoplasmic reticulum
Sty1	synaptotagmin 1
T-tubule	transverse tubule
TGFβ	transforming growth factor beta
TX100	Triton X-100
VAChT	vesicular acetylcholine transporter
VEGF	vascular endothelial growth factor

List of Figures

List of Tables

Abstract

Neuromuscular junction (NMJ) research is vital to advance the understanding of neuromuscular (NM) pathologies and development of novel therapies for diseases associated with NM dysfunction and deterioration. Several *in vivo* animal models manifest phenotypes observed in NM diseases. Unfortunately, *in vivo* NMJ research with animal models present many challenges due to inaccurate reproduction of human disease. For example, the most widely used animal model for Duchenne muscular dystrophy, the mdx mouse, is a good genetic and biochemical model, presenting total deficiency of the protein dystrophin in the muscle. However, this *in vivo* model is not useful for clinical trials due to the very mild phenotype expressed. Therefore, *in vitro* models were established, yet limitations exist. For example, inclusion of serum influences translation of animal data into human trials, inclusion of complex neurotrophic/growth factors can interfere with drug discovery, the initiation of skeletal muscle (SkM) contractions requiring electric pulse or chemical stimuli, and time consuming culture methods to induce spontaneous SkM contractions. Therefore, the aim of this thesis was to establish and characterise a simplified co-culture system that allows *in vitro* research of functional NMJs, representative of *in vivo* conditions. Immortalised human SkM stem cells were co-cultured with motor neurons (MNs) from rat embryo spinal cord explants, using for the first time a culture media formulation free from serum and neurotrophic or growth factors. This co-culture resulted in NMJ formation and contractile SkM cells. The *de novo* formation of NMJs was validated via characterisation of pre- and post-synaptic structures of the junctional apparatus. Interactions between the specialised membranes of presynaptic MN terminals with postsynaptic motor end plates (MEPs) located on SkM cells, along with supporting neuroglia, permitted chemical transmission of acetylcholine from MNs across structural bridges to bind with receptors on the MEPs. These interactions were associated with contractile activity and advanced differentiation of innervated SkM fibres. Functionality of NMJs was verified through the application of known agonists and antagonists to the co-culture system and confirmed that the contractile activity observed in the innervated SkM fibres were driven via NMJs. An ELISA-based microarray identified the presence of trophic factors required for MN, SkM, and NMJ development. Ultimately, engineering of this novel *in vitro* NMJ system represents an accessible platform to investigate NMJ formation and function, as well as providing a breakthrough assay via the system's ability to respond to drug interventions through measurable output, initiate spontaneous SkM cell contractions, and induce advanced differentiation of SkM Cells. Therefore, this novel system provides a tool to screen pharmacological or genetic therapies for diseased linked with SkM, MNs, and NMJs.

Chapter 1: Introduction

This thesis describes the generation of a novel *in vitro* platform consisting of immortalised human skeletal muscle stem cells innervated by embryonic rat neurons in order to model neuromuscular junction formation and development. The *in vitro* differentiation of stem cells into the required terminal cells necessitates the recapitulation of the molecular signalling that transpires *in vivo* during development. Thus, a comprehensive understanding of the generation and development of cells being studied and used in this research project is required. The forthcoming introduction aims to set the context and scope of the project by detailing the developmental biology of skeletal muscle cells and motor neurons, beginning with embryotic development through postnatal maturation before discussing the fundamental genetic regulation of neuromuscular synapse formation and neuromuscular junction function.

1.0 Myogenesis

1.0.0 Embryonic Myogenesis

The genesis of skeletal muscle cells (SkMCs) is initiated during embryonic development. The primitive germ layers of the early embryo give rise to the paraxial mesoderm, which leads to the formation of the somites (Aulehla and Pourquié, 2010). The somites are prompted by factors from the dorsal ectoderm, neural tube, and notochord to differentiate further (Buckingham et al., 2003; Pourquie, 2001). As the somite transforms, the dorsal region produces the dermomyotome, which contains the precursors of the skeletal muscle (SkM) progenitor cells. The paired-homeobox transcription factors, paired box protein 3 (Pax3) and paired box protein 7 (Pax7) are two of the first genetic regulators of myogenesis observed in the genetic hierarchy of SkMC formation. The expression of one or both of these genes has been detected in all vertebrate animals, including humans (Balczarek et al., 1997). Both Pax3 and Pax7 are expressed upstream of myogenesis by dermomyotome cells that will differentiate to SkMC progenitors. Research has demonstrated that the expression of Pax3 is vital for the primary formation of myofibers, whereas Pax7 expressing cells are involved with secondary myofibre development and generating a population of satellite cells (SCs), which are the quiescent SkM stem cells (i.e. myoblasts) found in the postnatal basal lamina of SkM, needed for SkM repair and regeneration (Bismuth and Relaix, 2010).

Low expression of Myogenic Factor 5 (Myf5), a member of the basic helix–loop–helix (bHLH) transcription factors is also expressed by these SkMC precursors (Buckingham and Relaix, 2007; Kiefer and Hauschka, 2001). The dermomyotome cells situated at the dorsomedial lip of the paraxial mesoderm form the myotome (Figure 1.0), which generates committed muscle progenitor cells (embryonic myoblasts). Elevated expression of MyoD, another bHLH transcription factors, and Myf5 is also observed in the committed progenitors (Kiefer and Hauschka, 2001; Ordahl et al., 2001). It has been demonstrated that MyoD performs downstream from Pax3 and Pax7, but Myf5 can act simultaneously alongside Pax3/7 (Tajbakhsh, 2009; Hutcheson et al., 2009). Both MyoD and Myf5 are known to direct muscle lineage specification toward myoblast commitment (Tajbakhsh et al., 1997). Upon formation of embryonic myoblasts, the myogenic process is controlled by the bHLH myogenic regulatory factors (MRFs). Initially by the MRFs Myf5 and MyoD for their function in myoblast determination, activation, and proliferation, followed by myogenin (aka MyoG, Myf4) and MRF4 (aka Myf6) for early differentiation of myoblasts to myocytes and late differentiation of myocytes to myotubes and ultimately into mature myofibers.

One of the first bHLH transcription factors discovered was MyoD. This early research showed how MyoD could be used to transform certain fibroblast-like cells to commence cellular fusion and myotube formation (Davis et al., 1987). Shortly after the discovery of MyoD three additional bHLH factors were discovered, namely Myf5 (Braun et al., 1989), myogenin (Edmondson and Olson, 1989), and MRF4 (Rhodes and Konieczny, 1989), for their ability to induce the myogenic features of myoblasts in different cell types. Since it was determined that these bHLH factors were expressed throughout and involved with controlling development of SkMCs, they were labelled as the myogenic regulatory factors (Rudnicki and Jaenisch, 1995). The actions of the MRFs are executed by binding with regulatory regions of DNA. Heterodimers are formed with E proteins, which facilitate the identification of E-boxes, a pattern located in the promoters of numerous genes specific to SkM (Shklover et al., 2007).

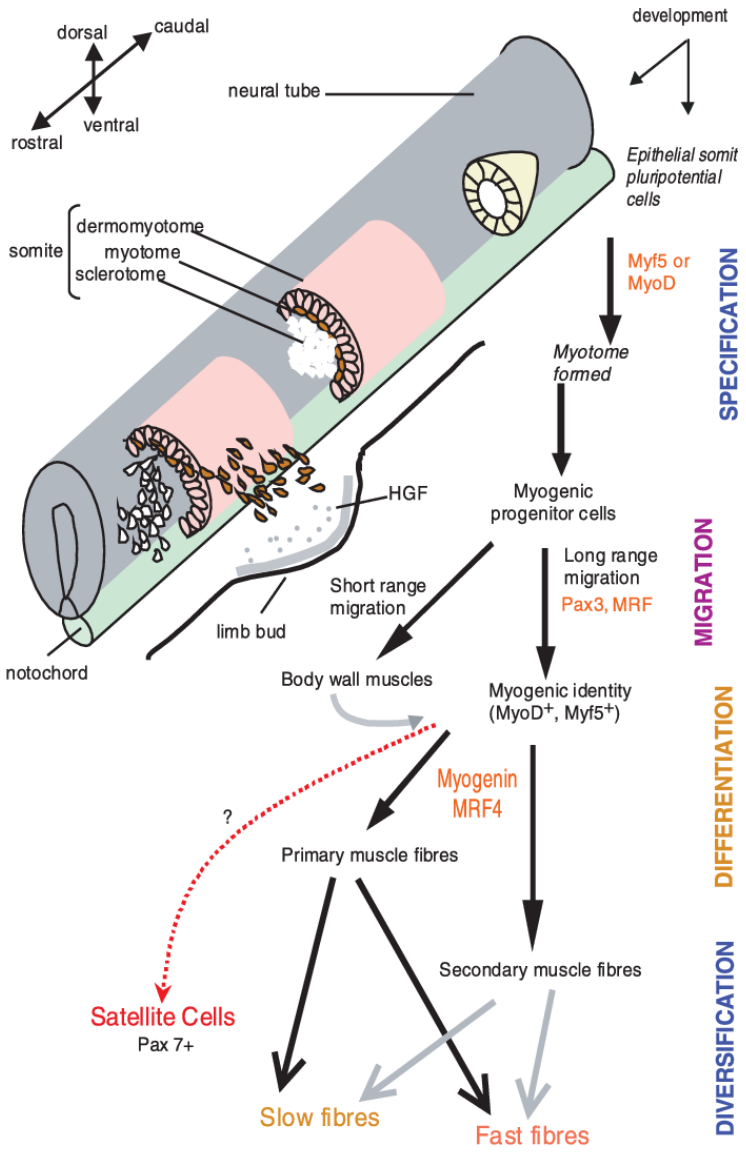

Figure 1.0: Schematic representation of somite maturation underlining embryonic myogenesis. Somite development and maturation follows a rostral to caudal gradient. The myotome arises from the dermomyotome to generate myogenic precursor cells. Myogenic genes and regulatory factors direct precursor cells toward a muscle lineage specification and myoblast differentiation. Adapted from (Sachidanandan and Dhawan, 2003; Buckingham, 2001)

1.0.1 Adult Myogenesis

The ability for SkM to repair and regenerate is a strictly regulated process involving four precisely programmed stages, which include deterioration, inflammation, repair-restoration and finally remodelling (Carosio et al., 2011). Damage to SkM induces prompt necrosis of SkMCs, which leads to the progressive infiltration of SkM by inflammatory cells, eliciting an inflammatory response in the damaged area (Tidball, 2005). Following inflammation, a regenerative phase is initiated by the activation of quiescent SCs. Under normal physiological conditions, upstream embryonic myogenesis generates Pax7 expressing cells within the dermomyotome, which become the SC population of SkM stem cells that remain present after birth and are required for future SkM regeneration. The specialised quiescent SCs are situated amongst the basal lamina and sarcolemma of SkM fibres and are governed by the same genetic hierarchy as embryonic myogenesis. Thus, SkM regeneration can only occur when the mitotically quiescent SCs are activated and develop into myoblasts (Siegel et al., 2011). Upon activation, the SCs become proliferative myoblasts and promptly re-enter the cell cycle and commence proliferation (Sousa-Victor et al., 2015). As the proliferative threshold for myofibrillar protein synthesis is reached, a population of SCs undergo asymmetric division for self-renewal and replenishment of the SkM stem cell pool. This population of SCs return to the periphery of the muscle fibres and remain in a state of quiescence with the intention of responding to future muscle damage upon subsequent activation (Relaix and Zammit, 2012). After several rounds of proliferation the committed myoblasts exit the cell cycle, they migrate to the site of injury and begin fusing into myocytes and then myotubes. As the myotubes mature, they fuse with pre-existing intact myofibres as a scaffolding and replace the damaged area to complete the muscular repair and regeneration (Simionescu and Pavlath, 2011). Finally, the regenerated myofibres continue to mature, remodelling of the extracellular matrix (ECM) occurs, and function is restored (Carosio et al., 2011). There are many parallels between embryonic myogenesis and SkM regeneration, which are both regulated by genetic and myogenic transcriptions factors. During SkM regeneration, SCs express the myogenic regulator Pax7 in the initial stages of activation (Seale et al., 2000). Studies have shown SC activation and proliferation are dependent on Pax7. Inhibiting Pax7 expression leads to a diminished capacity for self-renewal, thus a diminished pool of quiescent cells for future sequences of repair (von Maltzahn et al., 2013). Research findings have demonstrated that activated Pax7 expressing SCs can travel amongst myofibers and can surmount obstacles such as the basal lamina and connective tissues to migrate across muscle during regeneration (Hughes and Blau, 1990; Jockusch and Voigt, 2003; Watt et al., 1987; Siegel et al., 2009). Investigations of Pax7 deficient mice revealed the premature arrest of myoblast proliferation and accelerated myoblast differentiation, which ultimately resulted in diminished muscle growth and significant muscle

degeneration and a total deficiency of functional SCs (Kuang et al., 2006). This validates the vital functions of Pax7 in the initial phase of SkM regeneration and is necessary for normal myogenic development. Furthermore, Pax7 initiates the successive activation of the MRFs Myf5, MyoD, myogenin, and MRF4 (Jones et al., 2015). Myf5 expression is detected in the early stages of the regenerative process after injury, suggesting a primarily proliferative function. Variable amounts of myoblast differentiation can be initiated *in vitro* by MyoD, myogenin, and MRF4, but not Myf5, signifying its functions as a MRF involved with the primary proliferation of SCs (Yin et al., 2013). Mice devoid of Myf5 display minor impairment of SkM regeneration, manifesting as endomysium fibrosis and adipocyte accumulation (Gayraud-Morel et al., 2007). Similar impairments are observed in MyoD deficient mice (White et al., 2000). During SkM regeneration, SC proliferation persists until a protein synthesis threshold is reached. Subsequently, proliferative MRFs decrease while differentiation MRFs increase. Myogenin is recognised as a mandatory MRF for the normal myoblasts-to-myocytes-to-myotube differentiation. Thus, Myogenin deficient mice exhibit severe deficiencies in muscle regeneration (Venuti et al., 1995). Research has revealed that a flawed muscle regeneration is possible without myogenin, mice devoid of myogenin can regenerate muscle, but are one-third the size of wild-type mice (Knapp et al., 2006). Suggesting MRF-independent mechanism can moderately compensate during postnatal myogenesis. During normal SkMC regeneration, the final MRF to be expressed is MRF4 (Charge and Rudnicki, 2004). Modifying the timing of MRF4 expression impairs SkM regeneration. Early expression of MRF4 in transgenic mice causes a transient delay in SkM regeneration (Pavlath et al., 2003). Premature myotube development and delays in SkM regeneration are also observed when MRF4 is expressed early. In summary, the complex and essential process of proliferation and differentiation via MRF expression during adult myogenesis occurs upon activation of quiescent SCs (Figure 1.1), ensuring proper SkM repair and regeneration.

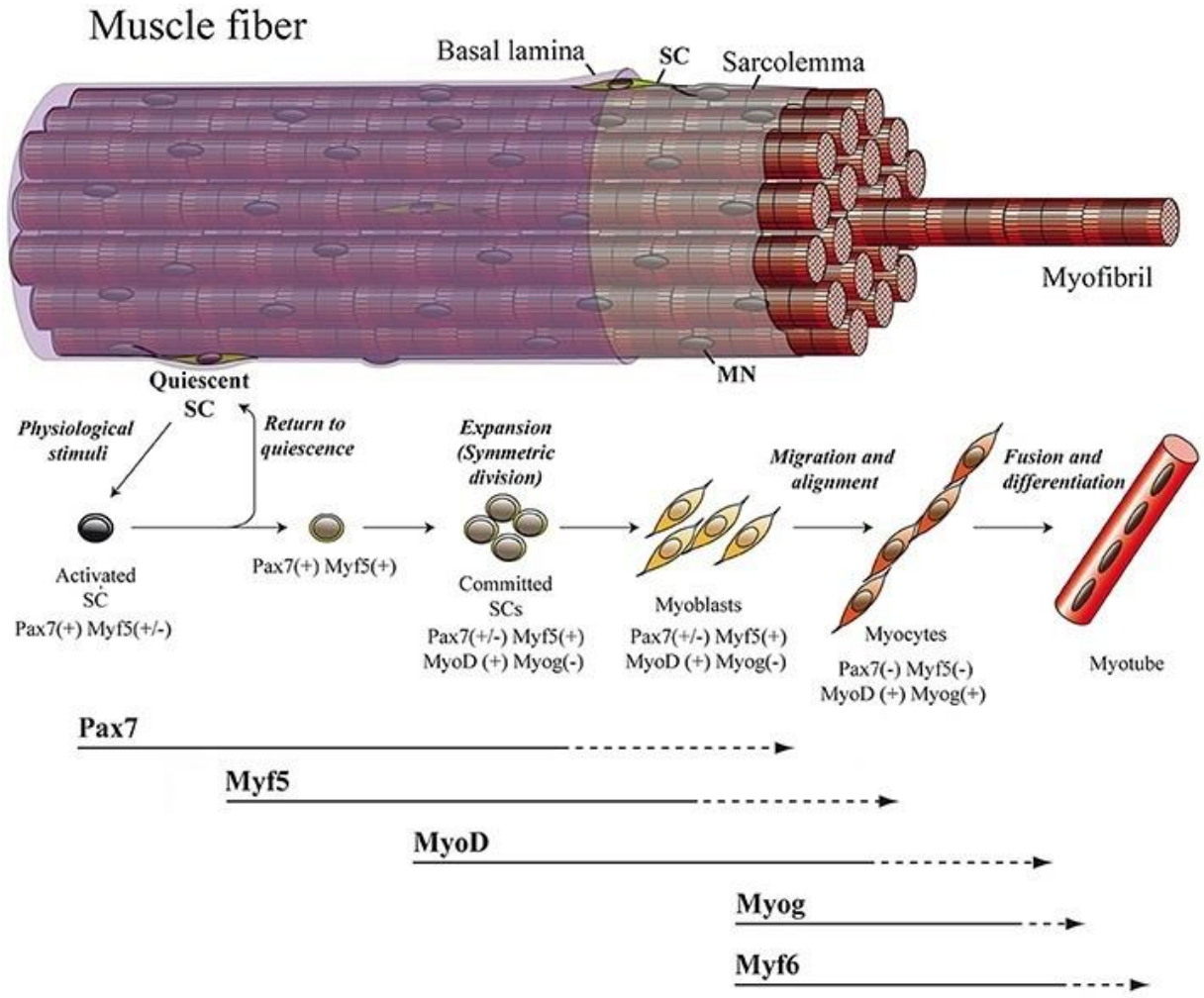

Figure 1.1: Adult myogenesis. The activation, proliferation, and differentiation of SCs from a state of quiescence to mature muscle fibre is regulated by the precise expression of myogenic transcription and regulatory factors. Adapted from (Hernandez-Torres et al., 2017).

1.1 Skeletal Muscle

1.1.0 Anatomy

Accounting for ~50% of the mass in healthy adult human males (Yin et al., 2013) and consisting of over 650 designated muscles, SkM is the largest metabolically active tissue in the human body. Distinct from both the other major muscle types (cardiac and smooth); SkM is regulated via the somatic nervous system, allowing the individual to command its function. Preparation, regulation, and implementation of voluntary locomotion of the body is regulated in the motor cortex region of the brain (Biswal et al., 1995). Upper motor neurons transmit information from the motor cortex of brain through the spinal cord to lower motor neurons. Although the primary function of SkM is to power physical movement, metabolism regulation via macronutrient storage and substrate oxidation to replace depleted adenosine triphosphate stores (ATP) (Leto and Saltiel, 2012) is also vitally performed by SkM, as well as executing crucial tasks in respiration and endocrine functions (Pedersen and Febbraio, 2008). Local and systemic environments in the body are also influenced by the growth factors, myokines, and cytokines secreted by SkM fibres into the ECM (Pedersen, 2011).

Development of SkM involves the fusion of myoblasts to form multinucleated fibres called myotubes, eventually maturing into myofibres. These singular contractile cells of SkM are innervated by a motor neuron (MN). A single MN can innervate hundreds of muscle fibres, but each mature muscle fibre is innervated by just one MN. This arrangement of a MN and all of the muscle fibres innervated by that neuron is known as a functional motor unit (Sherrington, 1925). Individual myofibres are ensheathed by endomysium and arrange in bundles. These bundles of myofibres known as muscle fascicle are bound by perimysium. Subsequently, fascicles are wrapped and encapsulated by the fibrous outer connective tissue called epimysium, to procedure a whole muscle (Figure 1.2), with numerous motor units residing within (Light and Champion, 1984; McComas et al., 1971).

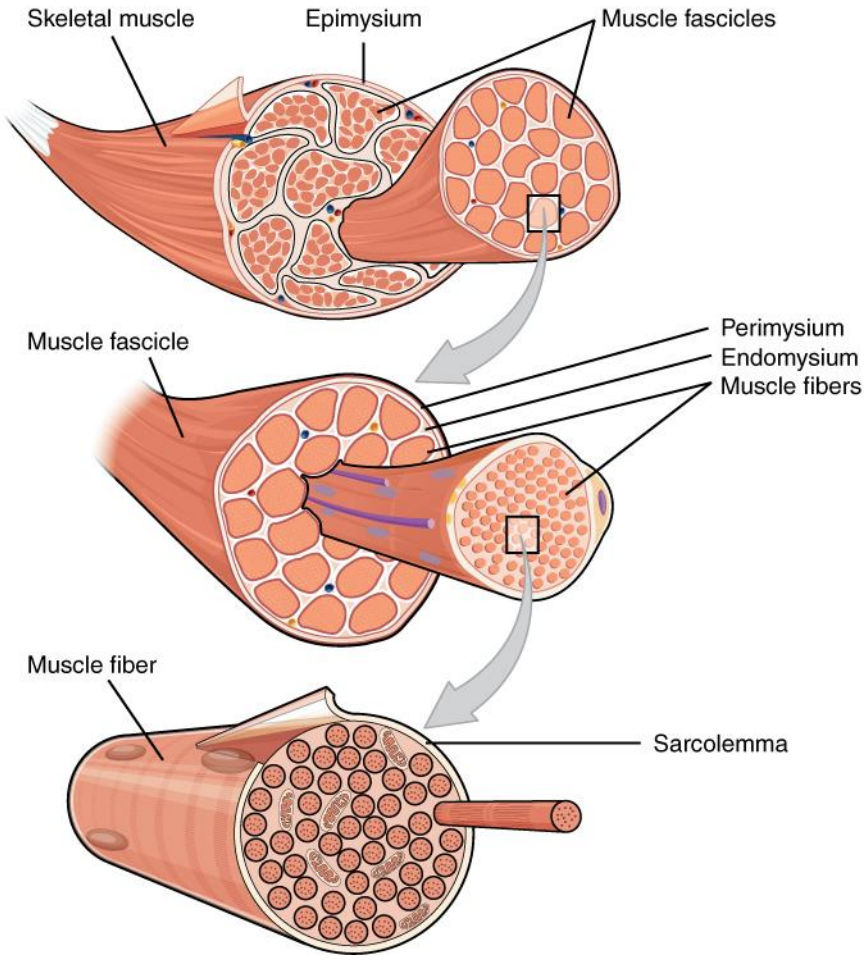

Figure 1.2: Gross anatomy of a skeletal muscle belly. A specialized cell membrane termed the sarcolemma wraps the individual skeletal muscle fibres. The fibres are bound together with a fine coating of connective tissue called the endomysium, which also functions to deliver nerve axons, nutrients, and oxygen via blood and lymphatic vessels. Bound muscle fibres are packed together with perimysium, this thin fibrous layer of connective tissue separates a muscle belly into fascicles. The muscle fascicles are then enveloped by the dense fibrous epimysium, constructing the complete skeletal muscle. Image "1007_Muscle_Fibes_(large).jpg" available for free public reuse at OpenStax CNX (https://cnx.org/contents/FPtK1zmh@12.8:bfiqsxdB@6/Skeletal-Muscle), licenced under Attribution 4.0 International (CC BY 4.0) (https://creativecommons.org/licenses/by/4.0/).

1.1.1 Skeletal Muscle Fibres

Mature myofibres are comprised of sequences of myofibrils, which include the thick filaments protein myosin and thin filaments protein actin (Rayment et al., 1993), supported by the protein titin. The repeated arrangement of these proteins in the myofibrils are known as sarcomeres, which are the single contractile units within myofibres (Figure 1.3), manifesting as striations on the myofibres. Actin molecules at the ends of a sarcomere are anchored to a position called the Z-discs, which are the defined boarders between each sarcomere. Actin bound to a Z-disc at one end of the sarcomere projects towards the M-line at the centre. Myosin filaments, which interact with the fixed actin filaments, are located centred over the M-line, with the myosin filament ends delicately attached to the Z-discs by titin. When prompted by nervous input, a cross-bridge is formed and the actin filaments are drawn and slide along the myosin filaments, shortening the sarcomere to induce contraction of the myofibre (Denoth et al., 2002).

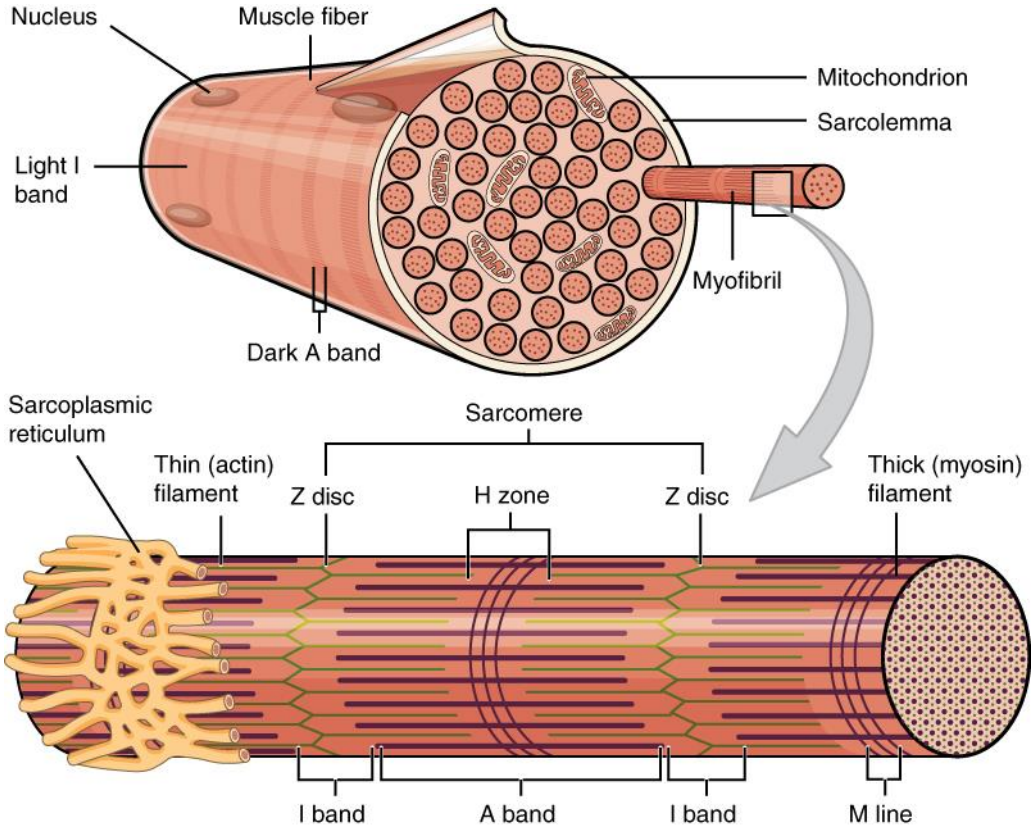

Figure 1.3: Structures of a myofibril. A muscle fibre is full of myofibrils, which are composed of individual sarcomeres joined in series. A single sarcomere is located between a set of Z-discs, making a distinct contractile unit, composed of a thin (actin) filament and thick (myosin) filament. The I-band of the sarcomere is the region where the myosin does not overlap the actin, giving a lightened appearance on the muscle fibre. The A-band appears visually darker on the muscle fibre as it contains the anisotropic myosin protein. This alternate banding gives muscle fibres the appearance of striations. The H-zone is located within the A-band where actin is absent. The M-line appears centrally in the sarcomere within the H-zone to provide structural stability. Image "1022_Muscle_Fibers_(small).jpg" available for free public reuse at OpenStax CNX (https://cnx.org/contents/FPtK1zmh@12.8:bfiqsxdB@6/Skeletal-Muscle), licenced under Attribution 4.0 International (CC BY 4.0) (https://creativecommons.org/licenses/by/4.0/).

1.1.2 Skeletal Muscle Fibre Types

Muscle fibres are commonly categorised as a type 1 (slow twitch) or type 2 (fast twitch) phenotype, according to their function, which is determined by the specific myosin heavy chain (a constituent of the myosin filament) isoforms that they express (Pette and Staron, 2000). Type 2 muscle fibres are further sub-classified as types 2a, 2x, and 2b. Type 1 fibres operate via aerobic metabolism attributed to a large concentration of mitochondria and myoglobin within the cells. This cellular composition means type 1 fibres produce low force contractions in a slow sustained manner with a high resistance to fatigue. Conversely, type 2x and 2b fibres generate fast, short, and high force contractions, which are quick to fatigue, due to the mainly glycolytic metabolism of these fibre types. In type 2a fibres, a combination of aerobic and anaerobic metabolism is observed. Therefore, this particular fibre type is able to generate force greater then type 1 fibres and fatigue more slowly than type 2x/b fibres (Schiaffino and Reggiani, 2011). Interestingly, it has been determined that only small mammals retain the type 2b fibres, which contract and fatigue at the fastest rate when compared to the other type 2 fibres. Thus, the hierarchy of type 2 fibre contraction speed begins with 2a, followed by 2x, and 2b being the fastest. However, this also means the demand for ATP is significantly higher in type 2b fibres, which in turn increases tension cost (Rundell et al., 2004). It is thought that humans as well as other large mammals have evolved to lack the type 2b fibre to moderate energy expenditure. Thus, human SkM fibres are a combination of type 1, 2a, and 2x. Although these general classifications of fibre types provide valuable fundamental information, fibre types have the ability to adapt to environmental or *in vivo* stimuli and can switch between fibre types or exhibit hybridized characteristic of several fibre types (Stephenson, 2001). In general, a SkM is composed of a combination of fibre types, which have varying degrees of particular characteristics (Table 1.0) and are determined by the function of the particular muscle. For example, postural muscles of the neck and spine contain higher concentrations of type 1 fibres as they mostly produce low force contractions and require a greater endurance for sustained activity. The high capacity for endurance of type 1 fibres means this fibre type is also observed in higher overall concentration in the muscles of athletes performing long distance events such as marathons. Conversely, the composition of fibres found in the muscles of the upper arms, shoulders, and chest are predominantly that of the type 2a/x fibres. This is apparent in athletes performing tasks that involve quick surges of explosive activity (Rockl et al., 2007).

Table 1.0: Characteristics of type 1, 2a, and 2x/b skeletal muscle fibres.

Feature	*Type 1*	*Type 2a*	*Type 2x/b*
Force production	+	++	+++
Contraction speed	+	+++	+++
Fatigue resistance	+++	++	+
Glycolytic capacity	+	+++	+++
Oxidative capacity	+++	++	+
Capillary density	+++	++	+
Mitochondrial density	+++	++	+
Endurance capacity	+++	++	+

Note: + = low; ++ = moderate; +++ = high

1.1.3 Muscle Contraction

Excitation–contraction coupling is the well-established molecular interaction and exchange involved with SkM contraction. Nervous input causes depolarisation of the muscle fibre membrane called the sarcolemma (Figure 1.4), the cascading action potential (AP) travels down the invaginated transverse tubule (T-tubule) of the sarcolemma into the cell. As the AP travels down the T-tubule into the sarcoplasm of the muscle fibre, it stimulates the opening of voltage-gated L-type calcium channels, subsequently depolarising the interior of the muscle fibre. The inner depolarisation of the muscle cell results in the opening of calcium channels in the terminal cisternae of the sarcoplasmic reticulum (SR). Since calcium ions (Ca^{2+}) are higher in concentration in the SR than the cell sarcoplasm, they rapidly diffuse into the sarcoplasm. The Ca^{2+} then bind with the protein troponin, which is located on the actin filaments. The Ca^{2+} bound troponin causes the troponin-tropomyosin-complex to undergo a conformational change, which exposes active binding sites for the myosin filament heads along the length of the actin filament, to allow for cross-bridge formation and cycling (Figure 1.5).

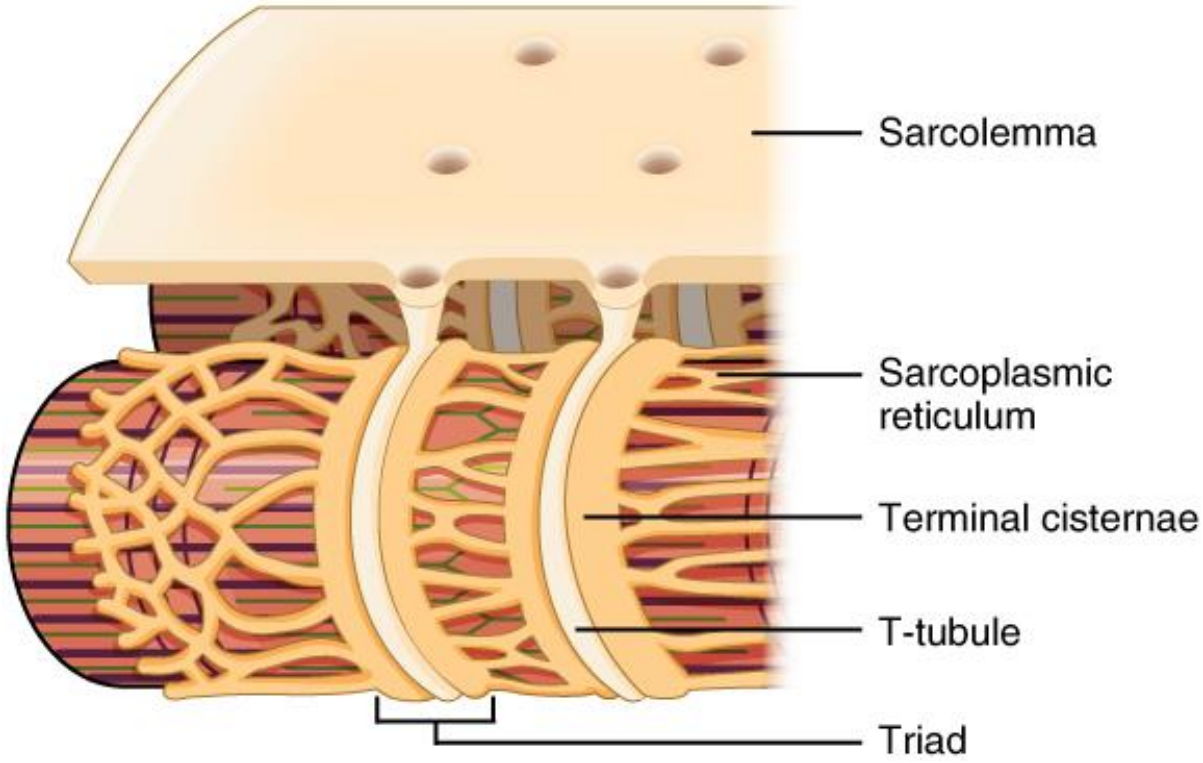

Figure 1.4: Arrangement and assembly of skeletal muscle triads. A triad is formed when a transverse tubule originating from the sarcolemma is sandwiched between two terminal cisternae of the sarcoplasmic reticulum. This tight configuration allows for efficient nerve signal transmission, depolarisation, and opening of gated ion channels. Image "1023_T-tubule.jpg" available for free public reuse at OpenStax CNX (https://cnx.org/contents/FPtK1zmh@12.8:bfiqsxdB@6/Skeletal-Muscle), licenced under Attribution 4.0 International (CC BY 4.0) (https://creativecommons.org/licenses/by/4.0/).

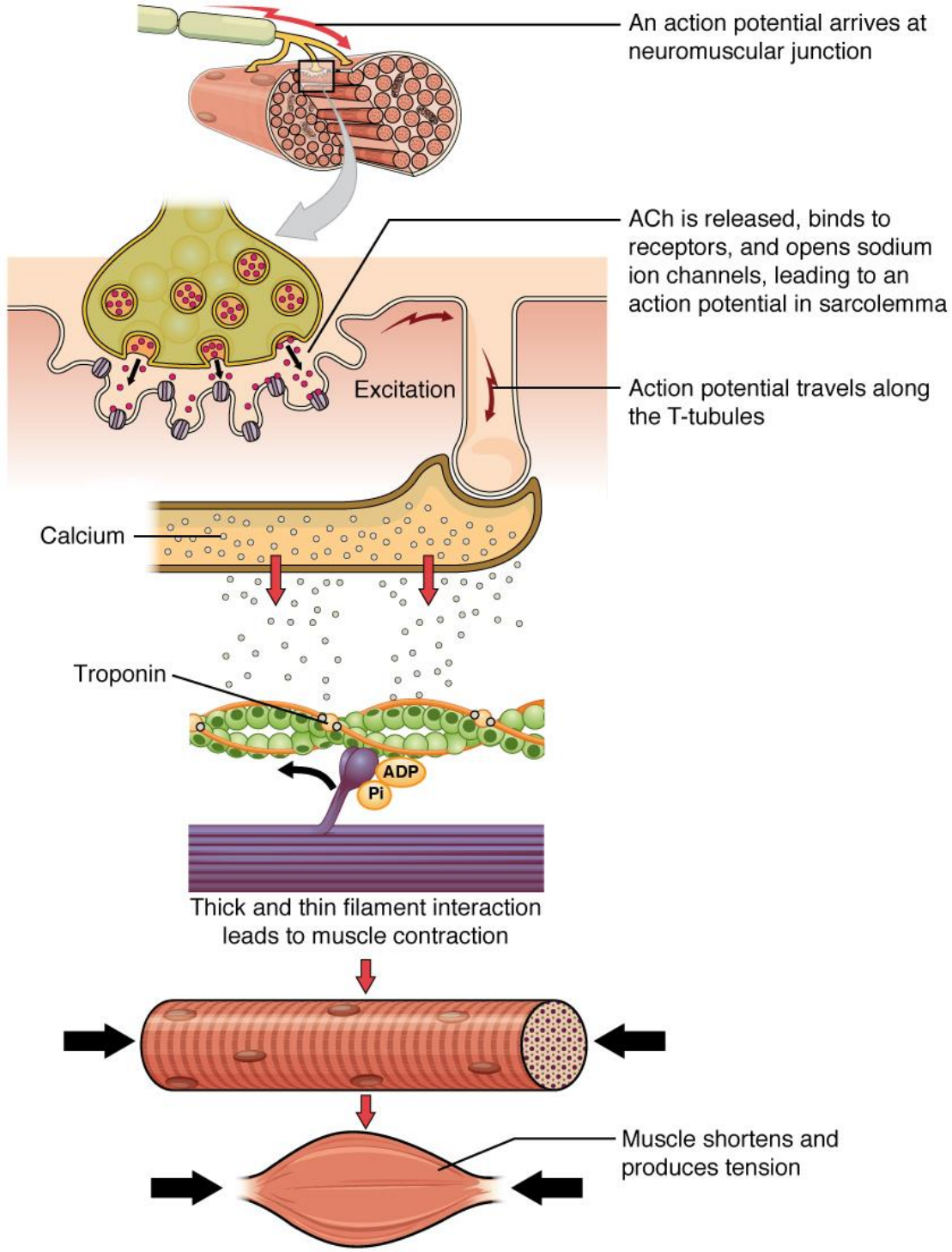

Figure 1.5: Cross-bridge formation. Depolarisation triggers the influx of calcium ions into the cytosol of the muscle fibre. The calcium binds with troponin and shifts the position of tropomyosin to expose binding site for myosin to form the cross-bridge needed for muscle contraction. Image "1010a_Contraction_new.jpg" available for free public reuse at OpenStax CNX (https://cnx.org/contents/FPtK1zmh@12.8:EtWWcJM-@10/Muscle-Fiber-Contraction-and-Relaxation), licenced under Attribution 4.0 International (CC BY 4.0) (https://creativecommons.org/licenses/by/4.0/).

A cross-bridge cycle can only occur after the myosin head has been activated. An ATP molecule binding with the myosin head, which is hydrolysed to adenosine diphosphate (ADP) and inorganic phosphate (IP), triggers activation through the energy liberating action of ATP hydrolysis, which fixes the myosin head into a 'cocked' configuration. A cross-bridge is formed between the activated myosin head and actin; the IP is then freed increasing the binding capacity of the myosin head and actin filament. The ADP is then liberated causing the myosin head to pivot. The actin filament then slides towards the centre of the sarcomere, this action is called the 'power stroke'. Another ATP then binds with the myosin head, the cross-bridge is weakened and the myosin head detaches from the binding site, before being activated again for another cross-bridge formation (Figure 1.6). Cross-bridge cycling will continue to re-engage while the binding sites on the actin filament remain available. Repeated cycling pulls the actin filaments together and the sarcomere shortens, inducing muscle contraction. Termination of Cross-bridge cycling occurs when Ca^{2+} are actively returned to the SR. The troponin-tropomyosin-complex returns to its primary formation, blocking the myosin binding sites on the actin filaments, initiating muscle relaxation. (ter Keurs et al., 2003).

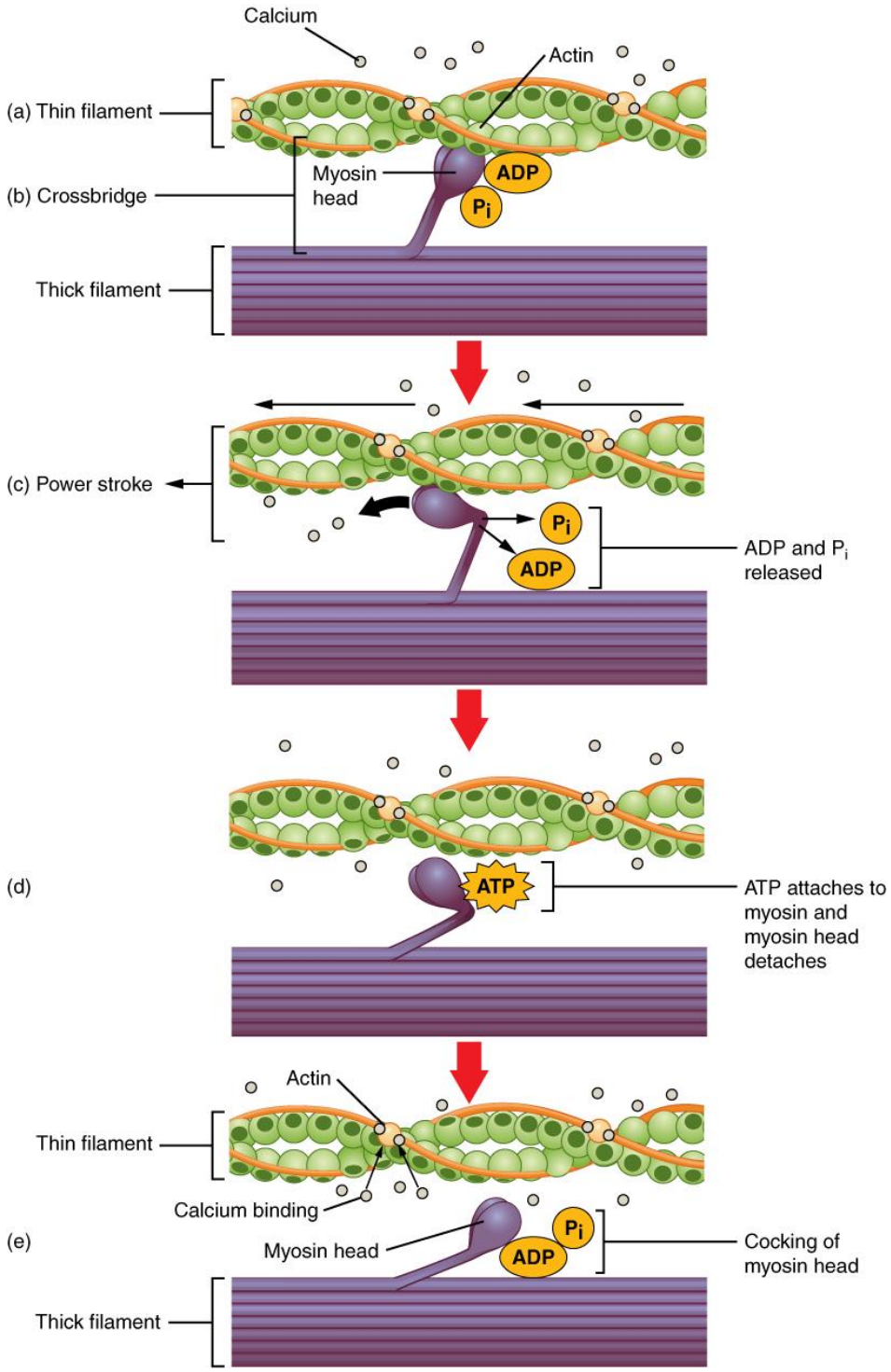

Figure 1.6: Molecular mechanisms of muscle contraction. a) Calcium ions bind with troponin to prompt a change in the structural position of tropomyosin, revealing the actin binding sites. b) Cross-bridge formation occurs between the bindings sites on the myosin heads and actin filaments. c) The power stroke is executed through the release of inorganic phosphate (IP) then adenosine diphosphate (ADP). d) The attachment of adenosine triphosphate (ATP) uncouples the binding of myosin and actin. e) The conversion of ATP to ADP and IP configures the myosin head for cross-bridge formation and cycling. Image "1008_Skeletal_Muscle_Contraction.jpg" available for free public reuse at OpenStax CNX (https://cnx.org/contents/FPtK1zmh@12.8:EtWWcJM-@10/Muscle-Fiber-Contraction-and-Relaxation), licenced under Attribution 4.0 International (CC BY 4.0) (https://creativecommons.org/licenses/by/4.0/).

1.2 Motor Neurons

Motor neurons (MNs) are neuronal cells that originate in the central nervous system (CNS) and project axons into the periphery to form synapses with their target tissues. Vital for life in all vertebrates, effective and accurate MN activity and signal transmission with target tissues in the periphery, such as SkM, is required for fundamental behaviours such as breathing and locomotion. Although typically described as a distinct cell type, MNs have vast diversity with varied expression of genes, molecular profiles, and target muscles. This diverse nature of MNs allows for separate innervation of the numerous individual SkM groups in the vertebrate body (Kanning et al., 2010). For example, in humans there are over 600 SkM throughout the body with most muscles making up one part of a bilateral pair (Frontera and Ochala, 2015). Thus, strict regulation of CNS signal transmission to MN and MN outputs to the target SkM is vital for the refined, organised motor control observed in sophisticated motor behaviours. Some research has suggested that MN subtype identity regulates the MNs innervation sequence and connection with the target SkM (Milner and Landmesser, 1999; Landmesser, 2001). Therefore, MN subtype diversity needs to be explored to appreciate the function of MNs and their motor units.

1.2.0 Motor Neuron Subtype Diversity

Divided into three distinct classifications, MNs can be labelled as branchial, visceral and somatic (Stifani, 2014). The MNs that reside in the brainstem and innervate muscles of the head and neck through the cranial nerves are known as the branchial MNs (Chandrasekhar, 2004). Visceral MNs are an element of the autonomic nervous system, which is comprised of the sympathetic division and parasympathetic division. Found in the preganglionic column (PGC) of the spinal cord, the sympathetic MNs innervate the adrenal medulla and sympathetic chain ganglia. Whereas parasympathetic MNs are found in the sacral division of the spinal cord, as well as the brainstem, innervating peripheral ganglia located close to vital organs of the body (Purves et al., 2001). Located in the hindbrain nuclei and spinal cord ventral horn, the axons of the somatic MNs extend from the CNS alongside the spinal nerves and into the periphery. Here the somatic MNs make contact with SkM and form the highly specialised synapses called neuromuscular junctions (NMJs) (Wu et al., 2010). By identifying their location within the spinal cord, the somatic MNs are separated into groups called motor columns, such as the PGC mentioned above, with each motor column innervating a specific collection of muscles. One of the five motor columns groups, called the medial motor column (MMC), tracks the entirety of the spinal cord and

contains the MNs that innervate the dorsal back muscles and axial thoracic muscles (Fetcho, 1987; Agalliu et al., 2009). Located exclusively at the limb regions of the spinal cord, the MNs of the lateral motor columns (LMCs) innervate the forelimbs via the LMC MNs in the brachial segment of the spinal cord, while innervation of the hindlimbs occurs via the LMC MNs of the lumbar segment (Landmesser, 1978). Innervating the muscles of the ventral trunk, such as the anterior abdominal wall and intercostal muscles, the hypaxial motor columns (HMCs) are located at cervical and thoracic segments of the spinal cord (Gutman et al., 1993). Positioned at the thoracic segment of the spinal cord, MNs from the forth group of motor columns called the PGC innervates the peripheral nervous system sympathetic chain ganglia (Prasad and Hollyday, 1991). Finally, the fifth group is called the phrenic motor column (PMC) which is a MN group that provides the sole source of diaphragm innervation, thus responsible for respiration in mammals (Philippidou et al., 2012) (Figure 1.7). The most comprehensively researched motor column is the LMC, which is additionally partitioned into a medial subdivision (LMC_m), responsible for ventral innervation of the limb muscles (e.g. flexors) and a lateral subdivision (LMC_l), in control of the dorsal innervation of limb muscles (e.g. extensor) (Tosney and Landmesser, 1985; Kania and Jessell, 2003).

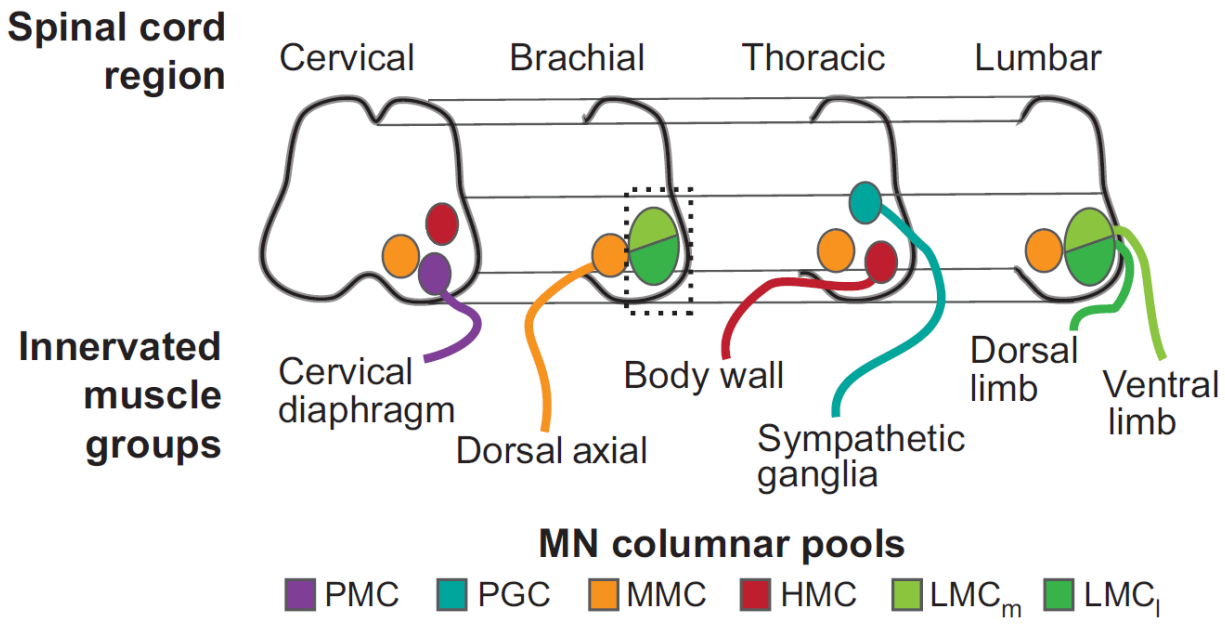

Figure 1.7: Spinal motor column organisation. The motor neuron (MN) columnar pools dictate the location of MN cell bodies along the spinal cord in relation to the body and regulates MNs to their target muscles. The MNs from the phrenic motor column (PMC) innervate the diaphragm. The preganglionic column (PGC) MNs innervate the sympathetic ganglia. The MNs originating from the medial motor column (MMC) innervate the dorsal axial muscles and the hypaxial motor columns (HMC) MNs innervate the muscles of the body wall. The medial lateral motor columns (LMC_m) and its lateral counterpart the LMC_l innervate the ventral and dorsal limb respectively. Adapted from (Davis-Dusenbery et al., 2014)

Depending on morphology, function, and the intended SkM target, MNs from a columnar pool can be further separated into three distinct classifications. Specifically, alpha motor neurons (αMNs), beta motor neurons (βMNs), and gamma motor neurons (γMNs) (Kanning et al., 2010). The αMNs are the biggest most abundant subtype of MNs and are responsible for innervating extrafusal SkM fibres, which are the muscle fibres that produce physical movements upon contraction. The αMNs send the communication through their axons to the intended target where they synapse with muscles directly to induce muscle contraction (Dalla Torre di Sanguinetto et al., 2008). The smaller γMNs are responsible for innervating the proprioceptive intrafusal SkM spindle and are involved with modulation of sensory neuron sensitivity to stretch forces on the SkM spindle (Jessell, 2000; Proske and Gandevia, 2009). Interestingly, the functions of βMNs requires further exploration before their functional role is accurately elucidated, despite βMNs axon collaterals innervating extrafusal SkM fibres and intrafusal SkM fibres (Manuel and Zytnicki, 2011; Kanning et al., 2010). Finally, further MN subtype diversification of αMNs is implemented based on their functional properties. These properties are defined by the metabolic and molecular attributes of the motor unit formed with the type of SkM fibre being innervated. The αMN subtype innervating type 1 SkM fibres are known as slow-twitch fatigue resistant (αS), type 2a SkM fibres are innervated by fast-twitch fatigue-resistant (αFR) MNs, and innervating the 2x/b fibres are the fast-twitch fatigable (αFF) MNs (Figure 1.8). Containing an assortment of the MN subtypes, the motor pool regulates the ultimate contractile function of SkM depending on the ratio of MN subtypes within the pool. However, hormones, physical requirements, and neuronal activity permits conversion of SkM fibre types, as observed *in vivo* (Staron, 1997; Pette and Staron, 2000; Friese et al., 2009).

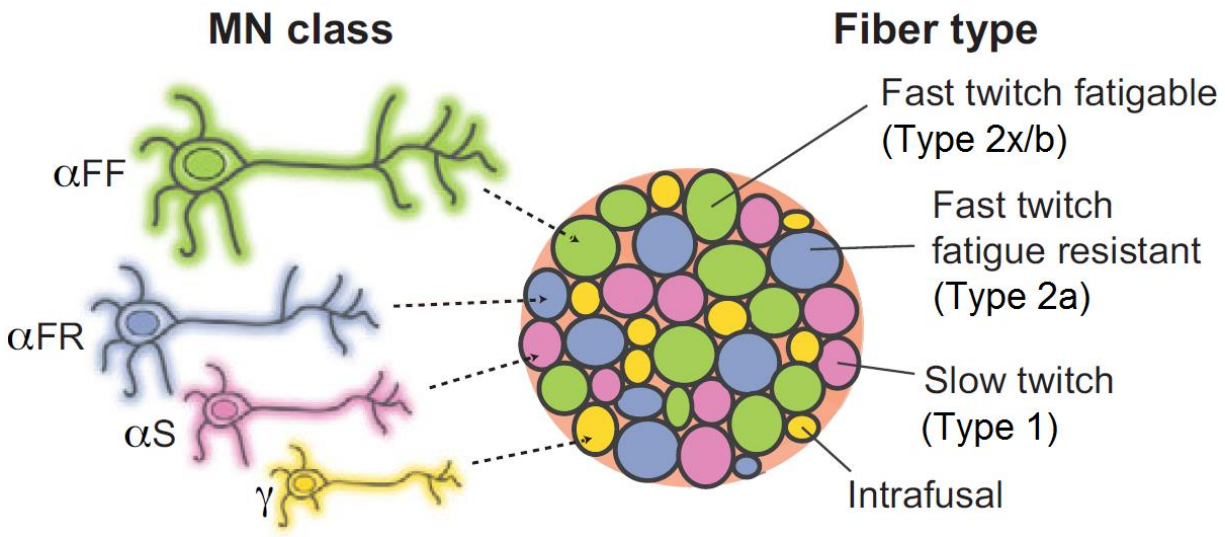

Figure 1.8: Functional classification of alpha motor neuron subtypes. Fast-twitch fatigable (αFF), fast-twitch fatigue-resistant (αFR), and slow-twitch fatigue resistant (αS) motor neurons (MNs) innervate their corresponding type 2x/b, type 2a, and type 1 extrafusal muscle fibres. The smaller gamma motor neurons (γMNs) innervate the intrafusal muscle fibres. Adapted from (Davis-Dusenbery et al., 2014)

1.3 The Neuromuscular Junction

In order to appreciate the vital function of neuromuscular junctions (NMJs) and the cellular specialisation they exhibit, the complex regulation of NMJ formation, development, and maturation need to be understood in relation to fundamental molecular and cellular mechanisms.

1.3.0 Agrin

In the initial stages of NMJ formation, clusters of acetylcholine receptors (AChRs) emerge centrally on myofibers in advance of nervous input in a process known as intrinsic pre-patterning of muscle (Lin et al., 2001; Yang et al., 2001). While this preliminary pre-patterning occurs without a nervous component, the differentiation of postsynaptic structures can only occur after synapse formation and presynaptic input. One of the fundamental components that regulates postsynaptic differentiation is *agrin.* Produced and secreted by motor neuron terminals (MNTs), agrin is a mandatory heparan sulphate proteoglycan needed for NMJ formation (Bezakova and Ruegg, 2003). The obligate nature of agrin has been shown in agrin-deficient mice, which present with failed NMJ formation and death (Gautam et al., 1996). Agrin deficient mice also fail to undergo presynaptic differentiation and have persistent MN growth. It is suggested that a lack of regressive termination signalling from postsynaptic structures and the lack of intrinsic agrin discontinuation signals cause the failure of presynaptic differentiation and excessive axon sprouting (Campagna et al., 1995; Campagna et al., 1997). However, when agrin deficient mice express a miniaturized form of agrin from their developing SkMCs, which have muscle-specific tyrosine kinase activating domains essential for AChR clustering, a restoration of NMJ formation is witnessed (Lin et al., 2008). Equally, the forced over expression of agrin in non-synaptic regions of SkMCs leads to the formation of postsynaptic structures usually only observed at the NMJ, such as developed junctional folds (Bezakova et al., 2001). There is also genetic expression of AChR genes usually only found at the synapse (Jones et al., 1997). These studies present evidence that the secretion of agrin from MNs to agrin-receptive SkMCs instigates the preliminary formation of NMJs. Formation and maturation of the NMJ is also facilitated by agrin through the binding of the dystrophin-glycoprotein complex, which is dystrophin-associated transmembrane glycoproteins, namely dystroglycan (Bowe et al., 1994; Gee et al., 1994). Some research also implies that the downregulation of agrin, facilitated by proteolytic cleavage, regulates maturation of the NMJ by manipulating AChR clusters and the topology of junctional fold (Bolliger et al., 2010).

1.3.1 Muscle-Specific Tyrosine Kinase

Agrin regulates the formation and development of the NMJ via a single transmembrane receptor tyrosine kinase, known as the muscle-specific tyrosine kinase (MuSK) receptors at the motor end plate (MEP) (Wu et al., 2010). MuSK signalling activation occurs after binding to the low-density lipoprotein receptor-related protein 4 (LRP4), which is a MuSK co-receptor (Zhang et al., 2008; Kim et al., 2008), prompting differentiation of postsynaptic structures after binding to neural agrin. Structurally, the activation of MuSK occurs when two heterodimers of agrin and LRP4 form a tetrameric complex. Communication with the cytoplasmic adaptor docking protein 7 aka downstream of tyrosine kinase 7. (Dok7) and the 43 kDa receptor-associated protein of the synapse (rapsyn) is also essential for MuSK activation and formation of the NMJ (Okada et al., 2006). As already mentioned, during preliminary NMJ formation intrinsic pre-patterning of muscle occurs on myofibers through the emergence of AChR clusters, along with supplementary postsynaptic proteins. Although pre-patterning of muscle occurs in advance of nervous input, the establishment of the MuSK–LRP4–Dok7–rapsyn complex (Figure 1.9) is required. During myogenesis, MuSK induces clustering of AChRs on aneural myotubes and facilities the assembly of postsynaptic structures needed to secure AChRs in mature developed MEPs (DeChiara et al., 1996; Lin et al., 2001). Furthermore, transcriptional specialisation of myonuclei at the synapse occurs after MuSK-mediated recruitment of the vital myonuclei. A lesser retrograde signalling from MuSK to MNs also occurs to induce presynaptic differentiation

Expression of MuSK is first observed at the premature myotome and is expressed throughout SkM development and thereafter. Following innervation of SkMCs, a down regulation of MuSK expression occurs in the myonuclei adjacent to the NMJ. However, recruited myonuclei at the synapse have sustained expression of elevated MuSK. Upon denervation, the NMJ-adjacent myonuclei begin to upregulate MuSK expression once again (Bowen et al., 1998). Accordingly, expression of MuSK mRNA occurs during myocyte to myotube fusion following the same expression pattern as AChR subunit genes (Kim and Burden, 2008). Research with MuSK knockout mice has provided valuable insight into the functions of MuSK during NMJ formation. Mice devoid of MuSK exhibit the same failed NMJ formation and death after birth due to respiratory failure as observed in the agrin-deficient models (DeChiara et al., 1996). Noteworthy, mice lacking LRP4, Dok7 or rapsyn suffer the same fate (Okada et al., 2006; Weatherbee et al., 2006; Gautam et al., 1995). MuSK devoid mice also have persistent MN growth engulfing the myotube as witnessed in agrin deficient mice (Lin et al., 2001). Additionally, MuSK-deficient *in vitro* cultured myotubes lack AChR cluster prepatterning and are unresponsive to the application of exogenous agrin (Glass et al., 1996). Interestingly, marginally defective regulation of

MuSK signalling during development may have minor effects on the primary formation of the NMJ. However, subsequent development and maturation of the NMJ can be disturbed by MuSK signalling dysfunction, only manifesting after birth or develop at delayed postnatal stages as congenital myasthenic syndromes (CMS) (Engel et al., 2010). Research conducted using loxP/Cre recombination to inactivate MuSK expression in mice during postnatal development results in the advance of symptoms consistent with myasthenic syndromes, leading to death from severe muscle weakness. A diffusion of AChR clusters, errors in postsynaptic configuration, and withdrawal of innervating MNs were also observed in conditionally inactivated MuSK mice (Hesser et al., 2006). When examining humans with CMS, distinct abnormalities of the postsynaptic apparatus are observed. The junctional folds lack the characteristics of MEP maturation and a significant decline in clustering of AChRs is displayed. These dysfunctions are a consequence of MuSK mutations that restrict MuSK expression and hinder communication with Dok7 (Maselli et al., 2010). Similar observations are made in CMS mouse models with MuSK mutations. Postnatal development of the CMS mouse reveals underdeveloped junctional folds, a decreased clustering of AChRs with obvious fragmentation, improper plaque-to-pretzel formation of AChRs, and faulty MN transmission (Chevessier et al., 2008). Along with being compulsory for the launch of postsynaptic NMJ differentiation, the initiation of postsynaptic assembly can be activated by MuSK alone. This has been confirmed via MuSK dimerization and subsequent overexpression of MuSK through self-activation (Punga et al., 2011; Sander et al., 2001), crosslinking via antibody mediation (Hopf and Hoch, 1998) or through transmembrane domain mutant dimerization (Jones et al., 1999). Applying any of the mentioned MuSK activation techniques to aneurally-cultured myotubes induces AChR cluster formation. The formation of postsynaptic features are also detected in innervated SkMCs on non-synaptic locations of the myofibres. MuSK activation also includes the aggregation of synaptic myonuclei, important for upregulation of AChR and MuSK gene expression (Jones et al., 1999; Moore et al., 2001). Minor presynaptic differentiation of MNs in Agrin deficient mice is possible when MuSK is overexpressed in SkM via self-activation. However, the mice have a short lifespan and only a few weeks of stunted growth (Kim and Burden, 2008). MuSK expression can act on MNs via indirect methods as well, to assist their presynaptic differentiation. MuSK-induced secreted factors from SkM such as the laminin isoform laminin-β2 has been shown to regulate the formation of MNT active zones during MNT differentiation (Jones et al., 1999; Nixon et al., 2008). Possibly regulated in a similar way by MuSK, collagen IV and fibroblast growth factor (FGF) proteins are increased in the synaptic basal lamina and can influence MNT differentiation (Fox et al., 2007).

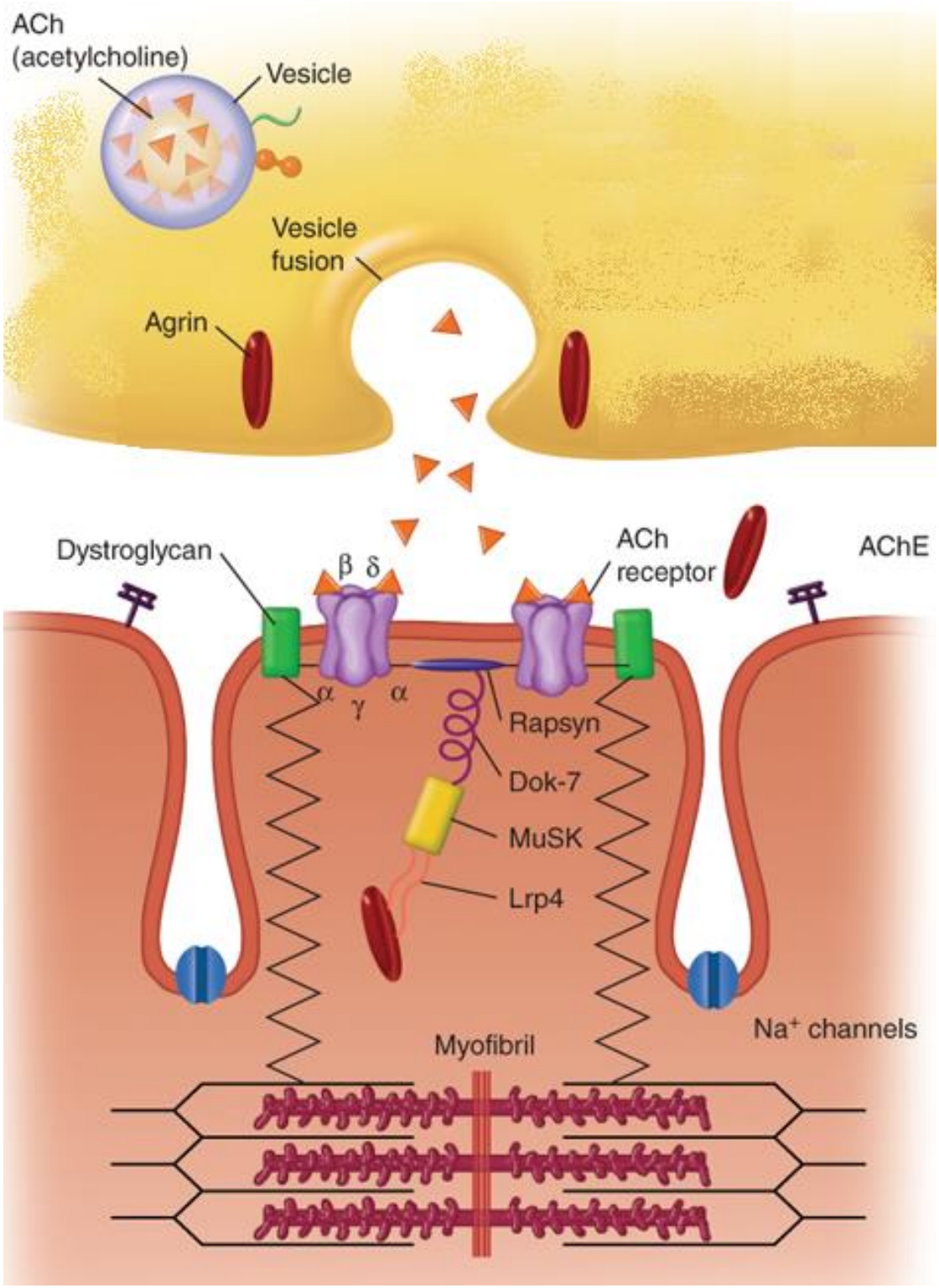

Figure 1.9: The Agrin-MuSK–LRP4–Dok7–rapsyn-AChR complex. Agrin and acetylcholine (ACh) are released by the motor neuron terminal. Muscle-specific tyrosine kinase (MuSK) phosphorylation occurs following the binding of Agrin and low-density lipoprotein receptor-related protein 4 (LRP4), which stimulates the organisation of Musk-LRP4. The recruitment of docking protein 7 (Dok7) stabilizes MuSK through dimerization. Subsequently, activated MuSK sites anchor AChRs with 43 kDa receptor-associated protein of the synapse (rapsyn) after the tyrosine phosphorylation of Dok7. Adapted from (Amato, 2018).

1.3.2 43 kDa Receptor-Associated Protein of the Synapse

Expressed in SkMCs throughout the early development of NMJs and in mature SkM, rapsyn is a cytoplasmic support protein underlying the postsynaptic cytoskeleton, with expression principally limited to the synapse. A high-density protein construct is formed by the rigid binding of rapsyn with AChRs and dystroglycan (Unwin, 2013; Bartoli et al., 2001). This complex is believed to maintain cytoskeletal-anchoring of AChRs. However, the AChR-rapsyn clustering initiated by MuSK activation is poorly understood from the perspective of molecular signalling pathways. Both *in vivo* and *in vitro* studies have confirmed rapsyn as an essential protein in the formation of AChR clusters. Thus, evident failure of postsynaptic specialization of the NMJ in rapsyn deficient mice is witnessed (Gautam et al., 1995). Unlike the stark phenotypes reflected in MuSK, Lrp4, and Dok7-null mice, rapsyn deficient mice have some respiratory function and laboured breathing allows them to live a few hours. Inspection of the failed MEP exposed a lack of cytoskeletal specializations and unsuitable AChR clusterisation. Nevertheless, aggregations of synaptic basal lamina constituents such as laminin-β2 and acetylcholinesterase are still supplied in abundance. Surprisingly, an accumulation of MuSK below the MNT and elevated expression of AChR genes by the synaptic myonuclei are exhibited (Apel et al., 1995; Gautam et al., 1995). These findings established that rapsyn is not involved with synaptic gene transcription but is vital for affixing of AChRs at the MEP apparatus. It is also implied that miniature muscle contraction are possible at premature NMJs before proper anchoring of AChRs by rapsyn is complete.

1.3.3 Acetylcholine Receptors

In addition to the vital functions AChRs perform during signal transmission, they are also involved with MEP formation during NMJ development. Rapsyn has been shown to form clusters in non-myogenic cells when forced overexpression is induced. However, SkMCs require AChRs to initiate clusterisation. For instance, a loss of associated rapsyn clusters occurs when AChRs are removed from *in vitro* myotube cell membranes using lasers or antibodies to induce the AChR depletion (Bruneau et al., 2008; Marangi et al., 2001). Research has also revealed that AChRs are joined with and escorted by rapsyn early in the exocytic pathway (Marchand et al., 2002; Moransard et al., 2003). Further findings support the notion that AChRs are fundamental for formation of the MEP, since deletion of the AChR γ-subunit gene, which is needed for fabrication of physiological AChRs during embryogenesis, results in unbridled MN growth (Liu et al., 2008). Noteworthy, mice in these experiments still conveyed clustering of MuSK at the

diaphragm, whereas rapsyn clustering was imperceptible. Ultimately, AChRs are perceived to participate in MEP differentiation, as well as assisting in distribution of rapsyn to the MEP apparatus.

1.3.4 Neuromuscular Junction Function

Contractions of SkM are governed by the CNS. MNs transmit communications from the CNS via nerve impulses to SkM fibres to induce contractile activity in muscle. The fusion of a MNT with the MEP of a SkM fibre forms a highly specialised chemical synapse where signal transmission takes place (Figure 1.10).

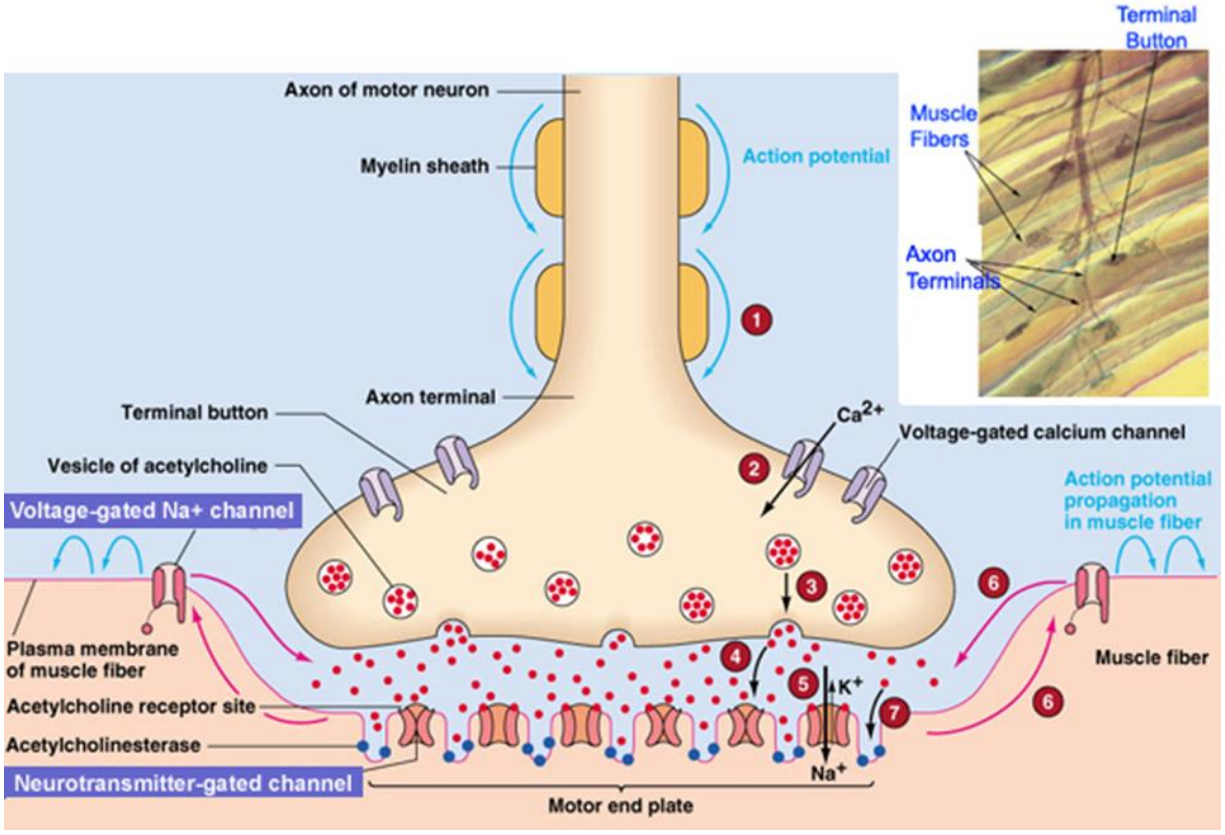

Figure 1.10: Neuromuscular junction signal transmission. 1) The action potential (AP) propagates down the motor neuron (MN) to the axon terminal. 2) Calcium channels are opened once the AP reaches the axon terminal, inducing influx of calcium ions (Ca^{2+}) into the presynaptic terminal. 3) Increased intracellular calcium concentration at the axon terminal prompts synaptic vesicle fusion with the membrane of the axon terminal. 4) Upon fusion, the vesicle releases acetylcholine (ACh) into the synaptic cleft. 5) ACh crosses the synaptic cleft to bind with acetylcholine receptors (AChRs), opening voltage-gated sodium ion (Na^{+}) channels on the motor end plate (MEP). 6) An AP generating muscle contraction is produced. 7) Termination of synaptic transmission occurs upon ACh degradation via acetylcholinesterase and presynaptic reuptake. Adapted from (Song, 2014)

This synapse is one of the first to be formed during embryonic development and is called the neuromuscular junction (NMJ). Although initial NMJ formation occurs early, full maturation requires several weeks of structural and molecular configuration (Sanes and Lichtman, 2001). The NMJ maturation process is significantly longer than observed in the formation of CNS synapses, which take just hours to mature in comparison and have a rapid turnover rate. Following NMJ maturation the synapse is maintained throughout life for appropriate signal transmission (Sanes and Lichtman, 1999). Consequently, erroneous formation, development, or impaired maintenance through aging could instigate muscle weakness, paralysis, or manifest as various neuromuscular (NM) or neurodegenerative (ND) diseases. Disorders that directly target the NMJs function are characteristically genetic (e.g. congenital myasthenia), autoimmune (e.g. Myasthenia gravis, Lambert-Eaton myasthenic syndrome), or neurotoxic (e.g. botulism). Additionally, particular disorders of the NM system target MNs directly, causing presynaptic signal transmission deficiency, such as amyotrophic lateral sclerosis (ALS) or spinal muscular atrophy (SMA). There are also nine major forms of muscular dystrophy (i.e. myotonic, Duchenne, Becker, limb-girdle, facioscapulohumeral, congenital, oculopharyngeal, distal, Emery-Dreifuss) that attack the postsynaptic SkM MEP. The peripheral nerve is also venerable to MN disorders that impair myelination, for instance, Charcot-Marie-Tooth disease.

The NMJ shares many fundamental similarities with chemical synapses located throughout the central and peripheral nervous system. The presynaptic MNT of the NMJ is occupied by vesicles containing the neurotransmitter acetylcholine (ACh). The synaptic cleft, which has a width of ~50-80 nm, separates the presynaptic terminal from the postsynaptic SkMC sarcolemma. The MEP has deep indentations called junctional folds that are saturated with AChRs; the binding of ACh with AChRs opens voltage-gated sodium channels. The diffusion of sodium ions (Na^+) into the sarcoplasm depolarises the MEP at the junctional folds, triggering an AP on the flanking sarcolemma, which spreads outward from the NMJ (Flucher and Daniels, 1989).

The basal lamina and ECM coating SkM fibres has a unique muscle specific composition, comprised of molecules derived from the SkMCs. Correspondingly, the ECM components at the synaptic cleft have their own unique molecular constituents, as secreted molecules at the cleft are derived from the SkMCs and MNs (Patton et al., 1997). Along with SkMCs and MNs, the anatomy of a NMJ *in vivo* consists of two other essential cell types, the terminal Schwann cells and kranocytes. Schwann cells at the NMJ are specialised non-myelinating neuroglia that cover the MNT, generating their own distinctive basal lamina, which interacts with the ECM of SkMCs in close proximity to the NMJ. Finally, the insufficiently understood kranocytes cover the Schwann cells, encasing the entire NMJ (Figure 1.11). Both the terminal Schwann cells and kranocytes help to maintain NMJ stability and regenerative response to injury (Son et al., 1996; Court et al., 2008). For successful transmission of nervous input at the NMJ, an

AP induces Ca^{2+} influx in the MNT. The incoming Ca^{2+} stimulates synaptic vesicles to fuse with the membrane of the MNT at specific locations known as the 'active zones'. The ACh released into the synaptic cleft by the membrane-bound vesicles quickly diffuses across and binds with AChRs on the SkMC. As mentioned, AChRs open voltage-gated sodium channels, but are also permeable to potassium ions (K^+), as well as Ca^{2+} to a degree. The fusion and release of ACh from a single presynaptic vesicle, called quantal release, produces a depolarising current in the SkMC of ~3-4 nA. This small depolarizing quantal release of ACh is known as a miniature endplate current, which is the minimum stimulation that can be sent between neurons. The fusion and release of ACh from a group of membrane-bound vesicles simultaneously produces what is known as the endplate potential (EPP). The EPP is generated when a presynaptic AP causes vesicle release to generate a current that is hundreds of nanoamperes and depolarizes SkMCs by ~30–40 mV. The EPP produced is considerably larger than needed to generate an AP in SkMCs. This greater than that required EPP is called the 'safety factor' and allows NM transmission to remain operative through varying physiological conditions and stressors (Wood and Slater, 2001).

The magnitude of the safety factor is determined by NMJ physiology and morphology. Firstly, the quantity of active zones at the MNT and the density of voltage-gated calcium channels, determined by the size of the MNT. The density of synaptic vesicle fusion upon stimulation of an AP and the amount of ACh released also influence safety factor. The concentration of AChRs found on the postsynaptic SkMC also controls the quantal current amplitude, though in a non-sequential manner, as the concentration of AChRs is usually greater than required for effective commandeering of ACh from the synaptic cleft. Additionally, voltage-gated sodium channels and AChRs on the junctional folds of MEPs orient in a specific manner, with AChRs located at the peak of the fold and sodium channels in the trenches (Flucher and Daniels, 1989). This orientation ensures effective transmission and reliable initiation of the AP in the sarcolemma (Slater, 2008).

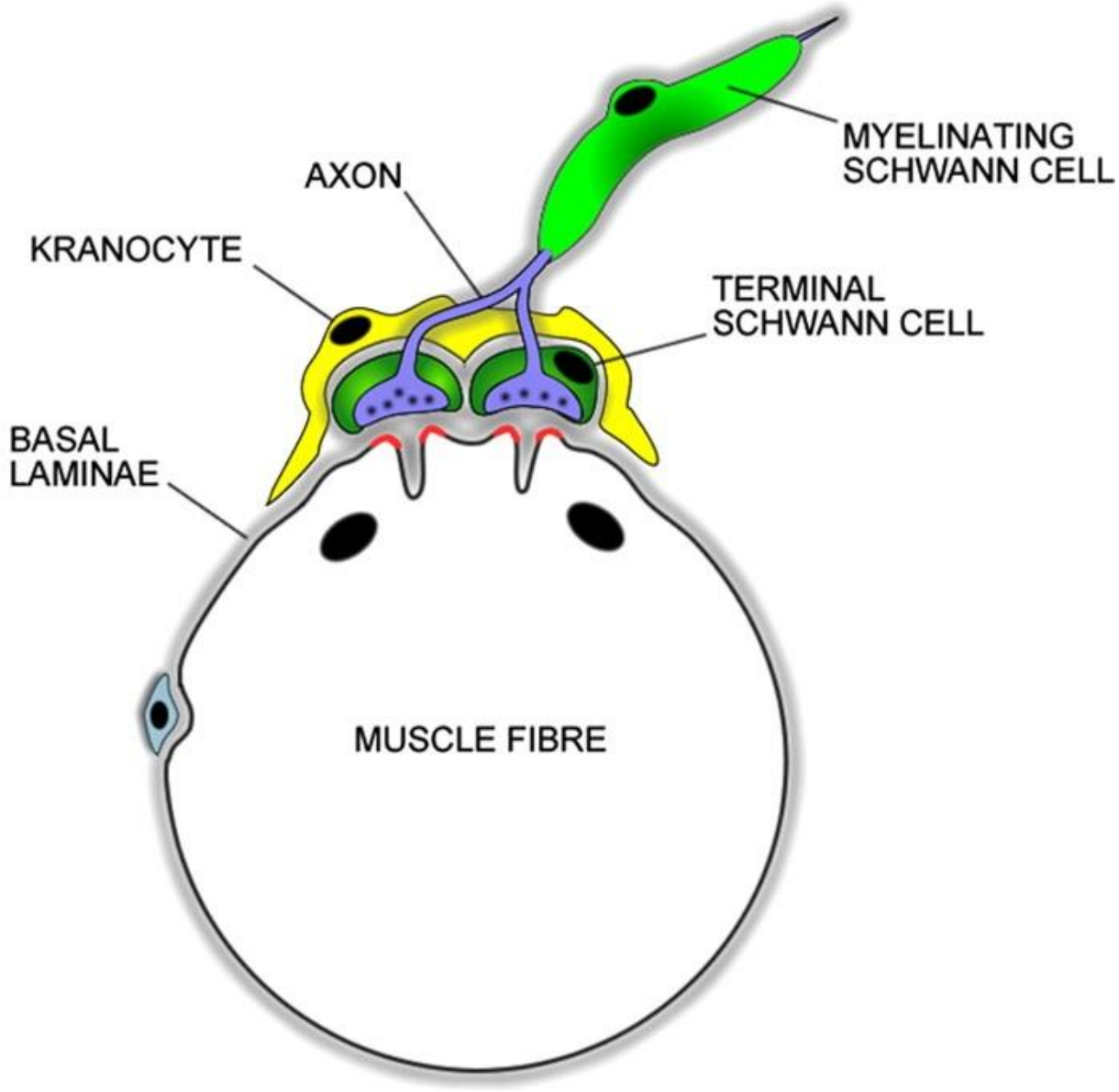

Figure 1.11: Cells comprising the neuromuscular Junction. The anatomy of the *in vivo* NMJs is comprised of the four main cell types. Motor neurons, muscle fibres, terminal Schwann cells and kranocytes. Adapted from (Court et al., 2008)

1.4 Aims and Objectives

In this introduction, many studies were used to detail the *in vivo* formation and development of NMJs, as well as SkM and the contribution of MNs toward synapse formation. By examining the current literature, it is clear that the existing methods to study how degenerated NMJs contribute to NM diseases are limited. Accordingly, most *in vivo* NMJ animal models do not properly reflect disease in humans. Thus, *in vitro* models of NMJs have the potential to elucidate NM disease pathogenesis and provide a platform for testing novel therapies. Previously established *in vitro* NMJ models suffer from a variety of limitations, due to the complex nature of the systems, resulting in inadequate experimental reproducibility. The limitations of the existing *in vitro* NMJ models will be explored in detail in the forthcoming chapters.

Thus, the primary **aim** of this project is to establish viable *in vitro* nerve-muscle co-cultures that generate functional NMJs, providing a practical system for the examination of NMJ formation, development, maturation, and functionality.

The main **objectives** are:

1. Develop and optimise cell culture conditions to compare young (25 years old) and old (83 years old) immortalised human SkMC lines.

2. Generate and optimise methods for a co-culture of human SkMCs innervated by nerve cells obtained from wild-type rat embryos at embryonic development day (ED) 13-14.

3. Use immunofluorescence and confocal microscopy to confirm SkMC innervation and NMJ formation via staining of pre- and post-synaptic proteins.

4. Use the application of known agonist and antagonists treatments to determine NMJ functionality via regulation of innervated SkMC contractions.

5. Use microarray analysis to identify the concentrations of endogenously generated growth and neurotrophic factors during NMJ formation and development.

Chapter 2: Materials and Methods

2.0 Materials

2.0.0 Cell Lines

The two immortalised human skeletal muscle cell (SkMC) lines used for this project were generated at the Institute of Myology (Paris, France) and provided to our research group. Both young and old SkMC lines were established using primary human myoblasts obtained anonymously from Myobank, a tissue bank affiliate of Eurobiobank, authorised by the French Ministry of Research (authorisation # AC-2013-1868). The primary myoblasts originated from biopsies of the semitendinosus muscle of a young 25-year-old male and an old 83-year-old man, both free of genetic defects and disease. Myoblast immortalisation was achieved through cyclin-dependent and telomerase-expressing kinase 4-expressing vector transduction (Mamchaoui et al., 2011). This project was the first use of these cells by our research group, meaning these cell lines were previously unestablished in our laboratory. Accordingly, training of cell culture techniques for the two cell lines used in this project was completed at the Institute of Myology.

2.0.1 Animals

Ethical approval for the animal work was obtained from the animal facility under a general S1 Home Office licence at the University of Manchester. Animal welfare was in accordance with the guidelines detailed in the Animals Scientific Procedures Act 1986, which regulates the use of living vertebrates and cephalopods in scientific procedures within the UK. Time-mated female Sprague Dawley rats obtained from Charles River Laboratories (Oxford, UK) were sacrificed with CO_2 when embryos were approximately embryonic development day (ED) 13.5.

2.0.2 Laboratory Equipment

Equipment	Company	Catalogue #
3-16KL refrigerated benchtop centrifuge	Sigma Laborzentrifugen	10360
appJET pipette controller	Appleton	AEL540
Axiovert 40 C inverted phase contrast microscope	Zeiss	MIC-990-130D
Axon Instruments GenePix 4000B microarray scanner	Molecular Devices	GENEPIX 4000B-U
BVC control, fluid aspiration system with VacuuHandControl VHC^{pro}	Vacuubrand	727202
Hausser Bright-Line 3100 haemocytometer	Hausser Scientific	3110
JB Nova unstirred water bath	Grant	JBN12
LabGard NU-437 class II, type A2 biosafety cabinet	Nuaire	NU-437-400E
Leica DMI6000 B inverted fluorescence microscope	Leica Microsystems	DMI6000B
Leica TCS SP5 confocal microscope	Leica Microsystems	TCSSP5
M3B stereomicroscope	Wild Heerbrugg	1171
MTS 2/4 digital microtiter shaker	IKA	0003208002
NU-5100E air-jacketed automatic CO_2 incubator	Nuaire	NU5100E
Omni tissue homogenizer (TH) package	Omni International	THP220
Synergy HT microplate reader	BioTek	7091000

2.0.3 Laboratory Plasticware

Plasticware	Company	Catalogue #
µ-Dish 35 mm, high glass bottom, D 263® M Schott glass	Ibidi	81158
CRYO.S™ 1 mL, conical bottom internal thread, polypropylene (Cryovial)	Greiner Bio-One	123278
EasYFlask™ 175 cm^2, polystyrene (T175)	Nunc	159910
Microlance™ 3 hypodermic needles 21G x 1.5” (0,8 x 40 mm)	Becton Dickinson	304432
Nalgene® Mr. Frosty™ freezing container	Thermo Scientific	5100-0001
Nunclon™ 6-well x 3mL MultiDish cell culture dish, polystyrene	Nunc	140675
Nunclon™ Delta Surface, petri dish with lid, 150 x 20mm, polystyrene	Nunc	168381
Sterilin™ Sterile sample container – 100 mL, polystyrene	Thermo Scientific	185BM
Tube 15 mL, 120x17mm, polypropylene	Sarstedt	62.554.001
Tube 50 mL, 115x28mm, polypropylene	Sarstedt	62.559

2.0.4 Reagents

Reagent	Company	Catalogue #
(+)-Tubocurarine chloride pentahydrate	Sigma-Aldrich	93750
1(S),9(R)-(−)-Bicuculline methiodide (Bicuculline)	Sigma-Aldrich	14343
4',6-Diamidine-2'-phenylindole dihydrochloride (DAPI)	Sigma-Aldrich	10236276001
Anti-calcium channel L type DHPR alpha 2 subunit antibody [20A] (DHPR)	Abcam	ab2864
Anti-choline acetyltransferase (ChAT)	Sigma-Aldrich	AB144
Anti-glial fibrillary acidic protein (GFAP)	Sigma-Aldrich	G3893
Anti-MUSK antibody (MuSK)	Abcam	ab92950
Anti-neurofilament H antibody (NFH)	Sigma-Aldrich	AB5539
Anti-rapsyn antibody [1234] (rapsyn)	Abcam	ab11423
Anti-ryanodine receptor 1 antibody (RyR)	Sigma-Aldrich	AB9078
Anti-synaptotagmin antibody [ASV30] (Syt1)	Abcam	ab13259
Anti-vesicular acetylcholine transporter (VAChT)	Sigma-Aldrich	ABN100
Beta-3 tubulin monoclonal antibody (2G10-TB3), Alexa Fluor® 488	eBioscience	53-4510-82
Dexamethasone	Sigma-Aldrich	D4902
Dimethyl sulfoxide (DMSO)	Fisher BioReagents	10103483
Donkey anti-goat IgG (H+L) cross-adsorbed secondary antibody, Alexa Fluor® 568	Invitrogen	A-11057
Donkey serum (DS)	Sigma-Aldrich	D9663
Dulbecco's modified eagle medium (DMEM)	Lonza	12-914F
Dulbecco's phosphate buffered saline 1X (DPBS)	Lonza	17-512F
Fetuin from fetal bovine serum	Sigma-Aldrich	F3004
Gelatin from porcine skin, type A	Sigma-Aldrich	G2500
Gentamicin	Gibco	15710-049
Goat anti-chicken IgY (H+L) cross-adsorbed secondary antibody, DyLight® 488	Invitrogen	SA5-10070
Goat anti-Mouse IgG (H+L) Cross-Adsorbed Secondary Antibody, Alexa Fluor® 555	Invitrogen	A-21422
Goat anti-rabbit IgG (H+L) cross-adsorbed secondary antibody, Alexa Fluor® 568	Invitrogen	A-11011
Goat serum (GS)	Sigma-Aldrich	G9023
Hanks' balanced salt solution w/ calcium, magnesium (HBSS)	Gibco	24020117
Heat-inactivated fetal bovine serum (FBS)	Gibco	10500-064
Horse serum (HS)	Sigma-Aldrich	H0146
Human recombinant basic fibroblast growth factor (FGFb)	Gibco	PHG0026
Human recombinant epidermal growth factor (EGF)	Gibco	PHG0311
Human recombinant hepatocyte growth factor (HGF)	Sino Biological Inc.	10463-HNAS
Human recombinant insulin	Sigma-Aldrich	91077C
L-Glutamic acid (L-Glut)	Sigma-Aldrich	G1251
L-glutamine	Lonza	17-605E
Matrigel® growth factor reduced basement membrane matrix, *LDEV-free	Corning	354230
Medium 199 with Earle's balanced salt solution	Lonza	12-119F
Myosin 4 monoclonal antibody (MF20), Alexa Fluor® 488 (anti-MHC)	eBioscience	53-6503-82
Paraformaldehyde	Sigma-Aldrich	P6148
Penicillin-streptomycin mixture (Pen/Strep)	Lonza	17-602E
Perm/Wash™ buffer (PWB)	BD Biosciences	554723
Plasmocin™ - mycoplasma elimination reagent	InvivoGen	ant-mpp
Quantibody® human growth factor array 1	RayBiotech	QAH-GF-1
Rabbit monoclonal anti-Ki67 antibody [SP6] (Anti-Ki67)	Abcam	ab16667
Rat Agrn / Agrin ELISA kit	Sigma-Aldrich	RAB0881-1KT
Skeletal muscle differentiation medium	PromoCell	C-23061
Texas Red®-X phalloidin	Invitrogen	T7471
Triton™ X-100 (TX100)	Sigma-Aldrich	T8787
Trypan Blue, 0.4% solution	Lonza	17-942E
TrypLE™ express enzyme 1X (TrypLE)	Gibco	12605-028
TWEEN® 20	Sigma-Aldrich	P1379
α-Bungarotoxin, Alexa Fluor™ 647 conjugate (α-BTX)	Invitrogen	B35450
γ-Aminobutyric acid (GABA)	Sigma-Aldrich	A2129

2.1 Methods

2.1.0 Human Skeletal Muscle Cell Culture

All cell culture work was carried out in a class II, type A2 biosafety cabinet, with strict adherence to aseptic techniques and practices. Two cryovials were retrieved from liquid nitrogen storage, each containing ~1x10^6 *25-year-old immortalised human myoblasts (C25)* or *83-year-old immortalised human myoblasts (C83).* The cells were cryopreserved in a 1 mL suspension of 90% fetal bovine serum (FBS) and 10% Dimethyl sulfoxide (DMSO). The frozen vials were placed into a water bath set to 37°C and rapidly thawed within 2 minutes. Subsequently, the thawed myoblasts were transferred into separate 15 mL tubes. Next, 9 mL of pre-prepared complete growth media (GM) (Table 2.0) was added to each tube to initiate myoblast proliferation.

Table 2.0: Complete growth media for skeletal muscle cell proliferation.

Media components	Concentration
Dulbecco's modified eagle medium (DMEM)	59% (v/v)
Medium 199 with Earle's balanced salt solution	19% (v/v)
Fetal bovine serum (FBS)	20% (v/v)
L-glutamine	1% (v/v)
Penicillin-streptomycin mixture (Pen/Strep)	1% (v/v)
Fetuin from fetal bovine serum	25 µg/mL
Basic fibroblast growth factor (FGFb)	0.5 ng/mL
Epidermal growth factor (EGF)	5 ng/mL
Hepatocyte growth factor (HGF)	2.5 ng/mL
insulin	5 µg/mL
Dexamethasone	0.2 µg/mL
Gentamicin	10 µg/mL
Plasmocin	25 µg/mL

The separate 10 mL suspensions of C25 and C83 were transferred into separate T175 flasks. The flasks were positioned onto a levelling plate and incubated at *37°C with a 5% CO^2 atmosphere (ATM),* until the density of cell growth was 80% confluent, which was determined by the percentage of area covered by cells in any random microscopic field of view. Phase contrast microscopy analysis with the Axiovert 40 C and DMI6000B inverted microscopes were used to assess and compare any difference in the percentage of confluence between the two cell lines at 24, 48, 72, and 96 hours. ImageJ, a Java-based image processing application developed at the National Institutes of Health and the Laboratory for Optical and Computational Instrumentation (Madison, WI, USA) (Collins, 2007; Schneider et al., 2012)

was used to quantify confluence at the stated time points by calculating the total myoblast area. Calculated by using the formula < [(total area of myoblasts in a field)/(total area of the field)](100) > (Ren et al., 2008; Ricotti et al., 2011). Ten fields chosen at random were visualized on a DMI6000B inverted microscope with the N Plan 10x/0.25na Ph1 objective.

2.1.1 Cell Count

When the flasks reached 80% confluence, the GM was aspirated and the cells were washed twice with 10 mL of Dulbecco's phosphate buffered saline 1X (DPBS) to remove any GM components that may inhibit the function of disassociation enzymes. The monolayers of cells were then disassociated from the flasks using 2 mL of the highly purified, recombinant cell-dissociation TrypLE express enzyme 1X and incubating at ATM for 5 minutes. The 2 mL of disassociated cell suspensions were pipetted from the flasks into separate 15 mL tubes. The flasks were then separately washed with 8 mL of GM to capture any residual cells that may have remained adherent to the flask after disassociation. The 8 mL of GM was collected from each flask and added to the corresponding 15 mL tube of C25 or C83, which contained the 2 mL of already collect cells. The 8 mL GM, 2 mL TrypPLE cell suspensions of both C25 and C83 were separately mixed by pipetting the cell suspension up and down in the 15 mL tube 5-10 times before aliquoting a sample for cell count. Comparison of total viable cells between C25 and C83 was quantified using established cell count protocols (Phelan and Lawler, 2001). The cells were counted by mixing a 1:1 dilution of cell suspension (50 µL) with Trypan Blue, which labels non-viable cells by penetrating the membrane and dyeing the cell blue, whereas viable cells remained transparent with a white halo around the membrane. The viable cells were counted using established techniques with a haemocytometer (Phelan and Lawler, 2001) viewed with an A-Plan 10x / .25 Ph1 objective on the Axiovert 40C inverted microscope . The number viable cells/mL of cell suspension was determined using the formula: [(Average number of live cells in eight large corner square) (dilution factor) (10^4)]. For example, (50)(2)(10000) = $1x10^6$ cell/mL of suspension, thus a hypothetical 10 mL suspension of harvested cells would yield $1x10^7$ cells . Dependant on experimental demands the counted cell suspension was either sub-cultured, cryopreserved, or seeded on tissue culture surfaces as required.

2.1.2 Subculture

Following cell count, aliquots of cell suspensions containing $1x10^6$ cell were transferred from the tubes of counted cells to new 15 mL tubes. A volume of GM needed to bring the total volume of the suspensions to 10 mL was added to the new 15 mL tubes of cells. Thus, the new cell suspensions of both C25 and C83 would have a concentration of $1x10^5$ cells/mL. The cell suspensions were homogenised with the GM in their respective tubes then pipetted into separate T175 flasks and incubated at ATM until 80% confluent.

2.1.3 Cryopreservation

Large stocks of cells were generated for storage and retrieval for experimental use when required. Both C25 and C83 were continually expanded and sub-cultured as described above to generate cells. Thus, the myoblasts retained a low number of passages to ensure fidelity throughout this project. Following disassociation and cell count (described in 2.1.1), the 10 mL cell suspensions of C25 and C83 were transferred to separate new 50 mL tubes. An equal volume of DPBS was added to the 50 mL tubes, diluting and washing the cells within the suspension. The 50 mL tubes was then centrifuged at 300 x *g* for 10 minutes at 23°C. After centrifuging the cells, the supernatants were aspirated from the tubes, ensuring the pelleted cells remained undisturbed. The required volume of FBS was added to the 50 mL tube to bring the concentration of cells to $1x10^6$ cell/mL, dependant on the cell count before centrifugation. The cell pellet was then thoroughly dispersed and homogenised in the FBS via pipetting the solution up and down in the tube 10-20X. A volume of 900 µL of the FBS cell suspension was pipetted into individual cryovials and 100 µL of DMSO was added to each vial thereafter. Thus, each vial contained ~$1x10^6$ cells suspended in 90% FBS and 10% DMSO. The vials were then placed into a Mr. Frosty freezing container and stored at -80°C for 24 hours. Subsequently, the vials were transferred from the -80°C storage freezer to liquid nitrogen tank for long-term storage at -200°C.

2.1.4 Differentiation Parameters

Following cell count, a quantity of cells was transferred from the 15 mL tubes of counted cells to new 50 mL tubes. The number of cells allocated to the 50 mL tubes was dependent on experimental needs. The volume of GM necessary to dilute the cells to a concentration of $1.5x10^5$ cells/mL was added to the 50 mL tubes in preparation for seeding in tissue culture plates. Before plating the cells, 6-well plates were pre-coated and dried with 1% gelatin solution for 1 hour. Subsequently, 2 mL of the GM cell suspension of both C25 and C83 were separately pipetted into the 6-well plates. Thus, the concentration of cells in each well of a 6-well plate was equal to $3x10^5$ cells or expressed as a density of 315 cells/mm^2. After seeding the cells, the 6-well plates were placed on a levelling plate and incubated for 24 hours at ATM, at which point the cells reached ~90-100% confluence. Following incubation the GM was aspirated from the wells and the cells were washed twice with 1 mL of DPBS. A volume of 2 mL of a simplified complete differentiation media (DM) (Table 2.1) was added to each well and the cells were incubated for 96 hours at ATM.

Table 2.1: Complete differentiation media for immortalised human skeletal muscle cell.

Media components	Concentration
Dulbecco's modified eagle medium (DMEM)	98% (v/v)
L-glutamine	1% (v/v)
Penicillin-streptomycin mixture (Pen/Strep)	1% (v/v)
Insulin	10 µg/mL
Gentamicin	10 µg/mL
Plasmocin	25 µg/mL

Immunofluorescence microscopy were used to determine any difference in the proportional decline of proliferating cells and to assess the phenotypic differentiation (alignment, elongation and fusion) of both the young and old cell lines as they differentiated over 96 hours. The expression of the proliferative marker Ki67 (Schonk et al., 1989; Bullwinkel et al., 2006) and the comparison of differentiation parameters were measured at 24, 48, 72, and 96 hours. At each time-point, the DM was aspirated from the wells and cells were washed twice with 1 mL of DPBS. Cell fixation was then performed by incubating the cells in a 500 µL 4% paraformaldehyde solution for 10 minutes at 23°C. The paraformaldehyde was then aspirated away and the cells were washed thrice with DPBS, followed by cell permeabilisation with a 1X concentration of Prem/Wash buffer (PWB). A volume of 1 mL of PWB was added to each well and then incubated for 30 minutes at 23°C. Once permeabilised the PWB was removed and the cells were washed once with 1 mL of DPBS. Subsequently, 1 mL of pre-prepared

blocking solution consisting of DPBS with 0.2% Triton X-100 (TX100) and 10% goat serum (GS) was added to each well and the cells incubated for 1 hour at 23°C. The blocking solution was then removed in preparation for primary antibody labelling. A 250-µL antibody diluent solution consisting of DPBS, 3% GS, 0.05% TWEEN 20, and anti-Ki67 at a dilution of 1:100 was applied to the cells and incubated for 18-24 hours at 4°C. Next, the primary antibody solution was removed from the wells and the cells were washed thrice with DPBS before the addition of fluorescent-labelled secondary antibody conjugates. The secondary antibody diluent had a volume of 250 µL and consisting of DPBS, 4',6-Diamidine-2'-phenylindole dihydrochloride (DAPI) at a dilution of 1:10000, anti-rabbit Alexa Fluor 568 at a dilution 1:500, anti-myosin heavy chain (MHC) Alexa Fluor 488 at a dilution 1:500, and phalloidin at a dilution 1:500 was applied to the cells and incubated for 30 minutes at 23°C. The stained cells were then washed a final two times with DPBS and maintained in DPBS thereafter for analysis. Visualisation of stained cells was achieved with fluorescence microscopy. ImageJ was used to measure and compare the differentiation parameters (Table 2.2) and quantify the percentage of Ki67 expression between both the young and old cell lines. Ten random fields of view were assessed for each experiment (n = 5) with a HCX PL FLUOTAR L 20X/0.40na CORR objective on the DMI6000B inverted microscope. The data was presented as mean with a ± SD of all the counted fields of view in the total number of experiments conducted.

Table 2.2: Differentiation parameters (Ren et al., 2008; Ricotti et al., 2011; Grubisic et al., 2014)

Differentiation parameters	**Formula**
Myotube area (MA)	[(total area of myotubes in a field)/(total area of the field)](100)
Fusion index (FI)	(total number of nuclei per myotube)/(total number of nuclei in the field)](100)
Aspect ratio (AR)	(myotube length)/(myotube width)

2.1.5 Co-culture

In vitro studies of muscular dysfunction utilising aneurally cultured SkMCs are limited by the lack of a nerve component, resulting in limited differentiation and non-contractile myotubes (Delaporte et al., 1986). For a valid reflection of physiological conditions found *in vivo,* SkMCs require MN stimulation. Accordingly, to overcome the limitations of aneurally cultured SkMCs a novel co-culture model was successfully established where functional innervation of myotubes was achieved using spinal cord explants (SCEs) from rat embryos (Figure 2.0).

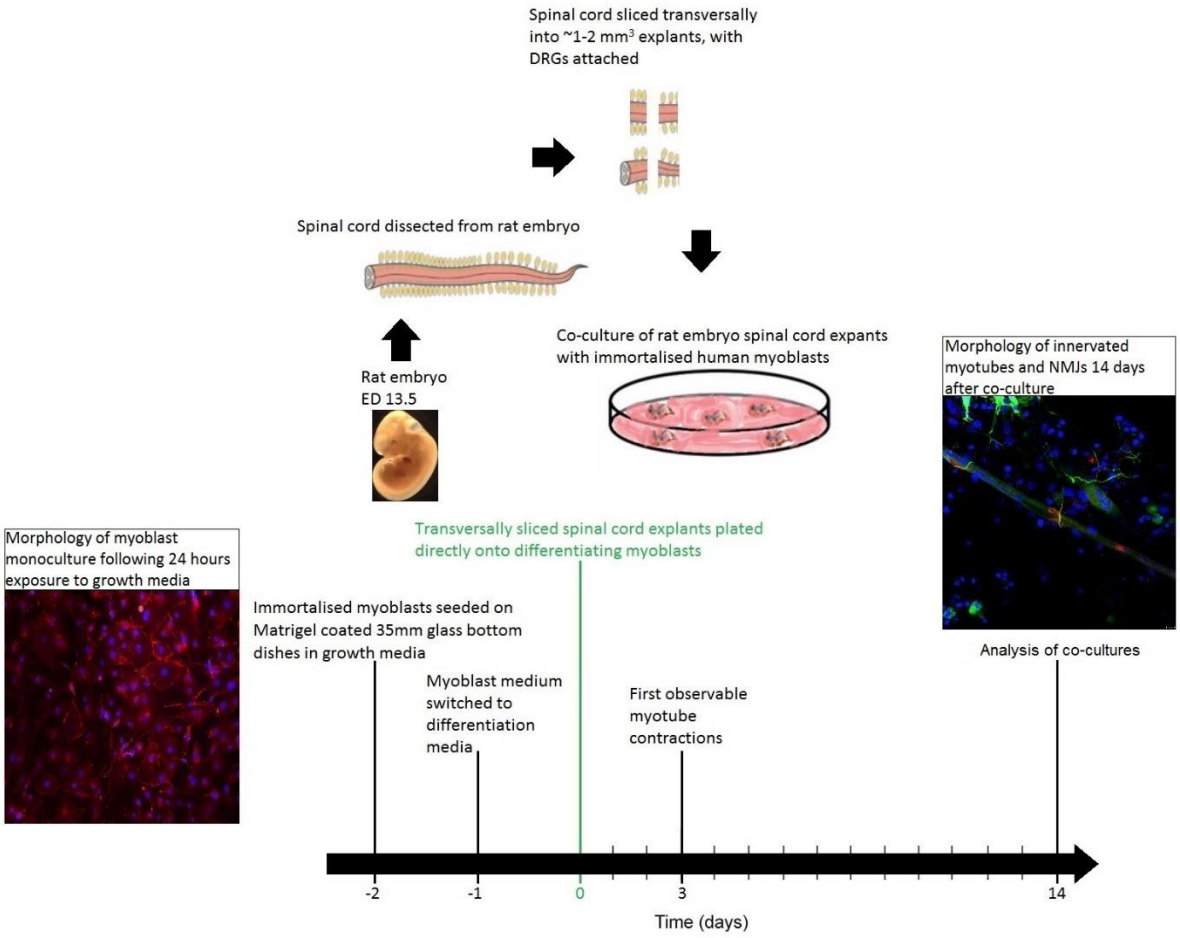

Figure 2.0: Timeline of human immortalised myoblasts co-cultured with rat embryo spinal cord explants. The time course of co-cultured cells is expressed in days, respective to plating of spinal cord explants with differentiating myoblasts. The first spontaneous myotube contractions were observed ~72 hours post co-culture. The co-cultures were characterised and functionally assessed on Day 14 post co-culture. Dorsal root ganglions (DRGs); embryonic development day (ED 13.5).

2.1.6 Isolation of Rat Embryo Spinal Cord

The uterine horn was dissected and removed from the sacrificed pregnant rat and transferred to a sterile sample collection container, containing Hanks' balanced salt solution (HBSS) with 10% FBS. Embryo dissection was carried out under sterile conditions in a biosafety cabinet using a stereomicroscope. The uterine horn was transferred to a 150 mm dish and saturated with HBSS plus 10% FBS. The embryos were individually cleaved from the uterine horn and transferred to a new 150 mm dish where they were dissected under a stereoscopic microscope using two sterile 40 mm 21-gauge hypodermic needles. The embryos were first decapitated, and then the spinal cord was dissected away from the main body as one piece. The surrounding connective tissue was removed from the spinal cord, ensuring the dorsal root ganglions (DRGs) remain attached. Following removal of connective tissue, the isolated spinal cord was transversally sliced into ~1-2 mm^3 explants and transferred to a 15 mL tube containing HBSS until ready for plating with SkMCs.

2.1.7 Preparation of Skeletal Muscle Cells for Co-culture

Preceding co-culture, 25-year-old immortalised human myoblasts (C25) were disassociated from a pre-incubated T175 flask and counted (as described in 2.1.1). The cells were then diluted to the desired concentration of $1.5x10^5$ cells/mL in GM. The cells were seeded at a density of 315 cells/mm^2 by adding 2 mL of GM cell suspension onto 35 mm glass bottom dishes, which were pre-coated for 1 hour with a 1 mL solution of DPBS supplemented with 100 µL of growth factor reduced Matrigel. The dishes were then incubated for 24 hours at ATM, at which time they reached 90-100% confluence. Following incubation, the GM was aspirated and the dishes washed twice with 1 mL of DPBS before the addition of 2 mL of DM to each dish. The dishes were then incubated for 24 hours at ATM before adding rat embryo SCEs.

2.1.8 Innervation of Skeletal Muscle with Embryonic Rat Motor Neurons

Following 24 hours of incubation with DM, the SkMCs were primed for innervation as they were in the initial phases of differentiation, transitioning from myoblast to myocyte, before substantial cell fusion and myotube formation occurred. The DM was removed from the dishes and the cells were washed twice with 1 mL of DPBS. Then, 750 µL of DM was added to each dish, thinly coating the cells on the glass bottom. Between three and six evenly spaced embryonic rat SCEs were placed into each dish then

incubated for 6 hour at ATM to allow the explants time to adhere with the SkMCs. Following incubation, the SCEs become slightly affixed to the SkMCs, at which time an additional 250 µL of DM was added dropwise to each dish to prevent dehydration of the SkMCs and the SCEs. However, adding too much DM too quickly or forcefully would not allow the SCEs to remain adherent to the SkMCs, causing SCEs to float. The dishes were then incubated for an additional 24 hours at ATM to reinforce unification of SCEs with the SkMCs before adding a further 1 ml of DM to each dish, bringing the total volume of DM in the dishes to 2 mL. Notably, the SCEs must be plated on the SkMCs after the SkMCs have been exposed to DM for 24 hours. As myoblasts fuse into immature myotube between 24 and 48 hours, sprouting neurites from the SCEs innervate the fusing myotubes at this stage of development. The co-cultures were maintained by changing half the DM every 72 hours and incubating at ATM. Live cell visualisation and real-time myotube contractions were video-captured at 24 frames per second with HCX PL FLUOTAR L 20X/0.40na CORR objective on a DMI6000 B inverted microscope.

2.1.9 Differentiation Parameters: Co-culture

In parallel experiments were conducted to compare the differentiation parameters (Table 2.2) of both aneurally cultured and co-cultured myotubes. Preceding assessment of phenotypic differentiation, aneurally cultured myoblasts were seeded and differentiated as described in 2.1.4, while co-cultured myoblasts were prepared for analysis as described in 2.1.7. The differentiation parameters were assessed at 72 hours, when spontaneous myotube contractions were first observed in the co-cultured myotubes. Phase contrast microscopy with a Leica DMI6000 B inverted microscope and the ImageJ image processing software package were used to quantify the differentiation parameters. Ten random fields of view were assessed with the N Plan 10x/0.25na Ph1 objective for each experiment (n = 3). The data was presented as a mean ± SD of the total number of fields observed in all experiments conducted.

2.1.10 Disassociation of Rat Embryo Spinal Cord

The efficacy of SCEs to induce myotube contractions and modulate contraction frequency (CF) was compared against myoblasts co-cultured with a disassociated rat embryonic spinal cord cell suspension. The spinal cord cell suspension was prepared by isolating spinal cords from ED 13.5 rat embryos as described in 2.1.6. Individually isolated intact spinal cords were transferred into 15 mL tubes containing 2 mL of DM. The spinal cord was then mechanically disassociated with a tissue homogenizer to generate a 2 mL cell solution of rat embryonic spinal cord cells suspended in DM. Young human immortalised

myoblasts were prepared for co-culture as described in 2.1.7. Following 24 of incubation with DM, the pre-plated myoblasts were co-cultured with SCEs as described in 2.1.8 or they were co-cultured with the 2 mL spinal cord cell suspension. The co-cultured myotubes were observed every 24 hours for 7 days to compare the initiation and frequency of contractions among the two culture conditions. The co-cultured cell dishes were positioned onto an inverted microscope stage, which was enclosed by an incubation chamber to maintain atmospheric conditions of 37°C with 5% CO_2. Worth mentioning, maintaining these conditions during assessment was vital to ensure persistent spontaneous myotube contractions, as fluctuations in temperature and atmospheric composition significantly influence spontaneous myotube contractions frequency. Following 5 minutes of live observation of uninterrupted spontaneous myotube contractile activity, live video analysis was conducted at 24 frames per second with phase contrast microscopy using the DMI6000 B inverted microscope with an N Plan 10x/0.25na Ph1 objective. Myotube CF was expressed as a mean ± SD.

2.1.11 Rat agrin ELISA

In parallel experiments were conducted to compare the concentration of agrin in aneural myotube cultures, co-cultured myotubes, and SCE only cultures. Both aneural and co-cultured myoblasts were prepared, seeded, and differentiated for 72 hours as described in 2.1.4 and 2.1.7. Similar to co-cultures, SCEs only were prepared and plated in 6-well plates pre-coated with a 1% gelatin solution and cultured in 2 mL of SkMC DM for 72 hours. Supernatant samples were collected from the three culture conditions for assessment using a rat agrin ELISA kit at 72 hour, when spontaneous myotube contractions were first observed in the co-cultured myotubes. Preparation of standards and reagents in the ELISA kit were completed using manufacturer guidelines. Subsequently 100 µl of standards, controls and supernatant samples were added to individually assigned wells of the agrin antibody-coated ELISA plate. The plate was then sealed to protect from light and incubated for 24 hours at 4°C on microplate shaker fixed to 500 rpm. After incubation, the wells were aspirated and the ELISA plate was washed four times with 300 µl of wash buffer, followed by inverting the plate and blotting it against clean paper towels to remove all residual wash buffer. Next, 100 µl of 1X biotinylated rat agrin detection antibody was added to all wells and the plate sealed. The detection antibody was incubated with the samples at 23°C for 1 hour on a plate shaker set to 500 rpm. Following incubation, the wells were washed four times with 300 µl of wash buffer then 100 µl of 1X HRP-Streptavidin solution was added to each well. The plate was sealed and incubated once more at 23°C for 45 minutes on a plate shaker set to 500 rpm. Following incubation, the plate was washed again four times with 300 µl of wash buffer. A volume of 100 µl of ELISA colorimetric TMB reagent was then added to each well before a final

darkened incubation for 30 minutes on the plate shaker set to 500 rpm at 23°C. Subsequently, 50 µl of stop solution was added to the wells and absorbance read immediately at 450 nm on the Synergy HT microplate reader.

2.1.12 Co-culture Fixation

The co-cultured cells were fixed in their dishes for analysis and characterisation on Day 14 post co-culture, which was 11 days after persistent spontaneous myotube contractions, though it was possible to maintain co-cultures beyond 30 days with regular media changes as described in 2.1.8. The DM was aspirated from the dishes and the cells washed thrice with 500 µL of DPBS. The cells were then incubated with a 4% paraformaldehyde solution for 12 minutes at 23°C. The paraformaldehyde was then removed from the dishes and the cells washed thrice with 500 µL of DPBS. The fixed cells were then stored in a DPBS solution for up to 7 days at 4°C. Alternatively, immunocytochemistry (ICC) was immediately performed for the evaluation and characterisation of pre- and post-synaptic components of neuromuscular junction (NMJ) formation in the co-culture model.

2.1.13 Co-culture Immunocytochemistry

After fixation of co-cultured cells, the cells were incubated with 500 µL of a 1X concentration of PWB for 30 minutes at 23°C to permeabilise the cells. Once permeabilised, the PWB was removed from the dishes and the cells washed twice with 500 µL of DPBS. A 500-µL volume of blocking solution consisting of 0.2% TX100 with 10% GS or donkey serum (DS) was applied to the cells and then incubated for 1 hour at 23°C, to block unspecific binding of antibodies. The blocking solution was removed after incubation and the cells washed once with 500 µL DPBS. A volume of 250 µL of primary antibody diluent consisting DPBS, 3% GS or DS, 0.05% TWEEN 20, and the primary antibodies (Table 2.3) was added to the cells and incubated for 18-24 hours at 4°C.

Table 2.3: Primary antibodies for co-culture.

Antibody	Concentration
Anti-calcium channel L type DHPR alpha 2 subunit (DHPR)	1:100
Anti-choline acetyltransferase (ChAT)	1:100
Anti-glial fibrillary acidic protein (GFAP)	1:100
Anti-muscle-specific kinase (MuSK)	1:100
Anti-neurofilament H (NFH)	1:100
Anti-receptor associated protein of the synapse (rapsyn)	1:100
Anti-ryanodine receptor 1 (RyR)	1:100
Anti-synaptotagmin (Syt1)	1:100
Anti-vesicular acetylcholine transporter (VAChT)	1:100

Following primary antibody incubation, the diluent was aspirated from the dishes and the cells were washed thrice with 500 µL of DPBS prior to adding the fluorescent-labelled secondary antibodies. A secondary antibody diluent consisting of 250 µL DPBS supplemented with DAPI at a dilution of 1:10000 and the corresponding secondary antibodies (Table 2.4) was added to each dish and incubated in darkness for 30 minutes at 23°C. The secondary antibodies were aspirated from the dishes and the stained cells were washed a final two times with 500 µL of DPBS and maintained in 1 mL of DPBS during analysis. Confirmation of myotube innervation and characterisation of NMJ formation was conducted with confocal and immunofluorescence microscopy using a Leica DMI6000 B inverted microscope with HCX PL FLUOTAR L 20X/0.40na CORR and N Plan 10x/0.25na Ph1 objectives; and a Leica TCS SP5 confocal microscope with HCX PL APO 40x 1.25-0.75 Oil CS ∞ and HCX PL APO 63x 1.40-0.60 oil CS ∞ objectives.

Table 2.4: Secondary antibodies for co-culture.

Antibody	Concentration
Anti-β-3-tubulin Alexa Fluor® 488 conjugate	1:400
Anti-chicken IgY DyLight® 488	1:400
Anti-goat IgG Alexa Fluor® 568	1:400
Anti-MHC Alexa Fluor® 488 conjugate	1:400
Anti-mouse IgG Alexa Fluor® 555	1:400
Anti-rabbit IgG Alexa Fluor® 488	1:400
Anti-rabbit IgG Alexa Fluor® 568	1:400
α-BTX Alexa Fluor® 647 conjugate	1:400

2.1.14 Quantification of Neuromuscular Junction Morphologies

In parallel experiments were conducted to compare the development of NMJ morphologies in co-cultured cells in contrast to aneurally cultured myotubes. Innervated and aneural cultures were differentiated, fixed, and stained on Day 14 post co-culture with α-bungarotoxin (α-BTX) and DAPI using the methods and concentrations detailed above. Distinctive NMJ morphologies were quantified into five previously established NMJ morphology development classifications (Valdez et al., 2010; Lee et al., 2013; Kummer et al., 2004; Sahashi et al., 2012). Specifically, NMJ morphology was classified as mature, fragmented, faint, premature or denervated. For each experiment (n = 4), individual wells were observed to assess twenty random fields of view for each morphological classification using the Leica TCS SP5 confocal microscope with a HCX PL APO 40x 1.25-0.75 Oil CS ∞ objective. For example, twenty fields from twenty different wells where assessed to determine the percentage of mature NMJs only, a different twenty fields from an alternative twenty wells where assessed to determine the percentage of fragmented NMJs only, until all classification were counted. The data was presented as a mean ± SD of the total number of all fields observed in all experiments conducted. A minimum of 100 NMJs was counted for each morphological classification over all experiments.

2.1.15 Quantification of Transversal Triad Formation

In parallel experiments were conducted to compare the development of transversal triads between co-cultured and anural myotubes. Innervated and aneural cultures were differentiated, fixed, and stained on Day 14 post co-culture for dihydropyridine receptors (DHPR), ryanodine receptors (RyR) and DAPI using the methods and concentrations detailed in 2.1.13. Myotubes were considered to have appropriate transversal triad formation, which is an indicator of advanced differentiation, when DHPR

and RyR staining was organised in an alternating sequence on a minimum of 50% of the myotubes length. In each experiment (n = 3), twenty random fields of view from five different plates were assessed using a Leica TCS SP5 confocal microscope with a HCX PL APO 63x 1.40-0.60 oil CS ∞ objective, to determine the percentage of myotubes displaying transversal triads. The data from all experiments was totalled and used to calculate the mean percentage ± SD.

2.1.16 Quantification of Peripheral Myonuclei

In parallel experiments were conducted to compare the positon of myonuclei in co-cultured myotubes as opposed to aneurally cultured myotubes, as peripherally located myonuclei are indicators of advanced differentiation. Innervated and aneural cultures were differentiated, fixed, and stained on Day 14 post co-culture for anti-MHC and DAPI using the methods and concentrations detailed in 2.1.13. Myonuclei were considered as peripherally situated if they were observed protruding the myotube membrane. In each experiment (n = 3), twenty random fields of view from five different plates were assessed using a Leica TCS SP5 confocal microscope with a HCX PL APO 40x 1.25-0.75 oil CS ∞ objective, to determine the percentage of myotubes displaying peripherally located myonuclei. The data from all experiments was totalled and used to calculate the mean percentage ± SD.

2.1.17 Quantification of Striation Formation

In parallel experiments were conducted to compare the striated myotubes in co-culture against aneurally cultured myotubes, as striations are indicators of advanced differentiation. Innervated and aneural cultures were differentiated, fixed, and stained on Day 14 post co-culture for anti-MHC and DAPI using the methods and concentrations detailed in 2.1.13. Myotubes were considered as striated if MHC expression was arranged as alternating banding on a minimum of 50% of the myotubes length. In each experiment (n = 3), twenty random fields of view from five different plates were assessed using a Leica TCS SP5 confocal microscope with a HCX PL APO 40x 1.25-0.75 oil CS ∞ objective, to determine the percentage of myotubes with striation formation. The data from all experiments was totalled and used to calculate the mean percentage ± SD.

2.1.18 Quantification of Myotube Thickness

In parallel experiments were conducted to compare the thickness of myotubes in co-culture to aneurally cultured myotubes. Innervated and aneural cultures were differentiated, fixed, and stained on Day 14 post co-culture for anti-MHC and DAPI using the methods and concentrations detailed in 2.1.13. Phase contrast microscopy with a Leica DMI6000 B inverted microscope and the ImageJ image processing software package were used to quantify the myotube thickness. In each experiment (n = 3), twenty random fields of view from five different plates were assessed using the HCX PL FLUOTAR L 20X/0.40na CORR objective, to measure and compare the thickness of innervated and aneural myotubes. The data from all experiments was totalled and used to calculate the mean myotube thickness ± SD.

2.1.19 NMJ Functionality Assessed via Measuring Spontaneous Contractions

Co-cultures were functionally evaluated to validate the formation NMJs via live phase contrast video analysis of myotube CF in response to agonist/antagonist treatments (Table 2.5). On Day 14, the co-cultured cell dishes were positioned onto an inverted microscope stage, which was enclosed by an incubation chamber to maintain atmospheric conditions of 37°C with 5% CO_2. Following 5 minutes of live observation of uninterrupted spontaneous myotube contractile activity, the co-cultures were treated with cholinergic antagonists to block AChRs at the NMJ.

Table 2.5: Treatments to inhibit or augment myotube contraction frequency via NMJ signal transmission.

Drug	Concentration
1(S),9(R)-(−)-Bicuculline methiodide	10 µM
γ-Aminobutyric acid (GABA)	1 mM
L-Glutamic acid (L-Glut)	400 µM
(+)-Tubocurarine chloride pentahydrate	8 µM
α-Bungarotoxin (α-BTX)	1:400

The co-cultures were also treated with the glutamatergic and γ-aminobutyric acid (GABA) receptor agonists to stimulate glutamate and GABA receptors on the motor neurons (MNs). The specified concentrations where selected based on previously established studies (Das et al., 2007; Guo et al., 2011; Morimoto et al., 2013; Borodinsky and Spitzer, 2007). The myotube CF was measured 30 seconds before the application of the treatments to the cells, to establish a baseline spontaneous CF.

Subsequently, agonist or antagonist treatments were added to the dishes at the centre of the field of view. Modulation of CF was measured immediately upon application of the treatment to the cells. Live measurement of CF in response to treatment were also conducted again after 1 minute, 2 minutes, 5 minutes, 10 minutes, 30 minutes and 1 hour. Following 1 hour after treatment, the cells were washed thrice with 500 µL of DPBS then fresh untreated DM was added to the cells. The dishes were placed back onto the microscope stage in the incubation chamber and CF was immediately measured again following the washout and resupply of DM. The CF was measured once again at 1 hour 30 minutes and 24 hours after the initial treatments. In each experiment (n = 5), live video analysis of twenty random fields from one 6-well plate was conducted at 24 frames per second with phase contrast microscopy using the DMI6000 B inverted microscope with an N Plan 10x/0.25na Ph1 objective. The data from all experiments was totalled and used to calculate the myotube CF, which was expressed as a mean of all experiments ± SD.

2.1.20 Human Growth Factor Array

In parallel experiments were conducted to compare the concentration of 40 human growth factors (Table 2.6) in aneural myotube cultures and co-cultured myotubes. Both aneural and co-cultured myoblasts were prepared, seeded, and differentiated for 7 days as described above. Supernatant samples were collected from both conditions for assessment using a human growth factor array kit on day 7, when spontaneous myotube contractions were first observed contracting in unison as a motor unit. Preparation of standards and reagents in the array kit were completed using manufacturer guidelines. Subsequently, 100 µl of sample diluent from the array kit was added to each well and incubated at 23°C for 30 minutes to block slides. The wells were then decanted and 100 µl of standards, controls and supernatant samples were added to the individually assigned wells. The slides were sealed and incubated for 24 hours at 4°C on microplate shaker fixed to 500 rpm. Following incubation, the samples were decanted from the wells and the slides were washed 5 times for 5 minutes each time with 150 µl of 1X wash buffer 1, then washed 2 times for 5 minutes each time with 150 µl of 1X wash buffer 2. Next, 80 µl of detection antibody cocktail was added to each well and the slides incubated for 1.5 hours at 23°C. The detection antibody cocktail was aspirated from the wells and the wash steps with wash buffer 1 and wash buffer 2 were repeated once again. After washing slides, 80 µl of Cy3 equivalent dye-conjugated streptavidin was added to each well then sealed and incubated in darkness for 1 hour at 23°C. Following incubation, the wash steps were repeated once again. The slides were then separated from the well gaskets and placed into the provided slide washer/dryer tube. The tube was then filled with 30 mL of 1X wash buffer 1 to completely cover the slides and shaken gently for 15

minutes. The 1X wash buffer 1 was removed from the tube and 30 mL of 1X wash buffer 2 was added to completely cover the slides and gently shaken for 5 minutes. The slides were removed from the washer/dryer tube and dried with compressed air to remove residual buffer solution. Subsequently, the array was visualised with a GenePix 4000B laser scanner at 532nm wavelength. Raw data from the visualised array images was generated and processed with the GenePix Pro 4.1 Microarray Acquisition & Analysis Software, further statistical analysis of the data was performed with the RayBiotech Q-Analyzer® tool Software for QAH-GF-1.

Table 2.6: Descriptions of the human growth factors and neurotrophins quantified in aneural myotube cultures and co-cultured myotube supernatant.

Amphiregulin (AR) (Colorectum cell-derived growth factor) (CRDGF)
Brain-derived neurotrophic factor (BDNF) (Abrineurin)
Fibroblast growth factor 2 (FGF-2) (Basic fibroblast growth factor) (bFGF) (Heparin-binding growth factor 2) (HBGF-2)
Bone morphogenetic protein 4 (BMP-4) (Bone morphogenetic protein 2B) (BMP-2B)
Bone morphogenetic protein 5 (BMP-5)
Bone morphogenetic protein 7 (BMP-7) (Osteogenic protein 1) (OP-1) (Eptotermin alfa)
Beta-nerve growth factor (Beta-NGF)
Pro-epidermal growth factor (EGF) [Cleaved into: Epidermal growth factor (Urogastrone)]
Epidermal growth factor receptor (EC 2.7.10.1) (Proto-oncogene c-ErbB-1) (Receptor tyrosine-protein kinase erbB-1)
Prokineticin-1 (Endocrine-gland-derived vascular endothelial growth factor) (EG-VEGF) (Mambakine)
Fibroblast growth factor 4 (FGF-4) (Heparin secretory-transforming protein 1) (HST) (HST-1) (HSTF-1) (Heparin-binding growth factor 4) (HBGF-4) (Transforming protein KS3)
Fibroblast growth factor 7 (FGF-7) (Heparin-binding growth factor 7) (HBGF-7) (Keratinocyte growth factor)
Growth/differentiation factor 15 (GDF-15) (Macrophage inhibitory cytokine 1) (MIC-1) (NSAID-activated gene 1 protein) (NAG-1) (NSAID-regulated gene 1 protein) (NRG-1)
Glial cell line-derived neurotrophic factor (hGDNF) (Astrocyte-derived trophic factor) (ATF)
Somatotropin (Growth hormone) (GH) (GH-N) (Growth hormone 1) (Pituitary growth hormone)
Proheparin-binding EGF-like growth factor [Cleaved into: Heparin-binding EGF-like growth factor (HB-EGF) (HBEGF) (Diphtheria toxin receptor) (DT-R)]
Hepatocyte growth factor (Hepatopoietin-A) (Scatter factor) (SF) [Cleaved into: Hepatocyte growth factor alpha chain; Hepatocyte growth factor beta chain]
Insulin-like growth factor-binding protein 1 (IBP-1) (IGF-binding protein 1) (IGFBP-1) (Placental protein 12) (PP12)
Insulin-like growth factor-binding protein 2 (IBP-2) (IGF-binding protein 2) (IGFBP-2)
Insulin-like growth factor-binding protein 3 (IBP-3) (IGF-binding protein 3) (IGFBP-3)
Insulin-like growth factor-binding protein 4 (IBP-4) (IGF-binding protein 4) (IGFBP-4)
Insulin-like growth factor-binding protein 6 (IBP-6) (IGF-binding protein 6) (IGFBP-6)
Insulin-like growth factor I (IGF-I) (Mechano growth factor) (MGF) (Somatomedin-C)
Insulin [Cleaved into: Insulin B chain; Insulin A chain]
Macrophage colony-stimulating factor 1 receptor (CSF-1 receptor) (CSF-1-R) (CSF-1R) (M-CSF-R) (EC 2.7.10.1) (Proto-oncogene c-Fms) (CD antigen CD115)
Tumor necrosis factor receptor superfamily member 16 (Gp80-LNGFR) (Low affinity neurotrophin receptor p75NTR) (Low-affinity nerve growth factor receptor) (NGF receptor) (p75 ICD)
Neurotrophin-3 (NT-3) (HDNF) (Nerve growth factor 2) (NGF-2) (Neurotrophic factor)
Neurotrophin-4 (NT-4) (Neurotrophin-5) (NT-5) (Neutrophic factor 4)
Tumor necrosis factor receptor superfamily member 11B (Osteoclastogenesis inhibitory factor) (Osteoprotegerin)
Platelet-derived growth factor subunit A (PDGF subunit A) (PDGF-1) (Platelet-derived growth factor A chain) (Platelet-derived growth factor alpha polypeptide)
Placenta growth factor (PlGF)
Kit ligand (Mast cell growth factor) (MGF) (Stem cell factor) (SCF) (c-Kit ligand) [Cleaved into: Soluble KIT ligand (sKITLG)]
Mast/stem cell growth factor receptor Kit (SCFR) (EC 2.7.10.1) (Piebald trait protein) (PBT) (Proto-oncogene c-Kit) (Tyrosine-protein kinase Kit) (p145 c-kit)
Protransforming growth factor alpha [Cleaved into: Transforming growth factor alpha (TGF-alpha) (EGF-like TGF) (ETGF) (TGF type 1)]
Transforming growth factor beta-1 (TGF-beta-1) [Cleaved into: Latency-associated peptide (LAP)]
Transforming growth factor beta-3 (TGF-beta-3) [Cleaved into: Latency-associated peptide (LAP)]
Vascular endothelial growth factor A (VEGF-A) (Vascular permeability factor) (VPF)
Vascular endothelial growth factor receptor 2 (VEGFR-2) (EC 2.7.10.1) (Fetal liver kinase 1) (FLK-1) (Kinase insert domain receptor) (KDR)
Vascular endothelial growth factor receptor 3 (VEGFR-3) (EC 2.7.10.1) (Fms-like tyrosine kinase 4) (FLT-4) (Tyrosine-protein kinase receptor FLT4)
Vascular endothelial growth factor D (VEGF-D) (c-Fos-induced growth factor) (FIGF)

2.1.21 Statistical Analysis

The results presented from the experimental outcomes of this work are representative of a minimum of three independent experiments. Results were analysed using GraphPad Prism v6.05 statistical analysis software. Data was expressed as mean plus/minus standard deviation (± SD). Statistical differences were analysed with unpaired t test or one-way ANOVA with Tukey correction for multiple comparison test as appropriate. Statistical significance was accepted if $P < 0.05$.

Chapter 3: Proliferation and Differentiation of Young and Old Immortalised Human Myoblasts.

3.0 Background

3.0.0 Introduction

The persistent mechanical forces produced by skeletal muscle (SkM) and its corresponding cellular and metabolic functions place it at a relatively high risk for injury or damage. This risk is further exacerbated by disuse-associated deconditioning, muscle disease, and aging. Although SkM has a remarkable capacity for repair and self-renewal, a reduction in functional capacity along with the progressive loss of SkM mass manifest in a range of conditions. From simple disuse-induced physiological atrophy, to muscular dystrophies (e.g. Duchenne muscular dystrophy), MN conditions (e.g. amyotrophic lateral sclerosis), metabolic muscle disorders (e.g. acid maltase deficiency), conditions of the peripheral nerve (e.g. Friedreich's ataxia) NMJ diseases (e.g. myasthenia gravis), neuromuscular myopathies (e.g. myotonia congenita), as well as the pathophysiological effects of aging, diabetic neuropathy and myopathy, cancer cachexia and heart failure.

Muscle loss and compromised muscle function are traits universally witnessed in aging mammals. As aging occurs, considerable reductions in the regenerative capability of SkM is witnessed. A 1–2% annual muscle loss after the age of 50 years old is considered normal human ageing (Kim and Choi, 2013; Kaasik et al., 2012), with those over the age of 80 years old losing upwards of 40% of their SkM mass. (McPhee et al., 2013). This progressive age-linked decline of SkM mass, quality, and function is termed sarcopenia (Dodds et al., 2015). The advancing loss of SkM also results in remodelling of the muscle with increasing connective and adipose tissue (Crane et al., 2010). The underlying mechanisms responsible for sarcopenia remain unclear. However, dysregulation of metabolic and hormonal factors, along with alterations to the immune system and inflammatory responses, as well as reduced SkM protein synthesis in response to nutrient and physical activity stimulus are all considered candidates contributing to the development of sarcopenia (Degens, 2010). It has also been indicated that age-linked reduction in satellite cell (SC) concentration and activation attenuates self-repair of muscle after damage induced through physical activity, possibly promoting sarcopenia (Brooks and Faulkner, 1990). Typical disuse-induced atrophy of SkM is entirely a consequence of decreased myofibre size, whereas SkM loss observed in elderly individuals presenting with sarcopenia have reduced myofibre size along

with a reduction in the number of myofibres (Machida and Booth, 2004). Alterations to myofibre phenotype are also apparent, predominantly a decrease in fast-twitch (type II) myofibre size and number is witnessed (Nilwik et al., 2013), resulting in a muscle composition with greater quantities of slow-twitch (type I) myofibres (Gannon et al., 2009). Along with a transitioning fast-to-slow twitch myofibre phenotype, dysregulation of motor neuron (MN) denervation and reinnervation leads to an increasing net deficit of MN units (Drey et al., 2014). Moreover, aging produces deviations in the microenvironment of regenerating SkM, potentially contributing to further reductions in regenerative potential of ageing SCs (Dhawan and Rando, 2005). The maintenance and self-reparative capability of SkM is implemented through the actions of SCs (Lepper et al., 2011). Thus, the fundamental issue of whether SCs from old or young individuals diverge in their intrinsic myogenic function requires elucidation.

To resolve the problem, experiments in this study were conducted by utilising SCs originating from young or old SkM to compare the *in vitro* responses of activated SCs (i.e. myoblasts) when examined under standardised conditions. The origin of the immortalised human skeletal muscle cell (SkMC) lines used in this study were generated from young myoblasts obtained from a healthy 25-year-old male and old myoblasts from a healthy 83-year-old male. Thus, the myoblasts used in this study differ in age by roughly six decades. The proliferative capacity, progression of myotube differentiation, and expression of proteins indicative of proliferation and differentiation were examined and compared to establish any differences in intrinsic myogenic behaviour among young and old myoblasts.

3.0.1 Aims

The hypothesis is immortalised myoblasts originating from young muscle differ in their intrinsic myogenic behaviour compared to immortalised myoblasts derived from old muscle. Thus, the aims are:

1. Characterise and compare young and old immortalised human myoblast proliferation.

2. Generate culture conditions for functional differentiation studies of young and old immortalised myoblasts.

3. Assess old and young myoblast-to-myotube differentiation in culture.

3.1 Results

3.1.0 Myoblast Revival

Two new human SkM cell lines were used for this project, which were not previously employed or established in our laboratory (as described in 2.0.0). Therefore, optimisation of culture conditions, such as seeding conditions, seeding density, and differentiation conditions were required before further studies could be conducted. Individual vials of 25-year-old immortalised human myoblasts (C25) and 83-year-old immortalised human myoblasts (C83) containing ~$1x10^6$ cryogenically preserved cells were retrieved from liquid nitrogen storage to compare cellular revival rates between old and young myoblasts following cellular passaging by quantifying the differences in adherent cells. Prior to seeding the revived cells (as described in 2.1.0), a cell count was performed (as described in 2.1.1) to establish a baseline seeding concentration. Following 24 hours incubation with growth media (GM) (Table 2.0), both C25 and C83 cells were collected from their respective flasks and counted to determine the percentage of adherent cells after seeding. The results showed that there was no significant difference ($p = 0.31$) in the number of baseline seeded cells between C25 ($1.08x10^6 \pm 6.1x10^5$ cells) and C83 ($1.11x10^6 \pm 7.5x10^5$ cells) (Figure 3.0). There was also no significant difference ($p = 0.97$) between the number adherent C25 ($7.7x10^5 \pm 8x10^4$) and C83 ($7.8 \pm 9x10^4$) following 24 hours of being seeded in GM. However, a significant reduction ($P < 0.0001$) in the number of adherent cells 24 hours after being seeded in GM was observed in both cell lines. There was a 28.4% decrease in the number of adherent C25 compared to the number of cells seeded. Similarly, a 30% reduction in the number of adherent C83 compared to the number of cells seeded was also observed. Thus, indicating a non-significant 1.6% difference in revival rate of C25 and C83 following cryogenic passaging of cells.

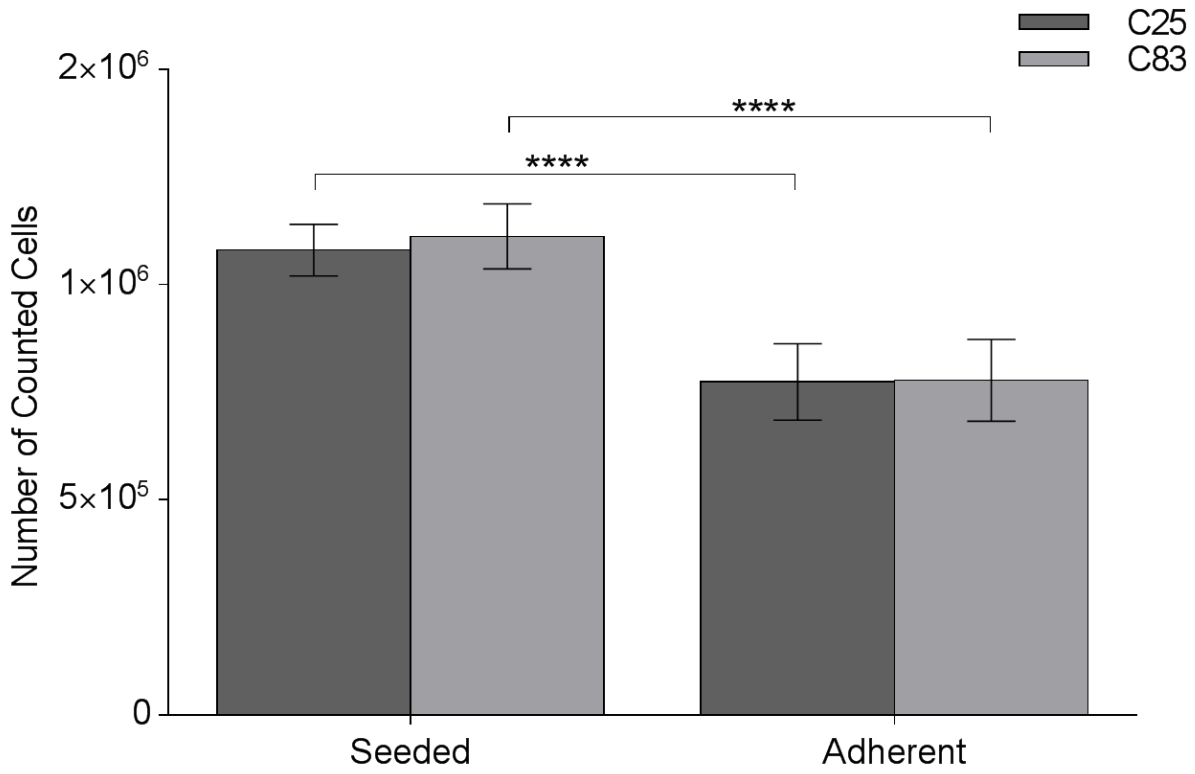

Figure 3.0: Myoblast revival after cryogenic passage. Comparison of the number adherent young and old myoblasts to the number seeded following 24 hours of incubation in growth media. Data quantified by counting cells in 10 random fields of view from 3 separate wells on each cell culture plate. Data presented as a mean, error bars signify ± SD. n = 4 independent experiments. **** denotes $P < 0.0001$. 25-year-old immortalised human myoblasts (C25); 83-year-old immortalised human myoblasts (C83).

3.1.1 Myoblast Proliferation

Upon determining no differences between the revival of old and young immortalised myoblasts following cryogenic passaging of the cells, the ensuing experiment set out to ascertain any differences in the rate of proliferation between the two cell lines. The cells were seeded in T175 flask as described in 2.1.1 and confluence was quantified by calculating the myoblast area of both C25 and C83 (Figure 3.1). At 24 hours there was no significant difference (P = 0.058), as the myoblast area was 9.1% ± 1.4 for the young cell line, where as the old cells had a myoblast area of 10.2% ± 1. After 48 hours the myoblast area of young proliferating myoblasts was 19% ± 1.5, while old myoblasts had a non-significantly (P = 0.067) different myoblast area of 20.3% ± 1.4. At 72 hours, the myoblast area of young cells had expanded to 50.8% ± 2.3 and the old myoblasts increased to 49.1% ± 1.2, though the difference was insignificant as P = 0.063. Similarly, at 96 hours there was no significant difference (P = 0.066). The proliferating young myoblasts had grown to cover an area of 88.5% ± 1.7, with old myoblasts covering a comparable area of 90% ± 1.6.

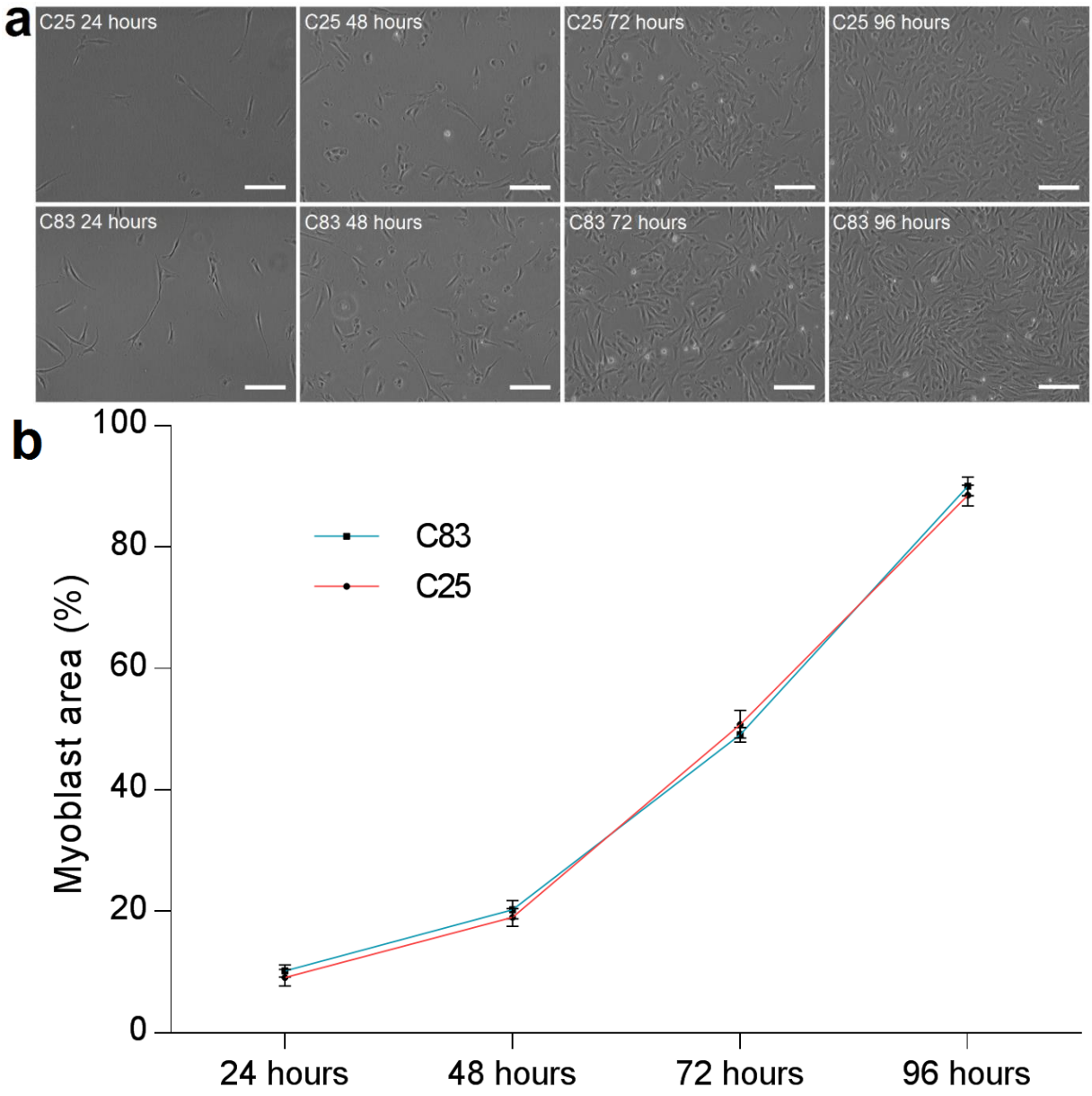

Figure 3.1: Young and old myoblast proliferation. a) The top row of panels are phase contrast images representative of young myoblast proliferation. The bottom row of panels are phase contrast images representative of old myoblast proliferation. b) A line graph showing the difference in proliferation rates between the two cells lines at 24, 48, 72, and 96 hours, quantified as myoblast area. Data presented as a mean, error bars signify ± SD. n = 5 independent experiments. 25-year-old immortalised human myoblasts (C25); 83-year-old immortalised human myoblasts (C83). Bar = 100 µm.

3.1.2 Myoblast Viability

Both young and old myoblasts were cultured for 96 hrs in T175 flasks at a seeding concentration of ~$1x10^6$ cell in GM, at which point confluence of both C25 and C83 reached ~80-90%. The cells were collected and counted to determine any discrepancy in the total number of viable cells after 96 hours of proliferation. The results revealed there was no significant difference (P = 0.112) in total number of young viable myoblasts (C25 = $7.91x10^6$ ± $6.2x10^5$) compared to the total number of old viable myoblasts (C83 = $7.46x10^6$ ± $3.3x10^5$) after 96 hours of proliferation (Figure 3.2).

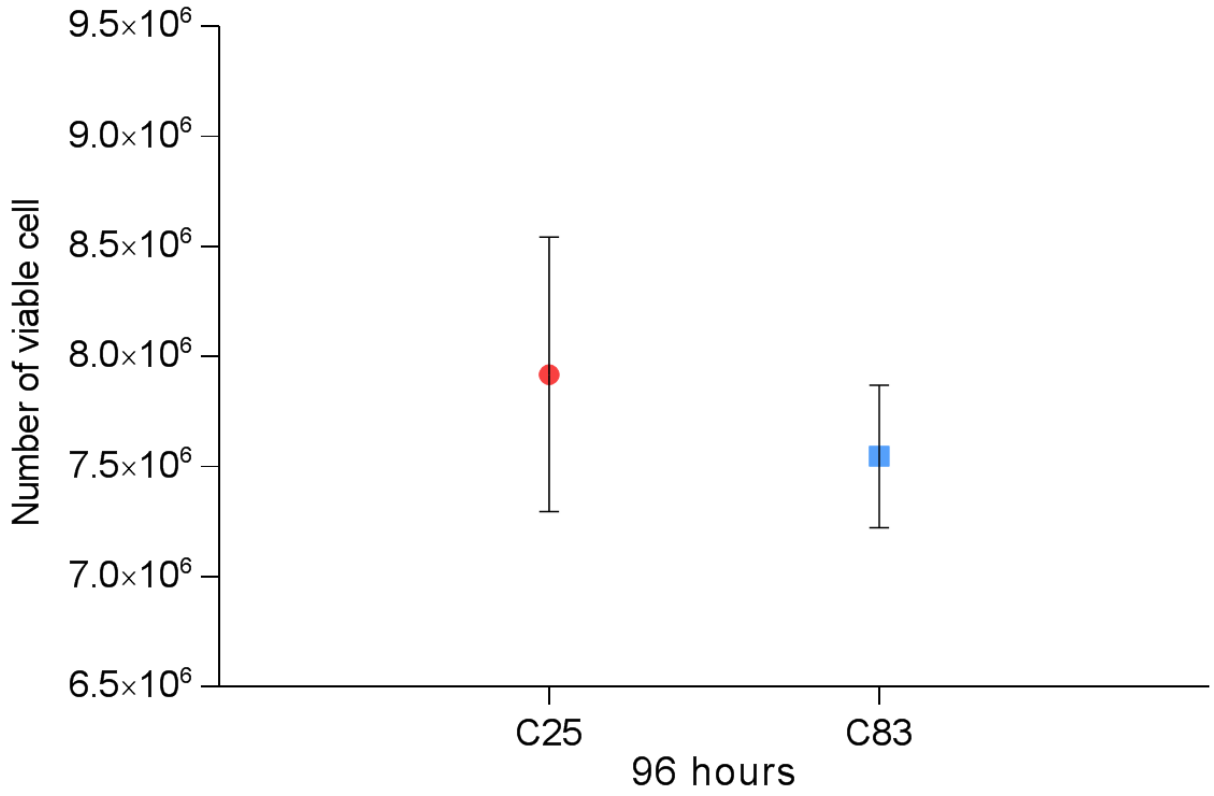

Figure 3.2: Total viable myoblasts. Comparison of the total number of young viable myoblasts to the number of old viable myoblasts following 96 hours of incubation in growth media. Data presented as a mean, error bars signify ± SD. n = 3 independent experiments. 25-year-old immortalised human myoblasts (C25); 83-year-old immortalised human myoblasts (C83).

3.1.3 Optimisation of Myoblast Seeding Density

Before functional studies of myoblast differentiation and development could be conducted, the density of myoblasts must be adequately concentrated to allow for cell-to-cell contact. Thus, to achieve an optimal cell density of ~90-100% confluence after 24 hours of being seeded in GM, four concentrations of C25 and C83 were concurrently cultured in 6-well plates pre-coated with a 1% gelatin solution (as described in 2.1.1). The myoblasts were seeded at $5x10^4$ (C1), $1x10^5$ (C2), $1.5x10^5$ (C3), or $2x10^5$ (C4) cells/mL. Phase contrast microscopy was used to assess 20 random fields of view at 10X magnification and ImageJ software was used to process the images and quantify confluence after 24 hrs by calculating the total myoblast area. The myoblast area was calculated for each seeding density to determine the percentage of confluence. For C25 the results showed C1 = 50.2% ± 4.3, C2 = 74.9% ± 2.4, C3 = 92.9% ± 2.5, and C4 = >100%. Similarly, for C83 the results were C1 = 49.9% ± 4.1, C2 = 75.4% ± 2.1, C3 = 95.1% ± 3.5, and C4 = >100% (Figure 3.3). A concentration of $1.5x10^5$ cell/mL was established as the optimal seeding cell density for functional studies in both cell lines. Although the concentration of $2x10^5$ cell/mL presented as 100% confluent after 24 hours, the cells were over confluent resulting in abnormal morphology and excessive cell detachment from the culture surface and death in both cell lines.

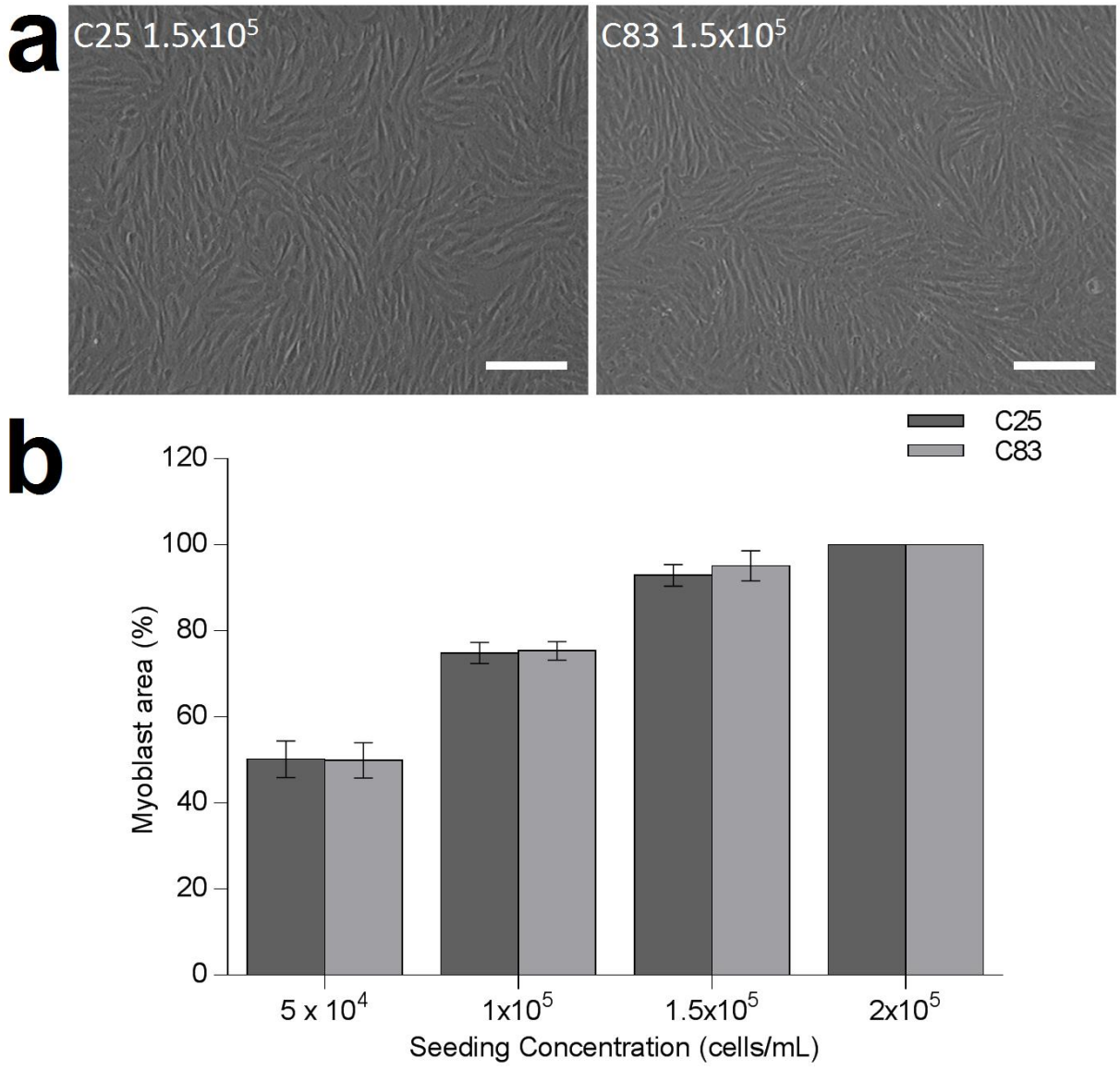

Figure 3.3: Optimal cell density for differentiation. a) The left panel is representative of young myoblast after 24 hours of being seeded at a density of $1.5x10^5$ cell/mL. The right panel is representative of old myoblasts after 24 hours of being seeded at a density of $1.5x10^5$ cell/mL. b) A graph showing the difference in confluence between the two cells lines 24 hours after being seeded at a density of $5x10^4$, $1x10^5$, $1.5x10^5$, or $2x10^5$ cells/mL, quantified as myoblast area. Data presented as a mean, error bars signify ± SD. n = 3 independent experiments. 25-year-old immortalised human myoblasts (C25); 83-year-old immortalised human myoblasts (C83). Bar = 100 µm.

3.1.4 Optimisation of Differentiation Media

To achieve optimal differentiation of myoblasts to myotubes in both C25 and C83 cell lines, the efficiency of the in-house DM formulation (DM1) (Table 2.1) was compared to the commercially available 'low-serum cell culture medium for differentiation of skeletal muscle cells' manufactured by PromoCell (DM2). The DM1 was also compared with the previously established in-house differentiation media for mouse myoblast (C2C12 cell line) differentiation in our laboratory. The C2C12 differentiation media (DM3) consisted of 96% Dulbecco's modified eagle medium (DMEM), 2% horse serum (HS), 1% penicillin-streptomycin (Pen/Strep), and 1% L-glutamine. Optimal differentiation was quantified by using phase contrast and immunofluorescence microscopy to assess 20 random fields of view at 10X magnification and ImageJ was utilised to calculate the fusion index (FI) (Table 2.2).After 24 hours of exposure to DM1, DM2, or DM3, cellular fusion was imperceptible in both C25 and C83. After 48 hours, the first instances of multinucleated cells (cells with > 2 nuclei) were discernible in both young and old cell lines. Thus, FI was quantified 48 hours after the application of the DM formulations to C25 and C83. The DM formulation exhibiting the highest percentage of FI in both young and old SkMC lines after 48 hours was established as optimal for functional studies. The DM1 formulation exhibited the largest percentage of FI in C25 with 69.7% ± 2.8 (Figure 3.4). The DM2 displayed a slightly lower, though insignificantly different FI percentage of 68% ± 6.3. The C25 cells exposed to DM3 had a FI percentage of 55.9% ± 5.8, which was significantly less ($P < 0.0001$) than both DM1 and DM2. Similarly, DM1 prompted a FI of 71.75% ± 3.5 in C83 after 48 hours (Figure 3.5). The C83 cells exposed to DM2 also had a slightly reduced yet insignificantly different FI of 69.3% ± 3. There was also a significant reduction ($P < 0.0001$) in the FI percentage (56.8% ± 6.7) of C83 after 48 hours of incubation with DM3 compared to both DM1 and DM2.

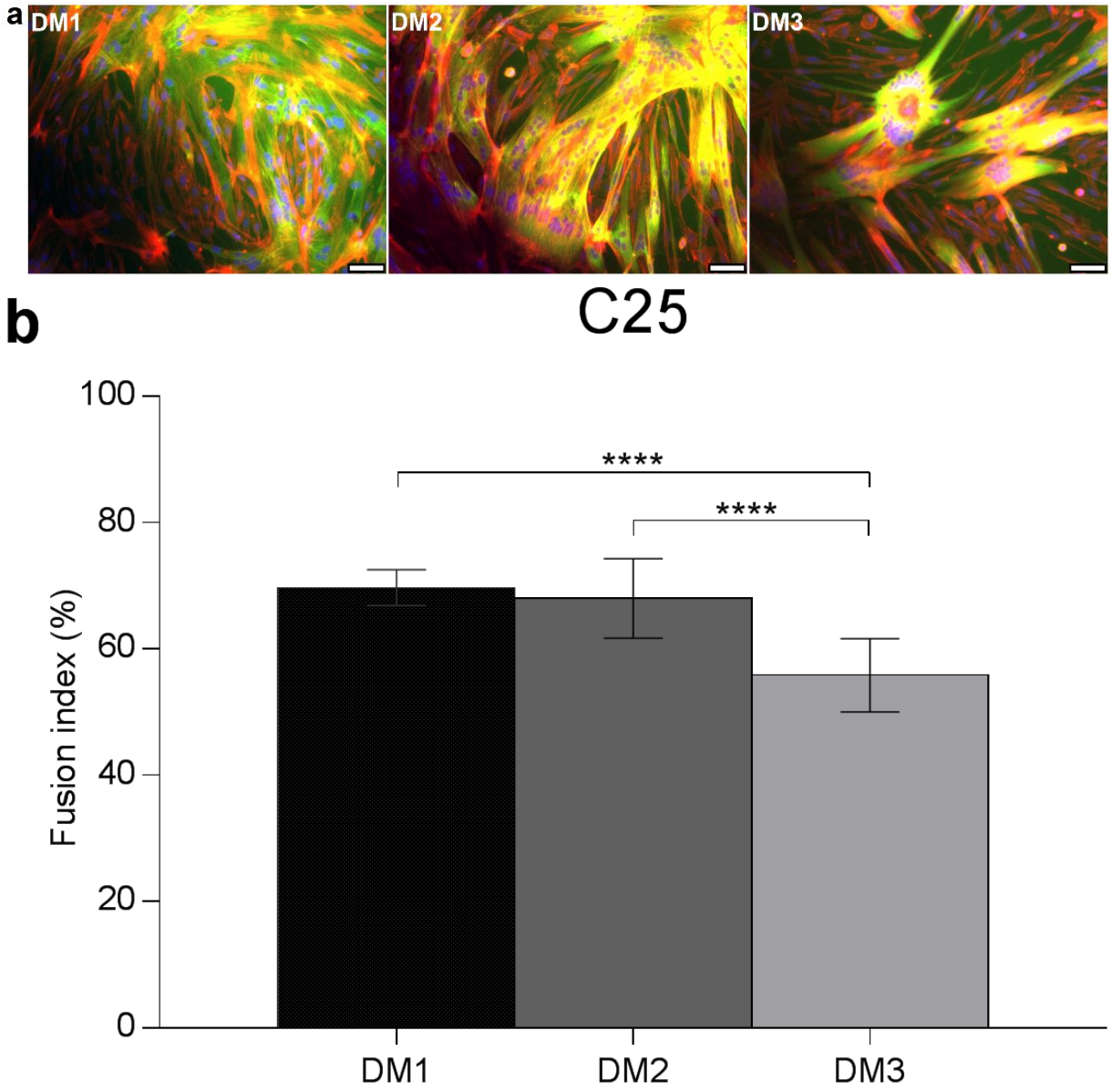

Figure 3.4: Optimal differentiation of young myoblasts. a) Image panels are representative of young immortalised human myoblasts treated with in-house differentiation media formulation (DM1), commercial differentiation media formulation by PromoCell (DM2), or in-house C2C12 differentiation media (DM3). The cells were stained for actin with phalloidin (red), differentiated cells with anti-myosin heavy chain (green), and nuclei with DAPI (blue). b) Comparison of the percentage of cellular fusion in young myoblast when incubated with DM1, DM2, or DM3 after 48 hours. Data presented as a mean, error bars signify ± SD. n = 3 independent experiments. **** denotes $P < 0.0001$. Bar = 75 µm. 25-year-old immortalised human myoblasts (C25).

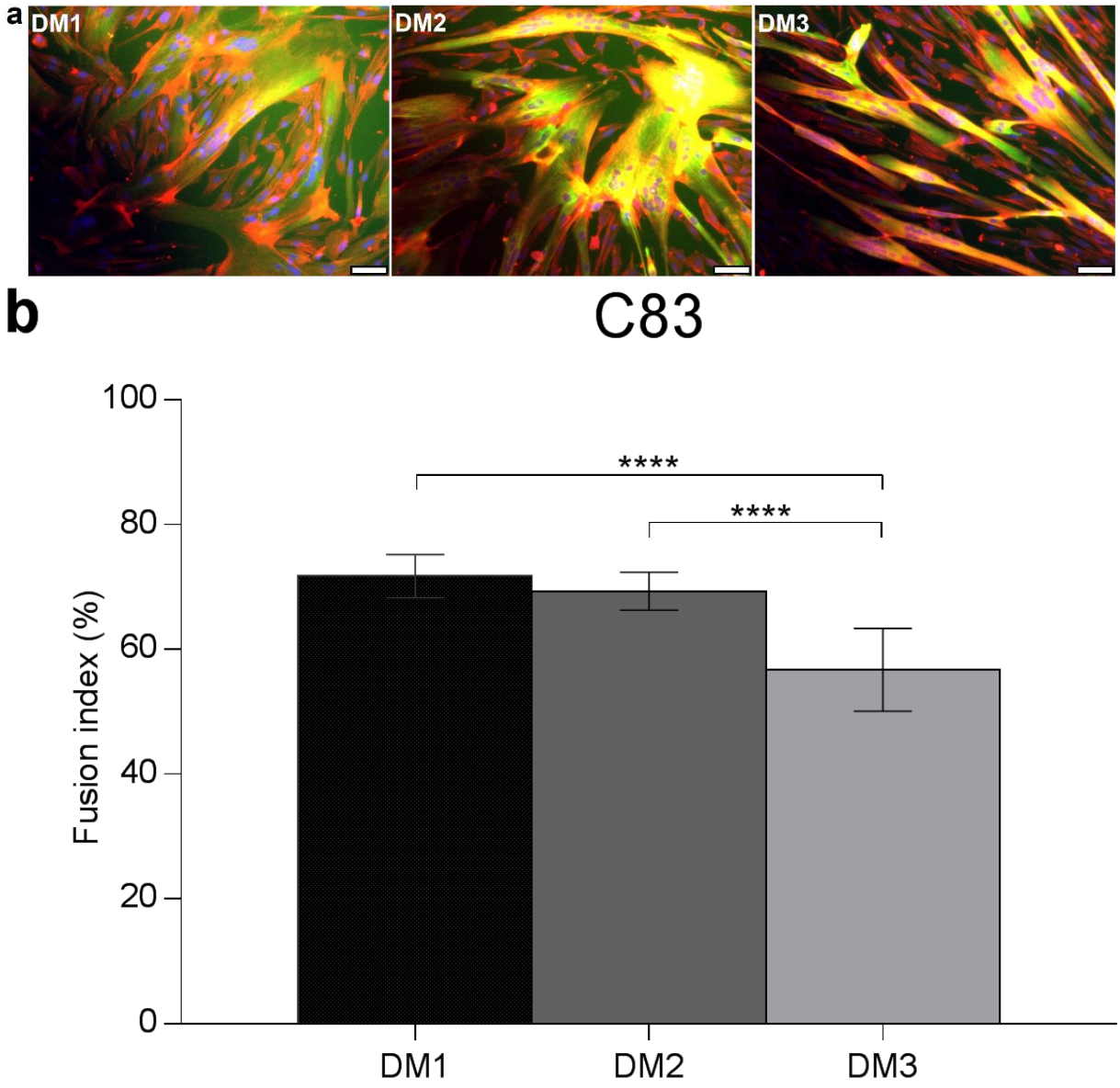

Figure 3.5: Optimal differentiation of old myoblasts. a) Image panels are representative of old immortalised human myoblasts treated with in-house differentiation media formulation (DM1), commercial differentiation media formulation by PromoCell (DM2), or in-house C2C12 differentiation media (DM3). The cells were stained for actin with phalloidin (red), differentiated cells with anti-myosin heavy chain (green), and nuclei with DAPI (blue). b) Comparison of the percentage of cellular fusion in old myoblast when incubated with DM1, DM2, or DM3 after 48 hours. Data presented as a mean, error bars signify ± SD. n = 3 independent experiments. **** denotes $P < 0.0001$. Bar = 75 µm. 83-year-old immortalised human myoblasts (C83).

3.1.5 Differentiation Parameters

To determine if there were any significant differences in the differentiation of young myoblasts to myocytes and ultimately myotubes compared to the differentiation of old myoblast, the differentiation parameters were calculated using the methods described in 2.1.4 (Table 2.2). Quantification was conducted using phase contrast and immunofluorescence microscopy to assess 20 random fields of view at 20X magnification and ImageJ was utilised to process the myotube area (MA), FI, and aspect ratio (AR) of both cell lines. There was no measurable difference in the differentiation parameters between C25 and C83 at 24 hours. Both young and old cell lines exhibited morphology consistent with mononucleated myoblasts and myocytes. Thus, the criteria for FI (>2 nuclei per cell), MA, and AR were not met, since there was no measurable myotube formation at 24 hours. After 48 hours, there was no significant difference ($P = 0.09$) in the FI of C25 (69.7% ± 3.2) and C83 (67.9% ± 3.3). After 72 hours the FI of C25 was 70.1% ± 5.1 with C83 being non-significantly ($P = 0.07$) higher at 72.8% ± 4.1. Similarly, there was no difference ($P = 0.16$) after 96 hours as the FI of C25 was 83% ± 4.1 and C83 at 84.7% ± 3.3 (Figure 3.6b). The results of MA comparison at 48 hours between C25 (49.5% ± 4.2) and C83 (50.2% ± 4.9) revealed no significant difference ($P = 0.63$). When measured at 72 hours, the MA of C25 was 58.5% ± 4.2 while the MA of C83 was insignificantly ($P = 0.38$) higher at 60% ± 4.3. After 96 hours, the MA of C25 was measured at 72.4% ± 4.1 and C83 was 70.3% ± 4.4, though the difference was insignificant ($P = 0.12$) (Figure 3.6c). Finally, the AR was compared amongst the cell lines. At 48 hours, the AR was not significantly different ($P = 0.34$) between C25 (20.1 ± 8) and C83 (17.8 ± 7.4). After 72 hours, the AR of C25 was 15.4 ± 5.8 and C83 measured at an insignificantly different ($P = 0.57$) 16.7 ± 8.3. Similarly, there was no difference ($P = 0.14$) after 96 hours as the AR of C25 was 18.5 ± 7.4 and C83 was 14.8 ± 7.8 (Figure 3.6d).

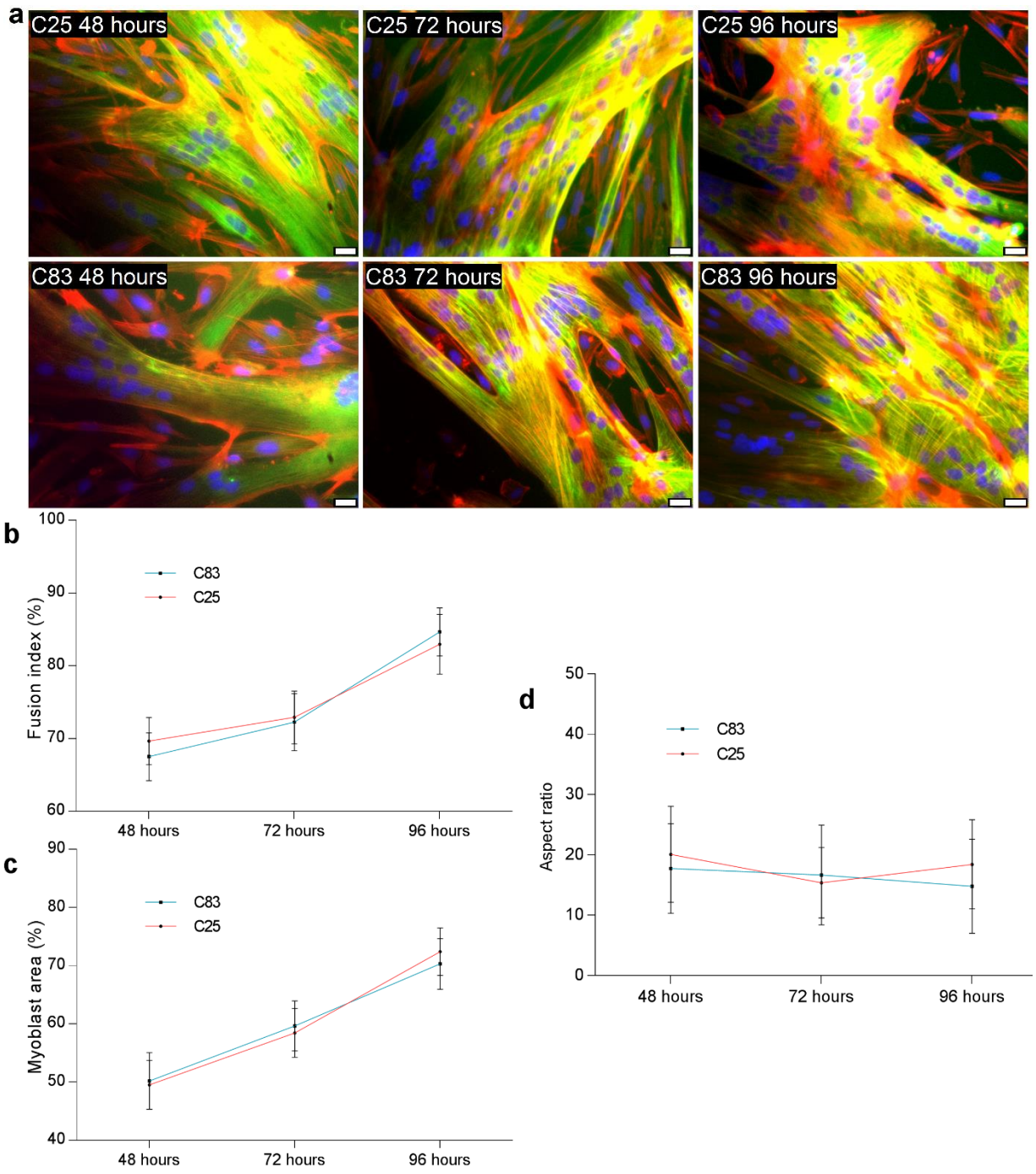

Figure 3.6: Differentiation parameters of young and old myoblasts. a) The upper row of images are representative of young myotube morphology during differentiation at 48, 72, and 96 hours. The lower row of images are representative of old myotube morphology during differentiation at 48, 72, and 96 hours. The cells were stained for actin with phalloidin (red), differentiated cells with anti-myosin heavy chain (green), and nuclei with DAPI (blue). b) Comparison of the percentage of cellular fusion in old and young myoblasts incubated with differentiation media at 48, 72, and 96 hours. c) Comparison of myotube area between old and young differentiated myotubes at 48, 72, and 96 hours. d) Comparison of aspect ratio at 48, 72, and 96 hours amongst young and old myotubes. Data presented as a mean, error bars signify ± SD. n = 5 independent experiments. Bar = 25 µm. 25-year-old immortalised human myoblasts (C25); 83-year-old immortalised human myoblasts (C83).

3.1.6 Proliferation & Differentiation Marker Expression

Protein expression was assessed to identify the differences in the proportional decline of proliferative myoblasts and the upregulation of differentiating myotubes during the preliminary stages of young and old myoblasts differentiation. The expression of the proliferative antigen Ki67 (Scholzen and Gerdes, 2000), which is strictly associated with cell proliferation and is only present during the active phases of the cell cycle (i.e. G1, S, G2 and M), and absent in resting cells (G0) (Hooghe et al., 2008; Shirendeb et al., 2009), was used as a the marker of proliferation in the skeletal muscle cells (SkMCs). Declines in Ki67 levels occur in later phases of mitosis (during anaphase and telophase) (Modlin et al., 2008). Thus, Ki67 expression is associated with the proliferative activity of intrinsic cell populations. Using the methods detailed in 2.1.4, the expression of Ki67 and the expression of myosin heavy chain (MHC), a marker of terminal differentiation in SkMCs (Schiaffino et al., 1986), were quantified and compared at 24, 48, 72, and 96 hours after cultured C25 and C83 were switched from GM to DM. Immunofluorescence microscopy was used to assess 20 random fields of view at 20X magnification. ImageJ was used to calculate the percentage of Ki67 expression and the percentage of MHC expression in both cell lines. Following 24 hours exposure to DM, 69.5% ± 6.6 of young myoblasts were positive for Ki67 (Figure 3.7) and devoid of any MHC expression. Expression of Ki67 in old myoblasts was similar ($P = 0.65$) at 70.4% ± 6.2 with no MHC expression as seen in the young myoblasts. After 48 hours, C25 expression of Ki67 decreased to 29.7% ± 6.6. A similar decrease ($P = 0.57$) was observed in C83, which decreased Ki67 expression to 31% ± 6.1. The expression of MHC had increased to 49.3% ± 3.6 in young cells and 51.2% ± 4.3 in old cell (Figure 3.8), though this difference was insignificant ($P = 0.15$). Following 72 hours of incubation with DM, expression of Ki67 in young cells decreased further to 2.6% ± 1.2. Expression of Ki67 also decreased in old cells to 2.8% ± 1.1, though this difference was insignificant ($P = 0.58$). An insignificant difference ($P = 0.08$) in MHC expression was also observed between the cell lines after 72 hours. Young cells increased MHC expression to 61% ± 4.3, while old cells expressed MHC at a similar 63.6% ± 4.8. Following 96 hours of DM exposure, the expression of Ki67 was measured at 0.5% ± 0.3 in the young cells and a similar ($P =0.6$) 0.41% ± 0.3 in old cells. There was also no significant difference ($P = 0.31$) in the expression of MHC between the cell lines. As C25 expressed MHC at 79% ± 5 and C83 expression of MHC was 77.3% ± 5.7.

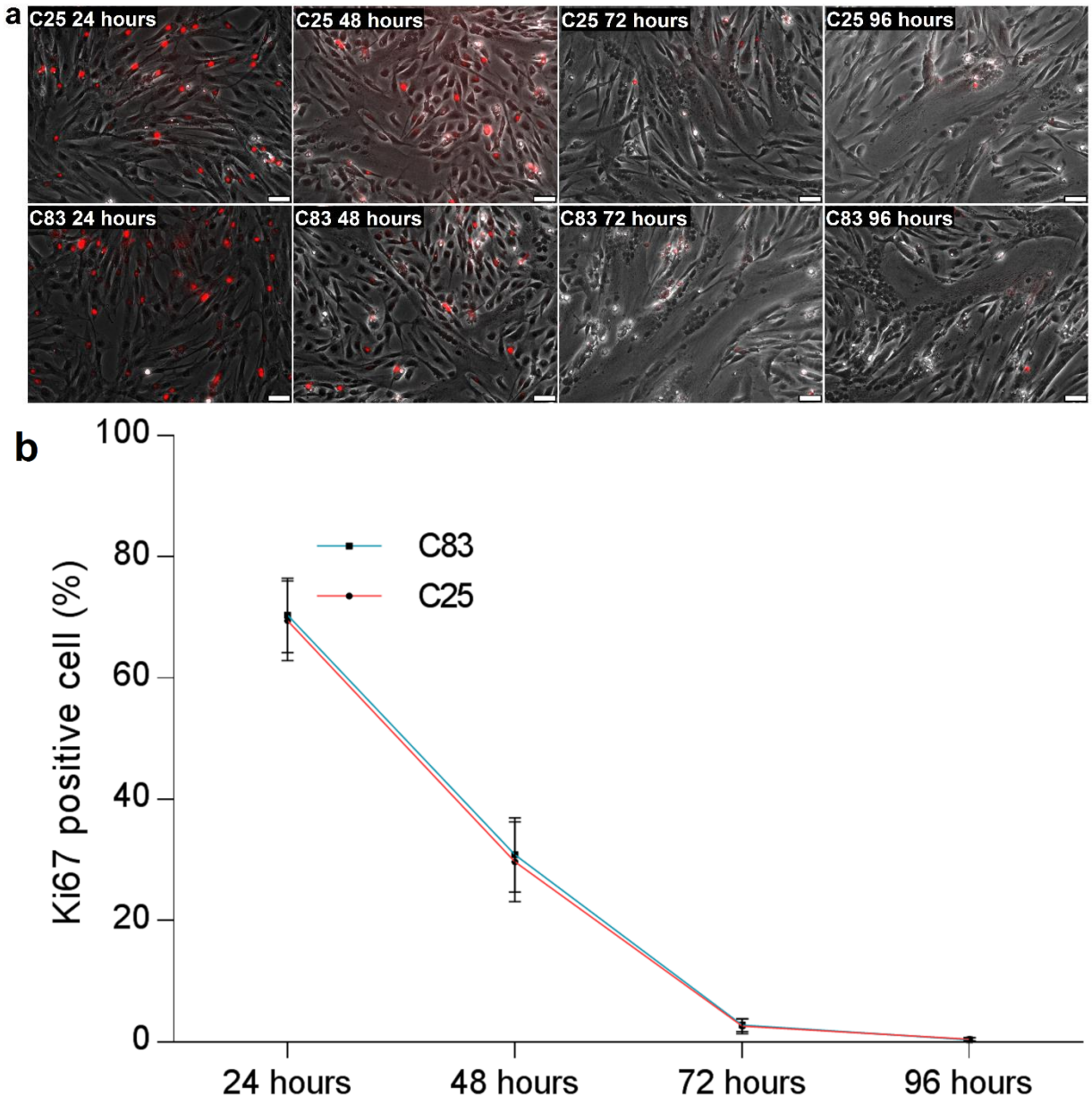

Figure 3.7: Expression of proliferation marker Ki67. a) The upper image panels are representative of Ki67 expression in young myoblasts as they differentiate to myotubes at 24, 48, 72, and 96 hours after exposure to differentiation media. The lower row of images are representative of Ki67 expression in old myoblasts as they differentiate to myotubes at 24, 48, 72, and 96 hours after exposure to differentiation media. The cells were stained for Ki67 (red). b) A line graph showing the percentage of cells positive for Ki67 between both cell lines at 24, 48, 72, and 96 hours. Data presented as a mean, error bars signify ± SD. n = 4 independent experiments. Bar = 50 µm. 25-year-old immortalised human myoblasts (C25); 83-year-old immortalised human myoblasts (C83).

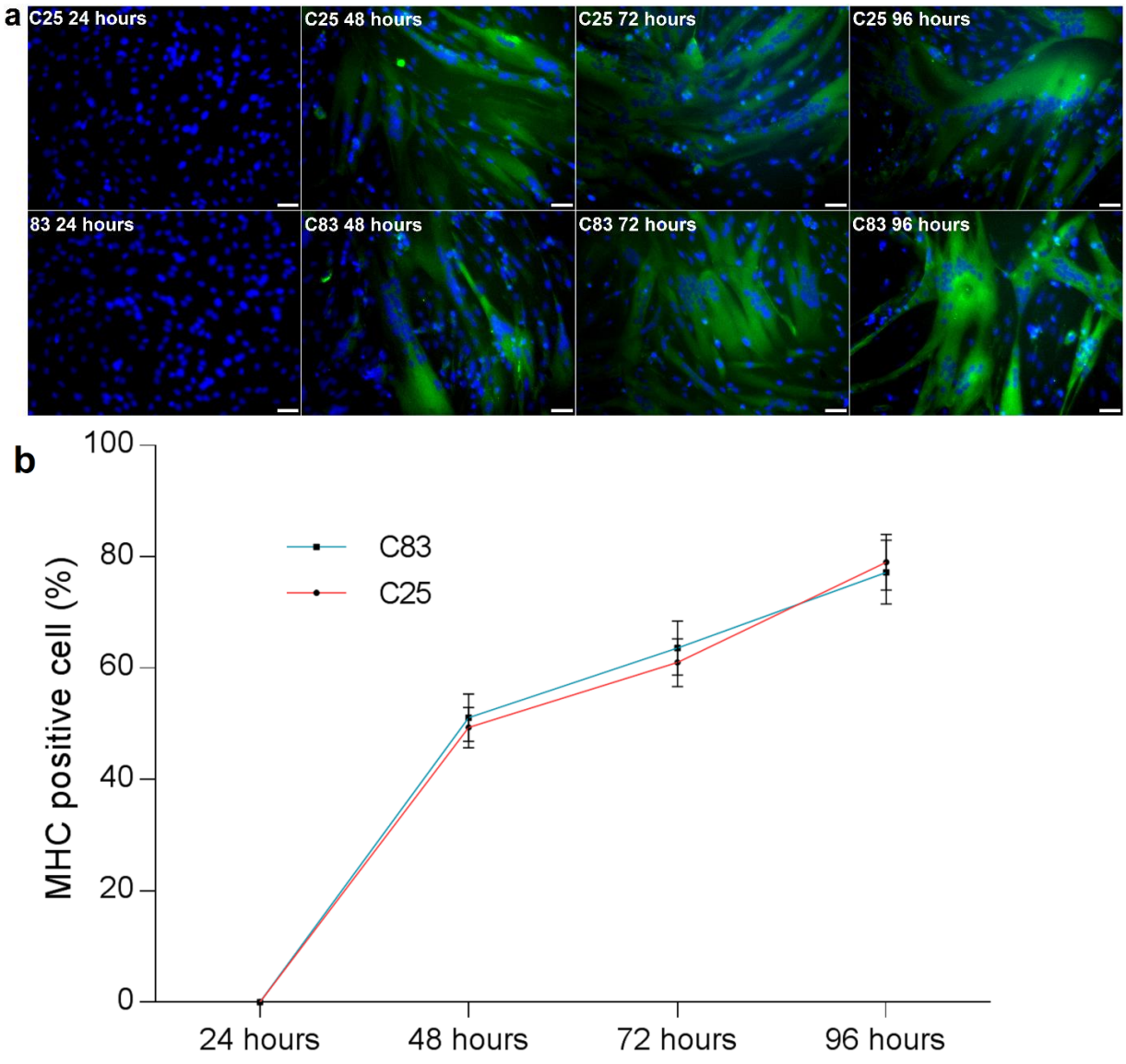

Figure 3.8: Expression of differentiation marker myosin heavy chain. a) The upper image panels are representative of myosin heavy chain (MHC) expression in young myoblasts as they differentiate to myotubes at 24, 48, 72, and 96 hours after exposure to differentiation media. The lower row of images are representative of MHC expression in old myoblasts as they differentiate to myotubes at 24, 48, 72, and 96 hours after exposure to differentiation media. The differentiated cells with anti-myosin heavy chain (green), and nuclei with DAPI (blue). b) A line graph showing the percentage of cells positive for MHC between both cell lines at 24, 48, 72, and 96 hours. Data presented as a mean, error bars signify ± SD. n = 4 independent experiments. Bar = 50 µm. 25-year-old immortalised human myoblasts (C25); 83-year-old immortalised human myoblasts (C83).

3.2 Discussion

The primary findings of this research demonstrated that immortalised human myoblasts originating from old or young muscle did not influence their *in vitro* function when cultured in matching microenvironments. This was determined through the analysis of various experiments including cellular passage of myoblasts, myoblast proliferation and differentiation, as well as the expression of markers demonstrating proliferative and differentiation capacity in young and old myoblasts. The passaging and revival of both young and old myoblasts from cryogenic suspension resulted in a net loss of viable cells that were able to adhere to the tissue culture surface and begin the process of proliferation. Although there was a significant loss of cells from the quantity seeded to the number that adhered when passaging cells, the numbers of myoblasts that were able to adhere and begin proliferating did not differ between the old and young cell lines. As serial passaging is unavoidably necessary for *in vitro* investigations of SkM formation and development, experiments moving forward were conducted with old and young myoblasts passaged an equal number of times to nullify any passage-induced variability among the cell lines. Various studies and subsequent cell line handling and utilisation guidelines have shown that serial passaging of cell lines can induce alterations in cell morphology and function (Geraghty et al., 2014). The C2C12 mouse myoblast cell line, which is one of the most commonly used cell line for *in vitro* investigations of SkM, has been shown to have dysfunctional apoptotic response when excessively serial passaged (Pronsato et al., 2013). This phenotypic drift may lead to the same cell line differing significantly between researchers and laboratories, making it difficult to distinguish between experimental treatments and intrinsic cellular mechanisms. Thus, to mitigate any unintended comparable morphological and functional changes in the two human immortalised SkMC lines used throughout this project, all forthcoming experiments were conducted with matched low number (< 4) passaged young and old myoblasts. To ascertain differences in the proliferative capacity of young and old myoblasts both the SkMC lines were first expanded following revival from cryogenic suspension. The proliferation of C25 and C83 were comparable over a period of 96 hours, with no statistical difference in the number of viable cells upon elimination of proliferative conditions. The expansion of both cell lines yielded a comparable ~10-fold increase of viable cells after 96 hours, indicating the intrinsic capacity for proliferation of early passaged immortalised human myoblast is not determined by the age of the donors muscle tissue. Research conducted with primary human myoblasts have similarly found that the mean population doubling of cells was not influenced by the age of the myoblast donor, as the replicative lifespan of both young and elderly primary myoblasts was found to be similar before replicative senescence occurs (Pietrangelo et al., 2009; Decary et al., 1997). However, the proliferative capacity of myoblasts *in vitro* is regulated by complex biochemical interactions, which

require significant elucidation before being fully understood. Next, both young and old cell lines were differentiated using three variations of DM. The standard in-house DM formulation (DM1) (Table 2.1) was tested for efficacy against a commercial serum free media formulated for primary myoblast differentiation (DM2) and a serum containing media used to differentiate C2C12 myoblasts (DM3). It was discovered that both the serum free formulations, DM1 and DM2, performed equally to induce cellular fusion after 48 hours of the myoblasts being incubated with the media. Various low serum containing DM formulations have been used to induce the differentiation of C2C12 myoblasts, with some studies using up to 5% FBS (Katagiri et al., 1994) and other experiments using as low as 1% FBS (Yoshiko et al., 2002). Thus, the standard low serum (2% horse serum) DM media formulation formerly used in our laboratory to induce differentiation in C2C12 myoblasts (DM3) (Al-Dabbagh et al., 2015) was tested for its ability to differentiate human myoblast. Although DM3 was able to induce an objective degree of differentiation in C25 and C83 (Figure 3.4, 3.5), myotube formation was morphologically abnormal and underdeveloped. Manifesting as smaller myotubes with a lower concentration of myonuclei. Interestingly, it has been demonstrated that that C2C12 differentiation is dependent on endogenous insulin-like growth factor expression and not on serum concentration (Yoshiko et al., 2002). These data demonstrated that DM1 was the most suitable for functional experiments of human myoblast-to-myotube differentiation. Once optimal DM conditions were determined, C25 and C83 were incubated with DM (Table 2.1) and the differentiation parameters along with proliferation/differentiation marker expression were evaluated every 24 hours over a 4-day period. The data in Figure 3.6 show no difference in myotube size when myoblasts from young or old muscle were differentiated. Additionally, regardless of myoblasts being young or old they displayed strikingly similar morphological behaviour in culture. This was also exhibited by C25 and C83 having a comparable ability to undergo cellular fusion, indicated by MHC expressing cells having similar concentrations of myonuclei between the cell lines throughout the process of differentiation. The Ki67 protein is a cellular marker strictly associated with cell proliferation. (Scholzen and Gerdes, 2000). Thus, Ki67 is exclusively detected within the cell nucleus during interphase with most of the protein relocated to the surface of the chromosomes during mitosis (Cuylen et al., 2016). Furthermore, Ki67 is observed during all active phases of the cell cycle (G1, S, G2, and mitosis) and absent in non-proliferating cells (G0) (Bruno and Darzynkiewicz, 1992). The content of Ki67 in cells is also markedly increases during cell progression through S phase of the cell cycle (Darzynkiewicz et al., 2015) The data in Figure 3.7 showed the relative decline in the expression of Ki67 in young and old myoblasts incubated with DM was unaffected by the age of the donor myoblasts. The inverse increase of MHC expression also revealed young and old myoblasts express the differentiation marker in equal proportion when differentiated. The findings of this study suggest no intrinsic age-associated deficits in myogenic function between

young and old immortalised human myoblasts when cultured in identical microenvironments *in vitro*. This data is largely consistent with established *in vitro* SkM research. Experimentation with satellite cells (SCs) harvested from 3-month-old (young) and 32-month-old (old) rats were cultured *in vitro* and found to have comparable rates of proliferation and differentiation (Dumke and Lees, 2011). Similarly, *in vivo* single fibre engraftment assays reveal that SCs from old myofibres possess a regenerative and self-renewal capacity comparable to young myofibre-linked SCs (Collins et al., 2007). Interestingly, studies have shown that muscle from aged mice was estimated to contain around 65% fewer functioning SCs than muscle from young mice (Cosgrove et al., 2014) and the overall number of SCs was also lower in aged mouse muscle (Chakkalakal et al., 2012). However, this was not the main cause of age-linked muscle loss, at least not in mice, where induced depletion of SCs in young adults had little impact on the rate of muscle ageing (Fry et al., 2015). There is strong evidence implicating the aged microenvironment with reduced SC responses (Barberi et al., 2013; Chakkalakal et al., 2012). Transplanted muscle from young into old mice fails to regenerate, but transplanted muscle from old mice into a young mouse did regenerate (Carlson and Faulkner, 1989) but might have a delayed regenerative response (Smythe et al., 2008). Moreover, 'rejuvenating' the microenvironment in older mice enhanced activation of SCs through increased Notch signalling, as shown in heterochronic parabiosis models (Conboy et al., 2003; Conboy et al., 2005; Carlson et al., 2008). Furthermore, lower SC function with ageing was linked to increased activity of the transforming growth factor beta (TGFβ) family of molecules within SCs that are negative regulators of growth and restrict the proliferative responses (Carlson et al., 2009; Sousa-Victor et al., 2014; Yousef et al., 2015). Circulating soluble factors, such as hormones, or other molecules released locally into the microenvironment may influence the intracellular SC signalling to regulate proliferative and differentiation responses. For example, elevating the circulating oxytocin had rejuvenating effects for SCs (Elabd et al., 2014); increasing circulating levels of growth differentiation factor 11 (GDF-11) also rejuvenated SCs (Sinha et al., 2014). However, alternative research investigating the effect of GDF-11 on myogenesis observed a significant inhibition of SkM regeneration (Brun and Rudnicki, 2015). Additionally, elevated levels of osteopontin in aged mice was associated with impaired SC responses to damage and this was overcome by reducing osteopontin *in vitro* and *in vivo* (Paliwal et al., 2012). Thus, a key detail, which has not yet been fully understood, is how the SCs respond to the rapidly changing microenvironment occurring soon after muscle damage, which is heavily influenced by the infiltrating immune cells (reviewed by the author of this thesis in (Saini et al., 2016)). Furthermore, some studies have also shown that geriatric mice were able to regenerate muscle autographs similar to whole muscle grafts transplanted between 27-29 month-old (geriatric) and 3-month-old (young) mice irrespective of the observed preliminary delay in myogenesis activation (Shavlakadze et al., 2010). Research with human SCs from old donors (> 76-

years-old) transplanted into young mice has also revealed that aged human SCs can appropriately supply their myonuclei to facilitate regeneration of *in vivo* mouse muscle (Schafer et al., 2006). Furthermore, it has been suggested that the reduction of SC migratory function observed in old mice is not the underlying factor for the diminished *in vivo* regeneration of muscle (Collins-Hooper et al., 2012). Investigations of human SCs in old muscle being activated via physiological stimuli have found the activation to be adequate for muscle regeneration (George et al., 2010). These findings indicate signalling pathways required for SC activation function correctly, however, significant investigation of SC activity *in vivo* is still required to explain SC behaviour completely. In opposition to the findings of this study, alternative research has indicated age-linked alterations in the proliferation and differentiation of primary human myoblasts, though it is important to note some studies provide limited data as only a single young and old donor were compared (Lorenzon et al., 2004; Fulle et al., 2005; Jacquemin et al., 2004). Additionally, some studies compare young and old SC populations that have varying desmin expression. This variable desmin expression may influence myogenic potential thus altering differentiation capacity of young and old myoblasts regardless of age (Pietrangelo et al., 2009; Beccafico et al., 2007). Ultimately, several reports attribute the loss of *in vivo* myoblast regenerative capacity in SkM to changes in the local microenvironment and not the SCs themselves. Meaning young and old myoblasts are intrinsically similar, but what makes them 'old' or 'young' is their microenvironment.

3.3 Conclusions

In conclusion, *in vitro* cell culture conditions were successfully generated and optimised to assess the proliferation and differentiation of young and old immortalised human myoblast. It was discovered proliferative capacity, decline of proliferative markers, differentiation progression and marker expression were indistinguishable between myoblasts that have a ~60-year age difference when cultured in duplicate culture microenvironments.

Chapter 4: A Novel System of Immortalised Human Myoblasts Co-cultured with Rat Embryonic Spinal Cord Explants

4.0 Background

4.0.0 Introduction

The previous chapter examined the differences between young and old immortalised human myoblasts and established immortalised human myoblasts maintain their myogenic potential *in vitro*, regardless of age. These findings were consistent with similar research with primary myoblasts obtained from young and old donors (Alsharidah et al., 2013). Therefore, the decision was made for the impending research to be conducted with the 25-year-old immortalised human myoblasts (C25) only, as there was no distinguishable difference between the old and young myoblast cell lines. However, the capability of aneurally-cultured myoblasts to provide insight into neuromuscular (NM) disorders is limited due to the lack nervous input, which does not accurately reflect the physiological conditions observed *in vivo*. Classic research has demonstrated that monocultures of primary human myoblasts almost never spontaneously contract and the lack of motor neuron (MN) stimulation inhibits advanced differentiation of myotubes (Delaporte et al., 1986), which puts limitations on *in vitro* investigations of NM disease in cultured skeletal muscle cells (SkMCs). To overcome these limitations a novel *in vitro* nerve-muscle co-culture model could provide a system for investigating NM disorders. The essential requirement of such a system would be the formation of *de novo* neuromuscular junctions (NMJs) on cultured human myotubes, due to the NMJ being the crucial synapse regulating motor unit function and dysfunction. The importance of the NMJ in relation to NM disease has been shown in amyotrophic lateral sclerosis (ALS) studies where destabilisation of the NMJ is one of the early detectable signs of the disease. Similar observations have been made in other NM diseases, which suggest insults to the NMJ are more closely linked to disease progression than the death and loss of MNs (Murray et al., 2008; Fischer et al., 2004; Gould et al., 2006). While degeneration of the NMJ plays a fundamental role in the pathology of NM disease, as well as diseases not traditionally thought of as NM disorders such as diabetes, which leads to diverse forms of peripheral neuropathy as the major NM complication (Bril, 2014). The existing methods to investigate the specific contribution of degenerated NMJs to the aetiology of NM diseases are limited. The majority of *in vivo* models established to explore NM disease are animal models that do not adequately replicate disease in humans (van der Worp et al., 2010).

Furthermore, typical *in vitro* models of NM disease are generally established using animal derived cells (Haase, 2006; Prather et al., 2013). As mentioned previously, *in vitro* models of NM disease with human SkMC monolayers lack the functional innervation required for NMJ formation and advanced muscle differentiation (Suuronen et al., 2004; Ashby et al., 1993; Wilson and Harris, 1993). Given the importance of SkMC innervation and formation of NMJs in the differentiation, maturation and function of SkM, systems and techniques that enable the analysis and manipulation of NMJs have the potential to enrich our understanding of NM disease pathogenesis. Furthermore, such a system may provide a platform to test new therapies. Some nerve-muscle co-culture models generated with mouse, rat, primary human myoblasts, human embryonic stem cells (hESCs) and human induced pluripotent stem cells (hiPSCs)-derived cells, as well as cross species systems have been established to address this problem (Umbach et al., 2012; Arnold et al., 2012; Demestre et al., 2015; Guo et al., 2014; Harper et al., 2004). However, such co-culture models suffer from inadequate experimental reproducibility, attributable to the intricate nature of the culture system requiring an array of growth and neurotrophic factors. Furthermore, serum utilised in classically established nerve-muscle co-culture systems (Giller et al., 1973; Nelson et al., 1993; Li et al., 2001; Daniels et al., 2000; Dutton et al., 1995) introduces indeterminate variables due to differences in serum composition that diminishes experimental reproducibility and may even disturb the influence of experimental treatments on the system. Therefore, the addition of serum into a co-culture system makes describing the minimum factors required for the generation of *in vitro* NMJs impractical. In fact, there is some evidence that retarded MN myelination *in vitro* may well be the consequence of serum in the culture system (Rumsey et al., 2009). Co-culture models employing primary human SkM SCs (i.e. primary myoblasts) acquired from muscle biopsy have their own limitations, as they have a limited proliferative capacity, poor cell purity and exhibit cellular senescence due to cell expansion (Mouly et al., 2005; Webster and Blau, 1990). Advances in the application of cells derived from hESCs and hiPSCs to generate myoblasts (Tanaka et al., 2013) and MNs (Stockmann et al., 2013) may overcome part of these limitations. Nevertheless, besides the ethical issues of using hESCs, monocultures of stem cell-derived MNs are notoriously fragile in culture and require multifarious culture media formulations with mandatory neurotrophic and growth factors. Consequently, when co-cultured with myoblasts these trophic factors negatively affect SkMC differentiation. Furthermore, co-cultures of myoblasts with stem cell-derived MNs produce poor NMJs that are not viable for long-term studies of NMJ maturation and maintenance (Li et al., 2005). Thus, the use of immortalised human myoblasts in a co-culture model offers several advantages, such as reduced cost, ease of use, and provide an unlimited supply of material and minimise ethical concerns associated with the use of human tissue. Cell lines also provide a pure population of cells, which is valuable since it provides a consistent sample and reproducible results (Kaur and Dufour, 2012).

4.0.1 Aim

The objective of the present study was to establish a novel simplified and easily reproducible nerve-muscle co-culture system generating contractile myotubes and formation of NMJs. Thus, the aim was:

1. Generate co-culture conditions free from serum and growth/neurotrophic factors for ED 13.5 rat embryo spinal cord explants to innervate young immortalised human myoblasts during differentiation of myoblasts to myotubes.

4.1 Results

4.1.0 Isolation of Embryonic Rat Spinal Cord

Spinal cords from embryonic rats were selected and isolated as the source tissue of MNs using the methods described in 2.1.6 to innervate C25 in the co-culture system. Rats were chosen over mice as they are genetically, physiologically morphologically closer to humans than mice and provide substantially more material for high throughput tissue culture experimentation than mice (Zhao et al., 2004). Additionally, microdissection of rat embryos is less technically challenging than mouse embryo dissection, streamlining the co-culture system for ease of reproducibility. Harvesting embryos from a pregnant rat when the embryos were ED 13.5 results in a yield of 13 ± 3 embryos. Each embryo was observable as individually compartmentalised protrusions along the uterine horn (Figure 4.0).

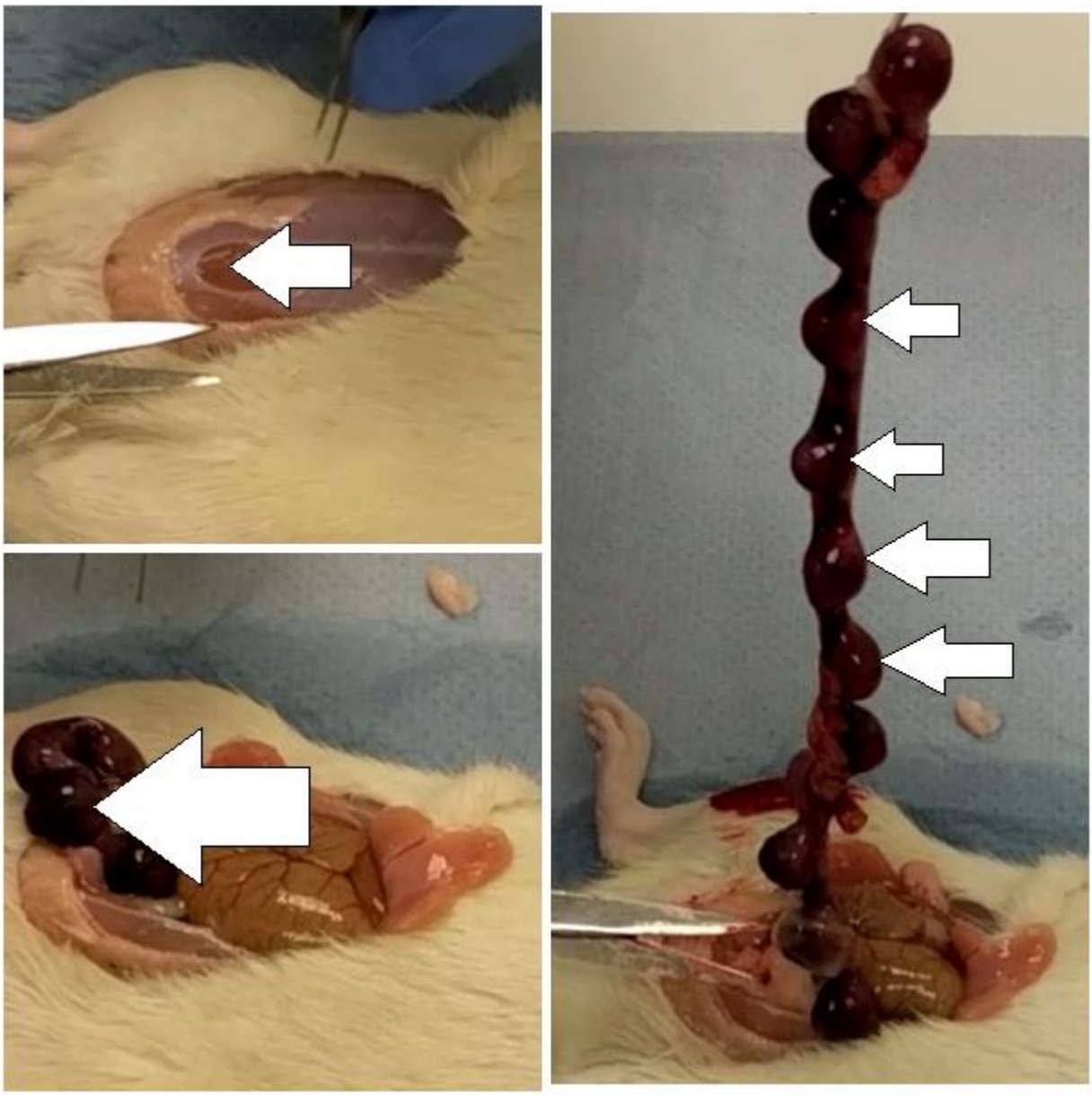

Figure 4.0: Isolation of embryos from rat. The upper left panel shows a sacrificed pregnant rat before extraction of the uterus, the white arrow indicates the incision site. The lower left panel indicates an exposed segment of the uterine horn after dissection of the sacrificed rat, highlighted by the white arrow. The right panel displays individual compartmentalised sections of the uterine horn during extraction of the uterus, each containing a single embryo; four examples are highlighted with white arrows.

Upon retrieval of the uterus, the segmented embryo compartments were individually cleaved from the uterine horn. A transverse incision made along the outer membrane of the embryo compartment resulted in the release of internal pressure and expelling of the amniotic fluid along with the embryo. The utilisation of 21 gauge hypodermic needles as dissection tools resulted in precision isolation of the spinal cord from the other tissues of the body, while allowing dorsal root ganglions (DRGs) to remain attached to the ventral horn. Transversely slicing the intact spinal cord into segments of 1-2 mm^2 explants provided 5 ± 1.5 spinal cord explants (SCEs) per embryo (Figure 4.1). Therefore, one pregnant rat yielded 65 ± 35 SCEs for each experiment.

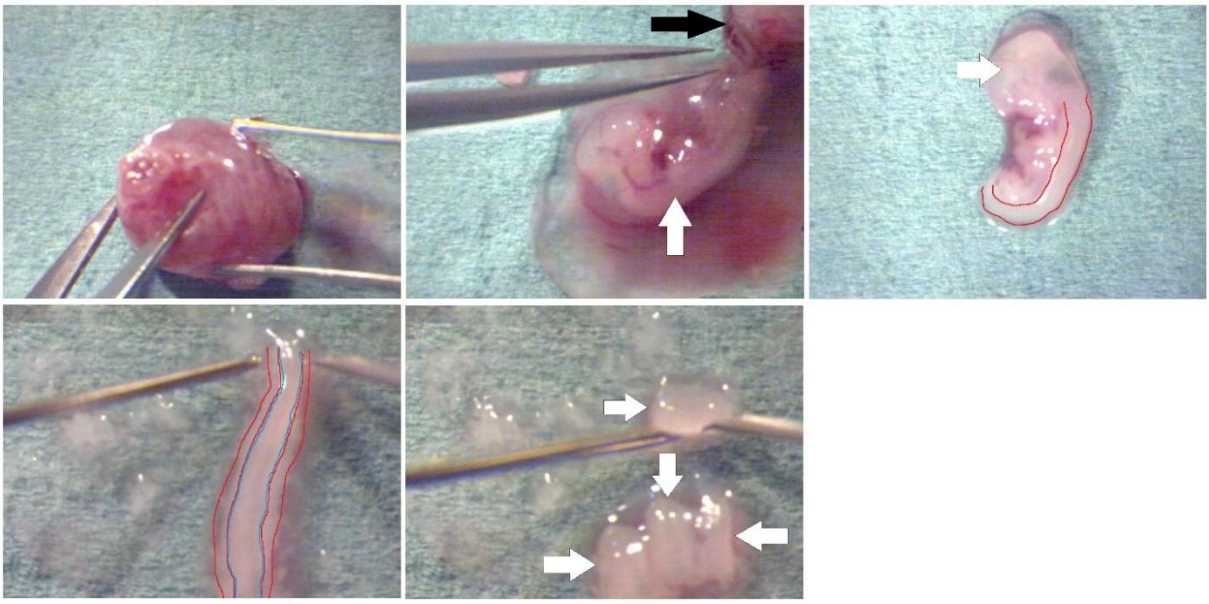

Figure 4.1: Isolation of spinal cord from ED 13.5 rat embryo. The upper left image panel displays an individually cleaved compartmentalised section of the uterine horn, which contains a single rat embryo. The upper middle panel shows the embryo (white arrow) being released from the uterine compartment, highlighted with the black arrow. The image panel on the upper right is representative of an isolated ED 13.5 rat embryo. The head of the intact embryo is highlighted with the white arrow and the spinal cord is shown between the two red lines. The lower left panel shows a dissected intact spinal cord. The dorsal root ganglions are located between the red lines as they flank both side of the ventral horn, shown between the blue lines. The lower right panel is representative of 1-2 mm^2 spinal cord explants cut from the intact spinal cord. The white arrows show four individual explants.

4.1.1 Viability of Spinal Cord Explants

Before functional studies of nerve-muscle co-cultures could be conducted, the viability of SCEs cultured in SkMC DM (Table 2.1) were evaluated. The SCEs were plated and cultured for 24 hours in 6-well plates pre-coated with a 0.5% gelatin solution using the methods for SkMC culture detailed 2.1.1. Viability was confirmed if SCEs were able to adhere with the culture surface and sprout neurites within 24 hours of being plated (Figure 4.2). Phase contrast microscopy at 10X magnification was used to assess the percentage of adherent and sprouting SCEs. Following 24 hours of incubation, the results showed that 92% ± 8 of the plated explants were able to adhere with the culture surface. However, only 85% ± 9 of the explants attached and sprouted spinal outgrowths within 24 hours.

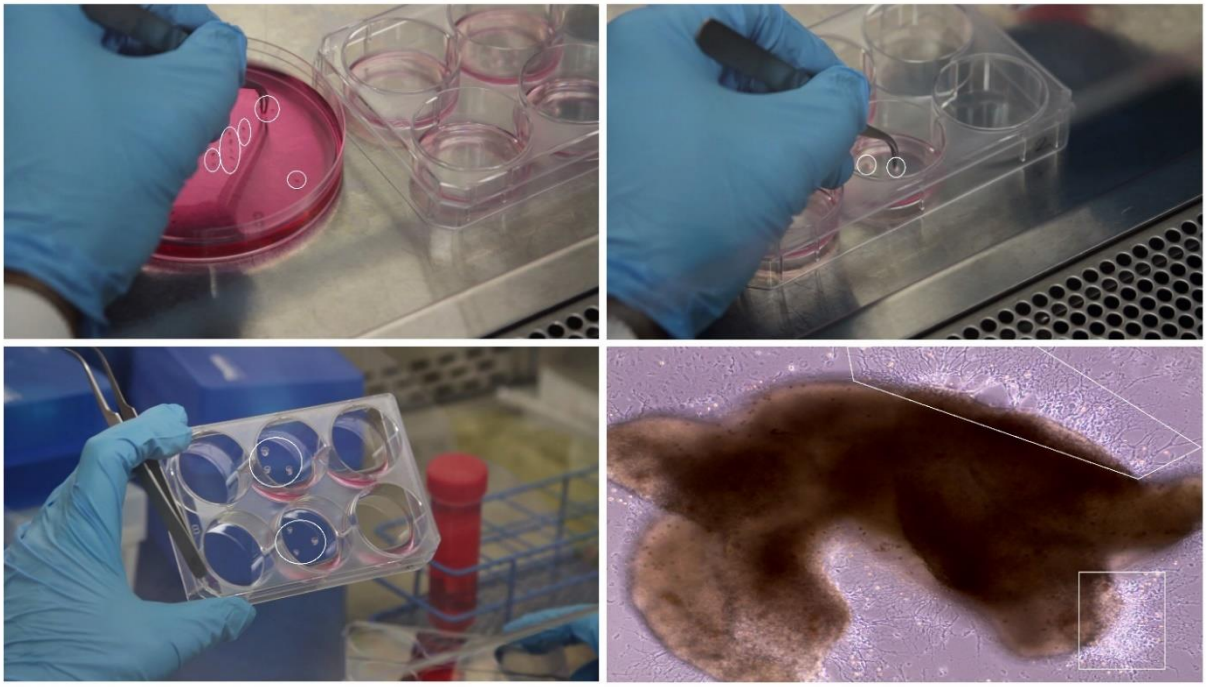

Figure 4.2: Viability of spinal cord explants in differentiation media. The upper left panel shows freshly isolated spinal cord explants in a 150 mm dish before being plated in 6-well plates, explants are encircled in white. The upper right image shows explants, circled in white, being plated onto the tissue culture surface immediately following isolation. The panel on the lower left exemplifies spinal cord explant adherence with the tissue culture surface after 24 hours of incubation. The lower right panel is a magnified image of a single spinal cord explant sprouting neurites after 24 hours. Examples of substantial sprouting are highlighted in the white boxes.

4.1.2 Validation of Neuron Proliferation

To verify the sprouting projections emerging from the SCEs were indeed neurons suitable for *in vitro* innervation of SkM myotubes, the methods detailed in 2.1.12 and 2.1.13 for immunocytochemistry (ICC) were applied to the cultured SCEs 72 hours after plating on the culture surface to detect protein expression indicating neuronal growth. The microtubule cytoskeletal element Class III β-tubulin (β-III-tubulin) is concentrated almost entirely in neurons (Sullivan and Cleveland, 1986; Caccamo et al., 1989) and prominently expressed during embryonic and postnatal development (Katsetos, Legido, et al., 2003). Making it an ideal target protein to identify neuronal growth, which has also been used to identify neurons in previous *in vitro* studies (Katsetos, Herman, et al., 2003). The use of immunofluorescence microscopy at 10X magnification resulted in the observation that neurite projections emerging from the SCEs do in fact express β-III-tubulin, verifying the proliferation of neurons emerging from the SCEs (Figure 4.3).

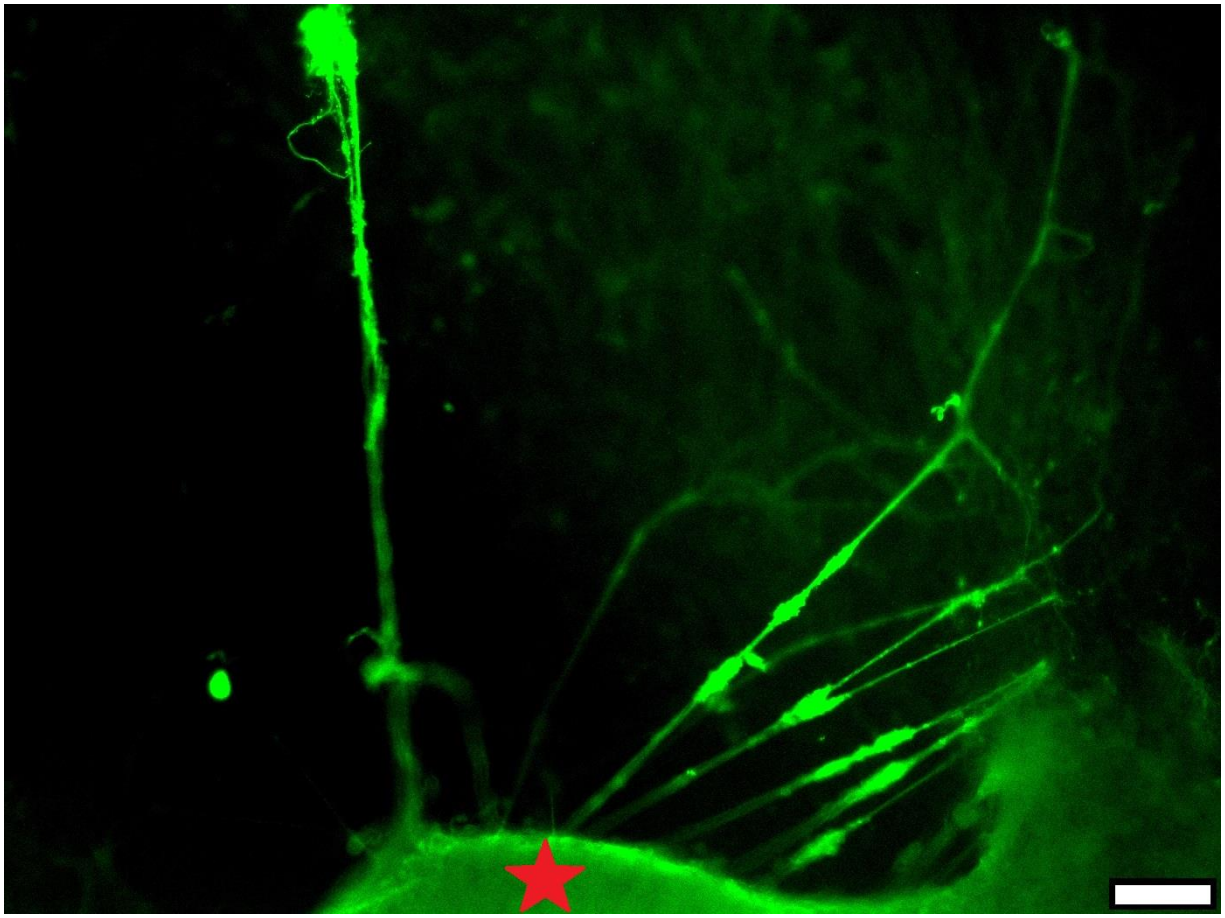

Figure 4.3: Neuronal outgrowth originating from ED 13.5 rat embryo spinal cord explant. A representative image of a cultured spinal cord explant (SCE) 72 hours after plating. The SCE is visible at the bottom of the image highlighted with a red star. Neurites were observed sprouting outward from the SCE. Stained for β-III-tubulin (green). Scale bar = 100 µm.

4.1.3 Characterisation of Co-culture Morphology

Upon confirmation of SCE viability in culture and their ability to generate β-III-tubulin^{+} neurons suitable for the innervation of SkMCs, the preliminary requirements for nerve-muscle co-culture were attained. Therefore, C25 were co-cultured with SCEs from ED 13.5 rat embryos using the methods described in 2.1.7 and 2.1.8 to induce functional innervation of differentiated myotubes and establish NMJ formation. A morphological assessment of the co-cultures was performed at 24, 48 and 72 hours after plating the explant with the myoblasts (Figure 4.4). At 24 hours, myoblasts fusion was absent and the cells displayed typical characteristics of mononucleated myocytes, indicating the cells were still in the initial stage of differentiation (Figure 4.4a). Successfully adhered explants sprouted neurites and expanded over the myocytes, exhibiting growth of 420 µm ± 36 emanating from the explant after 24 hours. If explants did not adhere to the myoblasts and initiate neurite sprouting by 24 hours, they were removed from the culture. At 48 hours, obvious myocyte-to-myotube differentiation had commenced and neurite length expanded further to 962 µm ± 57 (Figure 4.4b). After 72 hours, neurite growth expanded to 1503 µm ± 148, with progressive myotube maturation (Figure 4.4c). Importantly, connections of neuronal axon terminals with myotubes were visible (Figure 4.4d) and the first spontaneous contractions of individual myotubes were observed. This provides initial confirmation that the immortalised human myoblasts were innervated by neurons from rat embryo SCEs after as little as 3 days of co-culture.

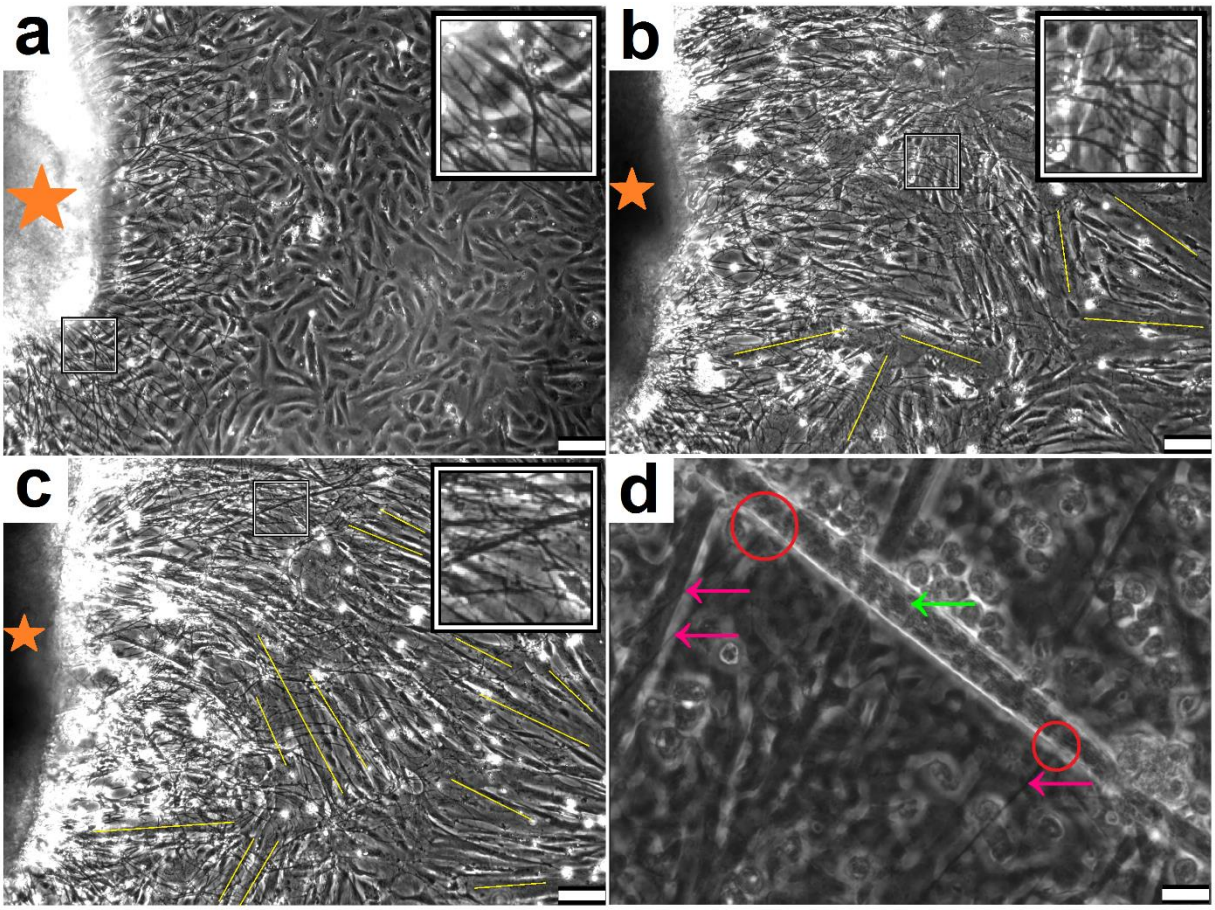

Figure 4.4: Young immortalised human skeletal muscle cells co-cultured with ED 13.5 rat embryo spinal cord explants. a) Phase contrast image of a spinal cord explant (SCE), highlighted with the orange star, sprouting neurites (shown in enlarged inset) after 24 hours over undifferentiated myocytes. Scale bar = 100 µm. b) Multinucleated myotube formation (indicated with yellow lines) after 48 hours with continued expansion of neural projections (shown in enlarged inset) emanating from the spinal cord explant (orange star). Scale bar = 100 µm. c) Maintained neurite growth (shown in inset) and continued myotube formation (yellow lines) at 72 hours. Scale bar = 100 µm. d) Neuronal axons (pink arrows) form a visible link (circled in red) with a myotube (green arrow) at 72 hours. Scale bar = 25 µm.

To determine if the first observable occurrences of myotube contractions (at 72 hours) in the co-culture system were due to neuron-induced morphological changes to myotubes, the myotube differentiation parameters were measured (Table 2.2). Phase contrast microscopy was utilised to quantify any significant differences in the differentiation of aneurally cultured and co-cultured myoblasts after 72 hours of incubation. Co-localisation of neuron axon terminals with differentiated myotubes were observed in the co-cultures (Figure 4.5a). Whereas aneurally cultured SkMCs (Figure 4.5b) display visually similar myotube differentiation without neurons. The fusion index (FI) did not significantly differ between the co-cultured and aneural cells (86.2% ± 4.6 vs. 86.8% ± 5.1, P = 0.846, Figure 4.4c). Additionally, no difference was detected between the myotube area (MA) of both culture environments (66.3% ± 3.9 in co-culture vs. 69.2% ± 7.3 for aneural culture. P = 0.458, Figure 4.4d). Indicating differentiation of myotubes at this time point of development occurs autonomously from neural input. Finally, myotube hypertrophy was determined by evaluating the aspect ratio (AR). Both culture conditions exhibited no difference in the AR of co-cultured cells (10.8 ± 8.3) vs. aneural cultures (9.9 ± 8.9, P = 0.881, Figure 4.4e).

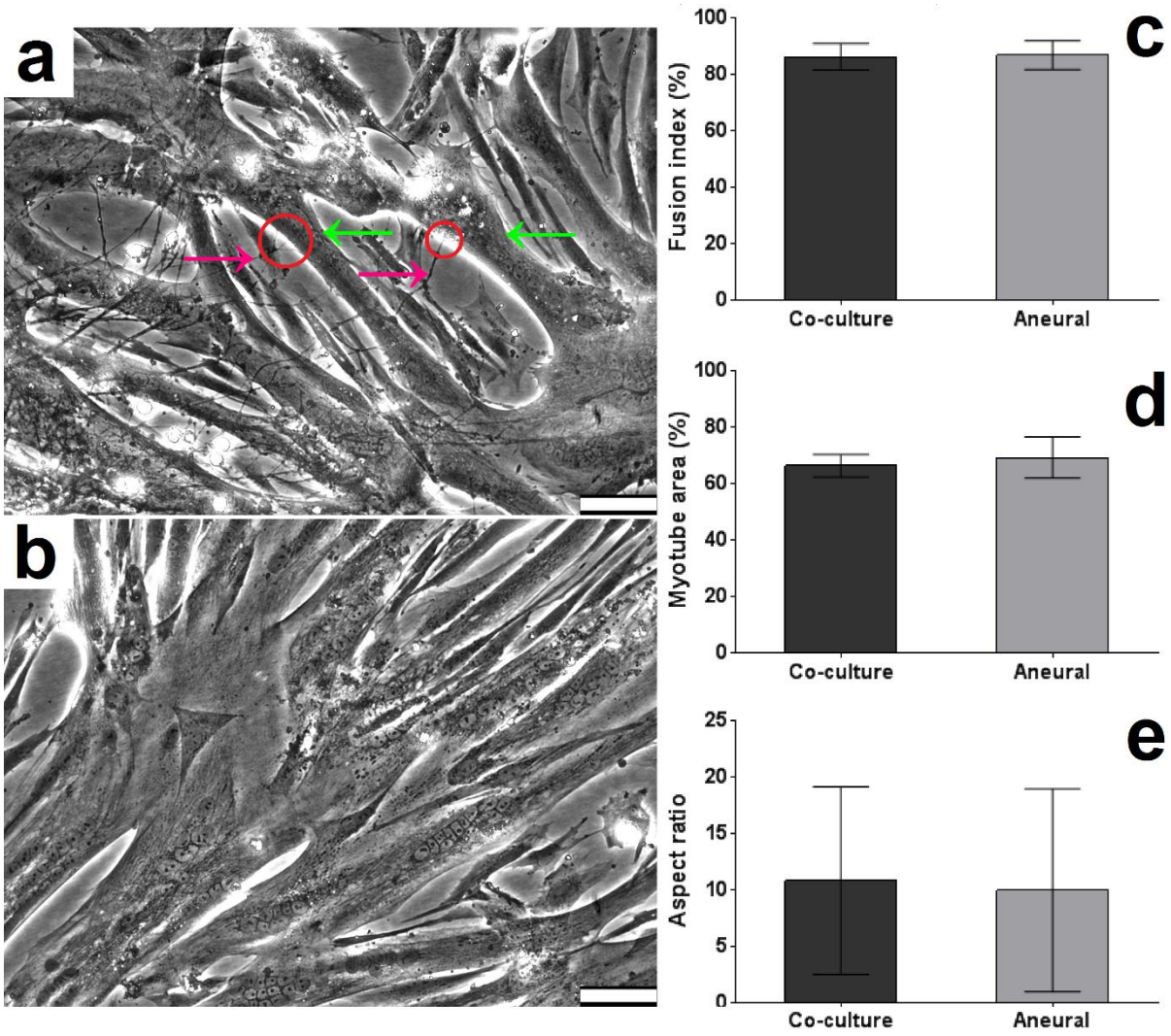

Figure 4.5: Differentiation parameters of aneural and co-cultured skeletal muscle cells at 72 hours. a) A representative image of co-culture morphology; neuronal axons (pink arrows) making contact (circled in red) with myotubes (green arrows). b) The image panel displays morphology of aneurally-cultured myotubes at 72 hours. c) Comparison of the percentage of cellular fusion in co-cultured and aneurally-cultured myotubes at 72 hours. d) Comparison of the myotube area in co-cultured and aneurally-cultured myotubes at 72 hours. e) Comparison of the aspect ratio in co-cultured and aneurally-cultured myotubes at 72 hours. Data presented as a mean, error bars signify ± SD. n = 3 independent experiments. Bar = 75 µm.

4.1.4 Spontaneous Myotube Contractions

The earliest contractions free of any external stimuli were observed in myotubes approximately 72 hours after co-culturing ED 13.5 rat embryo SCEs with C25. The co-cultures that had robust explant adherence with the myoblasts produced myotubes with contractile functionality, as long as atmospheric conditions were maintained at 37°C with a 5% CO_2. Even though co-cultures generated contracting myotubes observable within the first 72 hours, only individual arrhythmically contracting myotubes were perceived at this time point, with myotubes closest to the explant having the most frequent and forceful contractions. The co-cultures were monitored every 24 hours after witnessing the first contractions and maintained with regular media changes to promote further innervation, and continued maturation of myotubes. The co-cultures exhibited increasing myotube contraction frequency (CF), which was defined by the number of myotube contractions per minute, and an increase in the number of contracting myotubes. By co-culture Day 7, the myotubes were contracting continuously in a systematic pattern as large networks (Video 1). Suggesting myotube contractions functioned as a single motor unit receiving bursts of stimulation from MNs. However, multiple points of innervation were still visible on individual myotubes at this stage. Interestingly, contracting myotubes also took on the morphological characteristics of three-dimensional tubes whereas aneural myotubes maintained a flat two-dimensional morphology, firmly fixed to the culture plate surface.

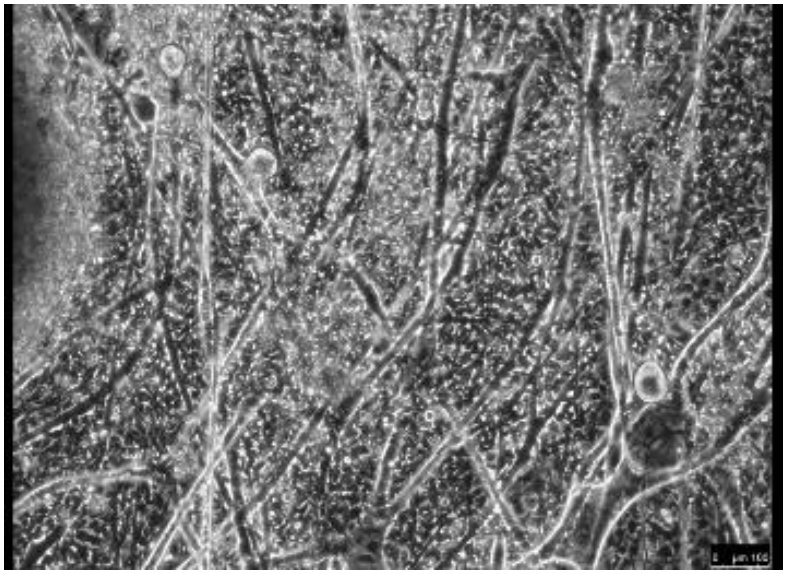

Video 1: Phase contrast video micrograph of young immortalised human myotube contractions at Day 7. Illustrative video of co-cultured myotubes spontaneously contracting as a network, devoid of serum, growth/neurotrophic factors, and external stimulus. Video captured at 24 frames per second. Bar = 100 µm. https://www.youtube.com/watch?v=Wg2is-SDdkE (Saini et al., 2019).

4.1.5 Spinal Cord Explant Co-culture vs Disassociated Spinal Cord Co-culture

To ensure optimal innervation of co-cultured myotubes, the efficiency of SCEs to induce contractions in the co-culture system was compared to myotubes co-cultured with disassociated spinal cord (DSC) cell suspensions, generated using the methods described in 2.1.10. The co-culture of myoblasts with DSC cell suspension was compared against SCEs due to disassociated cell suspension co-cultures being an established alternative to explant co-cultures (E Thomson et al., 2006). Optimal innervation of myotubes was quantified by analysing CF every 24 hours post co-culture for 7 days, using live phase contrast microscopy to assess 20 random fields of view at 10X magnification. The results revealed no observable myotube contractions in either SCEs or DSCs co-cultured with myoblast after the first 48 hours. Following 3 days of co-culture, initiation of myotube contractions were observable in the SCE co-cultures, contracting at a frequency of 0.18 Hz ± 0.09, no contractions were witnessed in the DSC co-cultures. On day 4, the myotubes in the SCE co-cultures increased CF to 0.43 Hz ± 0.24; no contractions were witnessed in the DSC co-cultures. The first measurable contractions in the DSC co-cultures were seen on day 5, contracting at a frequency of 0.13 Hz ± 0.08. However, this was significantly less ($P < 0.0001$) than the myotubes contracting in the SCE co-cultures, which increased CF further to 0.87 Hz ± 0.38. On day 6, SCE co-cultures were contracting at 1.04 Hz ± 0.36 and DSC co-cultures were contracting a significantly reduced ($P < 0.0001$) rate of 0.22 Hz ± 0.15. The myotubes in the SCE co-cultures has increased CF further on day 7 to 1.15 Hz ± 0.35. Whereas myotubes in the DSC co-cultures were contracting at a significantly reduced ($P < 0.0001$) rate of 0.38 Hz ± 0.14 (Figure 4.6). After confirming co-cultured SCEs are more efficient than DSC cell suspension at inducing myotube contractions, subsequent co-culture experiments where conducted with SCEs.

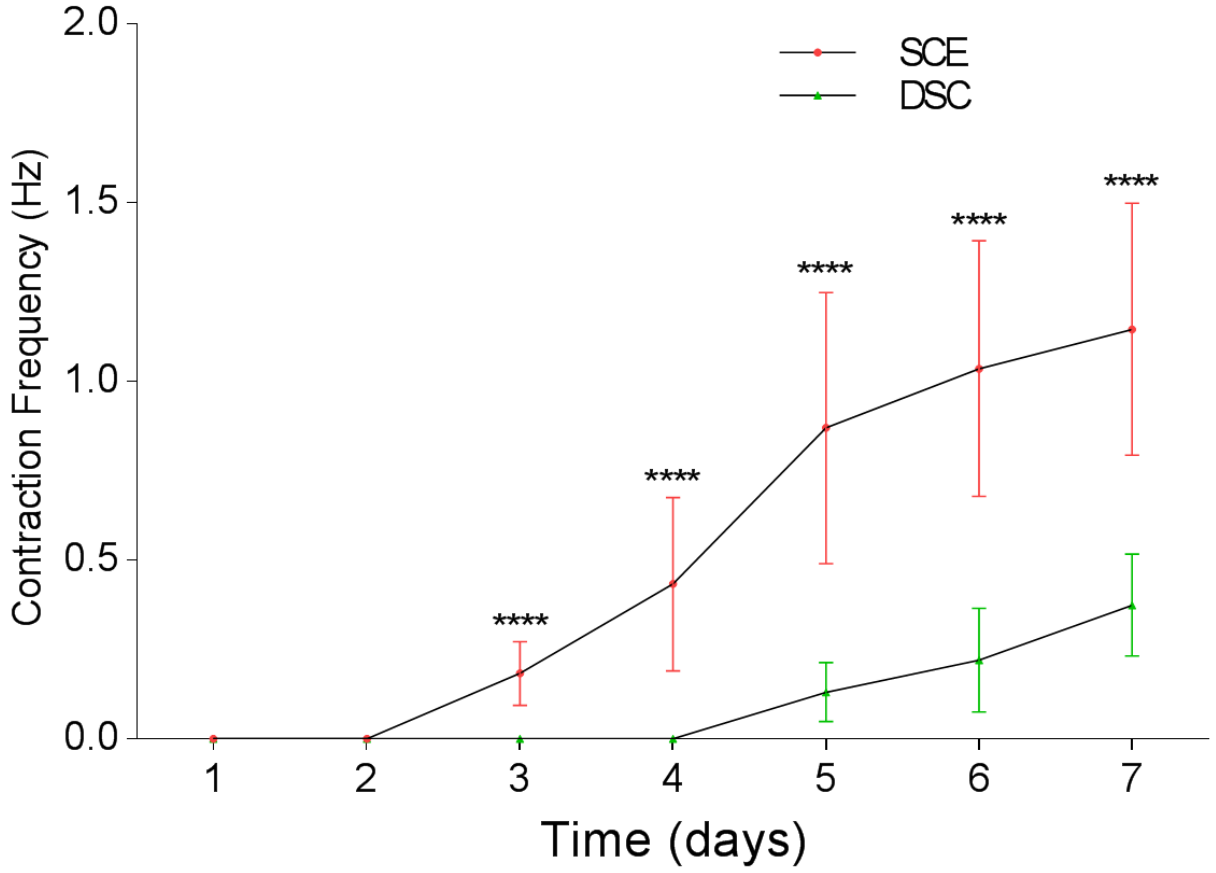

Figure 4.6: Contraction frequency in myotubes co-cultured with spinal cord explants or disassociated spinal cord cell suspension over 7 days. A line graph comparing the onset of myotube contractions and contraction frequency in young immortalised human myoblasts co-cultured with spinal cord explants (SCEs) or disassociated spinal cord (DSC) cell suspension, generated from ED 13.5 rat embryos. Data presented as a mean, error bars signify ± SD. n = 6 independent experiments. **** denotes $P < 0.0001$.

4.1.6 Expression of Rat Agrin

Neural agrin is a large (~400–600 kDa) heparan sulphate proteoglycan and is a prerequisite for NMJ formation. The release of agrin by motor neuron terminals (MNT) at the developing NMJ signals the transcription of select genes in the synaptic myonuclei to aggregate and stabilise postsynaptic acetylcholine receptors (AChRs) during synapse formation (Sanes and Lichtman, 2001). Accordingly, the methods described in 2.1.11 were applied and quantitative analysis was performed to verify the presence and concentration of agrin secreted in the SCE/myoblast co-cultures compared to SCE only cultures and myoblast only cultures. The concentration of agrin was measured at 72 hours with a rat agrin enzyme-linked immunosorbent assay. The results showed agrin expression in the co-cultured conditions was 1126 pg/mL ± 225, which was significantly higher ($P = 0.04$) than the agrin concentration in SCE only cultures (901 pg/mL ± 377) and the myoblast only cultures, which did not exhibit any measurable concentration of rat agrin.

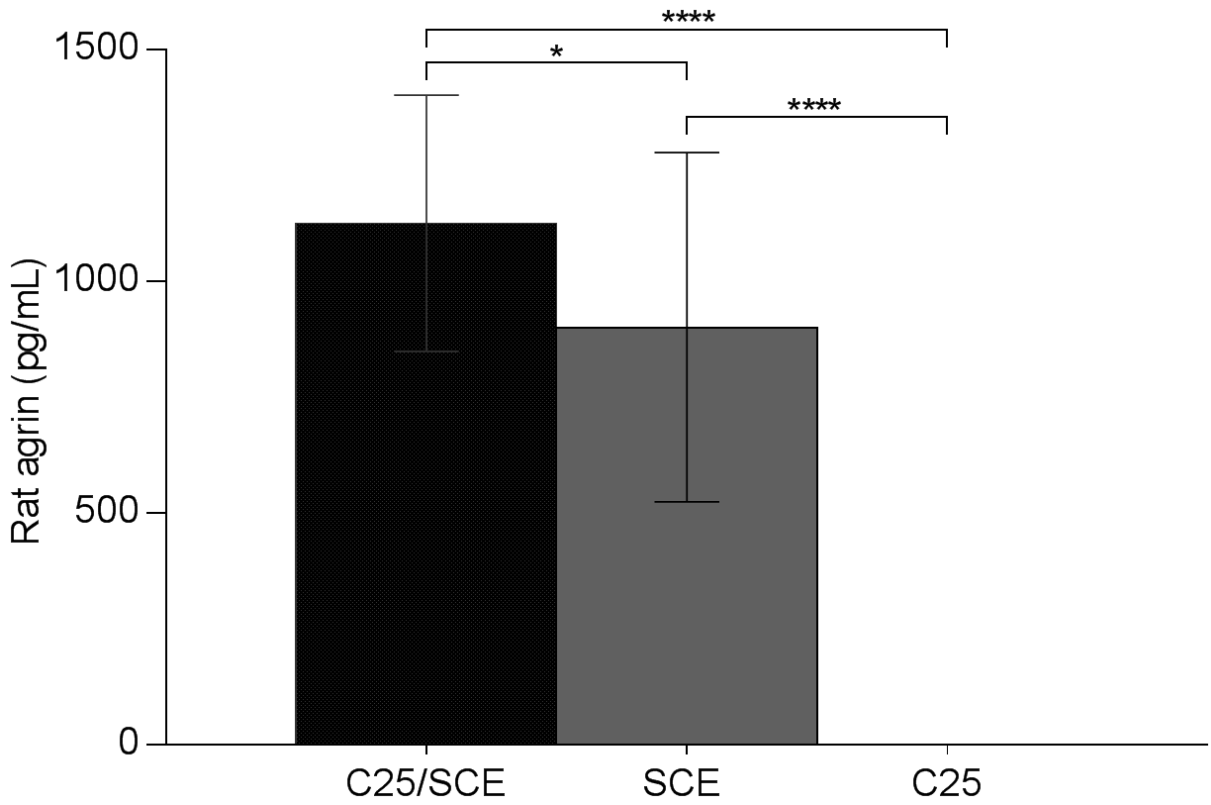

Figure 4.7: Concentration of rat agrin after 72 hours. A bar graph showing the concentration of rat agrin expressed in co-cultures of 25-year-old immortalised human myoblasts (C25) with spinal cord explants (SCEs) from ED 13.5 rat embryos compared with SCE only cultures and aneural C25 cultures. Data presented as a mean, error bars signify ± SD. * denotes $P < 0.05$; **** denotes $P < 0.0001$.

4.1.7 Preliminary Neuromuscular Junction Formation

The finding that agrin was indeed secreted by SCEs in the co-culture system and when cultured alone suggested that the co-culture system possessed the obligatory agrin needed for AChR clustering and NMJ formation (Wu et al., 2010; Tintignac et al., 2015). Thus, the subsequent experiment set out to determine if myotube contractions observed in the co-culture system were truly driven via MN stimulation due to NMJ formation. Using the methods detailed in 2.1.12 and 2.1.13, verification of preliminary NMJ formation was achieved with ICC of the co-cultures on day 7, when myotubes were observed to be contracting as a single motor unit. The co-cultures were stained with β-III-tubulin to show MN growth and with α-bungarotoxin (α-BTX), which binds as a competitive antagonist to nicotinic AChRs, to show AChR clustering on myotubes. Phase contrast and immunofluorescence microscopy were used to confirm the co-localisation of MNs emerging from the SCEs with AChRs on the myotubes. The results revealed multiple AChR clusters on differentiated myotubes integrated with MN axons and MNTs (Figure 4.8). Instances of multiple MN and AChR co-localisation (i.e. multiple points of innervation) were observed in 83.4% ± 12.6 of myotubes, indicating the early formation of NMJs in the co-culture system.

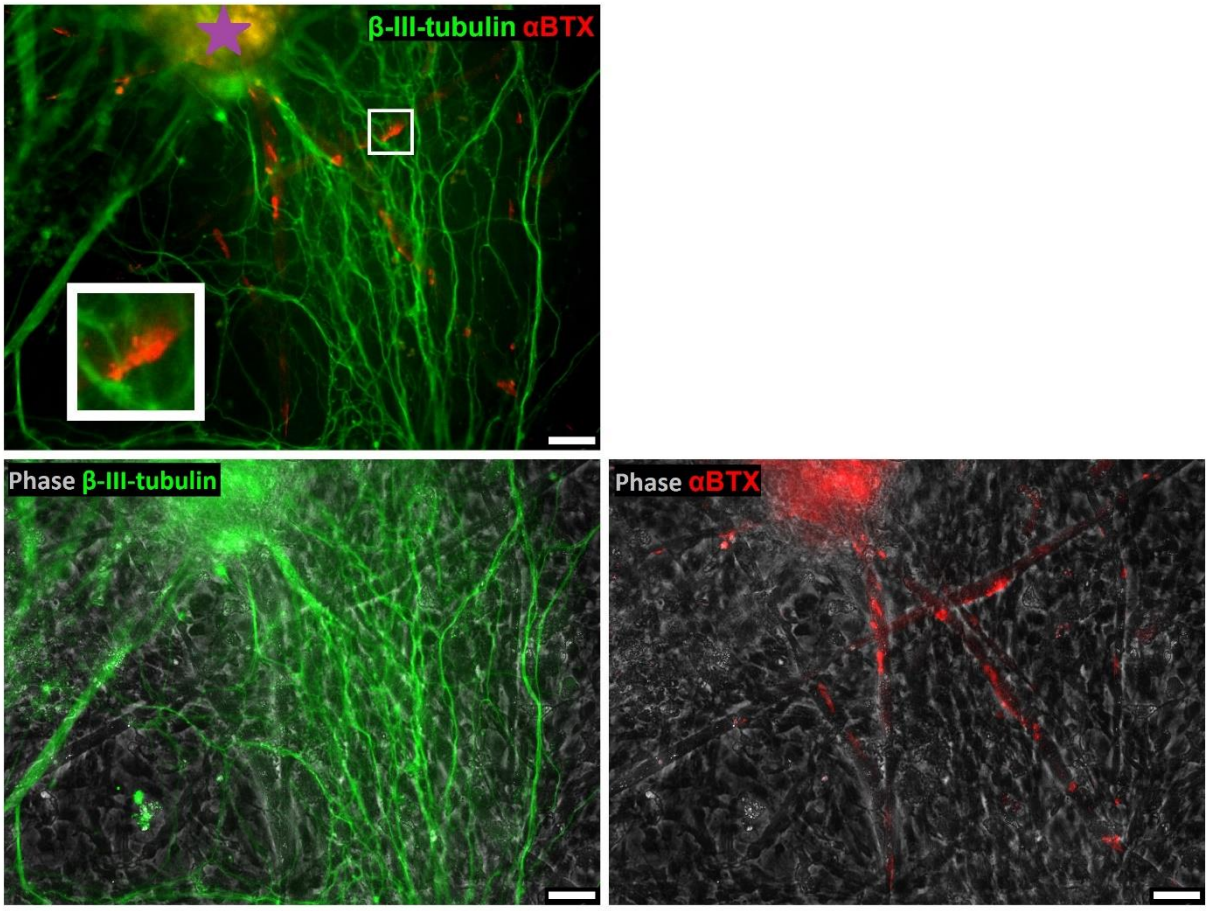

Figure 4.8: Co-localisation of embryonic rat neuron axons with acetylcholine receptor clusters on myotubes at day 7. The panel on the lower left is a phase contrast image of neuronal cells in the co-culture stained for β-III-tubulin (green). The lower right panel is phase contrast image of differentiated myotubes in the co-culture stained for α-bungarotoxin (α-BTX) (red). The panel on top is a combined immunofluorescence image showing the overlap of neuronal cells emanating from the spinal cord explant (indicated by the purple star) with acetylcholine receptor (AChR) clusters on the myotubes. The enlarged inset shows a cluster of AChRs (red) interacting with neuron axons (green). Bar = 50 µm.

4.2 Discussion

The findings from this study detail the successful establishment of a novel minimalist *in vitro* nerve-muscle co-culture system free from serum and growth/neurotrophic factors. The system enabled the survival of SCEs in simplified DM, promoted the proliferation of neuronal axons, generated contractile myotubes, and exhibited numerous instances of co-localisation between neuronal axons with AChRs, indicative of NMJ formation. The co-culture model was created by innervating C25 with neuronal outgrowths from ED 13.5 rat SCEs. This co-culture model delivers benefits beyond traditional myoblast monocultures as a research tool for investigating NM and muscle wasting disorders. For example, aneurally cultured human myotubes did not spontaneously contract in culture. However, as similarly witnessed *in vivo*, innervated myotubes in this co-culture system exhibited endogenously stimulated contractile functionality (Feher, 2017). Studies have been conducted using secreted proteins from rat-nerve/human-muscle co-cultures to treat aneurally cultured human myotubes, which resulted in some increased AChR clustering, mostly due to agrin exposure (Arnold et al., 2004; Bandi et al., 2008). However, treating anural myotubes with secreted proteins harvested from co-cultures failed to generate contractile function. This finding suggests that factors secreted by neuronal cells, such as agrin, are not independently adequate to induce contractions in myotubes *in vitro*, signifying the requirement of nerve-muscle contact via NMJs for physiological development of contractile myotubes, which are more representative of *in vivo* conditions. Interestingly, the co-culture model detailed in this current study displayed myotube contractions as early as 72 hours post co-culture, which may possibly be the first time contractile functionality has been observed at this time point of development in any nerve-muscle co-culture system. This finding suggests the initial emergence of NMJ formation, due to myotubes requiring nervous input from the MNs to induce contraction (Hong and Etherington, 2011). In addition to the benefit of this co-culture model being more physiologically similar to *in vivo* conditions of SkM development then aneurally-cultured myotubes, the system was also optimised for easy reproducibility. The co-culture model was established using the minimalist culture media listed in Table 2.1, which was devoid of serum, neurotrophic factors, and growth factors. This model is the first to generate contractile innervated myotubes using this simplified culture media composition, allowing for a drastic reduction in experimental variability. Contrastingly, previously established nerve-muscle culture systems require the use of serum or trophic factors to induce myotube innervation, NMJ formation, and spontaneous myotube contractions (Das et al., 2010; Guo et al., 2011; Rumsey et al., 2010; Demestre et al., 2015). Importantly, the potential reduction in experimental variability and ease of reproducibility this simplified co-culture model offers is evident when comparing the culture media formulation (Table 2.1) used to develop the co-culture model with some of the most contemporary

alternative nerve-muscle co-culture systems, which still require a complex of trophic factors to generate their systems successfully (Figure 4.9) (Guo et al., 2017).

Composition of enriched Co-culture media (medium 2).

Component	Full name	Concentration
Neurobasal/Neurobasal A		
B27 (50X)		1X
Glutamax (100X)		1X
rhNRG	Neuregulin-1-β1 EGF domain	100 ng/ml
Rhβ-NGF	Nerve Growth Factor	100 ng/ml
GDNF	Glial-derived Neurotrophic Factor	10 ng/ml
BDNF	Brain-derived Neurotrophic Factor	20 ng/ml
Shh	Sonic Hedgehog, N-terminal peptide	50 ng/ml
RA	Retinoic Acid	0.1 uM
IGF-1	Insulin-like Growth Factor -I	10 ng/ml
cAMP	Adenosine 3′,5′-cyclic Monophosphate	1 uM
CNTF	Ciliary Neurotrophic Factor	5 ng/ml
NT-3	Neurotrophin-3	20 ng/ml
NT-4	Neurotrophin-4	20 ng/ml
Vitronectin		100 ng/ml
Laminin	Mouse Laminin	4 μg/ml
G5 (100X)		1X
Agrin		100 ng/ml

Figure 4.9: Culture media components required for successful generation of a recently established nerve-muscle co-culture system. Adapted from (Guo et al., 2017)

Therefore, this co-culture model offers ideal conditions for high-throughput research of the mechanisms responsible for the formation and development of NMJs and the advanced differentiation of contractile myotubes. The methods applied throughout this study were designed to minimise the time required to induce observable spontaneous myotube contractions and produce an abundance of functional NMJs. Through the efficient application of embryonic material harvested from a single pregnant rat, a potential yield of 100 SCEs were available for each experiment, allowing for a wide variation of experimental conditions and time points. In this co-culture model, individual myotubes begin to contract by Day 3. The contracting cells continued to increase CF and synchronous unified contractions were apparent by Day 7 (Video 1). Previously established nerve-muscle co-culture models involve intricate methods requiring various culture media formulations for separate myotube or MN differentiation for at least 10 days before co-culturing (Guo et al., 2011). While other studies have

presented NMJ formation at 21 days (Demestre et al., 2015). These lengthy protocols lead to avoidable delays and possible unintended variation to experimental procedures.

Neurons generated in this co-culture model were derived from ~1-2 mm^2 transversally sliced SCEs with intact DRGs (Kobayashi et al., 1987; Arnold et al., 2012). Experiments were conducted with embryo spinal cords mechanically disassociated to create a neuronal cell suspension before culturing with myoblasts; these conditions resulted in delayed initiation of spontaneous myotube contractions, increased arrhythmic contractions and reduced CF. This suggests motor and sensory neurons originating from both the ventral horn and dorsal root function mutually to correctly innervate myotubes and form NMJs, representative of an *in vivo* environment (Mears and Frank, 1997). Additionally, SCEs with intact DRGs contain a range of progenitor and supporting cells types, such as Glial cells. For example, Schwann cells perform vital functions in MN development, differentiation, and maintaining NMJ integrity (Riethmacher et al., 1997). Thus, indicating the presence of supporting cells may possibly encourage NMJ robustness and improved function of MNs *in vitro*.

4.3 Conclusion

In summary, a novel co-culture system was engineered using neurons from rat embryo spinal cords to innervate C25 for the first time, resulting in the contractile myotubes with an abundance of potentially functional NMJs. The similarity to *in vivo* contractility demonstrated by mature myotubes in this co-culture system improves research capabilities into SkM physiology allowing for improved pathophysiological elucidation, diagnosis, and treatment. The simplified serum and trophic factor free culture media implemented in this co-culture model allows for precise manipulations in the systems variability, which could lead to greater insight into NMJ formation and development. This co-culture model offers a relevant means for high-throughput investigations of human muscle physiology, NM pathology, and NMJ-linked disease and disorder.

Chapter 5: Characterisation of *in vitro* Neuromuscular Junctions between Embryonic Rat Motor Neurons and Immortalised Human Myoblasts

5.0 Background

5.0.0 Introduction

The previous chapter outlined the establishment of a novel nerve-muscle co-culture system free from serum and trophic factors, which was able to induce spontaneous contractile activity in differentiated myotubes and displayed co-localisation between neuronal axons and acetylcholine receptor (AChR) clusters, suggesting the formation of neuromuscular junctions (NMJs). The NMJ is highly specialised peripheral synapse that regulates skeletal muscle (SkM) contraction by functionally joining lower motor neurons with skeletal muscle cells (SkMCs). Formed during pre-natal development *in vivo*, the NMJ consist of a presynaptic motor neuron terminal (MNT), synaptic cleft, and postsynaptic motor end plate (MEP) (Bloch-Gallego, 2015). The pathology of a variety of neuromuscular (NM) and neurodegenerative (ND) diseases target either the presynaptic or the postsynaptic integrity of the NMJ, consequently leading to SkM loss and weakness (Punga and Ruegg, 2012). Additionally, one effect of old age is the degradation of AChRs on MEPs, which can induce denervation and subsequent age-linked muscle loss and dysfunction (Gonzalez-Freire et al., 2014). Thus, innervation of SkMCs is essential for the appropriate development and function of SkM. Research has shown degeneration of myotubes during embryonic development when SkMCs lack innervation (Ashby et al., 1993). A reduction in myotube size and severe deficiency in secondary myotube development (Wilson and Harris, 1993; Condon et al., 1990) are also evident in the absence of innervation. The findings from these studies provide evidence for the crucial role motor neurons (MNs) and NMJs play in regulating SkM fibre development, size, and maturation. In order to investigate the physiological development of innervated myotubes and the formation of NMJs, a small number of *in vitro* models have cultured MNs with SkMCs attempting to replicate NMJ formation (Das et al., 2010; Das et al., 2007). In more recent times, co-culture systems have made use of MNs derived from stem cells as well as MN cell lines, (Morimoto et al., 2013; Umbach et al., 2012). While other models have made use of primary or stem cell derived myoblasts (Demestre et al., 2015; Steinbeck et al., 2016; Chipman et al., 2014; Puttonen et al., 2015). Furthermore, the development of newer human induced pluripotent stem cell

(hiPSC) NMJ models have potential for specialised drug screening or patient-specific MN disease modelling (Inoue et al., 2014; Lenzi et al., 2016; Abujarour and Valamehr, 2015; Faravelli et al., 2014). While hiPSCs have potential for creating a fully human NMJ model there are points of contention in regards to maturation of the NMJ, as well as development and differentiation of MNs and SkMCs in such models (Siller et al., 2013). Furthermore, many of these previously established systems provide evidence of NMJ formation by simply demonstrating the co-localisation of neuronal axons and AChR clusters without analysing or confirming vital elements in MNs needed for transmission at the NMJ. For example, choline acetyltransferase (ChAT) and the vesicular acetylcholine transporter (VAChT) are essential for the synthesis and transport of ACh in MNs, making the neurotransmitter available for secretion into the synaptic cleft (Brandon et al., 2003; Maeda et al., 2004). Additionally, activity at the presynaptic MNT is observable through analysis of synaptic vesicle proteins such as Synaptotagmin 1 (Syt1), which is a Ca^{2+} sensor that triggers fusion of acetylcholine (ACh) containing vesicles with the MNT membrane (Brose et al., 1992; Yu et al., 2013). Furthermore, co-culture systems need to be examined for alternative neuronal cell populations such as Glial cells, which are known to be involved with the formation and maintenance of the NMJs (Feng and Ko, 2008). Previously established *in vitro* NMJ models also commonly disregard the characterisation of innervated myotubes for markers of advanced differentiation, such markers include the formation of striated myotubes, transversal triads, and peripherally located nuclei. Furthermore, structures of the postsynaptic apparatus beyond AChRs have rarely been characterised in detail. For example, the agrin-induced formation of postsynaptic elements such as muscle-specific tyrosine kinase (MuSK) and the 43 kDa receptor-associated protein of the synapse (Rapsyn) are vital for the formation of AChRs. Therefore, experiments in this study were conducted with co-cultures of ED 13.5 embryonic rat spinal cord explants (SCEs) innervating 25-year-old immortalised human myoblasts (C25) to explore the formation of NMJs and examine the advanced differentiation of innervated myotubes.

5.0.1 Aims

The objective of the present study was to characterise the novel co-culture system of ED 13.5 rat SCEs innervating young immortalised human myoblasts established in the previous study. Thus, the aims were:

1. Establish the optimal time for co-culture characterisation.

2. Characterise pre- and post-synaptic elements of NMJs formed in the co-culture system.

3. Investigate the maturation of innervated myotubes for markers of advanced differentiation.

5.1 Results

5.1.0 Optimisation of Co-cultures for Characterisation

To ensure optimal innervation, NMJ formation, and advanced differentiation of myotubes had occurred before characterisation of the co-cultured cells was conducted, the peak contraction frequency (CF) of co-cultured myotubes was used as an indicator of the co-culture vitality. Optimal conditions for co-culture characterisation were determined by quantifying CF every 24 hours post co-culture for 30 days, using live phase contrast microscopy to assess 20 random fields of view at 10X magnification. The methods used to determine CF were detailed in 2.1.19. The results revealed no observable myotube contractions in the co-cultured myotubes after the first 48 hours. Following 3 days of co-culture, initiation of myotube contractions were observable, contracting at a frequency of 0.19 Hz ± 0.1. The co-cultured myotubes were observed gradually increasing synchronous CF over the next eleven day. On day 14, myotube contractions peaked at a frequency of 1.33 Hz ± 0.39 (Figure 5.0). The co-cultured myotubes roughly maintained peak CF until day 17, followed by a gradual decrease of contractile activity in the innervated myotubes. Although myotube contractions were still detectable until the termination of the experiment on day 30, the frequency of contractions had reduced to 0.69 Hz ± 0.33, with contractile activity becoming increasing asynchronous. Thus, the determination was made to conduct characterisation of the co-cultures on day 14.

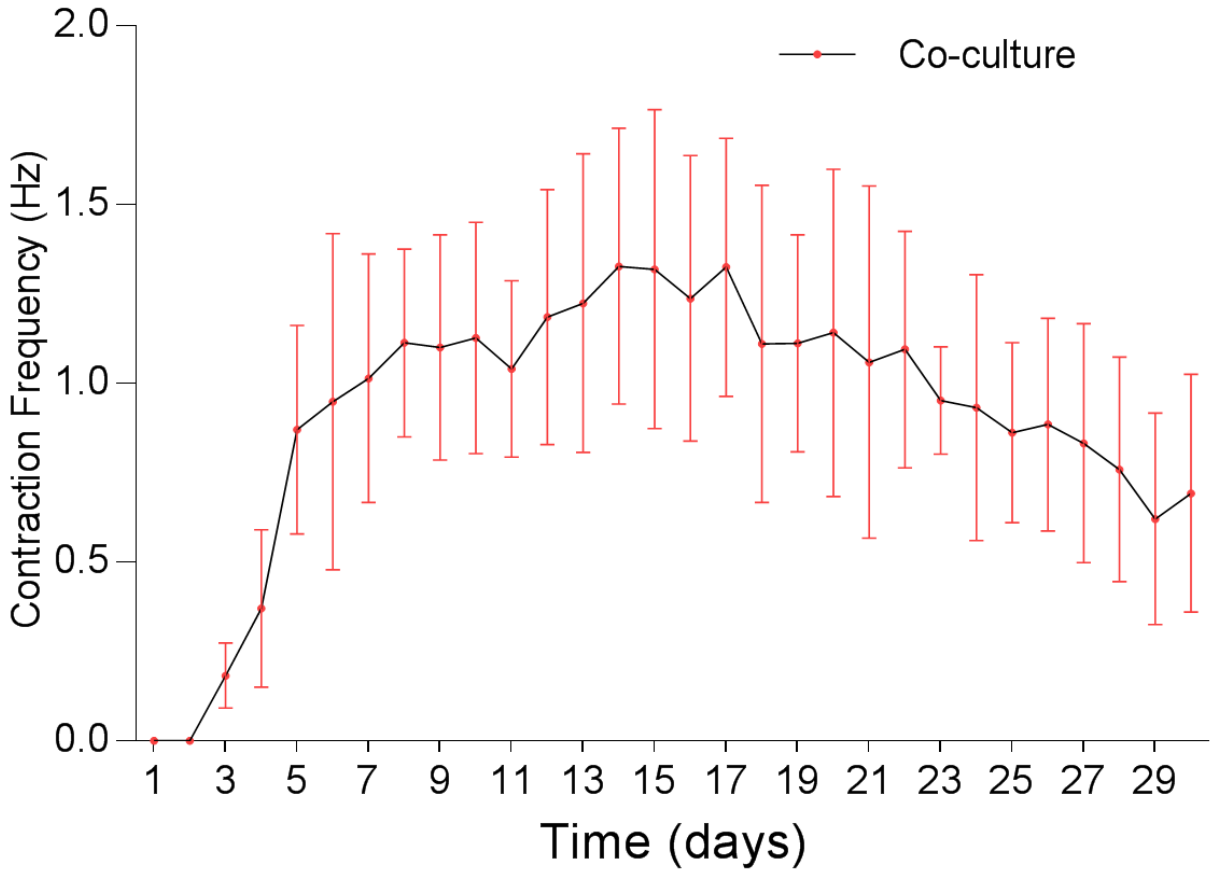

Figure 5.0: Contraction frequency in co-cultured myotubes over 30 days. A line graph showing the onset, increase, and decline of myotube contractions frequency in 25-year-old immortalised human myoblasts co-cultured with ED 13.5 rat embryo spinal cord explants. Data presented as a mean, error bars signify ± SD. n = 3 independent experiments.

5.1.1 Characterisation of Cholinergic Motor Neurons

By exploiting immunocytochemistry (ICC) techniques in the previous chapter, the preliminary observation was made that SCEs did indeed sprout neurites that positively expressed β-III-tubulin (Figure 4.3, 4.8), indicating the proliferation of neuronal cells in the co-culture system. The appropriate formation and development of NMJs is characterised by the convergence of cholinergic MNTs with MEPs on the SkMCs. Therefore, the following experiments were performed to confirm that sprouting neuronal cells from the SCEs did in fact include cholinergic MNs and to confirm the co-localisation of cholinergic MNs with SkM myotubes in culture. Confirmation of co-localisation was achieved via antibody staining visualised with confocal microscopy, detailed in methods sections 2.1.12 and 2.1.13. A cytoplasmic transferase enzyme found in elevated concentration in cholinergic neurons called ChAT (Oda, 1999) was stained to reveal cholinergic MNs in the co-cultures (Figure 5.1). To validate the presence of cholinergic MNs, supplementary staining was performed using VaChT, a functional mediator of ACh storage and transport by synaptic vesicles (Arvidsson et al., 1997) (Figure 5.2). Staining myotubes for myosin heavy chain (MHC) was used to show myotube differentiation. Staining of the co-cultured cells revealed $ChAT^{+}$ and $VaChT^{+}$ cholinergic MNs, with axons terminating on differentiated myotubes. Axon terminals were also observed establishing multiple points of contact with individual myotubes, comparable to similar observations of SkM innervation during embryonic myogenesis. *In vivo*, preliminary myotube innervation occurs via numerous branching axons, which originate from different MNs. Maturation of the innervation process causes axon pruning to occur, leaving individual MNs to innervate hundreds of mature muscle fibres, generating a functional motor unit (Low and Cheng, 2006). Notably, myotubes in this co-culture model also exhibited multiple innervations (e.g. 2 or more NMJs per myotube; Figure 5.6) similar to what is observed *in vivo* before axon pruning occurs.

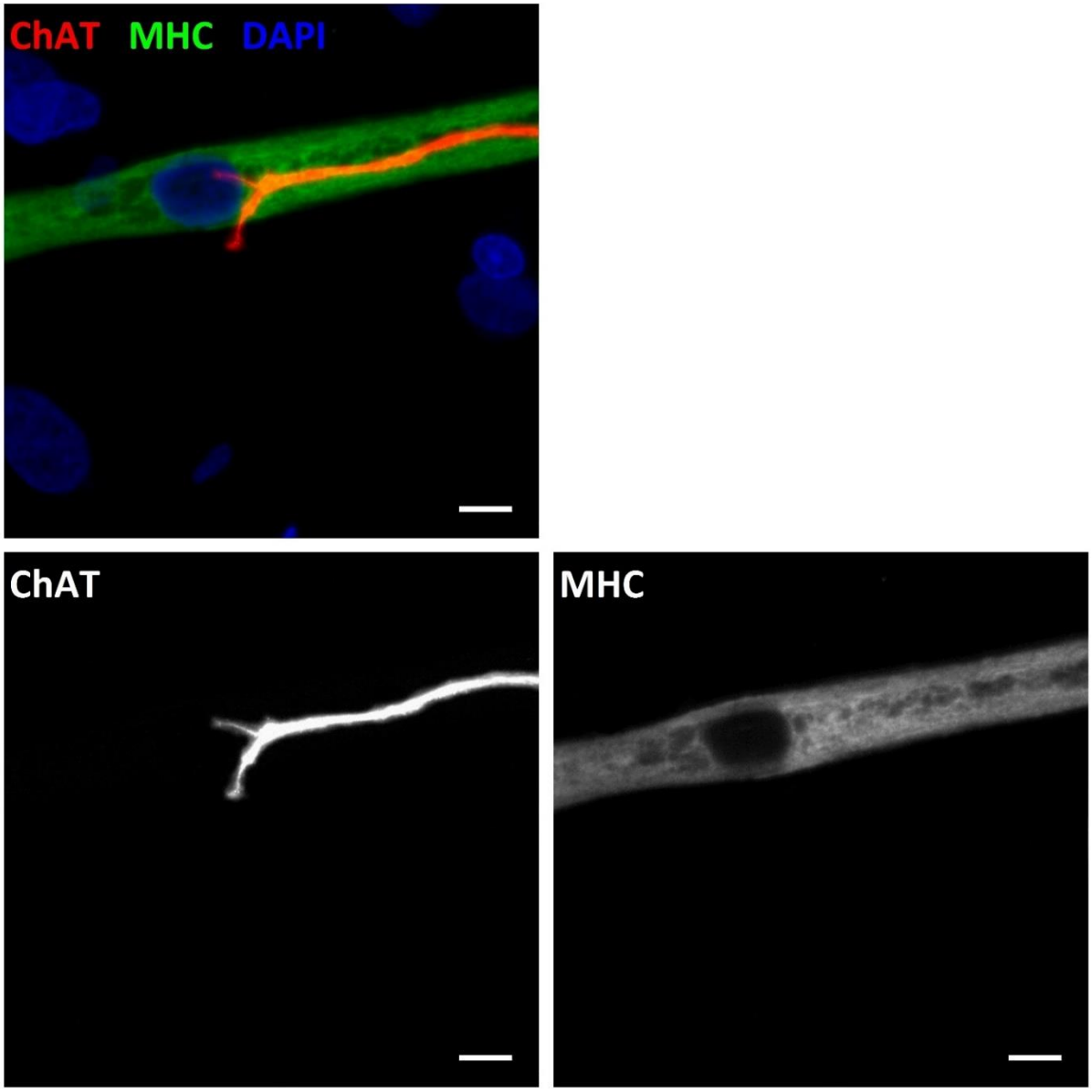

Figure 5.1: Co-localisation of cholinergic motor neurons with myotubes on Day 14. a) A representative image showing a single cholinergic motor neuron axon terminating on top of a single differentiated myotube. The co-culture stained for choline acetyltransferase (ChAT) (red), myosin heavy chain (MHC) (green), and DAPI (blue). Bar = 7.5 µm. Adapted from (Saini et al., 2019)

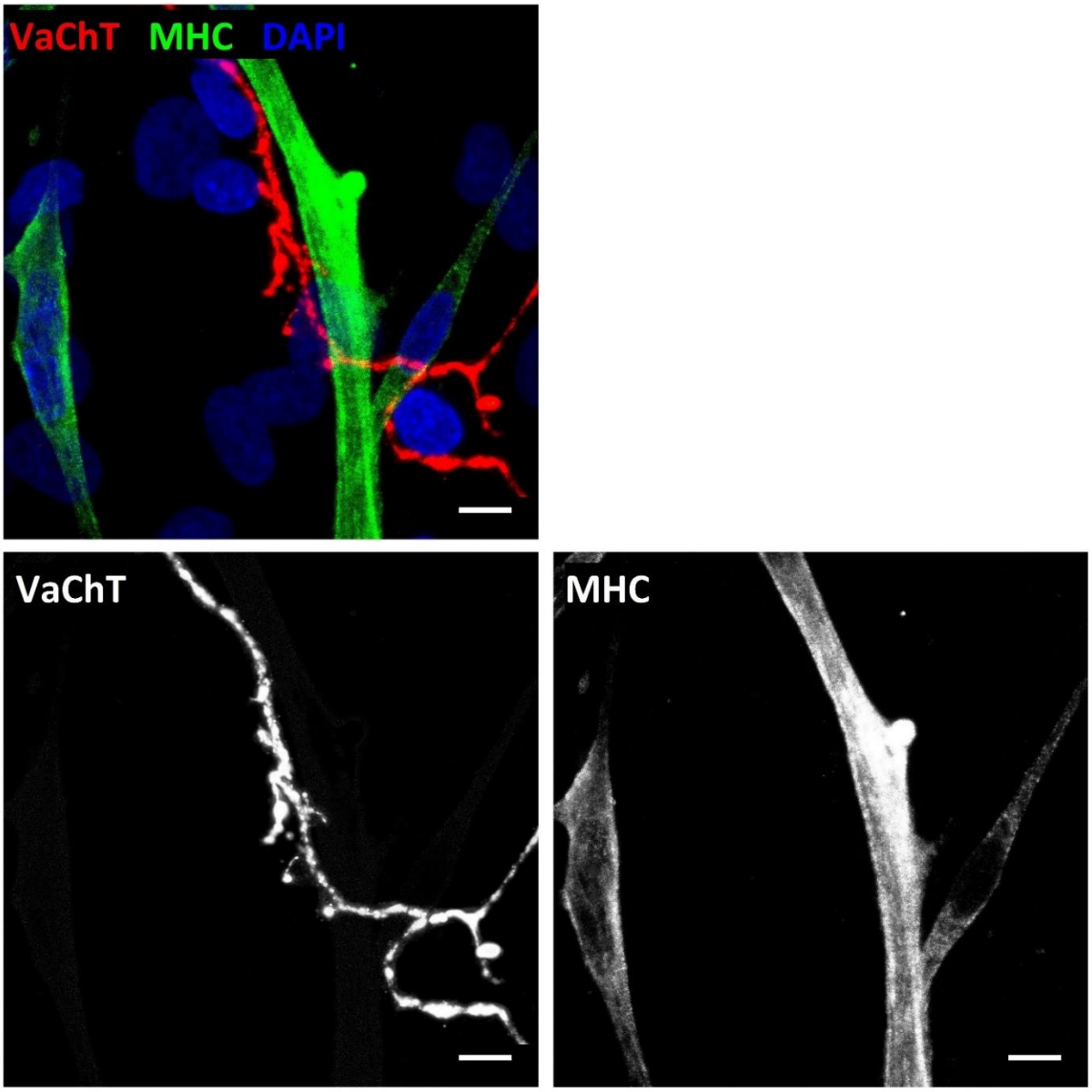

Figure 5.2: Confirmation of cholinergic motor neurons co-localising with myotubes on Day 14. A representative image showing cholinergic motor neuron axons co-localising with differentiated myotube. The co-cultures were stained for vesicular acetylcholine transporter (VaChT) (red), myosin heavy chain (MHC) (green), and DAPI (blue). Bar = 7.5 µm.

5.1.2 Characterisation of Neuroglia

The characterisation of many established *in vitro* NMJ models focus predominantly on describing aspects of the neurons and/or the myotube formation with marginal consideration for associated cells involved with NMJ generation, regulation, and development. The synapse-associated glial cells known as non-myelinating terminal Schwann cells cap motor nerve terminals *in vivo*, these cells are an essential component in NM synaptic maintenance and repair (Balice-Gordon, 1996). Thus, revealing Schwann cells in the co-culture system and the subsequent detection of interactions between MNs, Schwann cells, and myotubes may explain the formation of NMJs generated in this co-culture system. Using the methods described in 2.1.12 and 2.1.13, glial fibrillary acidic protein (GFAP), an intermediate filament cytoskeletal component involved in the structure and function of the neuroglia cytoskeleton (Jessen et al., 1990) was used as a marker to reveal the existence of non-myelinating Schwann cells. Neuronal cells were shown by staining the microtubule cytoskeletal component for β-III-tubulin (Figure 5.3). Myotubes were visualised by staining for MHC (Figure 5.4). The results showed co-localisation of neurons and Schwann cells was evident throughout the co-cultures. The enlarged inset image in Figure 5.3 illustrates the interaction between these cells, which may be indicative of Schwann cells capping axons, as observed *in vivo*. Furthermore, the results displayed co-localisation of Schwann cells and differentiated myotubes apparently throughout the co-cultures. The discovery of co-localisation and cellular interaction between myotubes, motor neurons, and Schwann cells within the co-culture system supports the concept that this co-culture model provides functional and robust innervation of myotubes via precisely coordinated NMJ formation, comparable to *in vivo* conditions.

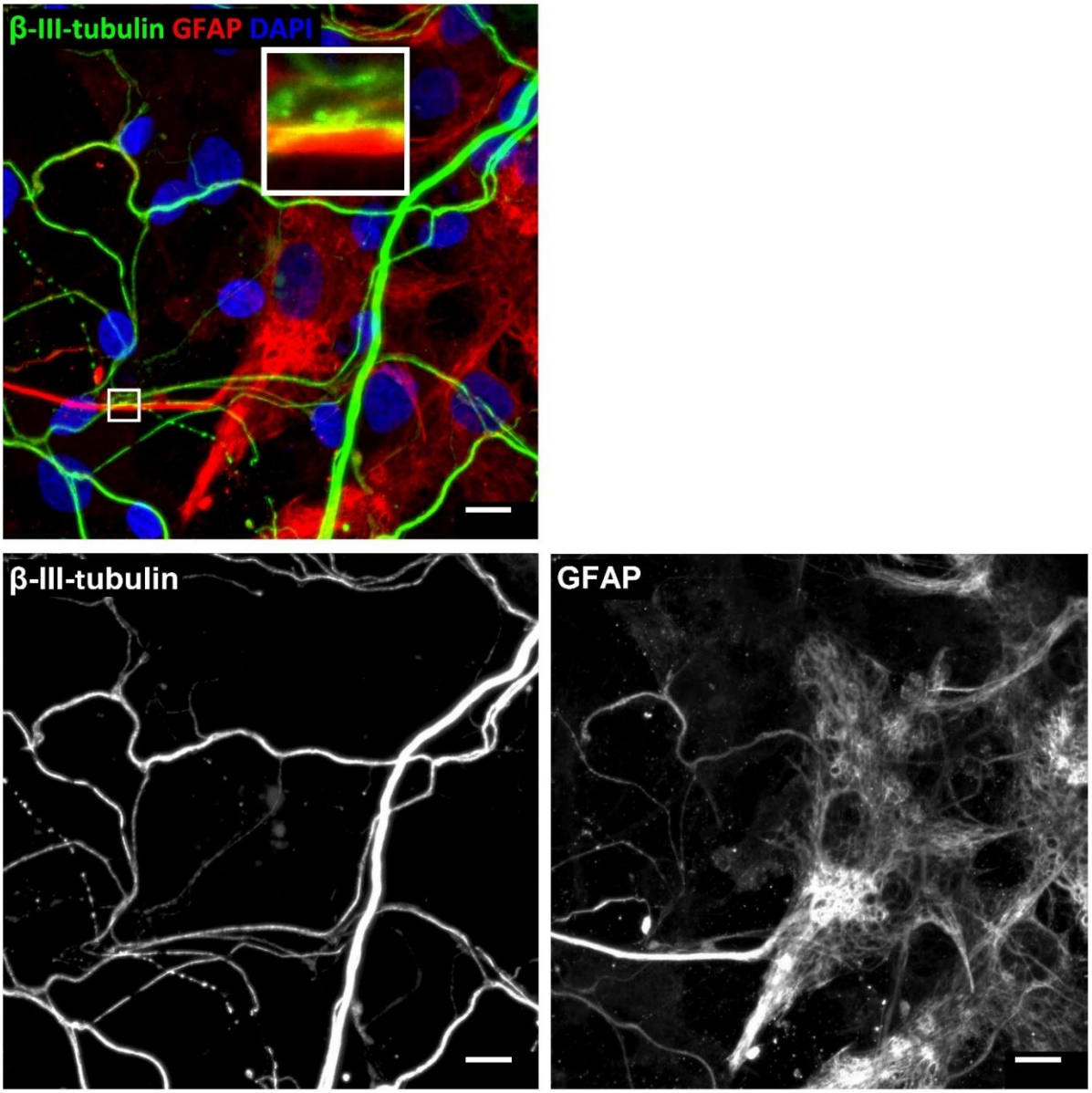

Figure 5.3: Interaction between neuronal axons and non-myelinating Schwann cells on Day 14. Image is representative of neuronal cells in the co-culture stained for β-III-Tubulin (green), Schwann cells stained for glial fibrillary acidic protein (GFAP) (red), and DAPI (blue). Enlarged Inset shows cellular interaction. Bar = 10 µm.

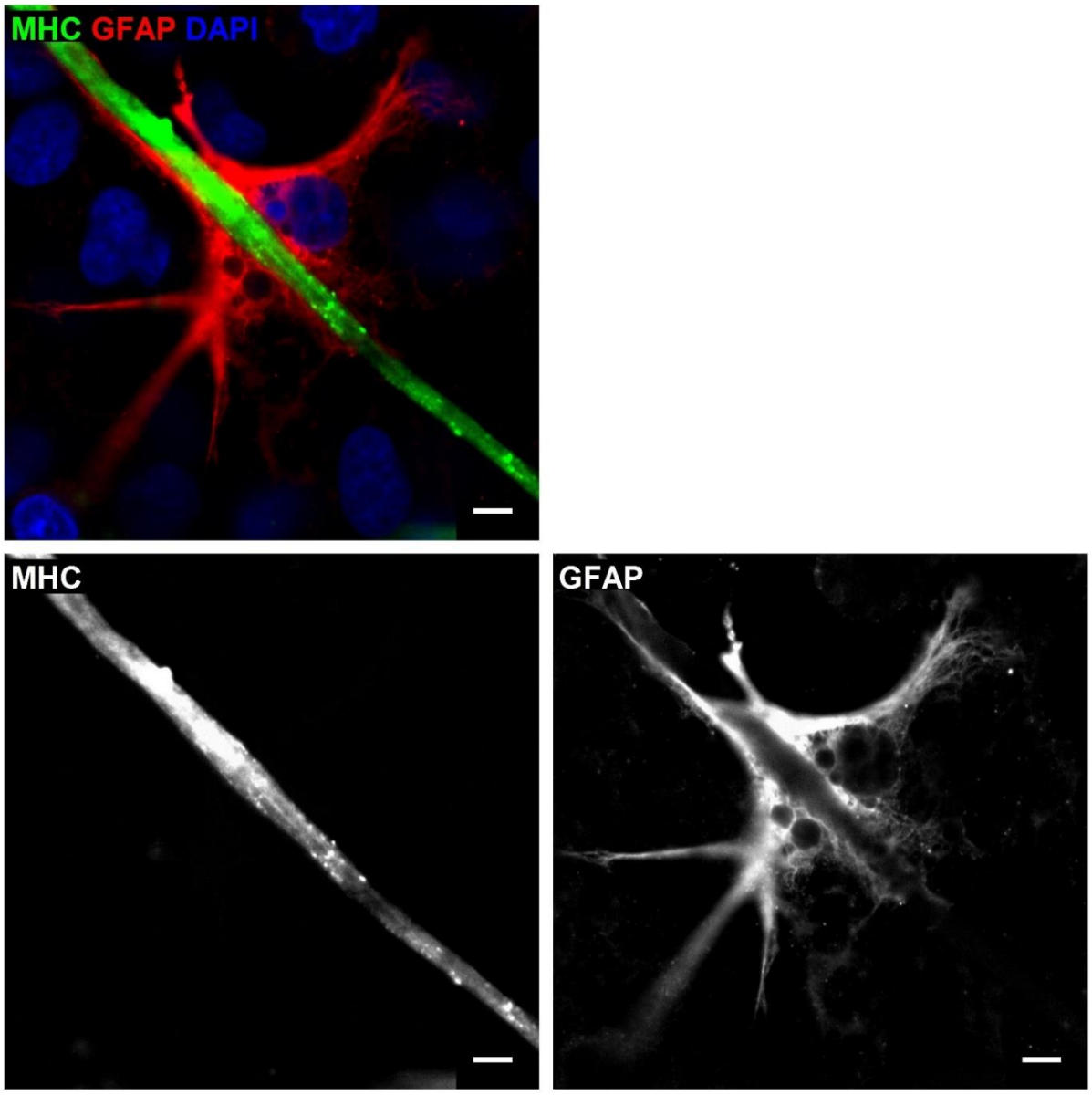

Figure 5.4: Co-localisation of non-myelinating Schwann cells and myotubes on Day 14. Image is representative of the interaction between myotube in the co-culture stained for myosin heavy chain (MHC) (green) and Schwann cells stained for glial fibrillary acidic protein (GFAP) (red), DAPI (blue). Bar = 5 µm.

5.1.3 Characterisation of NMJ formation

Following characterisation and validation of the co-localisation between cholinergic MN axon terminals and myotubes in the co-culture system, experiments were conducted to verify and characterise the formation of NMJs. The formation of NMJs is characterised by the substantial aggregation of AChRs on the myotube membrane in apposition of MN axon terminals. Using the methods described in 2.1.12 and 2.1.13, ICC was performed on the co-cultures, and axon terminals were identified by staining MNs for β-III-tubulin (Figure 5.5). To further validate NMJ formation, supplementary staining for MNs was also performed using neurofilament heavy (NFH) (Figure 5.6), an intermediate filament found in the cytoplasm of neurons (Lees et al., 1988). The accumulation of AChRs on the myotubes was characterised with fluorescently labelled α-bungarotoxin (α-BTX), known to bind specifically with AChRs on the myotube membrane (Young et al., 2003). The results revealed MN axons and terminals overlaying AChR clusters accumulated on the myotubes surface. Similar to *in vivo* observations, the AChR clusters in the co-cultures exhibited the greatest concentrations where MN axons and terminals overlapped the clusters, signifying the successful formation of NMJs. Experiments were also conducted to compare the development of NMJ morphologies in co-cultured myotubes in contrast to aneurally-cultured myotubes. Distinctive NMJ morphologies were quantified into five established NMJ morphological classifications (Valdez et al., 2010; Lee et al., 2013; Kummer et al., 2004; Sahashi et al., 2012), detailed in the methods section 2.1.14. Specifically, NMJ morphology was classified as mature, fragmented, faint, premature or denervated. The results showed no mature NMJs in the aneurally cultured myotubes. However, 43.5% ± 12.7 of the NMJs observed in the co-cultures were classified as exhibiting a mature morphology (Figure 5.7). When examining NMJs with a fragmented morphology, 6% ± 2.6 of the NMJs in the co-cultured cells were considered fragmented, no fragmented NMJs were observed in the aneural myotubes. The co-cultures displayed 4% ± 2.7 of NMJs classified as faint, no faint NMJs were seen in the aneural myotube cultures. The NMJ morphologies of mature, fragmented, and faint were all significantly higher ($P < 0.0001$) in the co-cultured myotubes when compared to the aneural myotube cultures. However, when comparing premature NMJ morphology, the aneurally-cultured myotube displayed 14.7% ± 5 as having premature NMJs, which was significantly higher ($P < 0.0001$) then the percentage of premature NMJs in the co-cultured cells (1.6% ± 1.6). Comparing the percentage of denervated myotubes resulted in 90.5% ± 6.2 of aneural cultures showing denervation, which was significantly higher than the 8.5% ± 5 of denervated myotubes in the co-cultured conditions.

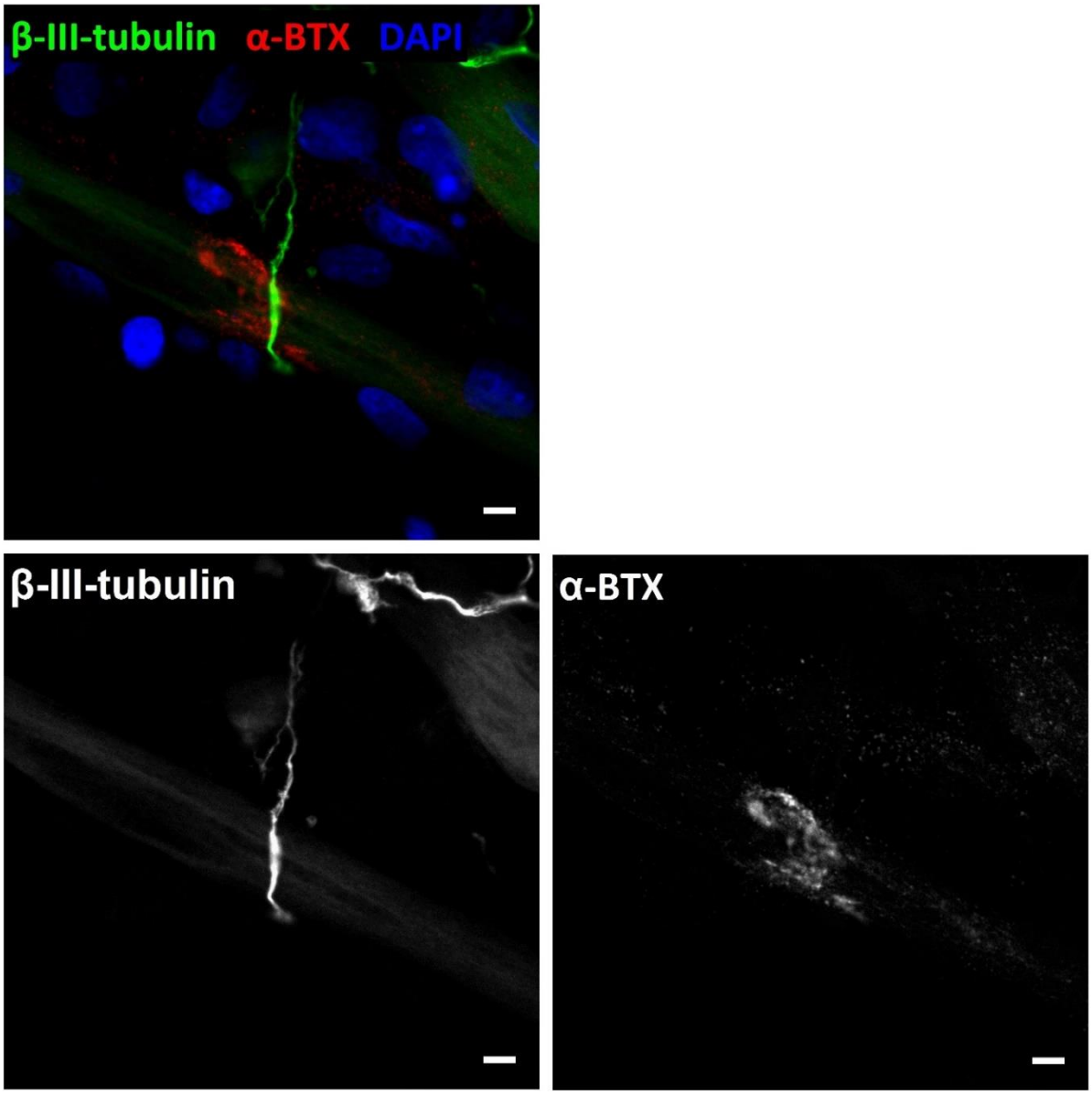

Figure 5.5: Characterisation of neuromuscular junction formation on Day 14. A Representative image showing an individual motor neuron axon terminal interacting with an acetylcholine receptor cluster in culture. The co-cultures were stained for β-III-tubulin (green), alpha-bungarotoxin (α-BTX) (red), and DAPI (blue). Scale bar = 5 µm. Adapted from (Saini et al., 2019)

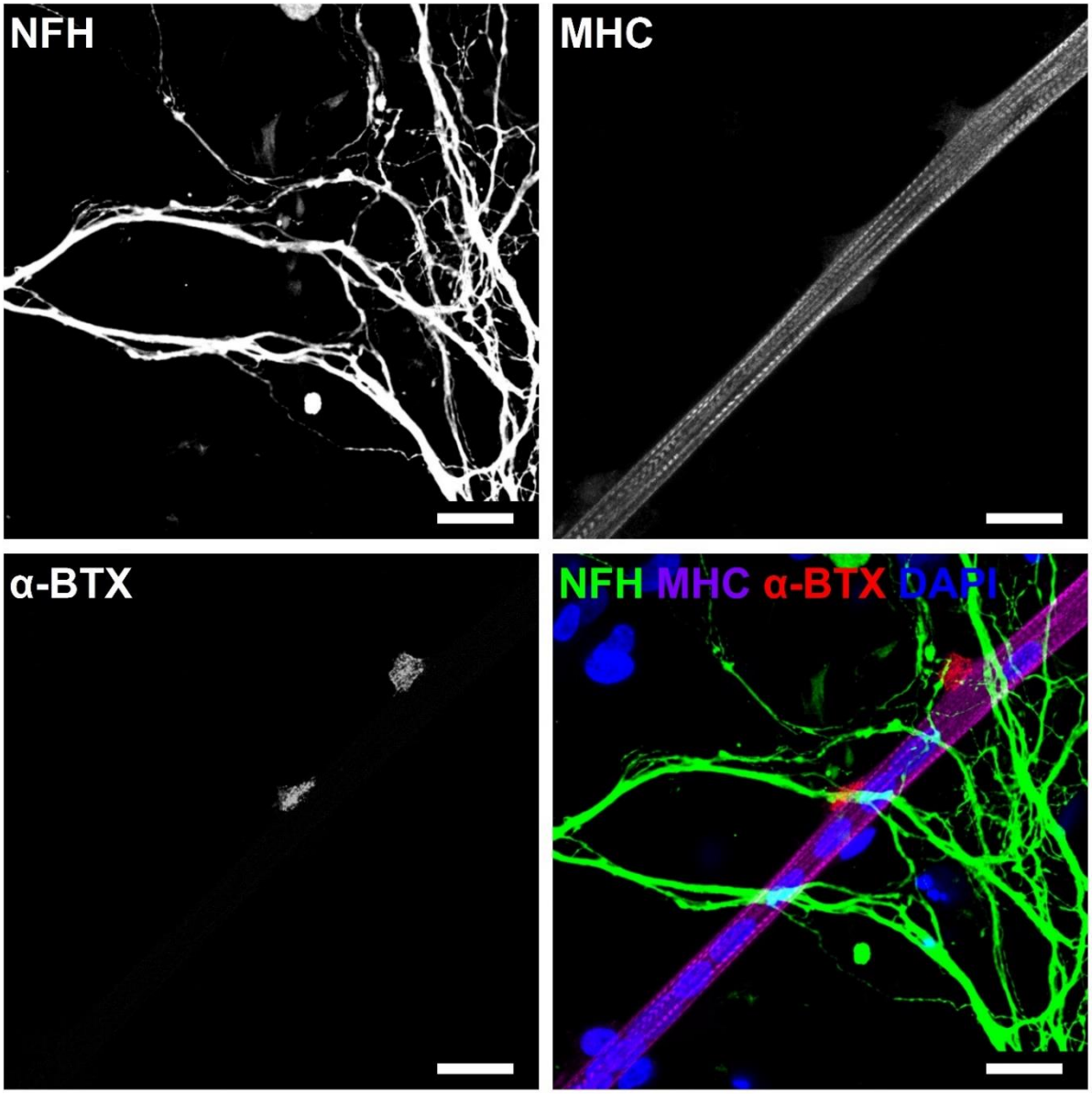

Figure 5.6: Confirmation of neuromuscular junction formation on Day 14. A Representative image showing motor neuron axons interacting with multiple acetylcholine receptor clusters on a differentiated myotube in culture. The co-cultures were stained for neurofilament heavy (NFH) (green), myosin heavy chain (MHC) (purple) alpha-bungarotoxin (α-BTX) (red), and DAPI (blue). Scale bar = 25 µm.

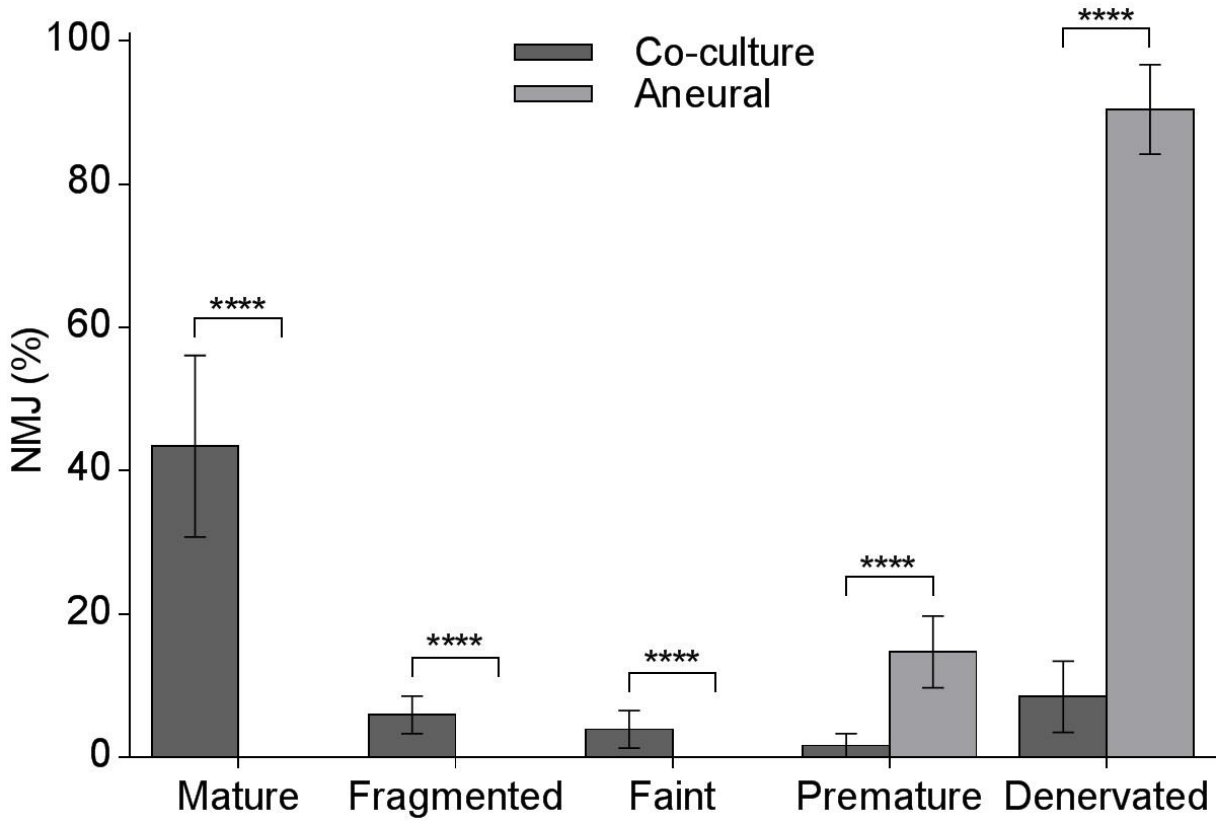

Figure 5.7: Neuromuscular Junction Morphologies on Day 14. A bar graph comparing the percentages of distinct neuromuscular junction (NMJ) morphologies in myotubes co-cultured with ED 13.5 rat embryo spinal cord explants against myotubes cultured aneurally. Each bar presents a mean of all wells with error bars signify ± SD from at least 100 NMJs. n = 4 independent experiments. **** denotes $P < 0.0001$. Adapted from (Saini et al., 2019)

5.1.4 Characterisation of Presynaptic Activity

Following confirmation of NMJ formation, subsequent experiments were conducted to assess NMJ functionality through the examination and characterisation of the presynaptic apparatus. When an action potential (AP) arrives at a presynaptic terminal, the local increase in the Ca^{2+} concentration triggers the release of ACh. This calcium-dependent exocytosis involves the precise docking of synaptic vesicles to the presynaptic membrane, which is regulated in part by the calcium sensor Syt1 (Brose et al., 1992). The methods described in 2.1.12 and 2.1.13 were used to confirm presynaptic NMJ activity, staining for NFH was used to visualise MN axons while activity at the terminal was shown by staining MN for Syt1 (Figure 5.8). The results revealed an elevated expression of Syt1 aggregated at the MNT, signifying presynaptic activity at the NMJ.

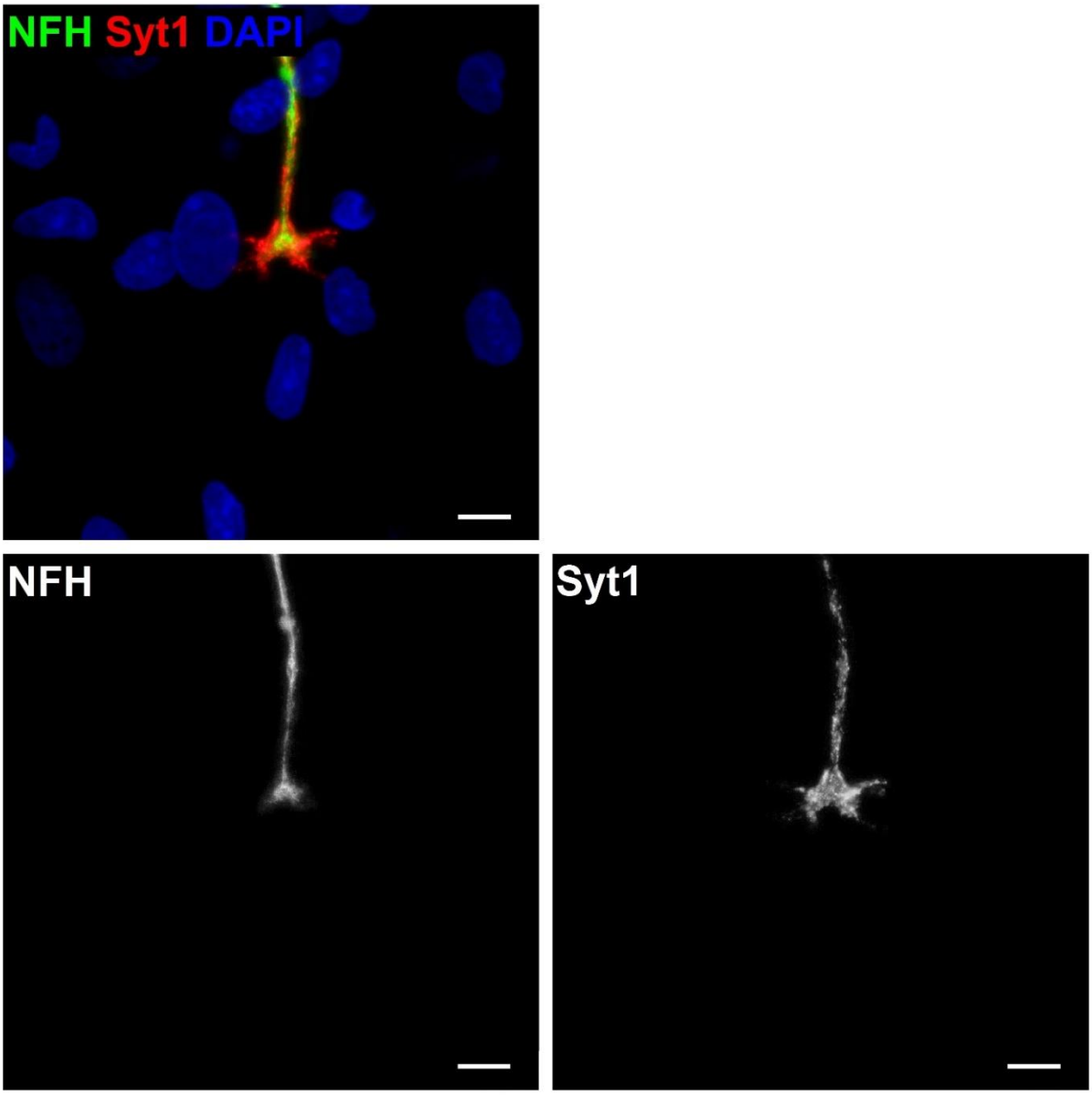

Figure 5.8: Characterisation of presynaptic neuromuscular junction activity on Day 14. A representative image of an individual neuronal axon expressing activity at the axon terminal. The co-cultures were stained for neurofilament heavy (NFH) (green), synaptotagmin 1 (Syt1) (red), and DAPI (blue). Bar = 7.5 µm.

5.1.5 Characterisation of Postsynaptic Elements

Upon determining MNT activity in the co-cultured cells, the next experiments were conducted to identify postsynaptic proteins known to co-localise with AChRs at the MEP. Agrin is crucial for AChR clustering in the MEP and is vital for precise NMJ formation. Presynaptic secretion of agrin by MNs induces activation and development of MuSK, which forms an initial scaffold for Rapsyn to advance recruitment of other postsynaptic MEP elements (Apel et al., 1995; Apel et al., 1997). The methods described in 2.1.12 and 2.1.13 were used to verify maturation and appropriate development of the MEP. The co-culture was stained with α-BTX to visualise AChRs along with antibodies for MuSK and Rapsyn. The results showed that both Rapsyn and MuSK were precisely overlaid the structure of the AChR clusters on the postsynaptic membrane (Figure 5.9).

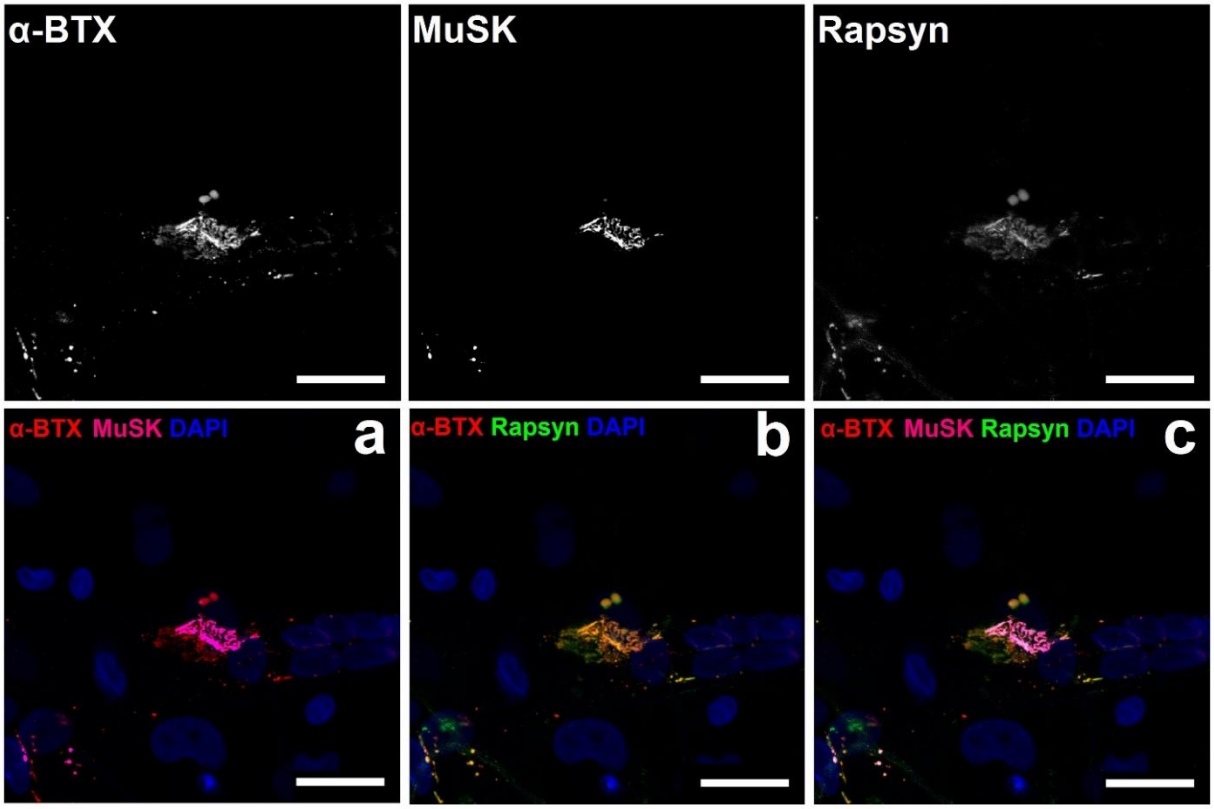

Figure 5.9: Characterisation of postsynaptic neuromuscular junction formation at Day 14. a) Image is representative of co-culture stained for alpha-bungarotoxin (α-BTX) (red), MuSK (magenta) and DAPI (blue). b) Image is representative of co-culture stained for alpha-bungarotoxin (α-BTX) (red), Rapsyn (green), and DAPI (blue). c) Image reveals interaction and detailed conformation of postsynaptic proteins MuSK (magenta) and Rapsyn (green) at the AChR stained with α-BTX (red), DAPI (blue). Scale bar = 25 µm

5.1.6 Characterisation of Innervated Myotubes

Mature myotubes *in vivo* display several features indicative of advanced differentiation. For instance, appropriately developed myotubes feature triads, which are arranged in a transversal manner. The structural composition of triads detected in myotubes having undergone advanced differentiation is formed by a transverse tubule (T tubule) with a sarcoplasmic reticulum (SR) known as the terminal cisterna on each side (Marty et al., 1994). The methods described in 2.1.12, 2.1.13, and 2.1.15 were used to determine if the co-culture system endorsed innervated myotubes to undergo advanced differentiation similar to developing myotubes observed *in vivo,* characterisation of both co-cultured and aneurally cultured myotubes was performed via antibody staining. T-tubules were identified by staining for dihydropyridine receptor (DHPR) a voltage-dependent calcium channel located in the T-tubule membrane (Rios and Brum, 1987). Antibody marking was also used to identify the ryanodine receptor (RyR), which is responsible for the release of Ca^{2+} from intracellular stores during excitation-contraction coupling in skeletal muscle and is located on the membrane of the SR (Coronado et al., 1994). Differentiated myotubes in the co-cultures were compared to aneurally-cultured myotubes to ascertain any differences in the percentage of myotubes exhibiting indicators of advanced differentiation. In each experiment (n = 3), twenty random fields of view from five different plates were assessed to determine percentage of myotubes displaying advanced differentiation. The data from all experiments was totalled and used to calculate the mean percentage ± SD from all observed fields of view. The results showed 32.4% ± 9.6 of innervated myotubes in the co-cultures had well developed and appropriately organised transversal triads (Figure 5.10), whereas aneural myotubes did not exhibit any triad formation. Along with the formation of transversal triads being an indicator of progressing advanced differentiation in innervated myotubes, peripherally located nuclei were also used to reveal features of advanced differentiation. The methods detailed in 2.1.12, 2.1.13, and 2.1.16 were used to perform characterisation of both co-cultured and aneurally cultured myotubes via antibody staining with MHC and DAPI to determine any differences in the percentage of myotubes having peripheral nuclei. The results showed 59.3% ± 17.1 of innervated myotubes in the co-cultures had peripherally located nuclei (Figure 5.11), contrastingly, no myotubes in the aneural cultures presented peripheral nuclei. Another feature of advanced differentiation in myotubes is the development of striations. Thus, myotube staining was performed with MHC and DAPI to determine any differences in the percentage of myotubes displaying striations in co-cultured and aneural conditions, using the methods detailed in 2.1.12, 2.1.13, and 2.1.17. The results show 46.2% ± 9.7 of the myotubes in the co-cultures presented with striations on their membranes. There was a significant reduction ($P < 0.0001$) in the percentage of striated myotubes (14.1% ± 3.5) when examining the aneural cultures (Figure 5.12). The methods

detailed in 2.1.18 were used to do a comparison of myotube thickness between co-cultured myotubes displaying features of advanced differentiation and aneurally-cultured myotubes. The results revealed that innervation and subsequent advanced differentiation endorsed the formation of thicker myotubes. The thickness of myotubes with characteristics of advanced differentiation was 20.3 µm ± 7.1, whereas aneurally cultured myotubes were measured at a significantly less ($P < 0.0001$) 11.2 µm ± 4.3 (Figure 5.13).

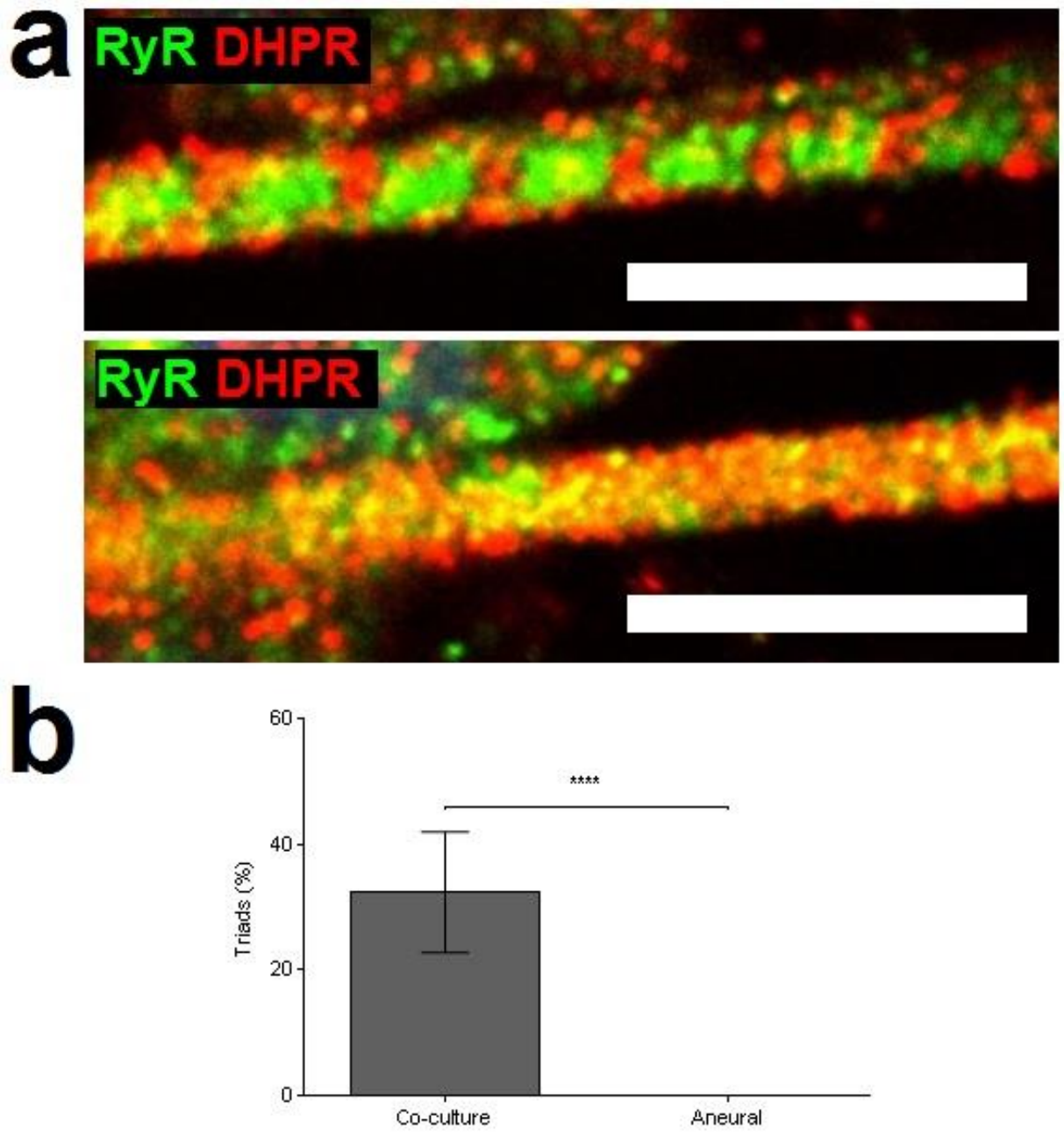

Figure 5.10: Formation of transversal triads on Day 14. a) The upper image panel is representative of an innervated myotube co-cultured with ED 13.5 rat embryo spinal cord explant displaying appropriate arrangement of transverse tubules and terminal cisterna. The lower image panel is representative of aneurally-cultured myotubes lacking formation of transversal triads. Myotubes were stained for ryanodine receptor (RyR) (green) and dihydropyridine receptor (DHPR) (red). b) A bar graph comparing percentage of myotubes with triad formation in the co-cultured conditions against aneural myotube conditions. Data presented as a mean, error bars signify ± SD. n = 3 independent experiments. **** denotes $P < 0.0001$. Bar = 7.5 µm. Adapted from (Saini et al., 2019)

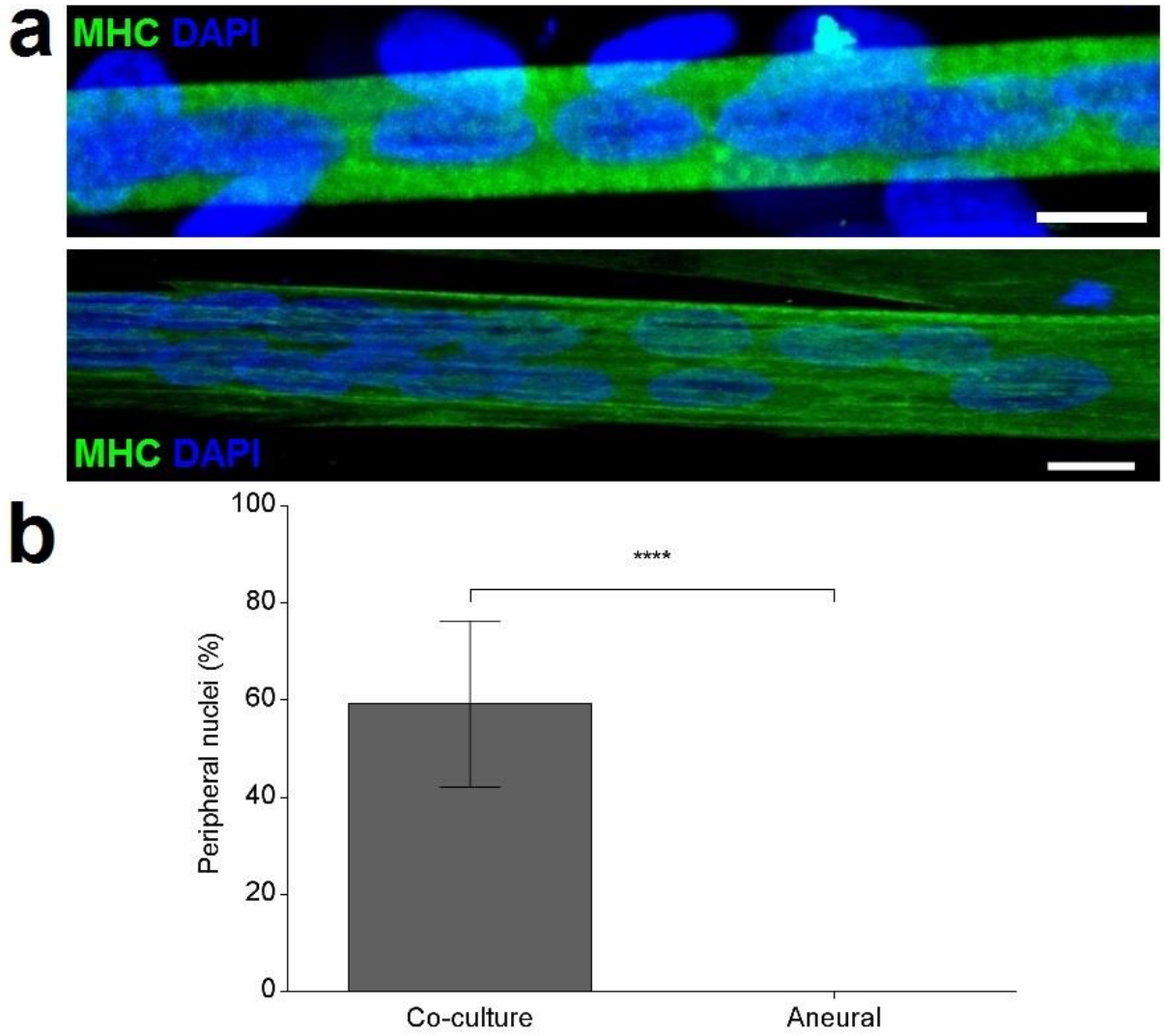

Figure 5.11: Generation of peripheral nuclei at Day 14. a) The upper image panel is representative of an innervated myotube co-cultured with ED 13.5 rat embryo spinal cord explant displaying peripherally located nuclei protruding from the myotube. The lower image panel is representative of aneurally-cultured myotubes with centrally located nuclei. Myotubes were stained for myosin heavy chain (MHC) (green) and DAPI (blue). b) A bar graph comparing percentage of myotubes with peripheral nuclei in the co-cultured conditions against aneural myotube conditions. Data presented as a mean, error bars signify ± SD. n = 3 independent experiments. **** denotes $P < 0.0001$. Bar = 10 µm.

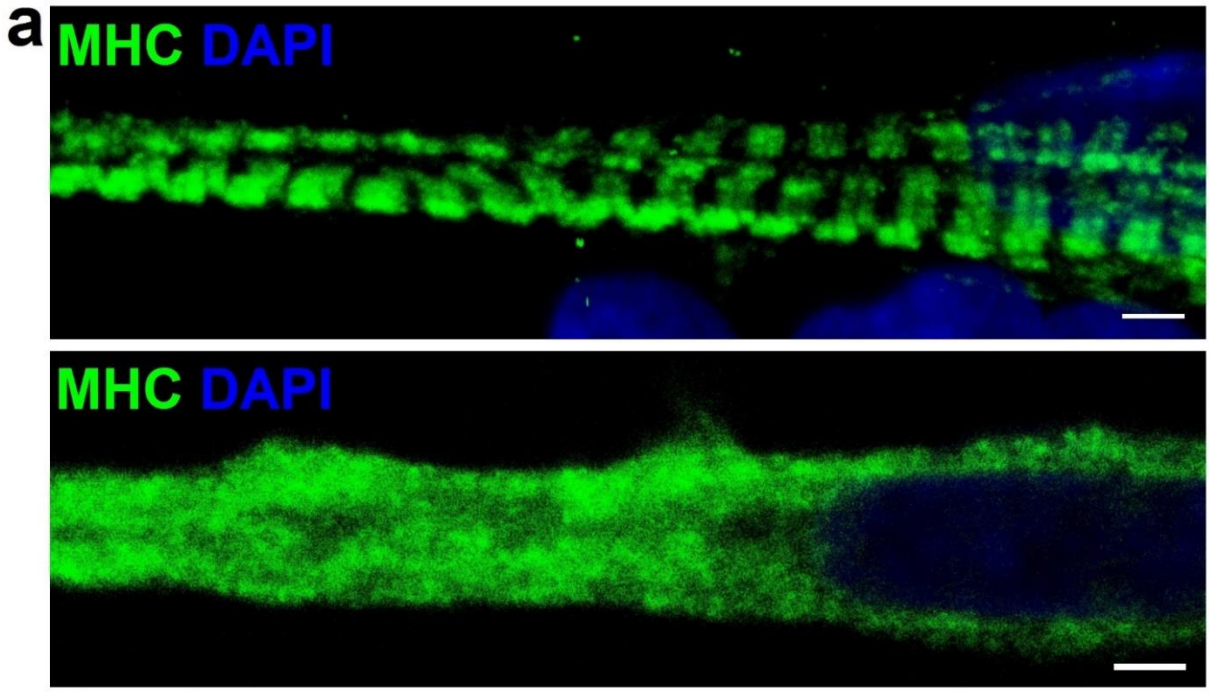

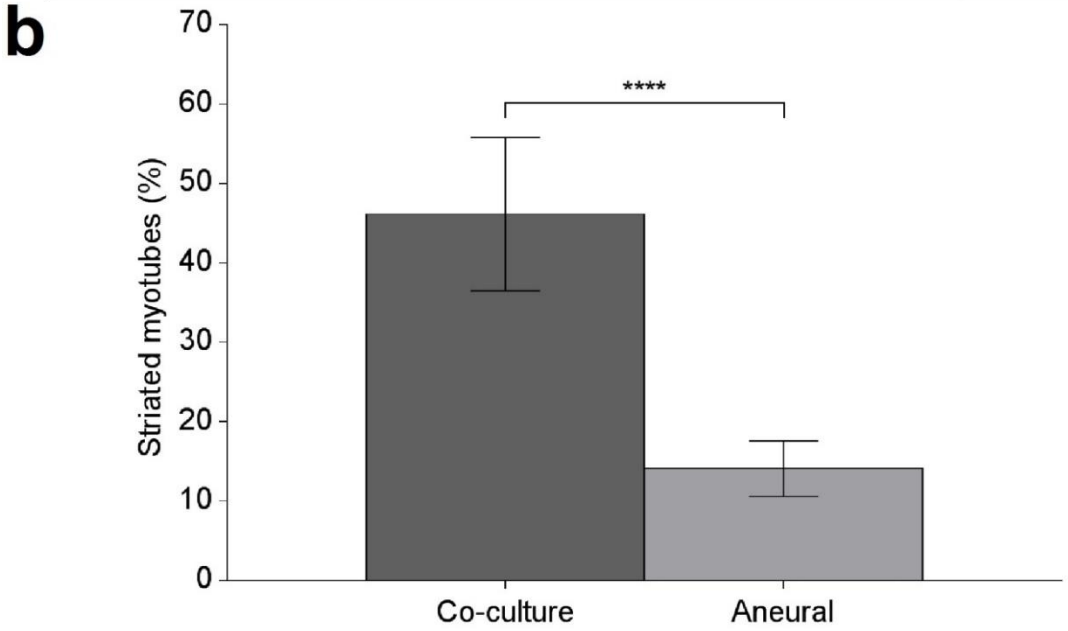

Figure 5.12: Myotube striations on Day 14. a) The upper image panel is representative of an innervated myotube co-cultured with ED 13.5 rat embryo spinal cord explant displaying striations on the myotube membrane. The lower image panel is representative of aneurally-cultured myotubes lacking striations. Myotubes were stained for myosin heavy chain (MHC) (green) and DAPI (blue). b) A bar graph comparing percentage of striated myotubes in the co-cultured conditions against aneural myotube conditions. Data presented as a mean, error bars signify ± SD. n = 3 independent experiments. **** denotes $P < 0.0001$. Bar = 2 µm.

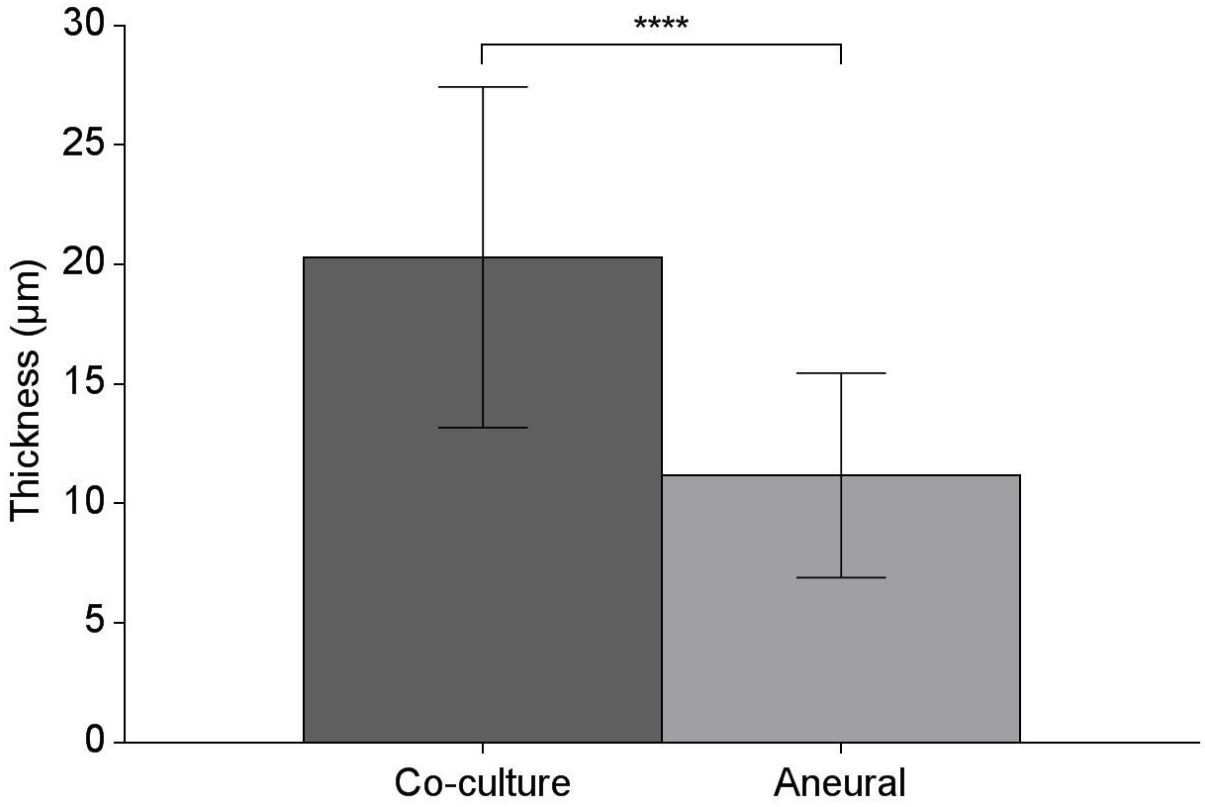

Figure 5.13: Myotube thickness on Day 14. A bar graph comparing the thickness of myotubes displaying features of advanced differentiation in the co-cultured conditions against aneurally cultured myotubes. Data presented as a mean, error bars signify ± SD. n = 3 independent experiments. *** denotes $P < 0.0001$.

5.2 Discussion

The primary outcome of this study presented characterisation of the *in vitro* NMJ model established in the previous chapter. The co-cultures of rat embryo SCEs with C25 demonstrated the co-localisation of cholinergic MNs with differentiated myotubes and promoted the interaction between neurons, myotubes, and neuroglia. Furthermore, co-cultures generated the formation and development of mature NMJs with presynaptic activity and postsynaptic structural organisation. Innervated myotubes in the co-cultures were also found to exhibit structural characteristics indicating the development of advanced differentiation. When preliminary experiments were conducted with the co-cultures to determine the optimal time for characterisation of the system, CF was used as the benchmark for NMJ formation and maturation. The observation that innervated myotubes were contracting at peak frequency after 14 days in the co-culture system provided evidence of effective mature NMJ development, which was reflected after characterisation was completed and revealed suitably differentiated MNs, NMJs, and myotubes. In comparison, some previously established co-culture systems require more than 20 days before NMJ formation occurs and involve extensive prior MN or myotube differentiation, further increasing the timeline of experimentation (Southam et al., 2013; Das et al., 2010). Moreover, contrasting the co-culture system presented in this current study, these previous co-culture models exhibited premature development of NMJs and myotubes lacked advanced differentiation. Although co-cultures were characterised on Day 14, the preliminary experiments used to determine the optimal date for characterisation also revealed long-term co-culture studies were possible with this novel simplified system, considering that myotube contractions persisted until experimental termination on Day 30, which could have been maintained further if desired. The characterisation of cholinergic MNs with ChAT and VaChT in the co-cultures resulted in the observation that interactions between MNs, ACh, and myotubes occurred in the system. Studies conducted with $ChAT^{-/-}$ mice have shown that embryos lacking ChAT have deficits in postsynaptic nerve potentials, resulting in embryo death at birth. The $ChAT^{-/-}$ mice display hyper-innervation due to excessive presynaptic nerve branching, smaller MNTs, and increased quantity of AChR agregations with fewer presynaptic contacts (Brandon et al., 2003; Misgeld et al., 2002). Although structural synaptic elements were present in the $ChAT^{-/-}$ mice, an assortment of both pre- and post-synaptic irregularities were evident at the NMJ. The findings from these *in vivo* ChAT deficient mice studies showed that neurotransmission is not the only function of ACh and synaptogenesis requires ACh and its biosynthetic enzyme ChAT. Research conducted with $VAChT^{-/-}$ mice similarly find severe abnormalities in NMJ development (de Castro et al., 2009). As seen in $ChAT^{-/-}$ mice, the studies with $VAChT^{-/-}$ mice have enlarged MEPs, excessive MN growth and necrotic SkM tissue, indicating VAChT is essential for the

release of ACh at the synapse and normal NMJ development. Thus, characterisation of ChAT and VaChT in the co-cultures provided data showing the *in vitro* NMJs generated in the system were an accurate physiological representation of NMJ development seen *in vivo*. Appropriate formation of NMJs requires interaction between the axon terminals of neurons, MEPs of myotubes and terminal Schwann cells. *In vivo* studies conducted with mutant mice lacking Schwann cells show MN axons are able to grow and extend towards developing SkM; however, significant axonal defasciculation is observed. This finding suggested Schwann cells are not required for axonal projection towards target myotubes but are necessary for nerve fasciculation. Additionally, Schwann cell deficient mice were able to establish preliminary NMJ formation but unable to maintain further development of the synapse (Lin et al., 2000; Morris et al., 1999; Riethmacher et al., 1997; Woldeyesus et al., 1999; Wolpowitz et al., 2000). These studies demonstrate that Schwann cells are not required for the initiation of contact between neurons and axons *in vivo*, but are vital for the subsequent advancement and maintenance of the developing synapse. Therefore, confirmation of Schwann cells in the co-culture system and the subsequent interaction observed between MNs and Schwann cells suggests the *in vitro* NMJ formation observed in the co-cultures were matured and maintained through Schwann cell/MN communication. Crucially, characterisation of the presynaptic nerve terminals with antibodies for Syt1 resulted in the discovery of presynaptic NMJ activity occurring in the co-cultured cells. Research investigating Syt1 revealed its function as a calcium sensor, facilitating the release of neurotransmitters from Ca^{2+}-dependent vesicles, which is mandatory for calcium-dependent vesicle exocytosis in invertebrates (Geppert et al., 1994; Littleton et al., 1993). However, investigations with $Syt1^{-/-}$ mice uncovered Syt1 was only required for fast synchronous release of neurotransmitters from Ca^{2+}-dependent vesicles, as synaptotagmin 2 can compensate for the lack of asynchronous exocytosis in $Syt1^{-/-}$ mice (Geppert et al., 1994). Studies conducted with spinal muscular atrophy (SMA) mouse models to explore the causes of impaired neurotransmitter release also discovered Syt1 was downregulated during development in the MNTs of the severely affected muscles, but not in MNT of less susceptible muscle (Lopez-Manzaneda et al., 2016). Therefore, identification of Syt1 in the co-cultures showed evidence that presynaptic activity at NMJs was illustrative of NMJ functionality, as would be similarly expected in appropriate *in vivo* NMJ formation and development. The formation of NMJs in the present co-culture system were characterised on the MEP with α-BTX to show the structure of postsynaptic aggregation of AChRs. Previously established nerve-muscle co-culture systems have demonstrated NMJ formation as diffused or speckled AChR clusters co-localising with MNs, primarily in the categories of faint or premature formation (Southam et al., 2013; Das et al., 2007). However, it is acknowledged that co-localisation alone does not represent *in vivo* NMJ formation (Thomson et al., 2012). Classic study of NMJs show that MN axons terminate at the MEP and overlap the AChR clusters precisely (Sanes and Lichtman,

1999; Englander and Rubin, 1987). Importantly, the NMJ formation observed in the co-culture system presented in this current study displayed MNs terminating on clusters of AChRs in the typical twisting knotted configuration. This finding signified *in vitro* NMJ formation, comparably observed *in vivo*. Confirming the co-cultures were able to generate NMJs with characteristics of maturely developed AChR clusters prompted the investigation of other postsynaptic NMJ elements. Essential for formation and maintenance of the NMJ, the observation of MuSK and Rapsyn at the MEP indicated activation of the MuSK signalling pathways triggered by agrin secretion from the MNT (Wu et al., 2010; Luo et al., 2003; Zhang et al., 2008; Kim and Burden, 2008). This finding was vital as it provided evidence toward successful postsynaptic differentiation at the NMJ via pre- and post-synaptic communication. Furthermore, the association of Rapsyn with AChRs is required for *in vivo* AChR clustering (Apel et al., 1997). Thus, the detection of co-localisation between Rapsyn, MuSK, and AChRs indicated that the postsynaptic development observed in the co-cultures were able to reach a level of maturation that would allow investigations of postsynaptic NMJ manipulation in the system. Co-cultured myotubes also displayed the morphological characteristics of advanced differentiation. Besides transversal triads being apparent in innervated myotubes, the co-cultured myotubes also contained peripherally located nuclei and the conventional actin-myosin striations expressed in mature differentiation, all characteristics which are similarly observed *in vivo* (Bruusgaard et al., 2003; Shadrin et al., 2016). This vital characterisation of mature innervated myotube development further exemplifies the advantage of this co-culture system over typical aneural *in vitro* myoblast cultures and previously established nerve-muscle co-culture models, which fail to achieve advanced stages of development. Thus, making this co-culture system a preferential alternative as a research tool for the accurate elucidation of skeletal muscle wasting and improve exploration of NM disorders.

5.3 Conclusion

In conclusion, this report characterised a novel *in vitro* NMJ system generated from ED 13.5 rat SCEs co-cultured with C25. The *de novo* formation of NMJs was verified by identifying pre- and post-synaptic structures of the junctional apparatus. Interactions with MN, myotubes and supporting neuroglia were shown to endorse the advanced differentiation of innervated myotubes. Thus, the SkMC line used in the generation of the system is a key aspect of this new system. The SkMC line allows for *de novo* formation of NMJs with easy reproducibility, while retaining the ability to differentiate regardless of the genetic programing performed on the cell line to achieve immortalisation.

Chapter 6: Functional Assessment of *in vitro* Neuromuscular Junctions between Embryonic Rat Motor Neurons and Immortalised Human Myoblasts

6.0 Background

6.0.0 Introduction

Experiments in the previous chapter detailed characterisation of NMJs and innervated myotubes in the ED 13.5 rat embryo SCE / C25 co-culture system. Successful NMJ formation with presynaptic cholinergic MN activity, maturation of postsynaptic MEP components, as well as cellular interaction between MNs, SkMCs, and supporting neuroglia were confirmed throughout the co-cultures. The formation of NMJs and development of innervated myotubes enabled the advanced differentiation of myotubes in the co-culture system, distinguished via characterisation of transversal triads, peripheral nuclei, and cross-striations on the myotubes. Furthermore, characterisation of the system verified the practicality of this heterologous co-culture model for NMJ disease modelling, as antibodies specific for rat or human can be used to study disorders that affect presynaptic and/or postsynaptic regions of the NMJ. The direct deterioration of NMJs is featured in a variety of disorders, such as congenital myasthenic syndromes (CMS), Lambert-Eaton myasthenic syndrome (LEMS) and myasthenia gravis (MG) (Engel and Sine, 2005; Vincent et al., 1989; Gilhus, 2016). These diseases and other NM disorders that affect MNs, such as amyotrophic lateral sclerosis (ALS) and spinal muscular atrophy (SMA) (Rosen et al., 1993; Lefebvre et al., 1995), can be initiated by autoimmunity, genetic mutations, and specific drugs or toxins. All of which can modify the function or quantity of synaptic proteins essential for regulating communication between MNTs and MEPs. Furthermore, disorders such as diabetic neuropathy and myopathy are associated with functional and morphological changes of the NMJ associated with muscle weakness (Garcia et al., 2012; Monaco et al., 2017). The degeneration of NMJs is also observed in several conditions including age-linked sarcopenia, cancer cachexia, heart failure, and NM transmission disorders, all of which lead to profound muscle wasting and weakness (Rudolf et al., 2016). The elucidation of mechanisms involved with deterioration of NMJs due to disease progression may allow for the development of therapies that can improve NMJ function and halt disease development. Animal models have been the traditional method to investigate the pathophysiology of NM disease, but are limited in the data they provide that translates to disease in humans. For example, the human *survival*

motor neuron 1 (SMN1) gene is mutated in SMA patients, but presence of the *survival motor neuron 2 (SMN2)* gene can mitigate some deleterious influences of the SMN1 gene mutation (Lefebvre et al., 1995). Contrastingly, deletion of the SMN1 gene in mice results in embryonic death as the mouse genome does not contain the SMN2 gene (Schrank et al., 1997). Therefore, the development of the SMA mouse model required insertion of the human SMN2 gene into the mouse genome of $SMN1^{-/-}$ mice to prevent embryo death (Monani et al., 2000; Hsieh-Li et al., 2000). Consequently, the resulting mouse exhibits an atrophied SkM phenotype due to a gene that the mouse genome does not naturally contain, yet this *in vivo* animal model and other similarly developed animal models are still the closest genetic representation of disease pathology in humans (Sleigh et al., 2011). Similarly, The superoxide dismutase 1 (SOD1) mouse model of ALS is the most commonly used animal model in ALS research, but has been unable to provide any significant insights into the mechanism of disease or possible therapies (Schnabel, 2008; Benatar, 2007). Thus, for effective interpretation of disease mechanisms and the screening of therapies designed to rectify NMJ function in NM disorders, a structurally robust and stable *in vitro* NMJ system that accurately reflects typical *in vivo* functionality is required. Data obtained through characterisation of the co-culture model presented in this project has already shown the system was able to emulate appropriate *in vivo* structural development of NMJs and exhibited long-term stability in culture. However, for the co-culture model to be considered a functional system the SkMCs contractile activity should respond physiologically to pre- or post-synaptic manipulation of the NMJ through pharmacological interventions. Importantly, unlike numerous SkMCs originating from animals, classic studies concluded that aneurally cultured human SkMCs, the most extensively utilised *in vitro* model to study human SkM (Aas et al., 2013), do not usually spontaneously contract or form differentiated postsynaptic components of NMJs under standard conditions (Delaporte et al., 1986; Kobayashi and Askanas, 1985). Thus, it is typically regarded that aneurally cultured human myotubes do not exhibit spontaneous contractile activity and any contraction has been considered to originate via innervation (Mis et al., 2017). Notably the first spontaneous aneural myotube contractions witnessed in differentiated human SkMCs was published in 2014 (Dixon et al., 2018), at which time the authors claimed that no spontaneous contraction had been reported from aneural human SkMCs *in vitro* (Guo et al., 2014). However, myotubes differentiated from the C2C12 mouse myoblast cell line have shown a capacity for spontaneous contractile activity when cultured aneurally (Manabe et al., 2012), indicating the possibility exists that aneurally cultured human myotubes could contract spontaneously, though unlikely. To demonstrate the formation of functional NMJs, some previously established nerve-muscle co-culture models have used the application of excitatory neurotransmitters such as glutamate to stimulate MNs, resulting in increased myotube contractions. In contrast, the cessation of myotube contractions has also been demonstrated through the application of reversible

and irreversible AChR inhibitors such as tubocurarine or bungarotoxin (Guo et al., 2011; Miles et al., 2004; Umbach et al., 2012; Bowman, 2006). Interestingly, recent research detected glutamate decarboxylase, which is an enzyme involved with γ-aminobutyric acid (GABA) synthesis, along with GABA, and a protein responsible for transmembrane transport of GABA called GAT-2, in the vertebrate NMJ (Nurullin et al., 2018). Though no previous compelling evidence existed that GABAminergic signalling occurred in the vertebrate NMJ. Furthermore, these new findings have yet to be explored in the context of NMJ functionality in heterologous nerve-muscle co-culture systems. Indicating that stimulation of *in vitro* NMJs with exogenous GABA is unknown, as well as the effects of GABA receptor antagonist such as bicuculline being insufficiently explored. Therefore, experiments in this study were conducted with co-cultures of ED 13.5 embryonic rat SCEs innervating C25 to explore the functional responses of NMJs to biochemical intervention.

6.0.1 Aims

The first aims of the present study was to verify spontaneous myotube contractions in the co-culture system were in fact driven via MN stimulation, as the unlikely possibility exists that spontaneous contractions may have been induced aneurally. The second aim was to ensure NMJs generated in the co-culture system respond to drug treatments in a physiological manner representative of *in vivo* NMJs. Thus, the objectives were:

1. Establish the co-culture model exhibiting spontaneous myotube contractions.

2. Treat the co-cultures with agonist and antagonist drugs (i.e. α-bungarotoxin, tubocurarine, bicuculline, L-glutamic acid, γ-aminobutyric acid).

3. Determine the functionality of NMJs generated in the co-culture system by assessing the myotube contraction frequency in response to pre- and post-synaptic NMJ manipulation via drug treatments.

6.1 Results

6.1.0 Functional Assessment of NMJs with α-Bungarotoxin

It is well known that α-BTX is a naturally occurring neurotoxic peptide found in the venom of the *Bungarus multicinctus* snake. When *in vivo* NMJs are exposed to α-BTX, an irreversible competitive antagonistic binding occurs between the neurotoxin and the AChRs on the postsynaptic MEP of the NMJ, leading to SkM paralysis, respiratory failure, and death (Lavoie et al., 1976). The methods described in 2.1.19 were used to determine if *in vitro* NMJs generated in the co-culture system reflect the SkM paralysis observed *in vivo,* the co-cultures were treated with a 1:400 concentration of α-BTX to induce permanent blockade of the postsynaptic AChRs. Experiments were conducted on day 14, when peak spontaneous contraction frequency (CF) was observed, which was determined in the previous chapter (Figure 5.0). Before exposing the co-cultures to α-BTX treatment, the culture dishes were placed on the microscope stage enclosed by an incubation chamber to maintain ideal atmospheric conditions for spontaneous myotube contractile activity. Continuous spontaneous myotube contractions were observed for no less than 5 minutes before baseline measurements were taken. This step was included to ensure any changes in myotube CF due to fluctuations in temperature or environmental conditions were mitigated, thereby removing false positive results, as the co-cultures were extremely sensitive to these fluctuations. Importantly, changing temperature and handling the culture plates can potentially reduce the possibility of locally triggered action potentials. This could potentially be tested by probing for local action potentials or by loading neurons with a calcium probe that would allow for the detection of waves of depolarisation. Baseline CF was measured 30 seconds before the application of α-BTX (Figure 6.0). There were no differences ($P = 0.64$) in baseline CF between the negative control (1.25 Hz ± 0.27) and the positive controls before treatment (1.18 Hz ± 0.33). All myotube contractions in the controls and α-BTX treated co-cultures stopped immediately upon addition of the treated and untreated diluent to the cultured cells. After 1 minute, myotube CF in the controls were measured at 0.08 Hz ± 0.08, while no myotube contractions were seen in the α-BTX treated cultures. Myotube contractions increased in the controls after 2 minutes to 0.27 Hz ± 0.08, no contractions were seen in the α-BTX treated cells. After 5 minutes, control myotubes were contracting at 0.96 Hz ± 0.19, no contractions were seen in the α-BTX treated cells. Following 10 minutes after treatment, CF in the controls returned to comparable baseline levels of 1.17 Hz ± 0.39. Controls continued to exhibit CF similar to baseline after 30mins (1.38 Hz ± 0.13) and 1 hour (1.23 Hz ± 0.2), though no contractions where observed in the α-BTX treated cells at these time points. The control and

α-BTX treated cells were washed out and fresh untreated DM was added to the cells after the 1 hour measurement, which resulted in the stoppage of contractions in both treated and control conditions. When measured again 30 minutes after washout (1 hour and 30 minutes after initial application of treatment), the controls were again contracting at a comparable baseline frequency of 1.18 Hz ± 0.26. This observation was also made 24 hours after treatment, where CF in the controls was 1.13 Hz ± 0.21. However, no observable contractile activity was witnessed in the α-BTX treated co-cultures at either of these final two time points.

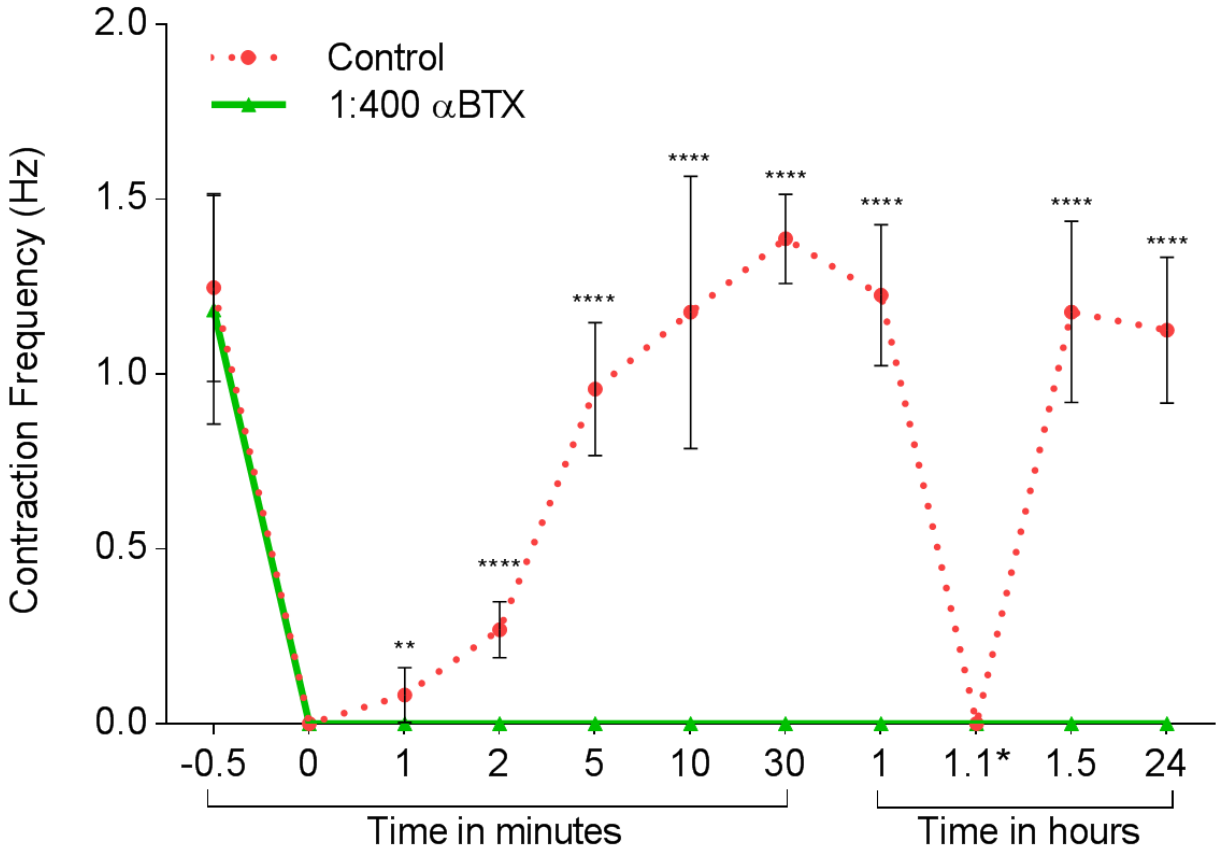

Figure 6.0: Assessment of the functional effects of a 1:400 concentration of α-bungarotoxin on co-cultured myotubes. A line graph comparing the contraction frequency of myotubes treated with α-Bungarotoxin (α-BTX) and untreated controls. Data presented as a mean, error bars signify ± SD. n = 5 independent experiments. ** denotes P < 0.01, **** denotes P < 0.0001. Time point 1.1* indicates washout.

6.1.1 Functional Assessment of NMJs with Tubocurarine

Tubocurarine is a toxic mono-quaternary alkaloid naturally occurring in the bark of the *Chondrodendron tomentosum* plant. The function of this toxin occurs by a reversible competitive binding of AChRs at the postsynaptic NMJ (Cooke and Grinnell, 1964). Similar to the effects of α-BTX, a sufficient dose of tubocurarine causes SkM paralysis and death from asphyxiation due to paralysis of the diaphragm. To determine if the innervated myotubes generated in the co-culture system parallels SkM paralysis observed *in vivo*, the co-cultures were treated with 8 µM tubocurarine to inhibit AChRs (Figure 6.1), as described in the methods section 2.1.19. There was no difference in baseline CF between treated and control co-cultured myotubes (1.18 Hz ± 0.25 vs 1.21 Hz ± 0.26, P = 0.75), recorded 30 seconds before addition of the treatment solution to the cells. Upon addition of tubocurarine to the treated cells and untreated diluent to the control cells, there was a halt in all observable contractions in both conditions. After 1 minute, CF of control myotubes was 0.12 Hz ± 0.06, no contractions were observed in the treated myotubes. After 2 minutes, CF of control myotubes was 0.22 Hz ± 0.06, no contractions were observed in the treated myotubes. After 5 minutes, myotube CF in the controls was 1.23 Hz ± 0.21, which was comparable to baseline CF, though no contractions were seen in the tubocurarine treated cultures. Controls continued to contract at a similar frequency of 1.25 Hz ± 0.31 after 10 minutes, no contractions were seen in the treated cells. Following 30 minutes after treatment, the tubocurarine treated cells were observed contracting at 0.13 Hz ± 0.09, which was significantly less ($P < 0.0001$) than the controls CF of 1.18 Hz ± 0.23. A slight increase in CF up to 0.51 Hz ± 0.16 was observed in the treated cells 1 hour after treatment, though this was still significantly less ($P < 0.0001$) than the controls, which were contracting at 1.03 Hz ± 0.22. Both control and treated conditions were washed out and fresh DM was added to the cells. The result was a complete stop of myotube contractions immediately following washout in both treated and control conditions. There was no difference ($P = 0.66$) in CF when measured 30 minutes after washout, controls were contracting at 1.15 Hz ± 0.28 and treated cells at 1.20 Hz ± 0.23. Similarly, when measuring CF 24 hours after initial treatment, the treated cells were contracting at 1.19 Hz ± 0.23 and the controls contracting at 1.1 Hz ± 0.17, indicating no significant difference ($P = 0.27$).

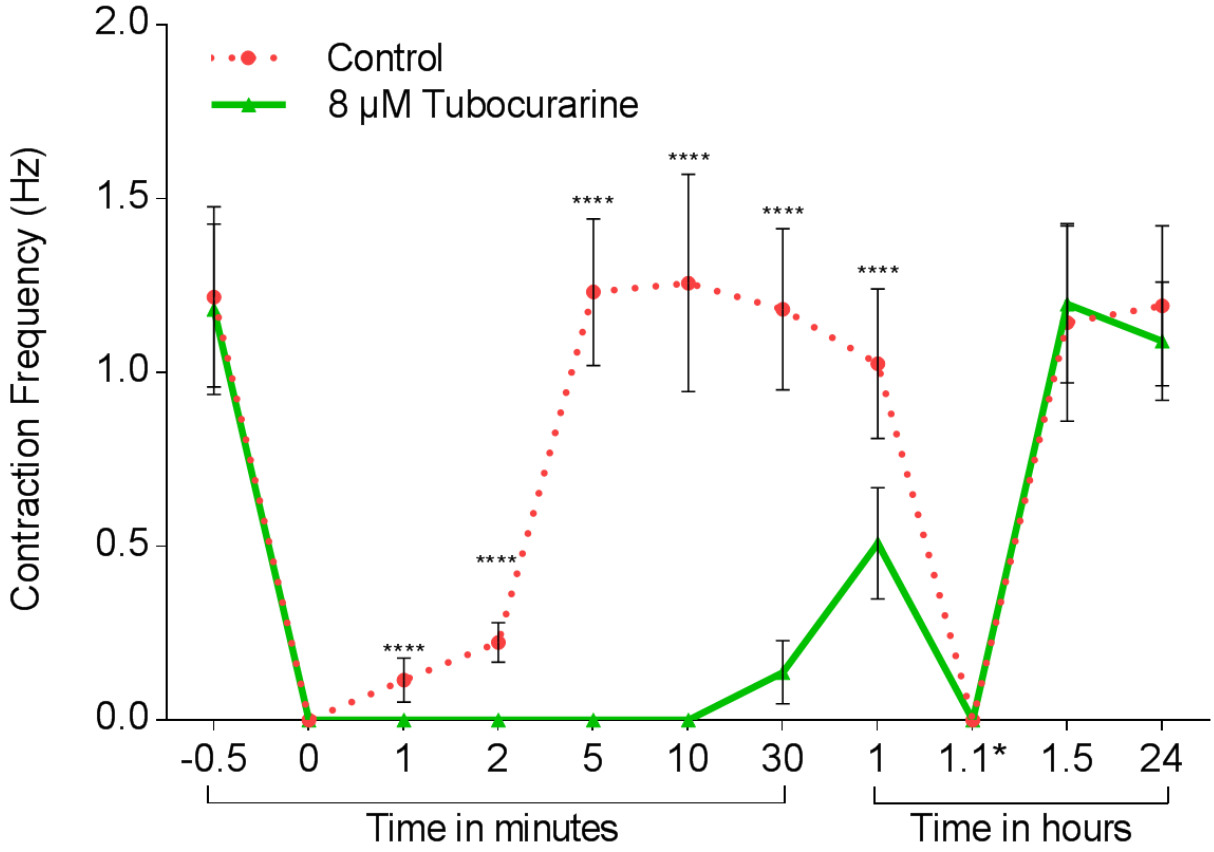

Figure 6.1: Assessment of the functional effects of 8 µM tubocurarine on co-cultured myotubes. A line graph comparing the contraction frequency of myotubes treated with tubocurarine and untreated controls. Data presented as a mean, error bars signify ± SD. n = 5 independent experiments. **** denotes $P < 0.0001$. Time point 1.1* indicates washout.

6.1.2 Functional Assessment of NMJs with Bicuculline

The phthalideisoquinoline alkaloid bicuculline is a competitive GABA receptor antagonist found in many plant species of the Fumarioideae subfamily (Manske, 1932). Previous studies have shown CF is modulated by the application of bicuculline in a homologous rat co-culture model (Mis et al., 2017). Thus, using the methods detailed in 2.1.19, 10 µM bicuculline was applied to the current *in vitro* NMJ system to determine its effects on myotube CF in this heterologous co-culture system (Figure 6.2). Baseline measurements of CF determined no difference between controls and treated cells 30 seconds before the addition of bicuculline treatment or untreated diluent to the co-cultures (1.26 Hz ± 0.27 vs 1.37 Hz ± 0.18, P = 0.26). All contractions stopped immediately upon addition of bicuculline or DM in both treated and untreated cells. After 1 minute, controls were observed contracting at 0.08 Hz ± 0.06, yet no contractions were seen in the treated cells. Measuring CF after 2 minutes showed an increase in the controls to 0.19 Hz ± 0.04, no contractions were observed in the bicuculline treated cells. Measurements of CF at 5 minutes found the bicuculline treated cells to be contracting at a rate of 0.05 Hz ± 0.04, which was significantly less ($P < 0.0001$) than the CF of controls, which were contracting at 1.1 Hz ± 0.19. After 10 minutes, a slight increase in CF was observed in the treated cells to 0.67 Hz ± 0.07, whereas CF in the controls was significantly higher ($P < 0.0001$) at 1.11 Hz ± 0.11. The CF measured 30 minutes after treatment in the controls was significantly higher than the treated cells (1.06 Hz ± 0.14 vs 0.6 Hz ± 0.13, $P < 0.0001$). Following 1 hour after treatment, the treated cells increased CF to 0.87 Hz ± 0.13, yet was still significantly less ($P = 0.003$) than the controls, which were measured at 1.06 Hz ± 0.12. All contraction stopped when the co-cultures were observed immediately following washout and replacement of DM in both conditions. When measured again 30 minutes after washout, there was no difference between the treated and control conditions (1.2 Hz ± 0.19 vs 1.1 Hz ± 0.15, $P = 0.2$). Similarly, after 24 hours no differences were seen between the treated and control conditions (1.27 Hz ± 0.23 vs 1.2 Hz ± 0.25, $P = 0.51$).

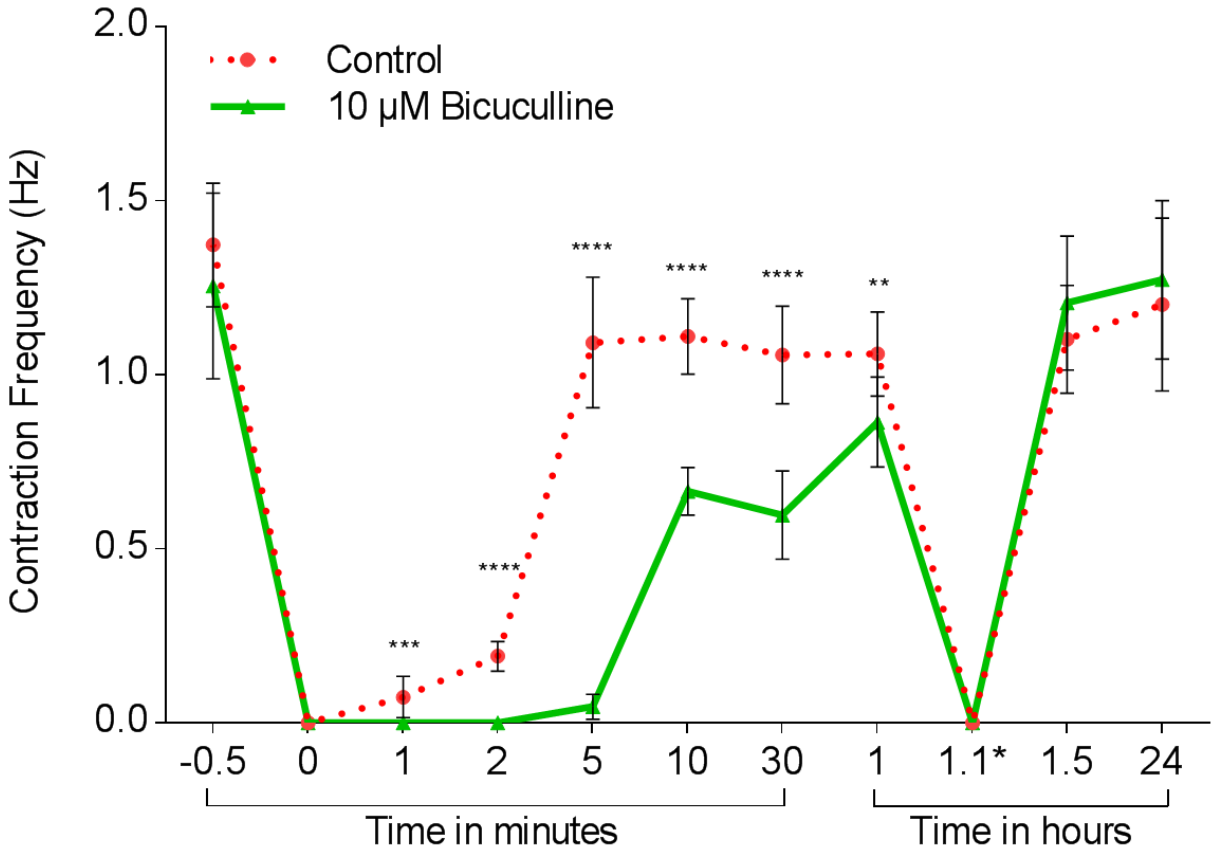

Figure 6.2: Assessment of the functional effects of 10 µM bicuculline on co-cultured myotubes. A line graph comparing the contraction frequency of myotubes treated with bicuculline and untreated controls. Data presented as a mean, error bars signify ± SD. n = 5 independent experiments. ** denotes $P < 0.01$, *** denotes $P < 0.001$, **** denotes $P < 0.0001$. Time point 1.1* indicates washout.

6.1.3 Functional Assessment of NMJs with L-Glutamic Acid

Upon determining contractile activity of myotubes in the co-culture system could be stopped or attenuated by the application of antagonist drugs that act on AChRs at the NMJ MEP, the next experiment set out to determine the impact of presynaptic agonist stimulation of the NMJ at the MNs. Thus, using the methods in 2.1.19, the excitatory neurotransmitter glutamate, in the form of 400 µM L-glutamic acid (L-Glut), was applied to the co-cultures to assess the influence of L-Glut on the CF of co-cultured myotubes (Figure 6.3). Baseline measurements of CF were recorded 30 seconds before the application of L-Glut to the positive controls and untreated diluent to the negative controls, which determined no significant differences (1.1 Hz ± 0.2 vs 1.2 Hz ± 0.3, P = 0.3). All contractions stopped immediately following the addition of the treatment solutions to the cultures. When CF was measured again 1 minute after the application of the treatment, the myotubes in the L-Glut treated cultures were contracting at a frequency of 0.18 Hz ± 0.05, which was significantly higher (P = 0.003) than the controls (0.1 Hz ± 0.05). After 2 minutes, the L-Glut treated cultures significantly increased (P < 0.0001) myotube CF to 1.7 Hz ± 0.18, while controls were measured at 0.23 Hz ± 0.06. After 5 minutes, myotube CF was measured at 1.3 Hz ± 0.22 in the controls, indicating CF had returned to levels comparable to baseline activity. However, myotubes in the L-Glut treated cultures were contracting at a frequency of 3.7 Hz ± 0.15, which was 2.5 Hz greater than the controls at this time point. When measuring contractile activity 10 minutes after application of the treatment, the myotubes in the L-Glut treated co-cultures exhibited a CF of 1.06 Hz ± 0.15, which was comparable to controls (P = 0.28), having a CF of 1.17 Hz ± 0.27. A Similar comparison was observed after 30 minutes (1.2 Hz ± 0.13 vs 1.3 Hz ± 0.14, P = 0.12) and 1 hour (1.26 Hz ± 0.19 vs 1.34 Hz ± 0.26, P = 0.44) between the control and L-Glut treated cultures respectively. Washing out and replacing the DM in both culture conditions 1 hour after the initial treatment resulted in stoppage of all contractions in the cultures. When measuring again 30 minutes after washout, both control and treated cultures where contracting at similar rates (1.1 Hz ± 0.21 vs 1.21 Hz ± 0.28, P = 0.3), comparable to baseline. At 24 hours following the initial treatment, both controls and L-Glut treated cultures showed no difference in CF (1.18 Hz ± 0.22 vs 1.23 Hz ± 0.17, P = 0.63), exhibiting spontaneous activity similar to baseline measurements.

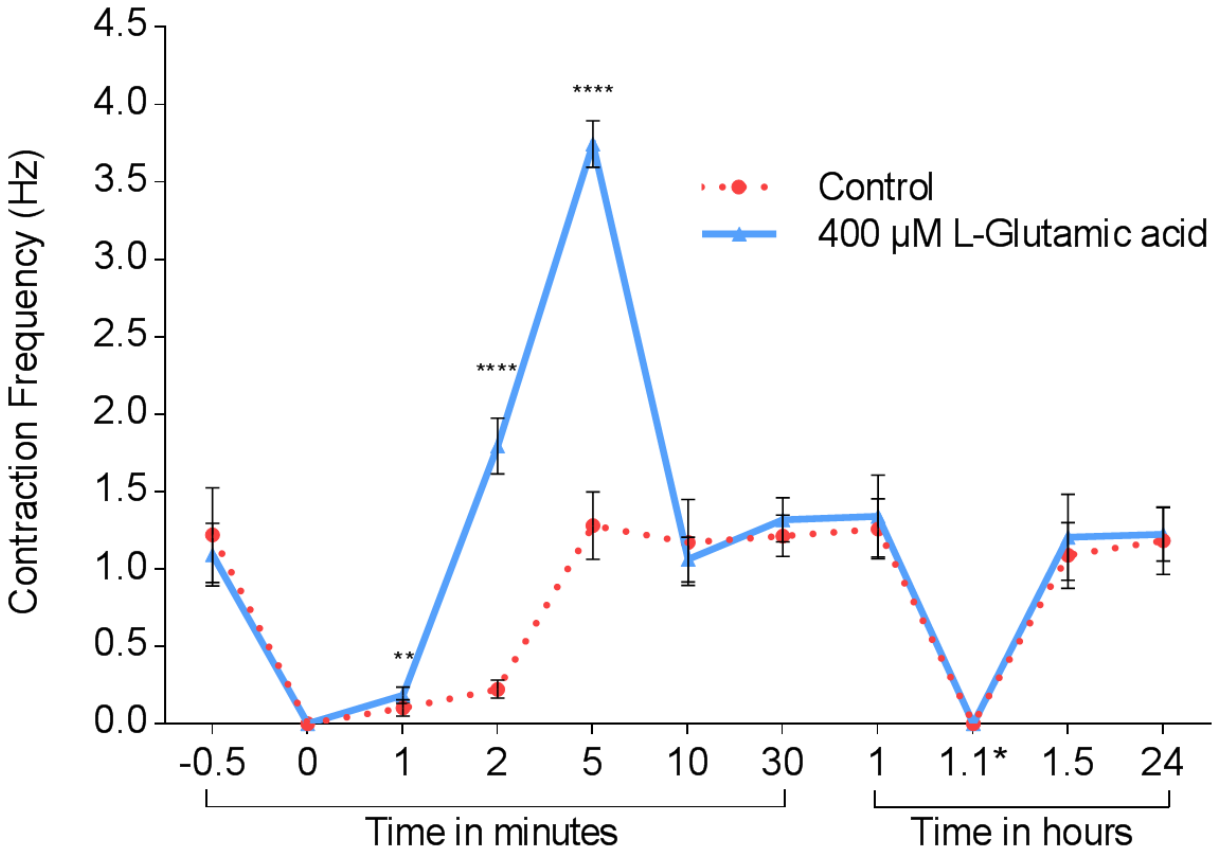

Figure 6.3: Assessment of the functional effects of 400 µM L-glutamic acid on co-cultured myotubes. A line graph comparing the contraction frequency of myotubes treated with L-glutamic acid and untreated controls. Data presented as a mean, error bars signify ± SD. n = 5 independent experiments. ** denotes P < 0.01, **** denotes P < 0.0001. Time point 1.1* indicates washout.

6.1.4 Functional Assessment of NMJs with γ-Aminobutyric Acid

Mainly found in the synapses of the CNS the inhibitory neurotransmitter GABA performs vital functions in the brain (Obata, 2013). Some studies have shown GABA signalling may occur in the periphery, with GABA transporters and receptors involved with GABA signalling being detected in a small number of endocrine and exocrine glands (Watanabe et al., 2002). Molecular studies have also found the $GABA_A$ receptor subunits α4 and β2/3 are present in cholinergic neurons (Elinos et al., 2016; Park et al., 2006). Although GABA functions to reduce neuronal activity in the CNS, the effects of increased GABA concentration in the *in vitro* NMJ environment requires clarification. Thus, using the methods described in 2.1.19 the co-cultures were treated with 1 mM GABA and CF was compared against control conditions (Figure 6.4). Baseline measurements of CF 30 seconds before treatment determined no difference between positive and negative conditions (1.32 Hz ± 0.18 vs 1.26 Hz ± 0.27, P = 0.6). There were no differences in myotube CF between the GABA treated and control co-cultures after 1 minute (0.11 Hz ± 0.05 vs 0.13 Hz ± 0.11, P = 0.65), or 2 minutes (0.19 Hz ± 0.06 vs 0.24 Hz ± 0.06, P = 0.09) following the addition of the treatment to the co-cultures. The CF of myotubes in the GABA treated co-cultures was significantly higher than the controls when observed 5 minutes after the treatment (1.7 Hz ± 0.33 vs 1.01 Hz ± 0.2, P < 0.0001). However, there were no differences in myotube CF between GABA and non-treated controls after 10 minutes (1.19 Hz ± 0.16 vs 1.22 Hz ± 0.23, P = 0.78), 30 minutes (1.08 Hz ± 0.2 vs 1.15 Hz ± 0.16, P = 0.39), 1 hour (1.11 Hz ± 0.14 vs 1.09 Hz ± 0.2, P = 0.79), 1 hour and 30 minutes (1.09 Hz ± 0.14 vs 1.2 Hz ± 0.2, P = 0.21), and 24 hours (1.36 Hz ± 0.22 vs 1.15 Hz ± 0.25, P = 0.07) after treatment.

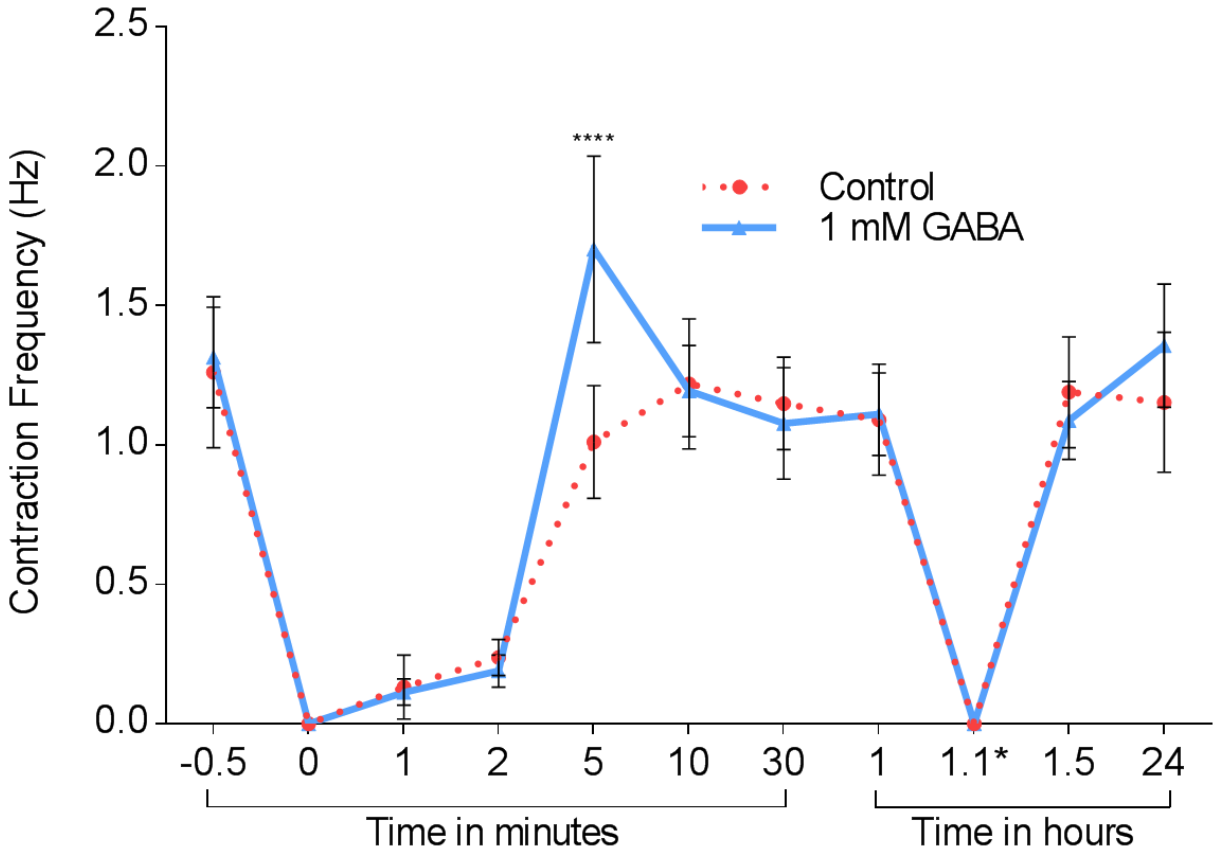

Figure 6.4: Assessment of the functional effects of 1 mM γ-aminobutyric acid on co-cultured myotubes. A line graph comparing the contraction frequency of myotubes treated with γ-aminobutyric acid (GABA) and untreated controls. Data presented as a mean, error bars signify ± SD. n = 5 independent experiments. **** denotes P < 0.0001. Time point 1.1* indicates washout.

6.2 Discussion

The main results from this chapter demonstrated the functional capacity of NMJs generated in the nerve-muscle co-culture system established in this project. The experiments conducted were designed to show spontaneous myotube contractile activity was indeed driven by MN signalling through the NMJ. Thus, functionality of NMJs was assessed through the analysis of myotube CF modulation, using agonist and antagonist pharmacological interventions that act on presynaptic MNs or postsynaptically on AChRs at the NMJ. The introduction of α-BTX to the co-cultures resulted in an immediate and permanent stoppage of spontaneous myotube contractions. This finding indicated binding of AChRs at the NMJ MEP with α-BTX, preventing ACh from binding with the postsynaptic receptors and consequently inducing paralysis in the co-cultured innervated myotubes. Although the co-cultures exposed to the α-BTX were washed out and reverted to normal culture conditions with fresh DM, spontaneous myotube contractile activity was indefinitely immobilised. Demonstrating the NMJs generated in this *in vitro* co-culture system responded physiologically to an irreversible competitive antagonist at the AChRs, as observed at the *in vivo* mammalian NMJ (Domet et al., 1995). Furthermore, the addition of tubocurarine to the co-cultures led to an immediate yet temporary halt in endogenously generated myotube contractions. Unlike the α-BTX treated cultures, which were unable to re-establish contractile activity, the myotubes in the tubocurarine treated co-cultures re-initiated spontaneous activity, beginning with low frequency irregular spasms rather than the typical synchronised contractions observed in control conditions. Although, the re-establishment of contractile activity was observed (30 minutes) after the application of tubocurarine, the spontaneous myotube contractions did not return to a typical synchronous frequency until the co-cultures were restored to pre-intervention conditions. Studies have shown the effects of ACh are not abolished in the presence of tubocurarine, but the ability of ACh to open the receptor channels is reduced, the result of which resembling a reduced concentration of ACh (Bowman, 2006). Dissimilar to the irreversible receptor antagonist α-BTX, which functionally inactivates the AChRs, tubocurarine acts by reducing the probability of ACh activating the receptor instead of inactivating it completely. Tubocurarine functions by repetitively associating and dissociating with its binding sites, as would be expected of a reversible competitive receptor antagonist, rather than remaining in constant contact with the AChR like α-BTX. The ability of myotube contractile activity in the co-cultures to recover from tubocurarine validates the accurate physiological nature of the neurotransmission witnessed in this *in vitro* NMJ system. The results from examining the application of bicuculline to the co-cultures revealed a preliminary cessation of myotube activity. Although spontaneous contractile function did partially recover, the frequency of myotube contractions were significantly attenuated prior to the removal of bicuculline from the

cultured cells. Previous research investigating the effects of the classic GABA type A receptor antagonist bicuculline on AChRs has demonstrated that bicuculline dose-dependently blocks the amplitude of the whole-cell current in cultured embryonic rat skeletal muscle (Liu et al., 1994). This study also showed the ability of bicuculline to reduce the maximum inducible ACh current without altering Kd value, this finding indicated that bicuculline non-competitively blocked the binding of ACh to AChRs. Ultimately, the study concluded that bicuculline was a blocker of embryonic nicotinic AChR channels (Liu et al., 1994). Furthermore, experiments conducted to investigate the effects of bicuculline on heteromeric mouse muscle αβγδ nicotinic AChRs demonstrated bicuculline diminished ACh-induced currents in a quick yet reversible manner, indicating the receptor is inhibited by bicuculline. Further investigation examining the effect of bicuculline at different membrane potentials revealed receptor inhibition was voltage-dependent, indicating bicuculline blocks nicotinic AChRs in a non-competitive way (Demuro et al., 2001). These studies provide evidence for the notion that the bicuculline-induced modulation of myotube contractions observed in the current co-culture system resulted from the prevention of ACh to bind with receptors on the MEP, further indicating that signalling at the NMJ was regulating contractile activity of myotubes in this *in vitro* NMJ model. Glutamic acid is a neuron-specific excitatory neurotransmitter that induces APs in MNs (Jiang et al., 1990). Despite the detection of glutamate receptors in mammalian NMJs, some research suggests these receptors are involved with regulation of muscle fibre membrane potentials via the nitric oxide synthase system (Urazaev et al., 1995), rather than signalling at the NMJ. When investigating the stimulation of associated neurons in the co-cultures via implementation of the neuron-specific excitatory neurotransmitter L-Glut, the frequency of myotube contractions in the system were significantly elevated. The impact of MN stimulation with L-Glut on myotube CF was immediately observable, causing myotubes activity to increase 1.5 Hz over the controls in 2 minutes and increase to 2.5 Hz greater than the controls in 5 minutes. However, myotube CF returned to levels comparable to spontaneous activity within 10 minutes following MN stimulation with L-Glut. In mammals, it is accepted that SkMC membranes are stimulated exclusively through AChRs, indicating that these findings show the successful enhancement of myotube contractions in the co-cultures via introduction of L-glut into the system was most probably achieved via the increased release of ACh from the cultured MNs into the synaptic cleft of the NMJs. Generally recognised as an inhibitory neurotransmitter in CNS synapses, GABA performs important tasks in neuronal function and development via activation of ionotropic and metabotropic receptors (i.e. $GABA_A$ and $GABA_B$ respectively) (Obata, 2013; Bowery et al., 2002; Olsen and Sieghart, 2008). Intriguingly, studies have shown that $GABA_B$ receptor 1 & 2 were detectable at the MNT in the synapses of rat extensor digitorum longus muscles and the soleus muscles (Malomouzh, Nurullin, et al., 2015). Further research investigating the effects of GABA on quantal and non-quantal ACh release from MNT suggests GABA

could reduce ACh release via activation of the $GABA_B$ receptors found in mammalian NMJs, mediated by phospholipase C (Malomouzh, Petrov, et al., 2015). Although recent studies have shown components of GABA synthesis and transport at the AChRs in mammalian NMJs, a determination could not be made on whether GABA plays the role of a co-mediator of ACh or as a gliotransmitter at the NMJ (Nurullin et al., 2018). However, the researchers maintain that activation of $GABA_B$ receptors influences the intensity of ACh release. Interestingly, when GABA was introduced into the co-culture system, the contractile activity of myotubes was increased. A transient but significant elevation in myotube CF was observed in the GABA treated cultures in the first 5 minutes following treatment. This finding suggests ACh release and binding at the NMJ was enhanced in the co-culture system, contrasting the findings in the above-mentioned studies. However, some research has shown that $GABA_A$ receptors are found at the embryonic vertebrate SkMCs and the expression of several transmitter receptor classes exist in early embryonic muscle and neuron development, including glutamate, glycine, ACh, as well as GABA (Borodinsky and Spitzer, 2007). Thus, further examination into the role and dynamic functions of GABA at the embryonic and mature mammalian NMJ is required, before the mechanisms of GABA action at the NMJ can be fully elucidated. Ultimately, the results in this chapter provided evidence that this nerve-muscle co-culture system permits assessment of NMJ functionality in real time. Offering a high-content platform for the evaluation of innovative therapies and *in vitro* disease modelling, as well as a system for refining the comprehension of NMJ formation and function in both healthy and disordered conditions.

6.3 Conclusion

In summary, a simplified *in vitro* nerve-muscle co-culture system was evaluated for NMJ functionality. Firstly, it was discovered that spontaneous myotube contractions in the co-cultures were indeed driven by MN signalling through NMJs. Additionally, it was verified the co-culture model responded in a physiologically appropriate manner to the drugs used in this study. Confirmed by reversible and irreversible paralysis of myotube contractile activity with AChRs antagonists, as well as augmenting myotube contractions with MN agonists.

Chapter 7: Investigation of Growth and Neurotrophic Factor Concentrations in Co-Cultures of Human Myoblasts Innervated by Rat Embryonic Spinal Cord Explants Compared with Human Myoblast Monocultures.

7.0 Background

7.0.0 Introduction

In the previous chapter, experiments were performed to validate the functionality of NMJs in the *in vitro* NMJ co-culture model comprised of human myoblasts co-cultured with embryonic rat nerves. Successful modulation of myotube contractile activity via manipulation of NMJs with postsynaptic AChR antagonists and presynaptic MN agonists was confirmed throughout the co-cultures. Indicating this *in vitro* NMJ system physiologically reflects *in vivo* mammalian NMJ function in response to known drugs and toxins. Thus, this novel co-culture system free from serum, growth, and neurotrophic factors would be an ideal *in vitro* NMJ model for screening potential drugs and molecules of interest in research concerning NM and ND disorders such as CMS, LEMS, MG, ALS, SMA, diabetic neuropathy and myopathy, sarcopenia, cancer cachexia and heart failure. The simplified nature of the co-culture system (i.e. serum, growth/neurotrophic factor free) also assures reliability in drug screening protocols. As the introduction of exogenous complex neural growth factors, as seen in alternative nerve-muscle co-culture models (Das et al., 2007; Guo et al., 2011; Guo et al., 2014; Rumsey et al., 2010; Puttonen et al., 2015), has the potential to influence and alter drug screening and development (Dugger et al., 2018). However, endogenously occurring growth factors and neurotrophins are vital for survival, development, plasticity, function and death of neurons *in vivo* (Oppenheim, 1991; Reichardt, 2006), as well as the maturation of myoblasts (Syverud et al., 2016). Accordingly, significant research has been conducted on the role of growth/neurotrophic factors in nervous system development and function. However, evidence from further research studies indicate that these factors have important functions in various cell populations across many tissues. One cell population of particular interest is that of SkMCs, which express receptors for several growth factors, cytokines, and neurotrophins, suggesting neurotrophic signalling occurs within SkMCs during formation, development and innervation (Griesbeck et al., 1995; Chevrel et al., 2006; Gonzalez et al., 1999). To our knowledge, the co-culture system established in this project is the first co-culture model engineered without exogenous neural

growth factors, suggesting all the factors required for the formation and maturation of NMJ, advanced differentiation of SkMCs, and maturation MNs were secreted endogenously. Studies with neurotrophin-4 (NT-4) and neurotrophin-5 (NT-5) null mice display clear defects in muscle development and function, indicating NT-4/5 are involved with SkM fibre differentiation (Carrasco and English, 2003). Additionally, neurotrophin-3 (NT-3) has been implicated in the formation of muscle spindles (Ernfors et al., 1994) and some dystrophic muscle pathologies have been linked with altered nerve growth factor (NGF) (Capsoni et al., 2000). Brain-derived neurotrophic factor (BDNF) expression studies have also shown various physiological and pathological conditions can influence the SkMC expression of BDNF (Chevrel et al., 2006). For example, research with healthy humans as well as people with multiple sclerosis has shown circulating BDNF can be increased with physical exercise (Ferris et al., 2007; Rojas Vega et al., 2006; Gold et al., 2003). Studies have also demonstrated that exercise with an ergometer bicycle for 2 hours was able to induce BDNF mRNA production in SkM (Matthews et al., 2009). Furthermore, the concentrations of SkM neurotrophins is altered in denervated SkMCs and studies with diabetic mice reveal reductions in the expression of NT-3 and NGF mRNA and increased expression of BDNF mRNA in the muscle (Fernyhough, Diemel, Brewster, et al., 1995; Fernyhough, Diemel, Hardy, et al., 1995; Ihara et al., 1996; Fernyhough et al., 1998; Fernyhough et al., 1996). The glial-cell-line-derived neurotrophic factor (GDNF) is known for its role in the support of CNS dopaminergic neurons and was first discovered in glial cells (Lin et al., 1993). Research has shown that overexpression of GDNF in SkM incudes hyper innervation of NMJs through increased MN sprouting (Nguyen et al., 1998). It has been suggested that GDNF can function to maintain cholinergic MNs throughout aging (Ulfhake et al., 2000) and a significant yet transient expression of GDNF at NMJs during embryonic myogenesis is also witnessed *in vivo*. Interestingly, GDNF expression has also been shown to be increased in denervated human SkM (Lie and Weis, 1998). The results from characterisation and functional assessment of the co-culture system communicated in the previous chapters of this project provided evidence that the NMJs generated in system physiologically mirror *in vivo* functionality and structural development. As mentioned in prior chapters of this project, alternative established nerve-muscle co-culture models typically require a complex neural growth media that contain serum and/or a cocktail of neural growth factors (some of which may derived from animals). This further complicates drug discovery and toxicology studies due to possible cross-communication of the novel compounds being studied with factors contained within culture media formulation, possibly explaining why many promising therapies do not translate to clinics. Even the most recent systems requiring up to 18 different trophic factors to establish their model successfully (Table 4.0). Furthermore, many systems induce myotube contractions via the application of electrical or chemical stimulation, which does not replicate the native physiological stimulation required for muscle contractions. Thus, the question remains how the

current co-culture model engineered during this project generated robust functional NMJs without serum and trophic factors, suggesting MNs and SkMCs in the system release all of the necessary factors needed to stimulate sprouting of MN axons and formation of NMJs with myotubes. Thus, to aid in clarifying this simplified co-culture system's ability to generate robust NMJs without the inclusion of exogenous serum, growth and neurotrophic, as is required by previously established nerve-muscle co-culture system, ELISA-based microarray experiments were conducted in the following study to examine the concentration of endogenously secreted growth factors and neurotrophins in this *in vitro* NMJ system.

7.0.1 Aims

The objective of the present study was to determine the concentration of growth and neurotrophic factors endogenously occurring in the co-cultures. Thus, the aim was:

1. Establish the co-culture model.

2. Culture myoblasts aneurally.

3. Collect, analyse, and compare the supernatant of C25 co-cultured with ED 13.5 rat embryo SCEs against aneurally cultured human myoblasts using an ELISA-based human growth factor microarray.

7.1 Results

7.1.0 Quantification of Growth and Neurotrophic Factors

To determine if there were any significant differences in the secretion of growth/neurotrophic factors in the supernatant of co-cultured and aneurally cultured human myoblasts, an ELISA-based microarray analysis of growth/neurotrophic factor concentrations was performed and compared between the two conditions. The methods used to perform the microarray analysis were described in section 2.1.20. The concentration of 40 growth/neurotrophic factors were quantified on day 7, shown in Table 7.0. The results revealed that twelve of the factors analysed were significantly different ($P < 0.05$) between co-cultures and aneural myotube cultures. Specifically, the concentrations of brain-derived neurotrophic factor **(BDNF)**, fibroblast growth factor 7 **(FGF-7)**, glial cell-derived neurotrophic factor **(GDNF)**, insulin-like growth factor-binding protein **(IGFBP)** -1, -3, -4, -6, insulin-like growth factor 1 **(IGF-1),** neurotrophin **(NT)** -3, -4, placental growth factor **(PIGF)**, and vascular endothelial growth factor **(VEGF)** were significantly higher in the supernatant collected from the co-cultures compared to the supernatant from aneurally-cultured myotubes.

Table 7.0: ELISA-based microarray analysis of growth and neurotrophic factor in supernatant collected from co-cultured and aneurally-cultured myotubes on Day 7.

Growth factors	Co-culture (pg/mL)	Aneural (pg/mL)	Fold change	*P* - value	Log-Log regression standard curve R^2
AR	4.03 ± 5.27	1.61 ± 1.87	2.5	0.26	0.987
BDNF	**52.33 ± 39.14**	**4.88 ± 1.73**	**10.72**	**0.005 ****	**0.976**
bFGF	2.55 ± 5.1	0.65 ± 1.06	3.91	0.31	0.943
BMP-4	10.55 ± 13.6	1.44 ± 3.25	7.33	0.09	0.961
BMP-5	215.8 ± 431.6	94.38 ± 109.3	2.29	0.45	0.996
BMP-7	3.67 ± 6.76	0.83 ± 1.55	4.42	0.26	0.994
b-NGF	0.4 ± 0.5	0.24 ± 0.29	1.6	0.48	0.991
EGF	0	0.01 ± 0.01	0	0.51	0.984
EGF R	179.2 ± 89.26	111.5 ± 32.68	1.61	0.08	0.995
EG-VEGF	0.43 ± 0.78	0.18 ± 0.36	2.39	0.45	0.986
FGF-4	16.65 ± 33.3	3 ± 8.49	5.55	0.28	0.997
FGF-7	**11.13 ± 7.19**	**2.91 ± 3.09**	**3.8**	**0.02 ***	**0.996**
GDF-15	410.3 ± 99.25	345.5 ± 71.91	1.18	0.22	0.999
GDNF	**7.37 ± 6.72**	**1.51 ± 1.43**	**6.41**	**0.05 ***	**0.996**
GH	0.83 ± 1.65	0.61 ± 1.11	1.39	0.79	0.994
HB-EGF	0.38 ± 0.45	0.48 ± 0.67	0.79	0.77	0.971
HGF	10.25 ± 11.84	13.85 ± 6.36	1.35	0.49	0.991
IGFBP-1	**50.43 ± 34.91**	**10.98 ± 2.98**	**4.59**	**0.008 ****	**0.997**
IGFBP-2	965.2 ± 1251	231 ± 74.01	4.18	0.11	0.999
IGFBP-3	**46859 ± 17230**	**14678 ± 2508**	**3.19**	**0.0003 *****	**0.988**
IGFBP-4	**30130 ± 14177**	**8351 ± 2221**	**3.61**	**0.001 ****	**0.999**
IGFBP-6	**877.6 ± 265.6**	**520.9 ± 149.9**	**1.68**	**0.01 ***	**0.987**
IGF-1	**86.73 ± 53.36**	**19.89 ± 46.82**	**4.36**	**0.05 ***	**0.975**
Insulin	3809 ± 3821	3796 ± 2547	1	0.99	0.989
MCSF R	1.33 ± 2.58	1.21 ± 1.82	1.1	0.93	0.991
NGF R	129.1 ± 81.12	161.8 ± 44.51	1.25	0.38	0.987
NT-3	**35.1 ± 10.32**	**10.08 ± 3.77**	**3.48**	**0.0002 *****	**0.997**
NT-4	**4 ± 4.1**	**0.64 ± 0.72**	**6.25**	**0.03 ***	**0.999**
OPG	1117 ± 194.7	875.7 ± 247.1	1.28	0.12	0.996
PDGF-AA	2378 ± 812.7	1828 ± 613.4	1.3	0.22	0.996
PlGF	**221.3 ± 36.89**	**171.8 ± 29.89**	**1.3**	**0.03 ***	**0.987**
SCF	0.73 ± 1.2	0.28 ± 0.4	2.61	0.34	0.996
SCF R	1.23 ± 1.46	0.66 ± 1.12	1.86	0.47	0.998
TGFa	0	0.01 ± 0.04	0	0.51	0.889
TGFb1	98.63 ± 197.3	15.71 ± 44.44	6.28	0.26	0.984
TGFb3	0.3 ± 0.6	0.21 ± 0.46	1.43	0.78	0.979
VEGF	**1060 ± 154.7**	**609.1 ± 105.9**	**1.74**	**0.0001 *****	**0.963**
VEGF R2	4.78 ± 6.74	1.96 ± 3.51	2.44	0.35	0.999
VEGF R3	4 ± 4.67	1.66 ± 1.92	2.41	0.23	0.991
VEGF-D	0.15 ± 0.24	0.13 ± 0.24	1.15	0.87	0.991

Note: * denotes P < 0.05; ** denotes P < 0.01; *** denotes P < 0.001

7.2 Discussion

Motor neurons and SkM are co-dependent tissues, each relying on the other for trophic stimulation. Indicating the bidirectional communications between these cells is vital for NMJ formation and maintenance. To understand how this co-culture model was established in the absence of exogenous neural growth factors, ELISA-based arrays were employed. The results from this study presented a quantitative measurement of 40 human growth factors and neurotrophins endogenously produced in the *in vitro* NMJ co-culture system, compared with endogenously produced factors in aneurally-cultured myotubes. Microarray experiments to quantify the concentration of growth factors were performed to show the formation and development of *in vitro* NMJs generated in the co-culture system were indeed supported by the endogenous regulation of specific growth or neurotrophic factors. When examining the results from Table 7.0, the concentration of a number of factors involved with NMJ formation, MN maintenance, and myotube development were discovered to be elevated in the co-culture system compared with aneural myotube cultures. Studies investigating the role BDNF in the development of NMJs suggest SkM innervation and MN survival are enhanced by SkM-derived BDNF, as well as transmission at the NMJ being potentiated by BDNF (Zhang and Poo, 2002; Yan et al., 1993). It has also been shown that myoblasts express high levels of BDNF during embryonic development *in vivo*, which is gradually down regulated as NMJ and SkM fibre maturation occurs (Griesbeck et al., 1995). Interestingly, research investigating chronic exposure to upregulated BDNF resulted in the inhibition of synaptogenesis in developing *in vitro* NMJs (Peng et al., 2003). Collectively, these results can be used as evidence to suggest that the endogenously regulated concentration of BDNF secreted in the present co-culture system allowed for the physiological formation and development of NMJs, which were representative of *in vivo* NMJ formation. Contrastingly, previously established nerve-muscle co-culture systems that require the inclusion of exogenous BDNF (Das et al., 2010; Rumsey et al., 2010; Das et al., 2007; Guo et al., 2017; Guo et al., 2011; Guo et al., 2014; Puttonen et al., 2015; Vilmont et al., 2016; Smith et al., 2016) may not generate the robust NMJ formation observed in the *in vitro* NMJ system generated during this project, due to unsuitable concentrations of exogenous BDNF inhibiting NMJ maturation (Song and Jin, 2015).

In addition to the significant BDNF upregulation measured in the co-cultures, FGF-7 was also significantly elevated. Studies have shown that organising molecules derived from SkM, such as members of the FGF family, have vital functions in regulating presynaptic specialisation at the NMJ (Umemori et al., 2004; Fox et al., 2007). An Investigation to determine if agrin can induced retrograde signalling of these muscle-derived organising molecules was conducted using real-time quantitative PCR analysis of RNA isolated from C2C12 myotubes treated with agrin. The researchers found that FGF-

7 was significantly elevated in agrin treated myotubes. Furthermore, it was shown that FGF-7 mRNA was inhibited in the diaphragm of agrin deficient mutant mice. The determination was made that agrin does in fact regulate FGF expression in SkM for the purpose of supporting presynaptic differentiation at the NMJ by opposing the deleterious impact of non-postsynaptic ACh signalling (An et al., 2010). Thus, the elevated FGF-7 observed in the co-culture system suggests interactions between agrin secreted by the ED 13.5 rat embryo SCE and the innervated myotubes during NMJ formation and development, as would be expected *in vivo*.

Results from the microarray also revealed elevated GDNF in the co-cultures in comparison to myotube monocultures. A key factor shown to be highly effective for MN survival *in vitro* is GDNF (Oppenheim et al., 1995). Intriguingly, GDNF is another example of a target-derived factor that is expressed by SkM with its receptor RET tyrosine kinase expressed in the MNs (Baudet et al., 2008). When conditionally ablating RET tyrosine kinase in the cranial MNs of mice, the outcomes were obvious disruptions to MNT maturation and reduced MEP size at NMJs (Baudet et al., 2008). Experiments with frogs to create a nerve-muscle co-culture system found that spontaneous synaptic current frequency and amplitude were increased when the co-cultures were treated with GDNF, indicating its possible role as a retrograde signalling factor (Wang et al., 2002). Furthermore, studies with transgenic mice that overexpress SkM-derived GDNF results in hyperinnervation of NMJs (Nguyen et al., 1998). Another study similarly found motor unit enlargement, hyperinnervation of NMJs, and slowed synapse elimination when GDNF was injected into mice during postnatal life (Keller-Peck et al., 2001). These findings suggest SkM derived GDNF plays a role in the regulation of MNT maturation at the NMJ. Thus, elevated GDNF observed in the co-culture system described in this project indicates interaction between pre- and post-synaptic components of NMJs in the system.

The growth factor IGF-1 is a potent anabolic hormone involved with growth throughout the body, shown to induce hypertrophic effects on SkM, which has been extensively documented in animal models and muscle cell culture systems (Velloso, 2008). The muscle specific expression of IGF-1 also functions to stabilise NMJs and enhanced motor neuronal survival (Dobrowolny et al., 2005). When injected directly into SkM, IGF-1 inhibits degeneration of MNs and NMJs, thus preventing age-related force decline in mice (Payne et al., 2006). Interestingly, the concentration of four (IGFBP -1, -3, -4, -6) of the five insulin-like growth factor binding proteins examined during the microarray experiments, along with IGF-1, were significantly elevated in the co-cultures. The primary function of the IGFBPs is to serve as membrane transporter proteins for IGF-1, with almost all IGF-1 being bound to at least one of the seven members of the IGFBP superfamily (Hwa et al., 1999). Binding to IGF-1 with a 1:1 ratio, IGFBP-3 is the most common protein of the superfamily and binds ~80% of circulating IGF-1 (Adachi et al., 2017). Noteworthy, the presence of IGFBP-3 was also the most abundant IGFBP observed in the co-

cultures and monocultures when compared to the other IGFBP measured during the array experiment. Studies examining the impact of IGFBPs on circulating IGFs found IGF-1 bioavailability is enhanced through the activity of the IGFBPs (Stewart et al., 1993). Thus, the observed upregulation of the IGFBPs and IGF-1 in the co-culture system supports the notion that interaction between SCEs and SkMCs in the system generates the necessary factors for MN maturation, advanced differentiation of myofibres, and the formation of robust NMJ, representative of *in vivo* formation.

Both NT-3 and NT-4 were also significantly elevated in the co-cultures when compared to aneural myotube cultures. Studies have demonstrated that NT-3 and NT-4 are important modulators of synaptic function and development and are required for maintenance of presynaptic and postsynaptic apparatus at the NMJ (Gonzalez et al., 1999; Belluardo et al., 2001). Studies exploring early postnatal development of NMJs and the NM system in NT-3 deficient mice found reductions in somal size, yet the number of αMNs developed normally (Woolley et al., 1999). Further research discovered decreased innervation of MEPs by MNTs and decreased number of SkM fibres in NT-3 deficient mice at birth, followed by a catastrophic postnatal loss of MNTs by postnatal development day 7 and complete denervation of hindlimb muscles with no observable NMJ remaining in the entire SkM endplate zones (Woolley et al., 2005). Additionally, mice with haploinsufficiency-induced reductions in NT-3 availability exhibit impaired MNT maturation, reduced recycling of synaptic vesicles, and a reduction in SkM fibre diameter (Sheard et al., 2010). Studies investigating NM transmission using a phrenic nerve / adult rat diaphragm-muscle system exposed that NT-4 treatment can improve synaptic transmission when transmission failure was induced in the system via repetitive nerve stimulation (Mantilla et al., 2004). The expression of NT-4 is also shown to be dependent on synapse activity at the NMJ, demonstrated via blockade of AChRs on the NMJ MEP with α-BTX causing reduced NT-4 expression, while electrical stimulation of MNs enhances SkM-derived NT-4 expression (Funakoshi et al., 1995). Considering these studies, it can be appreciated that the significantly elevated NT-3 and 4 expression observed in the co-culture system was due to NMJ formation, development and synaptic activity.

Intriguingly, the concentration of VEGF and PlGF, which is a member of the VEGF sub-family, were also significantly elevated in the co-cultures when compared to the anural myotube cultures. Originally described for their regulatory role in vascular growth and development (Ferrara, 2004), the VEGF family of factors have also demonstrated important functions in MN growth, guidance, migration, and survival (Rosenstein et al., 2010; Ruiz de Almodovar et al., 2009). Research with ALS transgenic mice found systemic administration of VEGF was able to increase the number of NMJs in the diseased mice (Zheng et al., 2007). Furthermore, Amelioration of SkM innervation is observed following administration of VEGF in mice with ischemic injury, promoting both regrowth and maintenance of damaged MN axons in the mice (Shvartsman et al., 2014). The researchers in that study also found VEGF was able to induce

the upregulation of GDNF and NGF to aid in MN axon regeneration (Shvartsman et al., 2014), pointing to the synergistic effects of growth factors during NMJ formation.

Finally, the results from the experiments conducted in this chapter provided important insights into the cellular signalling of this simplified co-culture system. Furthermore, the results demonstrated the capacity of the co-culture system to endogenously regulate formation and development of NMJ, as well as provide the conditions to allow the advanced differentiation of immortalised human myotubes *in vitro,* through the precise expression of essential growth factors and neurotrophins.

7.3 Conclusion

In conclusion, this report analysed the concentration of 40 human growth factors and neurotrophins in the *in vitro* NMJ system generated from ED 13.5 rat SCEs co-cultured with C25. Elevated concentrations of 12 factors involved with MN, SkM, and NMJ development were measured in the co-cultures system, providing evidence the *in vitro* NMJ generated in this project were representative of *in vivo* conditions.

Chapter 8: General Discussion & Conclusions

8.0 Discussion

The overarching aim of this project was to establish and validate a novel and simplified nerve-muscle co-culture system capable of generating functional in *vitro* NMJs, without the use of serum, growth, and/or neurotrophic factors. Thus providing a defined platform to investigate disease and disorders of the NM system via examination of NMJ formation and functionality. The fulfilment of this aim was first addressed through the optimisation of cell culture conditions for the two immortalised human SkMC lines newly acquired for this project. Optimisation of culture conditions for the two cell lines, one young (25 years old) and one old (83 years old), was completed before any co-culture studies were conducted, as both these cell lines had not been previously established or used in our laboratory. Upon successfully optimising culture conditions for the two cell lines, the myogenic potential of both C25 and C83 cells was compared to determine any differences in the *in vitro* proliferation and differentiation of immortalised human myoblasts originating from old or young muscle. Through the analysis of cellular passaging, examination of proliferative capacity and differentiation parameters, as well as investigating the expression of the proliferation marker Ki67 and differentiation marker MHC, the determination was made that *in vitro* function of immortalised human myoblasts was not influenced by the intrinsic age of the donor SkM. Preliminary cellular passaging experiments of both cell lines found that myoblasts from young or old origins had similar proliferative capacity and responses to cryogenic revival. Importantly, to eliminate any variability between the cell lines, possibly induced through serial passaging, experiments were conducted with myoblasts having been passaged an equal number of times. Studies have shown that serial passaging of cell lines can lead to phenotypic drift in the cell line (Geraghty et al., 2014). Thus, to diminish possible passage-induced phenotypic changes among the young and old cell lines, experiments were conducted with cells cryogenically passaged no more than four times. Subsequent investigations comparing the proliferative capacity of myoblasts between the young and old cell lines determined similar rates of cellular expansion when the cells were cultured, which was reflective of the published literature (Pietrangelo et al., 2009; Decary et al., 1997). Similarly, comparing the capacity of young and old myoblasts to differentiate using three different DM formulations revealed cellular fusion occurred at equal rates among the two cell lines in each of the three culture conditions. Further experimentation examining the differences between young and old myoblasts detailed the prominent similarities in the differentiation parameters and the expression of the proliferation and differentiation markers. Ultimately, the cell culture conditions generated in this

project revealed that immortalised human myoblasts maintained their myogenic potential and function when cultured *in vitro*, despite an almost 6-decade difference in the age of the donor SkM. Importantly, these finding coincide with studies utilising primary human myoblasts, which also showed persevered *in vitro* myogenic functionality regardless of the age of the donor SkM (Alsharidah et al., 2013). Indicating that age-linked changes to the SkM microenvironment rather than then intrinsic age of myoblasts induces the faulty SkM regeneration observed in aged SkM (Conboy et al., 2005; Carlson and Faulkner, 1989).

Upon determining no morphological differences between the young and old cell lines, the subsequent objectives of this project were executed utilising only the C25 cell line, as both cell lines performed equally when cultured under identical conditions. The next objective achieved in the fulfilment of the primary aim of this project was the generation of a novel simplified *in vitro* nerve-muscle co-culture system, free from serum, growth factors, and neurotrophins. Importantly, one of the biggest challenges in translating data from *in vitro* research to human trials is the inclusion of serum in the *in vitro* system. The role of serum in cell culture is extremely complex due to the occurrence of both growth factors and inhibitors. Thus, the use of serum in cell culture has many substantial drawback that can lead to misinterpretations of experimental results (Barnes and Sato, 1980; Ulreich and Chvapil, 1982; Sandstrom et al., 1994). For example, serum composition lacks uniformity, quality testing is required of each batch before use, growth-inhibiting factors may be present, an increased risk of contamination is possible, and the existence of serum in media can impede the isolation and purification of cells in culture. The experimental procedures conducted in the creation of the co-culture system permitted the proliferation of MN axons from ED 13.5 rat SCEs while simultaneously promoting innervation during myoblast-to-myotube differentiation of C25. Motor axons and their terminals were observed overlapping AChRs on contractile myotubes within the system, suggesting the formation of preliminary *in vitro* NMJs in the co-cultures. Importantly, myotubes in the co-culture system displayed contractile activity. This finding demonstrated the preliminary benefits of the co-culture system as a platform for studying SkM disorders in comparison to monocultures of SkMCs, which are less representative of *in vivo* conditions, as they do not exhibit contractile activity. In studies of SkMC monocultures treated with MN-derived growth factors involved with NMJ formation, such as agrin, no contractile activity is observed (Arnold et al., 2004; Bandi et al., 2008). Indicating that secreted factors alone did not promote the contractile activity observed in the co-culture system and cellular signalling via NMJ formation was most probably responsible for the contractile activity observed in the system. Myotube contractions in the system were observed as early as 72 hours after the co-culture of the SCEs with the C25. To the author's knowledge, this is the first nerve-muscle co-culture system to exhibit spontaneous myotube contractions at this stage of development without supplementing the co-culture environment with

serum, growth and/or neurotrophic factors. Thus, the simplified composition of the co-culture system allowed for easy reproducibility, along with being a more accurate reflection of *in vivo* SkM development compared to SkMC monocultures. Furthermore, previous co-culture systems attempting to induce *in vitro* innervation of myotubes have all required the inclusion of at least one growth factor in their systems in order to generate spontaneous contractile activity in myotubes via NMJ formation (Das et al., 2010; Das et al., 2007; Rumsey et al., 2010; Rumsey et al., 2009; Guo et al., 2017; Guo et al., 2011; Guo et al., 2014; Chipman et al., 2014; Demestre et al., 2015; Umbach et al., 2012; Vilmont et al., 2016; Puttonen et al., 2015; Morimoto et al., 2013; Larkin et al., 2006). The simplified methods and efficient use of resources used to generate the co-culture model were able to induce myotube contractions in as little as three days post co-culture and by seven days post co-culture myotube contractions were exhibiting synchronicity, implying an abundance NMJ formation generated in a time efficient manner. This observation suggested the co-culture model offers ideal conditions for high-throughput research of the mechanisms responsible for the formation of NMJs. Contrastingly, most of the previously established models cited above require weeks of separately cultured MNs and SkMCs before co-culturing the cells and several more weeks before NMJ formation and myotube contraction are observed. Thus, providing further evidence that the co-culture model generated in this project offers many advantages over the established systems. Additionally, other advantages of this system being free of serum and growth/neurotrophic factors include it being cost-effective as well as saving on labour. The co-culture model was also designed with the neural component originating from SCEs as opposed to a cell suspension created from intact embryo spinal cords. This was due to experiments revealing SCEs induced synchronous and high frequency myotube contractions in the shortest timeframe, suggesting ventral horn and dorsal root neurons as well as supporting cells types at the DRGs, such as glial cells function mutually to correctly innervate myotubes and form NMJs in the system.

After establishing the co-culture model, the next objective in this project was to characterise the system to verify the occurrence of physiological NMJ formation. Before characterisation of the co-cultures was performed, experiments were conducted to determine the optimal time point indicative of mature NMJ formation. Peak contraction frequency was used to determine mature NMJ formation, which was observed 14 days after co-culture. Additionally, these preliminary experiments also revealed the long-term viability of the co-cultured cells, as the experiments were not terminated until 30 days after co-culture and could have been maintained longer if required. Cholinergic MNs were identified and characterised in the system using antibodies for ChAT and VaChT, which revealed the interaction among cholinergic MNs and myotubes in the system. This important finding reflects NMJ development seen *in vivo,* as both ChAT and VaChT are required for correct MN development and function (Brandon

et al., 2003; Misgeld et al., 2002). Along with MN and SkMC interactions during *in vivo* NMJ formation, the presence of terminal Schwann cells is also required. Studies with mice have shown that preliminary NMJ formation is possible without Schwann cells, but for appropriate synapse development to occur *in vivo* Schwann cells must be involved (Lin et al., 2000; Morris et al., 1999; Riethmacher et al., 1997; Woldeyesus et al., 1999; Wolpowitz et al., 2000). Thus, characterisation of Schwann cells in the co-culture system with antibodies for GFAP suggests the interaction between MNs, myotubes, and Schwann cells in the system promoted the maintenance and maturation of the *in vitro* NMJs generated in the system. The co-cultures were then stained for Syt1, a presynaptic calcium sensor that can be used to expose presynaptic MNT activity and is known to be crucial for facilitating the release of neurotransmitters from Ca^{2+} dependent vesicles (Geppert et al., 1994; Littleton et al., 1993). Identifying Syt1 at MNTs in the co-culture system provided further evidence of successful structural formation of NMJs in the system as would be expected during *in vivo* signal transmission at the NMJ. Subsequently, NMJ characterisation was performed to show postsynaptic AChRs at the NMJ MEP co-localising with MNs and their terminals. Accordingly, evidence of physiological *in vitro* NMJ formation, comparably observed *in vivo* was attained by the identification of AChRs on the MEP in the typical twisting knotted configuration overlapped by MNs, which endorsed the notion that the co-cultures were generating NMJs and exhibiting attributes of successful maturation. Postsynaptic characterisation of the co-cultures was also conducted to determine if NMJs in the system exhibited appropriate postsynaptic development and structural organisation. Observations of MuSK and Rapsyn at the MEP suggested agrin secretion from the MNT was able to trigger the MuSK signalling pathways. This finding demonstrated synaptic communication at the NMJ allowed for successful postsynaptic differentiation, as was shown by the co-localisation between Rapsyn, MuSK, and AChRs. Co-cultured myotubes also displayed the morphological characteristics of advanced differentiation. Specifically, transversal triads, which are the precisely developed excitation-contraction coupling apparatus characterised by the tight apposition of RYRs on the SR membranes and DHPRs on the T-tubules, physiological sarcomeric development as demonstrated by the presence of striations on the myotube membrane, and peripherally nuclei were all observed in the co-culture system. All of which are observed *in vivo* during advanced differentiation of SkMCs (Bruusgaard et al., 2003; Shadrin et al., 2016). Thus, the advantage of this co-culture system over typical aneural *in vitro* myoblast cultures and previously established nerve-muscle co-culture models is apparent, as they do no exhibit the level of advanced myotube differentiation seen in this co-culture system. Thus, this co-culture system is a superior tool for researching SkM wasting associated with ageing (e.g. sarcopenia) and disease (e.g. cancer cachexia) and investigating NM disorders. Through characterisation of the co-culture system, evidence was provided showing the interaction between neurons, myotubes, and neuroglia, as well as confirmation

of mature NMJs with presynaptic activity and postsynaptic structural organisation, and advanced differentiation of myotubes.

Once characterised, the next objective was to ensure NMJs function physiologically and confirm spontaneous myotube contractions in the co-culture system were MN-driven via signalling at the NMJ. This was accomplished with agonist and antagonist drug-response experiments, designed to act presynaptically on MNs and postsynaptically on AChRs at the NMJ, consequently influencing myotube CF. When exposed to α-BTX a permanent stoppage of spontaneous contractions occurred. Demonstrating that NMJs in the co-cultures reacted correctly to an irreversible competitive antagonist at the AChRs, as observed at the *in vivo* NMJ (Domet et al., 1995). Co-cultures treated with tubocurarine similarly demonstrated a stop in myotube contractions. However, unlike the α-BTX treated cultures, contractile activity was able to restart in the tubocurarine treated co-cultures, which would also be expected of a reversible competitive receptor antagonist acting on NMJs to modulate the contractile activity of SkM *in vivo*. Therefore, the re-initiation of contractile activity in the co-cultures verified recovery from tubocurarine exposure and validated the accurate neurotransmission observed in this *in vitro* NMJ system. Interestingly, co-cultures treated with bicuculline resulted in a preliminary cessation of myotube contractions before the reestablishment spontaneous activity. Research with mice has shown that bicuculline can non-competitively block ACh from binding with AChRs (Liu et al., 1994; Demuro et al., 2001). Accordingly, results from these studies can be used to suggest that bicuculline was able to modulate NMJ activity, which was reflected in myotube contractions being diminished in the co-culture system by preventing ACh from binding with receptors at the postsynaptic NMJ, further indicating that signalling at the NMJ was regulating contractile activity of myotubes in the co-culture system. The co-cultures were also treated with L-Glut to determine if MNs in the system were receptive to the excitatory neurotransmitter. A marked but short-lived increase in myotube CF was observed within the co-cultures when exposed to L-Glut. As it is known that SkMC membranes are stimulated through AChRs, the increased CF witnessed after the application L-Glut indicated that MNs were stimulated by the neurotransmitter to increase the release of ACh into the synaptic cleft of the NMJ in the co-culture system, thus inducing the increased myotube activity. The final treatment applied to the co-cultures was with the inhibitory CNS neurotransmitter GABA, to determine if GABA signalling was occurring at the *in vitro* NMJs in this system. Interestingly, a brief increase in myotube activity was observed following GABA exposure. Contrasting this result, studies have shown $GABA_B$ receptors exist *in vivo* at MNTs and their modulation via GABA binding could reduce ACh release at the MNT (Malomouzh, Nurullin, et al., 2015; Malomouzh, Petrov, et al., 2015). However, the full function of GABA and its role in modulating ACh via $GABA_B$ receptors at the presynaptic NMJ is yet to be clarified (Nurullin et al., 2018). Alternately, Research has shown several transmitter receptor classes exist in

early embryonic muscle, with $GABA_A$ receptors expressed on embryonic SkMCs (Borodinsky and Spitzer, 2007). Thus, the role of GABA at the embryonic and mature NMJ requires additional exploration before GABA functions at the NMJ can be fully understood. Ultimately, through real time functional assessment of NMJs in the co-culture system, evidence was provided to show this system has the potential for use as a high-content platform for the evaluation of innovative therapies and *in vitro* disease modelling, as well as improve the understanding of NMJ formation, development, and function. Although establishing this model without exogenous growth factors and neurotrophins is a significant breakthrough in *in vitro* NMJ modelling, it was not surprising as MNs and SkM are co-dependent tissues that rely on each other for trophic support and synaptic transmission/stimulation. Additionally, the crosstalk between SkM and MNs is essential for the formation and development of SkM, MNs, and NMJs. Following the functional assessment of NMJs engineered in the absence of growth factors and neurotrophins, indicating cells in the system secreted all required factors to establish this functional system. The final objective was to quantify the concentration of growth and neurotrophic factors in the co-culture system in comparison to aneurally-cultured myotubes, to determine if the endogenous upregulation of specific trophic factors supported the formation and development of NMJs generated in the co-culture system. This was accomplished via ELISA-based microarray experiments, which revealed elevated expression of twelve growth factors. Studies have shown that BDNF, which is commonly used in *in vitro* NMJ systems, is involved with SkM innervation and MN survival *in vivo*, along with potentiation of signal transmission at the NMJ (Zhang and Poo, 2002; Yan et al., 1993). Thus, the upregulation of BDNF in the co-cultures provided evidence that the system permitted physiological formation and development of NMJs via endogenously regulated BDNF, which was representative of *in vivo* NMJ formation. The upregulation of FGF-7 was also observed in the co-cultures. Importantly, this organising molecule can function in regulating presynaptic specialisation at the NMJ (Umemori et al., 2004; Fox et al., 2007). Studies have also shown agrin can regulate FGF expression in SkM to support presynaptic NMJ differentiation (An et al., 2010). Thus, elevated FGF-7 in the co-culture system indicated interaction between MN-secreted agrin and innervated myotubes during NMJ formation and development, as would be expected *in vivo*. Another factor upregulated in the co-cultures was GDNF, which is known to be important for *in vitro* MN survival (Oppenheim et al., 1995). Studies have also argued GDNF may act as a retrograde signalling factor (Wang et al., 2002). Additionally, GDNF over expression experiments in mouse models result in abnormal MN overgrowth (Keller-Peck et al., 2001; Nguyen et al., 1998). Findings from these studies suggest GDNF is involved with MNT maturation. Thus, elevated GDNF observed in the co-culture system indicated interaction between pre- and post-synaptic NMJs elements in the system. When quantifying IGF-1 and the IGFBPs 1, 2, 3, 4, and 6 in the co-cultures, all were significantly elevated in the system except IGFBP-2. It is known that IGF-1 has important

functions in SkM, MN, and NMJ formation, development, and maintenance (Velloso, 2008; Dobrowolny et al., 2005) and 80% of IGF-1 is bound to at least one IGFBP (Adachi et al., 2017). Importantly, the elevation of the IGFBPs, which serve as membrane transporter proteins for IGF-1, have also been shown to enhance IGF-1 bioavailability (Stewart et al., 1993). Therefore, the observed elevated expression of IGF-1 and its binding proteins in the co-culture system suggests SCE and SkMC interaction in the system induced the upregulation of these factors to support MN maturation, advanced differentiation of myofibres, and the formation of robust NMJ, representative of *in vivo* formation. Both NT-3 and NT-4, which are essential for *in vitro* NMJ modelling, were also elevated in the co-cultures, which are involved with the modulation of synaptic function and required for maintenance of NMJs (Gonzalez et al., 1999; Belluardo et al., 2001). Animal studies have demonstrated lack of NT-3 causes disruptions in NMJ development and maintenance, as well as reductions in the size of SkM fibres (Woolley et al., 1999; Woolley et al., 2005). Studies investigating NT-4 expression reveal NT-4 is expressed dependent on synapse activity and functions to regulate NM transmission. Thus, it can be asserted that the elevated NT-3 and NT-4 observed in the co-cultures was most probably caused by NMJ formation, development and synaptic activity. The final two growth factors that were significantly elevated in the co-cultures were VEGF and PlGF. Both of which belong to the VEGF family of growth factors and prominently known for their functions in vascular growth and development (Ferrara, 2004), Importantly, these factors have demonstrated functions in MN growth, guidance, migration, and survival (Rosenstein et al., 2010; Ruiz de Almodovar et al., 2009). These factors have also been linked with improved reinnervation of SkM after injury, as well as VEGF having the ability to upregulate GDNF and NGF to support MN axon regeneration (Shvartsman et al., 2014), indicating the synergy of growth factors during NMJ formation. Thus, the observed upregulation of VEGF and PlGF in the co-cultures suggests these factors were needed for appropriate MN develop and NMJ formation the system.

Having examined the results from the microarray experiments valuable insights were gained concerning the cellular signalling of this simplified co-culture system. Additionally, the determination was made that the co-culture system had the capacity to self-regulate NMJ formation and promoted advanced differentiation of SkMCs via the specific expression of essential growth and neurotrophic factors.

8.1 Conclusion & Future Directions

In conclusion, this project detailed the establishment of a novel and simplified *in vitro* NMJ co-culture system, engineered for the first time with immortalised human skeletal muscle myoblasts innervated with neurons from rat embryo spinal cords. This unique breakthrough co-culture system free from serum, growth and neurotrophic factors generated contractile myotubes with indicators of advanced differentiation and the formation of structurally appropriate and functional NMJs, representative of *in vivo* conditions. Therefore, this *in vitro* co-culture system provides a platform for expanding research into skeletal muscle physiology, as well as NMJ formation and development. Furthermore, the nature of this co-culture system offers a relevant means for high-throughput investigations of neurological and/or muscular disease modelling, drug discovery, and regenerative medicine, through precise manipulation of components in the system.

For example, new potential drugs and molecules of interest that are being developed for the treatment of NM and ND disorders such as CMS, LEMS, MG, ALS, SMA, diabetic neuropathy/myopathy, and sarcopenia can be tested on this NMJ model as single or multiple doses over a protracted time interval, mimicking real drug evaluation conditions, which can be used to quantify how the NM system responds to the intervention. The model provides an accurate replica of live NMJs *in vivo*, permitting for fast, realistic, and non-invasive drug testing. Regardless of the ethical concerns of using live animal subjects to test drugs, animal testing is known to be extremely inaccurate. Studies have shown that only one out of 50 drugs that are tested on animals *in vivo* are suitable for human use, as well as the approval process for drug use in humans based on animal testing being a complex and largely unsuccessful endeavour. In contrast, the functional data generated by this *in vitro* NMJ model can be directly compared to what clinicians may be observing in clinical human trials. Thus, this model may influence the design of future clinical trials, and reduce the time required for drug development. Furthermore, the sensitivity of this model provides a highly accurate screening tool for new drugs due to the model having the capability to quantify the degree of loss-of-function caused by neuromuscular blocking agents with various modes of action. This model can also allow for future research into the behaviour of disease progression in the NM system, resulting in more informed treatment decisions for clinical patients. There is also the potential for future versions of this NMJ model being developed with diseased MNs or SkMCs, which could also be used to develop innovative therapies to treat neuromuscular diseases.

Chapter 9: References

9.0 References

Aas, V., Bakke, S. S., Feng, Y. Z., Kase, E. T., Jensen, J., Bajpeyi, S., Thoresen, G. H. and Rustan, A. C. (2013) 'Are cultured human myotubes far from home?' *Cell Tissue Res*, 354(3), Dec, pp. 671-682.

Abujarour, R. and Valamehr, B. (2015) 'Generation of skeletal muscle cells from pluripotent stem cells: advances and challenges.' *Front Cell Dev Biol*, 3 p. 29.

Adachi, Y., Nojima, M., Mori, M., Yamashita, K., Yamano, H.-O., Nakase, H., Endo, T., Wakai, K., Sakata, K. and Tamakoshi, A. (2017) 'Insulin-like growth factor-1, IGF binding protein-3, and the risk of esophageal cancer in a nested case-control study.' *World journal of gastroenterology*, 23(19) pp. 3488-3495.

Agalliu, D., Takada, S., Agalliu, I., McMahon, A. P. and Jessell, T. M. (2009) 'Motor neurons with axial muscle projections specified by Wnt4/5 signaling.' *Neuron*, 61(5), Mar 12, pp. 708-720.

Al-Dabbagh, S., McPhee, J. S., Murgatroyd, C., Butler-Browne, G., Stewart, C. E. and Al-Shanti, N. (2015) 'The lymphocyte secretome from young adults enhances skeletal muscle proliferation and migration, but effects are attenuated in the secretome of older adults.' *Physiological reports*, 3(11) p. e12518.

Alsharidah, M., Lazarus, N. R., George, T. E., Agley, C. C., Velloso, C. P. and Harridge, S. D. (2013) 'Primary human muscle precursor cells obtained from young and old donors produce similar proliferative, differentiation and senescent profiles in culture.' *Aging Cell*, 12(3), Jun, pp. 333-344.

Amato, A. A. (2018) 'Myasthenia Gravis and Other Diseases of the Neuromuscular Junction.' *In* Jameson, J. L., Fauci, A. S., Kasper, D. L., Hauser, S. L., Longo, D. L. and Loscalzo, J. (eds.) *Harrison's Principles of Internal Medicine, 20e*. New York, NY: McGraw-Hill Education,

An, M. C., Lin, W., Yang, J., Dominguez, B., Padgett, D., Sugiura, Y., Aryal, P., Gould, T. W., Oppenheim, R. W., Hester, M. E., Kaspar, B. K., Ko, C.-P. and Lee, K.-F. (2010) 'Acetylcholine negatively regulates development of the neuromuscular junction through distinct cellular mechanisms.' *Proceedings of the National Academy of Sciences*, 107(23) pp. 10702-10707.

Apel, E. D., Roberds, S. L., Campbell, K. P. and Merlie, J. P. (1995) 'Rapsyn may function as a link between the acetylcholine receptor and the agrin-binding dystrophin-associated glycoprotein complex.' *Neuron*, 15(1), Jul, pp. 115-126.

Apel, E. D., Glass, D. J., Moscoso, L. M., Yancopoulos, G. D. and Sanes, J. R. (1997) 'Rapsyn is required for MuSK signaling and recruits synaptic components to a MuSK-containing scaffold.' *Neuron*, 18(4), Apr, pp. 623-635.

Arnold, A.-S., Christe, M. and Handschin, C. (2012) 'A Functional Motor Unit in the Culture Dish: Co-culture of Spinal Cord Explants and Muscle Cells.' *Journal of Visualized Experiments : JoVE*, (62), 04/12, p. 3616.

Arnold, A. S., Gueye, M., Guettier-Sigrist, S., Courdier-Fruh, I., Coupin, G., Poindron, P. and Gies, J. P. (2004) 'Reduced expression of nicotinic AChRs in myotubes from spinal muscular atrophy I patients.' *Lab Invest*, 84(10), Oct, pp. 1271-1278.

Arvidsson, U., Riedl, M., Elde, R. and Meister, B. (1997) 'Vesicular acetylcholine transporter (VAChT) protein: a novel and unique marker for cholinergic neurons in the central and peripheral nervous systems.' *J Comp Neurol*, 378(4), Feb 24, pp. 454-467.

Ashby, P. R., Wilson, S. J. and Harris, A. J. (1993) 'Formation of primary and secondary myotubes in aneural muscles in the mouse mutant peroneal muscular atrophy.' *Dev Biol*, 156(2), Apr, pp. 519-528.

Aulehla, A. and Pourquié, O. (2010) 'Signaling gradients during paraxial mesoderm development.' *Cold Spring Harbor perspectives in biology*, 2(2) pp. a000869-a000869.

Balczarek, K. A., Lai, Z. C. and Kumar, S. (1997) 'Evolution and functional diversification of the paired box (Pax) DNA-binding domains.' *Molecular Biology and Evolution*, 14(8), Aug, pp. 829-842.

Balice-Gordon, R. J. (1996) 'Schwann cells: Dynamic roles at the neuromuscular junction.' *Current Biology*, 6(9), 1996/09/01/, pp. 1054-1056.

Bandi, E., Jevsek, M., Mars, T., Jurdana, M., Formaggio, E., Sciancalepore, M., Fumagalli, G., Grubic, Z., Ruzzier, F. and Lorenzon, P. (2008) 'Neural agrin controls maturation of the excitation-contraction coupling mechanism in human myotubes developing in vitro.' *Am J Physiol Cell Physiol*, 294(1), Jan, pp. C66-73.

Barberi, L., Scicchitano, B. M., De Rossi, M., Bigot, A., Duguez, S., Wielgosik, A., Stewart, C., McPhee, J., Conte, M., Narici, M., Franceschi, C., Mouly, V., Butler-Browne, G. and Musarò, A. (2013) 'Age-dependent alteration in muscle regeneration: the critical role of tissue niche.' *Biogerontology*, 14(3), Jun, pp. 273-292.

Barnes, D. and Sato, G. (1980) 'Serum-free cell culture: a unifying approach.' *Cell*, 22(3), Dec, pp. 649-655.

Bartoli, M., Ramarao, M. K. and Cohen, J. B. (2001) 'Interactions of the rapsyn RING-H2 domain with dystroglycan.' *J Biol Chem*, 276(27), Jul 6, pp. 24911-24917.

Baudet, C., Pozas, E., Adameyko, I., Andersson, E., Ericson, J. and Ernfors, P. (2008) 'Retrograde Signaling onto Ret during Motor Nerve Terminal Maturation.' *The Journal of Neuroscience*, 28(4) pp. 963-975.

Beccafico, S., Puglielli, C., Pietrangelo, T., Bellomo, R., Fano, G. and Fulle, S. (2007) 'Age-dependent effects on functional aspects in human satellite cells.' *Ann N Y Acad Sci*, 1100, Apr, pp. 345-352.

Belluardo, N., Westerblad, H., Mudo, G., Casabona, A., Bruton, J., Caniglia, G., Pastoris, O., Grassi, F. and Ibanez, C. F. (2001) 'Neuromuscular junction disassembly and muscle fatigue in mice lacking neurotrophin-4.' *Mol Cell Neurosci*, 18(1), Jul, pp. 56-67.

Benatar, M. (2007) 'Lost in translation: treatment trials in the SOD1 mouse and in human ALS.' *Neurobiol Dis*, 26(1), Apr, pp. 1-13.

Bezakova, G. and Ruegg, M. A. (2003) 'New insights into the roles of agrin.' *Nat Rev Mol Cell Biol*, 4(4), Apr, pp. 295-308.

Bezakova, G., Helm, J. P., Francolini, M. and Lomo, T. (2001) 'Effects of purified recombinant neural and muscle agrin on skeletal muscle fibers in vivo.' *J Cell Biol*, 153(7), Jun 25, pp. 1441-1452.

Bismuth, K. and Relaix, F. (2010) 'Genetic regulation of skeletal muscle development.' *Exp Cell Res*, 316(18), Nov 1, pp. 3081-3086.

Biswal, B., Yetkin, F. Z., Haughton, V. M. and Hyde, J. S. (1995) 'FUNCTIONAL CONNECTIVITY IN THE MOTOR CORTEX OF RESTING HUMAN BRAIN USING ECHO-PLANAR MRI.' *Magnetic Resonance in Medicine*, 34(4), Oct, pp. 537-541.

Bloch-Gallego, E. (2015) 'Mechanisms controlling neuromuscular junction stability.' *Cell Mol Life Sci*, 72(6), Mar, pp. 1029-1043.

Bolliger, M. F., Zurlinden, A., Luscher, D., Butikofer, L., Shakhova, O., Francolini, M., Kozlov, S. V., Cinelli, P., Stephan, A., Kistler, A. D., Rulicke, T., Pelczar, P., Ledermann, B., Fumagalli, G., Gloor, S. M., Kunz, B. and Sonderegger, P. (2010) 'Specific proteolytic cleavage of agrin regulates maturation of the neuromuscular junction.' *J Cell Sci*, 123(Pt 22), Nov 15, pp. 3944-3955.

Borodinsky, L. N. and Spitzer, N. C. (2007) 'Activity-dependent neurotransmitter-receptor matching at the neuromuscular junction.' *Proc Natl Acad Sci U S A*, 104(1), Jan 2, pp. 335-340.

Bowe, M. A., Deyst, K. A., Leszyk, J. D. and Fallon, J. R. (1994) 'Identification and purification of an agrin receptor from Torpedo postsynaptic membranes: a heteromeric complex related to the dystroglycans.' *Neuron*, 12(5), May, pp. 1173-1180.

Bowen, D. C., Park, J. S., Bodine, S., Stark, J. L., Valenzuela, D. M., Stitt, T. N., Yancopoulos, G. D., Lindsay, R. M., Glass, D. J. and DiStefano, P. S. (1998) 'Localization and regulation of MuSK at the neuromuscular junction.' *Dev Biol*, 199(2), Jul 15, pp. 309-319.

Bowery, N. G., Bettler, B., Froestl, W., Gallagher, J. P., Marshall, F., Raiteri, M., Bonner, T. I. and Enna, S. J. (2002) 'International Union of Pharmacology. XXXIII. Mammalian gamma-aminobutyric acid(B) receptors: structure and function.' *Pharmacol Rev*, 54(2), Jun, pp. 247-264.

Bowman, W. C. (2006) 'Neuromuscular block.' *British journal of pharmacology*, 147 Suppl 1(Suppl 1) pp. S277-S286.

Brandon, E. P., Lin, W., D'Amour, K. A., Pizzo, D. P., Dominguez, B., Sugiura, Y., Thode, S., Ko, C. P., Thal, L. J., Gage, F. H. and Lee, K. F. (2003) 'Aberrant patterning of neuromuscular synapses in choline acetyltransferase-deficient mice.' *J Neurosci*, 23(2), Jan 15, pp. 539-549.

Braun, T., Buschhausen-Denker, G., Bober, E., Tannich, E. and Arnold, H. H. (1989) 'A novel human muscle factor related to but distinct from MyoD1 induces myogenic conversion in 10T1/2 fibroblasts.' *The EMBO journal*, 8(3) pp. 701-709.

Bril, V. (2014) 'Neuromuscular complications of diabetes mellitus.' *Continuum (Minneap Minn)*, 20(3 Neurology of Systemic Disease), Jun, pp. 531-544.

Brooks, S. V. and Faulkner, J. A. (1990) 'Contraction-induced injury: recovery of skeletal muscles in young and old mice.' *Am J Physiol*, 258(3 Pt 1), Mar, pp. C436-442.

Brose, N., Petrenko, A. G., Sudhof, T. C. and Jahn, R. (1992) 'Synaptotagmin: a calcium sensor on the synaptic vesicle surface.' *Science*, 256(5059), May 15, pp. 1021-1025.

Brun, Caroline E. and Rudnicki, Michael A. (2015) 'GDF11 and the Mythical Fountain of Youth.' *Cell Metabolism*, 22(1) pp. 54-56.

Bruneau, E. G., Brenner, D. S., Kuwada, J. Y. and Akaaboune, M. (2008) 'Acetylcholine receptor clustering is required for the accumulation and maintenance of scaffolding proteins.' *Curr Biol*, 18(2), Jan 22, pp. 109-115.

Bruno, S. and Darzynkiewicz, Z. (1992) 'Cell cycle dependent expression and stability of the nuclear protein detected by Ki-67 antibody in HL-60 cells.' *Cell Prolif*, 25(1), Jan, pp. 31-40.

Bruusgaard, J. C., Liestol, K., Ekmark, M., Kollstad, K. and Gundersen, K. (2003) 'Number and spatial distribution of nuclei in the muscle fibres of normal mice studied in vivo.' *J Physiol*, 551(Pt 2), Sep 1, pp. 467-478.

Buckingham, M. (2001) 'Skeletal muscle formation in vertebrates.' *Current Opinion in Genetics & Development*, 11(4), 2001/08/01/, pp. 440-448.

Buckingham, M. and Relaix, F. (2007) 'The role of Pax genes in the development of tissues and organs: Pax3 and Pax7 regulate muscle progenitor cell functions.' *Annu Rev Cell Dev Biol*, 23 pp. 645-673.

Buckingham, M., Bajard, L., Chang, T., Daubas, P., Hadchouel, J., Meilhac, S., Montarras, D., Rocancourt, D. and Relaix, F. (2003) 'The formation of skeletal muscle: from somite to limb.' *Journal of Anatomy*, 202(1), Jan, pp. 59-68.

Bullwinkel, J., Baron-Lühr, B., Lüdemann, A., Wohlenberg, C., Gerdes, J. and Scholzen, T. (2006) 'Ki-67 protein is associated with ribosomal RNA transcription in quiescent and proliferating cells.' *Journal of Cellular Physiology*, 206(3) pp. 624-635.

Caccamo, D. V., Herman, M. M., Frankfurter, A., Katsetos, C. D., Collins, V. P. and Rubinstein, L. J. (1989) 'An immunohistochemical study of neuropeptides and neuronal cytoskeletal proteins in the neuroepithelial component of a spontaneous murine ovarian teratoma. Primitive neuroepithelium displays immunoreactivity for neuropeptides and neuron-associated beta-tubulin isotype.' *The American journal of pathology*, 135(5) pp. 801-813.

Campagna, J. A., Ruegg, M. A. and Bixby, J. L. (1995) 'Agrin is a differentiation-inducing "stop signal" for motoneurons in vitro.' *Neuron*, 15(6), Dec, pp. 1365-1374.

Campagna, J. A., Ruegg, M. A. and Bixby, J. L. (1997) 'Evidence that agrin directly influences presynaptic differentiation at neuromuscular junctions in vitro.' *Eur J Neurosci*, 9(11), Nov, pp. 2269-2283.

Capsoni, S., Ruberti, F., Di Daniel, E. and Cattaneo, A. (2000) 'Muscular dystrophy in adult and aged anti-NGF transgenic mice resembles an inclusion body myopathy.' *J Neurosci Res*, 59(4), Feb 15, pp. 553-560.

Carlson, B. M. and Faulkner, J. A. (1989) 'Muscle transplantation between young and old rats: age of host determines recovery.' *Am J Physiol*, 256(6 Pt 1), Jun, pp. C1262-1266.

Carlson, M. E., Hsu, M. and Conboy, I. M. (2008) 'Imbalance between pSmad3 and Notch induces CDK inhibitors in old muscle stem cells.' *Nature*, 454(7203), 07/24/print, pp. 528-532.

Carlson, M. E., Suetta, C., Conboy, M. J., Aagaard, P., Mackey, A., Kjaer, M. and Conboy, I. (2009) 'Molecular aging and rejuvenation of human muscle stem cells.' *EMBO Mol Med*, 1(8-9), Nov, pp. 381-391.

Carosio, S., Berardinelli, M. G., Aucello, M. and Musaro, A. (2011) 'Impact of ageing on muscle cell regeneration.' *Ageing Res Rev*, 10(1), Jan, pp. 35-42.

Carrasco, D. I. and English, A. W. (2003) 'Neurotrophin 4/5 is required for the normal development of the slow muscle fiber phenotype in the rat soleus.' *J Exp Biol*, 206(Pt 13), Jul, pp. 2191-2200.

Chakkalakal, J. V., Jones, K. M., Basson, M. A. and Brack, A. S. (2012) 'The aged niche disrupts muscle stem cell quiescence.' *Nature*, 490(7420), Oct 18, pp. 355-360.

Chandrasekhar, A. (2004) 'Turning heads: development of vertebrate branchiomotor neurons.' *Dev Dyn*, 229(1), Jan, pp. 143-161.

Charge, S. B. and Rudnicki, M. A. (2004) 'Cellular and molecular regulation of muscle regeneration.' *Physiol Rev*, 84(1), Jan, pp. 209-238.

Chevessier, F., Girard, E., Molgo, J., Bartling, S., Koenig, J., Hantai, D. and Witzemann, V. (2008) 'A mouse model for congenital myasthenic syndrome due to MuSK mutations reveals defects in structure and function of neuromuscular junctions.' *Hum Mol Genet*, 17(22), Nov 15, pp. 3577-3595.

Chevrel, G., Hohlfeld, R. and Sendtner, M. (2006) 'The role of neurotrophins in muscle under physiological and pathological conditions.' *Muscle Nerve*, 33(4), Apr, pp. 462-476.

Chipman, P. H., Zhang, Y. and Rafuse, V. F. (2014) 'A stem-cell based bioassay to critically assess the pathology of dysfunctional neuromuscular junctions.' *PloS one*, 9(3) pp. e91643-e91643.

Collins-Hooper, H., Woolley, T. E., Dyson, L., Patel, A., Potter, P., Baker, R. E., Gaffney, E. A., Maini, P. K., Dash, P. R. and Patel, K. (2012) 'Age-related changes in speed and mechanism of adult skeletal muscle stem cell migration.' *Stem Cells*, 30(6), Jun, pp. 1182-1195.

Collins, C. A., Zammit, P. S., Ruiz, A. P., Morgan, J. E. and Partridge, T. A. (2007) 'A population of myogenic stem cells that survives skeletal muscle aging.' *Stem Cells*, 25(4), Apr, pp. 885-894.

Collins, T. J. (2007) 'ImageJ for microscopy.' *BioTechniques*, 43(1S) pp. S25-S30.

Conboy, I. M., Conboy, M. J., Smythe, G. M. and Rando, T. A. (2003) 'Notch-mediated restoration of regenerative potential to aged muscle.' *Science*, 302(5650), Nov 28, pp. 1575-1577.

Conboy, I. M., Conboy, M. J., Wagers, A. J., Girma, E. R., Weissman, I. L. and Rando, T. A. (2005) 'Rejuvenation of aged progenitor cells by exposure to a young systemic environment.' *Nature*, 433, 02/17/online, p. 760.

Condon, K., Silberstein, L., Blau, H. M. and Thompson, W. J. (1990) 'Differentiation of fiber types in aneural musculature of the prenatal rat hindlimb.' *Dev Biol*, 138(2), Apr, pp. 275-295.

Cooke, I. M. and Grinnell, A. D. (1964) 'EFFECT OF TUBOCURARINE ON ACTION POTENTIALS IN NORMAL AND DENERVATED SKELETAL MUSCLE.' *The Journal of physiology*, 175(2) pp. 203-210.

Coronado, R., Morrissette, J., Sukhareva, M. and Vaughan, D. M. (1994) 'Structure and function of ryanodine receptors.' *Am J Physiol*, 266(6 Pt 1), Jun, pp. C1485-1504.

Cosgrove, B. D., Gilbert, P. M., Porpiglia, E., Mourkioti, F., Lee, S. P., Corbel, S. Y., Llewellyn, M. E., Delp, S. L. and Blau, H. M. (2014) 'Rejuvenation of the muscle stem cell population restores strength to injured aged muscles.' *Nat Med*, 20(3), 03//print, pp. 255-264.

Court, F. A., Gillingwater, T. H., Melrose, S., Sherman, D. L., Greenshields, K. N., Morton, A. J., Harris, J. B., Willison, H. J. and Ribchester, R. R. (2008) 'Identity, developmental restriction and reactivity of extralaminar cells capping mammalian neuromuscular junctions.' *J Cell Sci*, 121(Pt 23), Dec 1, pp. 3901-3911.

Crane, J. D., Devries, M. C., Safdar, A., Hamadeh, M. J. and Tarnopolsky, M. A. (2010) 'The effect of aging on human skeletal muscle mitochondrial and intramyocellular lipid ultrastructure.' *J Gerontol A Biol Sci Med Sci*, 65(2), Feb, pp. 119-128.

Cuylen, S., Blaukopf, C., Politi, A. Z., Müller-Reichert, T., Neumann, B., Poser, I., Ellenberg, J., Hyman, A. A. and Gerlich, D. W. (2016) 'Ki-67 acts as a biological surfactant to disperse mitotic chromosomes.' *Nature*, 535(7611) pp. 308-312.

Dalla Torre di Sanguinetto, S. A., Dasen, J. S. and Arber, S. (2008) 'Transcriptional mechanisms controlling motor neuron diversity and connectivity.' *Curr Opin Neurobiol*, 18(1), Feb, pp. 36-43.

Daniels, M. P., Lowe, B. T., Shah, S., Ma, J., Samuelsson, S. J., Lugo, B., Parakh, T. and Uhm, C. S. (2000) 'Rodent nerve-muscle cell culture system for studies of neuromuscular junction development: refinements and applications.' *Microsc Res Tech*, 49(1), Apr 1, pp. 26-37.

Darzynkiewicz, Z., Zhao, H., Zhang, S., Lee, M. Y. W. T., Lee, E. Y. C. and Zhang, Z. (2015) 'Initiation and termination of DNA replication during S phase in relation to cyclins D1, E and A, p21WAF1, Cdt1 and the p12 subunit of DNA polymerase δ revealed in individual cells by cytometry.' *Oncotarget*, 6(14) pp. 11735-11750.

Das, M., Rumsey, J. W., Bhargava, N., Stancescu, M. and Hickman, J. J. (2010) 'A defined long-term in vitro tissue engineered model of neuromuscular junctions.' *Biomaterials*, 31(18), Jun, pp. 4880-4888.

Das, M., Rumsey, J. W., Gregory, C. A., Bhargava, N., Kang, J. F., Molnar, P., Riedel, L., Guo, X. and Hickman, J. J. (2007) 'Embryonic motoneuron-skeletal muscle co-culture in a defined system.' *Neuroscience*, 146(2), May 11, pp. 481-488.

Davis-Dusenbery, B. N., Williams, L. A., Klim, J. R. and Eggan, K. (2014) 'How to make spinal motor neurons.' *Development*, 141(3) pp. 491-501.

Davis, R. L., Weintraub, H. and Lassar, A. B. (1987) 'Expression of a single transfected cDNA converts fibroblasts to myoblasts.' *Cell*, 51(6), Dec 24, pp. 987-1000.

de Castro, B. M., De Jaeger, X., Martins-Silva, C., Lima, R. D. F., Amaral, E., Menezes, C., Lima, P., Neves, C. M. L., Pires, R. G., Gould, T. W., Welch, I., Kushmerick, C., Guatimosim, C., Izquierdo, I.,

Cammarota, M., Rylett, R. J., Gomez, M. V., Caron, M. G., Oppenheim, R. W., Prado, M. A. M. and Prado, V. F. (2009) 'The Vesicular Acetylcholine Transporter Is Required for Neuromuscular Development and Function.' *Molecular and Cellular Biology*, 29(19) pp. 5238-5250.

Decary, S., Mouly, V., BenHamida, C., Sautet, A., Barbet, J. P. and ButlerBrowne, G. S. (1997) 'Replicative potential and telomere length in human skeletal muscle: Implications for satellite cell-mediated gene therapy.' *Human Gene Therapy*, 8(12), Aug, pp. 1429-1438.

DeChiara, T. M., Bowen, D. C., Valenzuela, D. M., Simmons, M. V., Poueymirou, W. T., Thomas, S., Kinetz, E., Compton, D. L., Rojas, E., Park, J. S., Smith, C., DiStefano, P. S., Glass, D. J., Burden, S. J. and Yancopoulos, G. D. (1996) 'The receptor tyrosine kinase MuSK is required for neuromuscular junction formation in vivo.' *Cell*, 85(4), May 17, pp. 501-512.

Degens, H. (2010) 'The role of systemic inflammation in age-related muscle weakness and wasting.' *Scand J Med Sci Sports*, 20(1), Feb, pp. 28-38.

Delaporte, C., Dautreaux, B. and Fardeau, M. (1986) 'Human myotube differentiation in vitro in different culture conditions.' *Biol Cell*, 57(1) pp. 17-22.

Demestre, M., Orth, M., Föhr, K. J., Achberger, K., Ludolph, A. C., Liebau, S. and Boeckers, T. M. (2015) 'Formation and characterisation of neuromuscular junctions between hiPSC derived motoneurons and myotubes.' *Stem Cell Research*, 15(2), 2015/09/01/, pp. 328-336.

Demuro, A., Palma, E., Eusebi, F. and Miledi, R. (2001) 'Inhibition of nicotinic acetylcholine receptors by bicuculline.' *Neuropharmacology*, 41(7), Dec, pp. 854-861.

Denoth, J., Stussi, E., Csucs, G. and Danuser, G. (2002) 'Single muscle fiber contraction is dictated by inter-sarcomere dynamics.' *Journal of Theoretical Biology*, 216(1), May, pp. 101-122.

Dhawan, J. and Rando, T. A. (2005) 'Stem cells in postnatal myogenesis: molecular mechanisms of satellite cell quiescence, activation and replenishment.' *Trends Cell Biol*, 15(12), Dec, pp. 666-673.

Dixon, T. A., Cohen, E., Cairns, D. M., Rodriguez, M., Mathews, J., Jose, R. R. and Kaplan, D. L. (2018) 'Bioinspired Three-Dimensional Human Neuromuscular Junction Development in Suspended Hydrogel Arrays.' *Tissue Eng Part C Methods*, 24(6), Jun, pp. 346-359.

Dobrowolny, G., Giacinti, C., Pelosi, L., Nicoletti, C., Winn, N., Barberi, L., Molinaro, M., Rosenthal, N. and Musarò, A. (2005) 'Muscle expression of a local Igf-1 isoform protects motor neurons in an ALS mouse model.' *The Journal of cell biology*, 168(2) pp. 193-199.

Dodds, R. M., Roberts, H. C., Cooper, C. and Sayer, A. A. (2015) 'The Epidemiology of Sarcopenia.' *J Clin Densitom*, 18(4), Oct-Dec, pp. 461-466.

Domet, M. A., Webb, C. E. and Wilson, D. F. (1995) 'IMPACT OF ALPHA-BUNGAROTOXIN ON TRANSMITTER RELEASE AT THE NEUROMUSCULAR-JUNCTION OF THE RAT.' *Neuroscience Letters*, 199(1), Oct, pp. 49-52.

Drey, M., Krieger, B., Sieber, C. C., Bauer, J. M., Hettwer, S. and Bertsch, T. (2014) 'Motoneuron loss is associated with sarcopenia.' *J Am Med Dir Assoc*, 15(6), Jun, pp. 435-439.

Dugger, S. A., Platt, A. and Goldstein, D. B. (2018) 'Drug development in the era of precision medicine.' *Nature reviews. Drug discovery*, 17(3) pp. 183-196.

Dumke, B. R. and Lees, S. J. (2011) 'Age-related impairment of T cell-induced skeletal muscle precursor cell function.' *American Journal of Physiology-Cell Physiology*, 300(6) pp. C1226-C1233.

Dutton, E. K., Uhm, C. S., Samuelsson, S. J., Schaffner, A. E., Fitzgerald, S. C. and Daniels, M. P. (1995) 'Acetylcholine receptor aggregation at nerve-muscle contacts in mammalian cultures: induction by ventral spinal cord neurons is specific to axons.' *J Neurosci*, 15(11), Nov, pp. 7401-7416.

E Thomson, C., M Hunter, A., R Griffiths, I., Edgar, J. and C McCulloch, M. (2006) *Murine spinal cord explants: A model for evaluating axonal growth and myelination in vitro.* Vol. 84.

Edmondson, D. G. and Olson, E. N. (1989) 'A gene with homology to the myc similarity region of MyoD1 is expressed during myogenesis and is sufficient to activate the muscle differentiation program.' *Genes Dev*, 3(5), May, pp. 628-640.

Elabd, C., Cousin, W., Upadhyayula, P., Chen, R. Y., Chooljian, M. S., Li, J., Kung, S., Jiang, K. P. and Conboy, I. M. (2014) 'Oxytocin is an age-specific circulating hormone that is necessary for muscle maintenance and regeneration.' *Nat Commun*, 5, 06/10/online,

Elinos, D., Rodríguez, R., Martínez, L. A., Zetina, M. E., Cifuentes, F. and Morales, M. A. (2016) 'Segregation of Acetylcholine and GABA in the Rat Superior Cervical Ganglia: Functional Correlation.' *Frontiers in cellular neuroscience*, 10 pp. 91-91.

Engel, A. G. and Sine, S. M. (2005) 'Current understanding of congenital myasthenic syndromes.' *Current Opinion in Pharmacology*, 5(3), Jun, pp. 308-321.

Engel, A. G., Shen, X. M., Selcen, D. and Sine, S. M. (2010) 'What have we learned from the congenital myasthenic syndromes.' *J Mol Neurosci*, 40(1-2), Jan, pp. 143-153.

Englander, L. L. and Rubin, L. L. (1987) 'Acetylcholine receptor clustering and nuclear movement in muscle fibers in culture.' *The Journal of Cell Biology*, 104(1) pp. 87-95.

Ernfors, P., Lee, K. F., Kucera, J. and Jaenisch, R. (1994) 'Lack of neurotrophin-3 leads to deficiencies in the peripheral nervous system and loss of limb proprioceptive afferents.' *Cell*, 77(4), May 20, pp. 503-512.

Faravelli, I., Frattini, E., Ramirez, A., Stuppia, G., Nizzardo, M. and Corti, S. (2014) 'iPSC-Based Models to Unravel Key Pathogenetic Processes Underlying Motor Neuron Disease Development.' *J Clin Med*, 3(4), Oct 17, pp. 1124-1145.

Feher, J. (2017) '3.6 - The Neuromuscular Junction and Excitation–Contraction Coupling.' *In Quantitative Human Physiology (Second Edition)*. Boston: Academic Press, pp. 318-333.

Feng, Z. and Ko, C. P. (2008) 'The role of glial cells in the formation and maintenance of the neuromuscular junction.' *Ann N Y Acad Sci*, 1132 pp. 19-28.

Fernyhough, P., Maeda, K. and Tomlinson, D. R. (1996) 'Brain-derived neurotrophic factor mRNA levels are up-regulated in hindlimb skeletal muscle of diabetic rats: effect of denervation.' *Exp Neurol*, 141(2), Oct, pp. 297-303.

Fernyhough, P., Diemel, L. T. and Tomlinson, D. R. (1998) 'Target tissue production and axonal transport of neurotrophin-3 are reduced in streptozotocin-diabetic rats.' *Diabetologia*, 41(3), Mar, pp. 300-306.

Fernyhough, P., Diemel, L. T., Brewster, W. J. and Tomlinson, D. R. (1995) 'Altered neurotrophin mRNA levels in peripheral nerve and skeletal muscle of experimentally diabetic rats.' *J Neurochem*, 64(3), Mar, pp. 1231-1237.

Fernyhough, P., Diemel, L. T., Hardy, J., Brewster, W. J., Mohiuddin, L. and Tomlinson, D. R. (1995) 'Human recombinant nerve growth factor replaces deficient neurotrophic support in the diabetic rat.' *Eur J Neurosci*, 7(5), May 1, pp. 1107-1110.

Ferrara, N. (2004) 'Vascular endothelial growth factor: basic science and clinical progress.' *Endocr Rev*, 25(4), Aug, pp. 581-611.

Ferris, L. T., Williams, J. S. and Shen, C. L. (2007) 'The effect of acute exercise on serum brain-derived neurotrophic factor levels and cognitive function.' *Med Sci Sports Exerc*, 39(4), Apr, pp. 728-734.

Fetcho, J. R. (1987) 'A review of the organization and evolution of motoneurons innervating the axial musculature of vertebrates.' *Brain Research Reviews*, 12(3), 1987/07/01/, pp. 243-280.

Fischer, L. R., Culver, D. G., Tennant, P., Davis, A. A., Wang, M., Castellano-Sanchez, A., Khan, J., Polak, M. A. and Glass, J. D. (2004) 'Amyotrophic lateral sclerosis is a distal axonopathy: evidence in mice and man.' *Exp Neurol*, 185(2), Feb, pp. 232-240.

Flucher, B. E. and Daniels, M. P. (1989) 'Distribution of Na+ channels and ankyrin in neuromuscular junctions is complementary to that of acetylcholine receptors and the 43 kd protein.' *Neuron*, 3(2), Aug, pp. 163-175.

Fox, M. A., Sanes, J. R., Borza, D. B., Eswarakumar, V. P., Fassler, R., Hudson, B. G., John, S. W., Ninomiya, Y., Pedchenko, V., Pfaff, S. L., Rheault, M. N., Sado, Y., Segal, Y., Werle, M. J. and Umemori, H. (2007) 'Distinct target-derived signals organize formation, maturation, and maintenance of motor nerve terminals.' *Cell*, 129(1), Apr 6, pp. 179-193.

Friese, A., Kaltschmidt, J. A., Ladle, D. R., Sigrist, M., Jessell, T. M. and Arber, S. (2009) 'Gamma and alpha motor neurons distinguished by expression of transcription factor Err3.' *Proc Natl Acad Sci U S A*, 106(32), Aug 11, pp. 13588-13593.

Frontera, W. R. and Ochala, J. (2015) 'Skeletal Muscle: A Brief Review of Structure and Function.' *Calcified Tissue International*, 96(3), Mar, pp. 183-195.

Fry, C. S., Lee, J. D., Mula, J., Kirby, T. J., Jackson, J. R., Liu, F., Yang, L., Mendias, C. L., Dupont-Versteegden, E. E., McCarthy, J. J. and Peterson, C. A. (2015) 'Inducible depletion of satellite cells in adult, sedentary mice impairs muscle regenerative capacity without affecting sarcopenia.' *Nat Med*, 21(1), 01//print, pp. 76-80.

Fulle, S., Di Donna, S., Puglielli, C., Pietrangelo, T., Beccafico, S., Bellomo, R., Protasi, F. and Fano, G. (2005) 'Age-dependent imbalance of the antioxidative system in human satellite cells.' *Exp Gerontol*, 40(3), Mar, pp. 189-197.

Funakoshi, H., Belluardo, N., Arenas, E., Yamamoto, Y., Casabona, A., Persson, H. and Ibanez, C. F. (1995) 'Muscle-derived neurotrophin-4 as an activity-dependent trophic signal for adult motor neurons.' *Science*, 268(5216), Jun 9, pp. 1495-1499.

Gannon, J., Doran, P., Kirwan, A. and Ohlendieck, K. (2009) 'Drastic increase of myosin light chain MLC-2 in senescent skeletal muscle indicates fast-to-slow fibre transition in sarcopenia of old age.' *Eur J Cell Biol*, 88(11), Nov, pp. 685-700.

Garcia, C. C., Potian, J. G., Hognason, K., Thyagarajan, B., Sultatos, L. G., Souayah, N., Routh, V. H. and McArdle, J. J. (2012) 'Acetylcholinesterase deficiency contributes to neuromuscular junction dysfunction in type 1 diabetic neuropathy.' *American journal of physiology. Endocrinology and metabolism*, 303(4) pp. E551-E561.

Gautam, M., Noakes, P. G., Mudd, J., Nichol, M., Chu, G. C., Sanes, J. R. and Merlie, J. P. (1995) 'Failure of postsynaptic specialization to develop at neuromuscular junctions of rapsyn-deficient mice.' *Nature*, 377(6546), Sep 21, pp. 232-236.

Gautam, M., Noakes, P. G., Moscoso, L., Rupp, F., Scheller, R. H., Merlie, J. P. and Sanes, J. R. (1996) 'Defective neuromuscular synaptogenesis in agrin-deficient mutant mice.' *Cell*, 85(4), May 17, pp. 525-535.

Gayraud-Morel, B., Chretien, F., Flamant, P., Gomes, D., Zammit, P. S. and Tajbakhsh, S. (2007) 'A role for the myogenic determination gene Myf5 in adult regenerative myogenesis.' *Dev Biol*, 312(1), Dec 1, pp. 13-28.

Gee, S. H., Montanaro, F., Lindenbaum, M. H. and Carbonetto, S. (1994) 'Dystroglycan-alpha, a dystrophin-associated glycoprotein, is a functional agrin receptor.' *Cell*, 77(5), Jun 3, pp. 675-686.

George, T., Velloso, C. P., Alsharidah, M., Lazarus, N. R. and Harridge, S. D. (2010) 'Sera from young and older humans equally sustain proliferation and differentiation of human myoblasts.' *Exp Gerontol*, 45(11), Nov, pp. 875-881.

Geppert, M., Goda, Y., Hammer, R. E., Li, C., Rosahl, T. W., Stevens, C. F. and Sudhof, T. C. (1994) 'Synaptotagmin I: a major Ca2+ sensor for transmitter release at a central synapse.' *Cell*, 79(4), Nov 18, pp. 717-727.

Geraghty, R. J., Capes-Davis, A., Davis, J. M., Downward, J., Freshney, R. I., Knezevic, I., Lovell-Badge, R., Masters, J. R. W., Meredith, J., Stacey, G. N., Thraves, P., Vias, M. and Cancer Research, U. K. (2014) 'Guidelines for the use of cell lines in biomedical research.' *British journal of cancer*, 111(6) pp. 1021-1046.

Gilhus, N. E. (2016) 'Myasthenia Gravis.' *New England Journal of Medicine*, 375(26), Dec, pp. 2570-2581.

Giller, E. L., Jr., Schrier, B. K., Shainberg, A., Fisk, H. R. and Nelson, P. G. (1973) 'Choline acetyltransferase activity is increased in combined cultures of spinal cord and muscle cells from mice.' *Science*, 182(4112), Nov 9, pp. 588-589.

Glass, D. J., Bowen, D. C., Stitt, T. N., Radziejewski, C., Bruno, J., Ryan, T. E., Gies, D. R., Shah, S., Mattsson, K., Burden, S. J., DiStefano, P. S., Valenzuela, D. M., DeChiara, T. M. and Yancopoulos, G. D. (1996) 'Agrin acts via a MuSK receptor complex.' *Cell*, 85(4), May 17, pp. 513-523.

Gold, S. M., Schulz, K. H., Hartmann, S., Mladek, M., Lang, U. E., Hellweg, R., Reer, R., Braumann, K. M. and Heesen, C. (2003) 'Basal serum levels and reactivity of nerve growth factor and brain-derived neurotrophic factor to standardized acute exercise in multiple sclerosis and controls.' *J Neuroimmunol*, 138(1-2), May, pp. 99-105.

Gonzalez-Freire, M., de Cabo, R., Studenski, S. A. and Ferrucci, L. (2014) 'The Neuromuscular Junction: Aging at the Crossroad between Nerves and Muscle.' *Front Aging Neurosci*, 6 p. 208.

Gonzalez, M., Ruggiero, F. P., Chang, Q., Shi, Y. J., Rich, M. M., Kraner, S. and Balice-Gordon, R. J. (1999) 'Disruption of Trkb-mediated signaling induces disassembly of postsynaptic receptor clusters at neuromuscular junctions.' *Neuron*, 24(3), Nov, pp. 567-583.

Gould, T. W., Buss, R. R., Vinsant, S., Prevette, D., Sun, W., Knudson, C. M., Milligan, C. E. and Oppenheim, R. W. (2006) 'Complete dissociation of motor neuron death from motor dysfunction by Bax deletion in a mouse model of ALS.' *J Neurosci*, 26(34), Aug 23, pp. 8774-8786.

Griesbeck, O., Parsadanian, A. S., Sendtner, M. and Thoenen, H. (1995) 'Expression of neurotrophins in skeletal muscle: quantitative comparison and significance for motoneuron survival and maintenance of function.' *J Neurosci Res*, 42(1), Sep 1, pp. 21-33.

Grubisic, V., Gottipati, M. K., Stout, R. F., Jr., Grammer, J. R. and Parpura, V. (2014) 'Heterogeneity of myotubes generated by the MyoD and E12 basic helix-loop-helix transcription factors in otherwise non-differentiation growth conditions.' *Biomaterials*, 35(7), Feb, pp. 2188-2198.

Guo, X., Gonzalez, M., Stancescu, M., Vandenburgh, H. H. and Hickman, J. J. (2011) 'Neuromuscular junction formation between human stem cell-derived motoneurons and human skeletal muscle in a defined system.' *Biomaterials*, 32(36), Dec, pp. 9602-9611.

Guo, X., Colon, A., Akanda, N., Spradling, S., Stancescu, M., Martin, C. and Hickman, J. J. (2017) 'Tissue engineering the mechanosensory circuit of the stretch reflex arc with human stem cells: Sensory neuron innervation of intrafusal muscle fibers.' *Biomaterials*, 122, 2017/04/01/, pp. 179-187.

Guo, X., Greene, K., Akanda, N., Smith, A., Stancescu, M., Lambert, S., Vandenburgh, H. and Hickman, J. (2014) 'In vitro Differentiation of Functional Human Skeletal Myotubes in a Defined System.' *Biomater Sci*, 2(1), Jan 1, pp. 131-138.

Gutman, C. R., Ajmera, M. K. and Hollyday, M. (1993) 'Organization of motor pools supplying axial muscles in the chicken.' *Brain Res*, 609(1-2), Apr 23, pp. 129-136.

Haase, G. (2006) 'Motor Neuron Diseases: Cellular and Animal Models.' *In Reviews in Cell Biology and Molecular Medicine*. Wiley-VCH Verlag GmbH & Co. KGaA,

Harper, J. M., Krishnan, C., Darman, J. S., Deshpande, D. M., Peck, S., Shats, I., Backovic, S., Rothstein, J. D. and Kerr, D. A. (2004) 'Axonal growth of embryonic stem cell-derived motoneurons in vitro and in motoneuron-injured adult rats.' *Proc Natl Acad Sci U S A*, 101(18), May 4, pp. 7123-7128.

Hernandez-Torres, F., Rodríguez-Outeiriño, L., Franco, D. and Aranega, A. E. (2017) 'Pitx2 in Embryonic and Adult Myogenesis.' *Frontiers in Cell and Developmental Biology*, 5(46), 2017-May-01,

Hesser, B. A., Henschel, O. and Witzemann, V. (2006) 'Synapse disassembly and formation of new synapses in postnatal muscle upon conditional inactivation of MuSK.' *Mol Cell Neurosci*, 31(3), Mar, pp. 470-480.

Hong, I. H. and Etherington, S. J. (2011) 'Neuromuscular Junction.' *In eLS*. Vol. 1. Chichester: John Wiley & Sons Ltd,

Hooghe, B., Hulpiau, P., van Roy, F. and De Bleser, P. (2008) 'ConTra: a promoter alignment analysis tool for identification of transcription factor binding sites across species.' *Nucleic Acids Res*, 36(Web Server issue), Jul 1, pp. W128-132.

Hopf, C. and Hoch, W. (1998) 'Dimerization of the muscle-specific kinase induces tyrosine phosphorylation of acetylcholine receptors and their aggregation on the surface of myotubes.' *J Biol Chem*, 273(11), Mar 13, pp. 6467-6473.

Hsieh-Li, H. M., Chang, J. G., Jong, Y. J., Wu, M. H., Wang, N. M., Tsai, C. H. and Li, H. (2000) 'A mouse model for spinal muscular atrophy.' *Nat Genet*, 24(1), Jan, pp. 66-70.

Hughes, S. M. and Blau, H. M. (1990) 'Migration of myoblasts across basal lamina during skeletal muscle development.' *Nature*, 345(6273), May 24, pp. 350-353.

Hutcheson, D. A., Zhao, J., Merrell, A., Haldar, M. and Kardon, G. (2009) 'Embryonic and fetal limb myogenic cells are derived from developmentally distinct progenitors and have different requirements for beta-catenin.' *Genes Dev*, 23(8), Apr 15, pp. 997-1013.

Hwa, V., Oh, Y. and Rosenfeld, R. G. (1999) 'The insulin-like growth factor-binding protein (IGFBP) superfamily.' *Endocr Rev*, 20(6), Dec, pp. 761-787.

Ihara, C., Shimatsu, A., Mizuta, H., Murabe, H., Nakamura, Y. and Nakao, K. (1996) 'Decreased neurotrophin-3 expression in skeletal muscles of streptozotocin-induced diabetic rats.' *Neuropeptides*, 30(4), Aug, pp. 309-312.

Inoue, H., Nagata, N., Kurokawa, H. and Yamanaka, S. (2014) 'iPS cells: a game changer for future medicine.' *Embo j*, 33(5), Mar 3, pp. 409-417.

Jacquemin, V., Furling, D., Bigot, A., Butler-Browne, G. S. and Mouly, V. (2004) 'IGF-1 induces human myotube hypertrophy by increasing cell recruitment.' *Exp Cell Res*, 299(1), Sep 10, pp. 148-158.

Jessell, T. M. (2000) 'Neuronal specification in the spinal cord: inductive signals and transcriptional codes.' *Nat Rev Genet*, 1(1), Oct, pp. 20-29.

Jessen, K. R., Morgan, L., Stewart, H. J. and Mirsky, R. (1990) 'Three markers of adult non-myelin-forming Schwann cells, 217c(Ran-1), A5E3 and GFAP: development and regulation by neuron-Schwann cell interactions.' *Development*, 109(1), May, pp. 91-103.

Jiang, Z. G., Shen, E. and Dun, N. J. (1990) 'Excitatory and inhibitory transmission from dorsal root afferents to neonate rat motoneurons in vitro.' *Brain Res*, 535(1), Dec 3, pp. 110-118.

Jockusch, H. and Voigt, S. (2003) 'Migration of adult myogenic precursor cells as revealed by GFP/nLacZ labelling of mouse transplantation chimeras.' *J Cell Sci*, 116(Pt 8), Apr 15, pp. 1611-1616.

Jones, A., Price, F., Le Grand, F., Soleimani, V., Dick, S., A Megeney, L. and Rudnicki, M. (2015) *Wnt/β-catenin controls follistatin signalling to regulate satellite cell myogenic potential.* Vol. 5.

Jones, G., Moore, C., Hashemolhosseini, S. and Brenner, H. R. (1999) 'Constitutively active MuSK is clustered in the absence of agrin and induces ectopic postsynaptic-like membranes in skeletal muscle fibers.' *J Neurosci*, 19(9), May 1, pp. 3376-3383.

Jones, G., Meier, T., Lichtsteiner, M., Witzemann, V., Sakmann, B. and Brenner, H. R. (1997) 'Induction by agrin of ectopic and functional postsynaptic-like membrane in innervated muscle.' *Proceedings of the National Academy of Sciences*, 94(6) p. 2654.

Kaasik, P., Aru, M., Alev, K. and Seene, T. (2012) 'Aging and regenerative capacity of skeletal muscle in rats.' *Curr Aging Sci*, 5(2), Jul, pp. 126-130.

Kania, A. and Jessell, T. M. (2003) 'Topographic motor projections in the limb imposed by LIM homeodomain protein regulation of ephrin-A:EphA interactions.' *Neuron*, 38(4), May 22, pp. 581-596.

Kanning, K. C., Kaplan, A. and Henderson, C. E. (2010) 'Motor neuron diversity in development and disease.' *Annu Rev Neurosci*, 33 pp. 409-440.

Katagiri, T., Yamaguchi, A., Komaki, M., Abe, E., Takahashi, N., Ikeda, T., Rosen, V., Wozney, J. M., Fujisawasehara, A. and Suda, T. (1994) 'BONE MORPHOGENETIC PROTEIN-2 CONVERTS THE DIFFERENTIATION PATHWAY OF C2C12 MYOBLASTS INTO THE OSTEOBLAST LINEAGE.' *Journal of Cell Biology*, 127(6), Dec, pp. 1755-1766.

Katsetos, C. D., Herman, M. M. and Mork, S. J. (2003) 'Class III beta-tubulin in human development and cancer.' *Cell Motil Cytoskeleton*, 55(2), Jun, pp. 77-96.

Katsetos, C. D., Legido, A., Perentes, E. and Mork, S. J. (2003) 'Class III beta-tubulin isotype: a key cytoskeletal protein at the crossroads of developmental neurobiology and tumor neuropathology.' *J Child Neurol*, 18(12), Dec, pp. 851-866; discussion 867.

Kaur, G. and Dufour, J. M. (2012) 'Cell lines: Valuable tools or useless artifacts.' *Spermatogenesis*, 2(1) pp. 1-5.

Keller-Peck, C. R., Feng, G., Sanes, J. R., Yan, Q., Lichtman, J. W. and Snider, W. D. (2001) 'Glial cell line-derived neurotrophic factor administration in postnatal life results in motor unit enlargement and continuous synaptic remodeling at the neuromuscular junction.' *J Neurosci*, 21(16), Aug 15, pp. 6136-6146.

Kiefer, J. C. and Hauschka, S. D. (2001) 'Myf-5 is transiently expressed in nonmuscle mesoderm and exhibits dynamic regional changes within the presegmented mesoderm and somites I-IV.' *Dev Biol*, 232(1), Apr 1, pp. 77-90.

Kim, N. and Burden, S. J. (2008) 'MuSK controls where motor axons grow and form synapses.' *Nat Neurosci*, 11(1), Jan, pp. 19-27.

Kim, N., Stiegler, A. L., Cameron, T. O., Hallock, P. T., Gomez, A. M., Huang, J. H., Hubbard, S. R., Dustin, M. L. and Burden, S. J. (2008) 'Lrp4 is a receptor for Agrin and forms a complex with MuSK.' *Cell*, 135(2), Oct 17, pp. 334-342.

Kim, T. N. and Choi, K. M. (2013) 'Sarcopenia: definition, epidemiology, and pathophysiology.' *J Bone Metab*, 20(1), May, pp. 1-10.

Knapp, J. R., Davie, J. K., Myer, A., Meadows, E., Olson, E. N. and Klein, W. H. (2006) 'Loss of myogenin in postnatal life leads to normal skeletal muscle but reduced body size.' *Development*, 133(4), Feb, pp. 601-610.

Kobayashi, T. and Askanas, V. (1985) 'Acetylcholine receptors and acetylcholinesterase accumulate at the nerve-muscle contacts of de novo grown human monolayer muscle cocultured with fetal rat spinal cord.' *Exp Neurol*, 88(2), May, pp. 327-335.

Kobayashi, T., Askanas, V. and Engel, W. K. (1987) 'Human muscle cultured in monolayer and cocultured with fetal rat spinal cord: importance of dorsal root ganglia for achieving successful functional innervation.' *J Neurosci*, 7(10), Oct, pp. 3131-3141.

Kuang, S., Charge, S. B., Seale, P., Huh, M. and Rudnicki, M. A. (2006) 'Distinct roles for Pax7 and Pax3 in adult regenerative myogenesis.' *J Cell Biol*, 172(1), Jan 2, pp. 103-113.

Kummer, T. T., Misgeld, T., Lichtman, J. W. and Sanes, J. R. (2004) 'Nerve-independent formation of a topologically complex postsynaptic apparatus.' *The Journal of cell biology*, 164(7) pp. 1077-1087.

Landmesser, L. (1978) 'The distribution of motoneurones supplying chick hind limb muscles.' *The Journal of physiology*, 284 pp. 371-389.

Landmesser, L. T. (2001) 'The acquisition of motoneuron subtype identity and motor circuit formation.' *Int J Dev Neurosci*, 19(2), Apr, pp. 175-182.

Larkin, L. M., Van der Meulen, J. H., Dennis, R. G. and Kennedy, J. B. (2006) 'Functional evaluation of nerve-skeletal muscle constructs engineered in vitro.' *In Vitro Cell Dev Biol Anim*, 42(3-4), Mar-Apr, pp. 75-82.

Lavoie, P. A., Collier, B. and Tenehouse, A. (1976) 'Comparison of alpha-bungarotoxin binding to skeletal muscles after inactivity or denervation.' *Nature*, 260(5549), Mar 25, pp. 349-350.

Lee, K.-Y., Li, M., Manchanda, M., Batra, R., Charizanis, K., Mohan, A., Warren, S. A., Chamberlain, C. M., Finn, D., Hong, H., Ashraf, H., Kasahara, H., Ranum, L. P. W. and Swanson, M. S. (2013) 'Compound loss of muscleblind-like function in myotonic dystrophy.' *EMBO molecular medicine*, 5(12) pp. 1887-1900.

Lees, J. F., Shneidman, P. S., Skuntz, S. F., Carden, M. J. and Lazzarini, R. A. (1988) 'THE STRUCTURE AND ORGANIZATION OF THE HUMAN HEAVY NEUROFILAMENT SUBUNIT (NF-H) AND THE GENE ENCODING IT.' *Embo Journal*, 7(7), Jul, pp. 1947-1955.

Lefebvre, S., Burglen, L., Reboullet, S., Clermont, O., Burlet, P., Viollet, L., Benichou, B., Cruaud, C., Millasseau, P., Zeviani, M., Lepaslier, D., Frezal, J., Cohen, D., Weissenbach, J., Munnich, A. and Melki, J. (1995) 'IDENTIFICATION AND CHARACTERIZATION OF A SPINAL MUSCULAR ATROPHY-DETERMINING GENE.' *Cell*, 80(1), Jan, pp. 155-165.

Lenzi, J., Pagani, F., De Santis, R., Limatola, C., Bozzoni, I., Di Angelantonio, S. and Rosa, A. (2016) 'Differentiation of control and ALS mutant human iPSCs into functional skeletal muscle cells, a tool for the study of neuromuscolar diseases.' *Stem cell research*, 17(1) pp. 140-147.

Lepper, C., Partridge, T. A. and Fan, C. M. (2011) 'An absolute requirement for Pax7-positive satellite cells in acute injury-induced skeletal muscle regeneration.' *Development*, 138(17), Sep, pp. 3639-3646.

Leto, D. and Saltiel, A. R. (2012) 'Regulation of glucose transport by insulin: traffic control of GLUT4.' *Nat Rev Mol Cell Biol*, 13(6), May 23, pp. 383-396.

Li, M. X., Jia, M., Jiang, H., Dunlap, V. and Nelson, P. G. (2001) 'Opposing actions of protein kinase A and C mediate Hebbian synaptic plasticity.' *Nat Neurosci*, 4(9), Sep, pp. 871-872.

Li, X. J., Du, Z. W., Zarnowska, E. D., Pankratz, M., Hansen, L. O., Pearce, R. A. and Zhang, S. C. (2005) 'Specification of motoneurons from human embryonic stem cells.' *Nat Biotechnol*, 23(2), Feb, pp. 215-221.

Lie, D. C. and Weis, J. (1998) 'GDNF expression is increased in denervated human skeletal muscle.' *Neurosci Lett*, 250(2), Jul 3, pp. 87-90.

Light, N. and Champion, A. E. (1984) 'CHARACTERIZATION OF MUSCLE EPIMYSIUM, PERIMYSIUM AND ENDOMYSIUM COLLAGENS.' *Biochemical Journal*, 219(3) pp. 1017-1026.

Lin, L. F., Doherty, D. H., Lile, J. D., Bektesh, S. and Collins, F. (1993) 'GDNF: a glial cell line-derived neurotrophic factor for midbrain dopaminergic neurons.' *Science*, 260(5111), May 21, pp. 1130-1132.

Lin, S., Maj, M., Bezakova, G., Magyar, J. P., Brenner, H. R. and Ruegg, M. A. (2008) 'Muscle-wide secretion of a miniaturized form of neural agrin rescues focal neuromuscular innervation in agrin mutant mice.' *Proceedings of the National Academy of Sciences*, 105(32) p. 11406.

Lin, W., Sanchez, H. B., Deerinck, T., Morris, J. K., Ellisman, M. and Lee, K. F. (2000) 'Aberrant development of motor axons and neuromuscular synapses in erbB2-deficient mice.' *Proc Natl Acad Sci U S A*, 97(3), Feb 1, pp. 1299-1304.

Lin, W., Burgess, R. W., Dominguez, B., Pfaff, S. L., Sanes, J. R. and Lee, K.-F. (2001) 'Distinct roles of nerve and muscle in postsynaptic differentiation of the neuromuscular synapse.' *Nature*, 410, 04/26/online, p. 1057.

Littleton, J. T., Bellen, H. J. and Perin, M. S. (1993) 'Expression of synaptotagmin in Drosophila reveals transport and localization of synaptic vesicles to the synapse.' *Development*, 118(4) pp. 1077-1088.

Liu, Q. Y., Dunlap, V. and Barker, J. L. (1994) 'gamma-Aminobutyric acid type A receptor antagonists picrotoxin and bicuculline alter acetylcholine channel kinetics in cultured embryonic rat skeletal muscle.' *Mol Pharmacol*, 46(6), Dec, pp. 1197-1203.

Liu, Y., Padgett, D., Takahashi, M., Li, H., Sayeed, A., Teichert, R. W., Olivera, B. M., McArdle, J. J., Green, W. N. and Lin, W. (2008) 'Essential roles of the acetylcholine receptor gamma-subunit in neuromuscular synaptic patterning.' *Development*, 135(11), Jun, pp. 1957-1967.

Lopez-Manzaneda, M., Tejero, R., Arumugam, S. and Tabares, L. (2016) 'Synaptotagmin-2, and -1, linked to neurotransmission impairment and vulnerability in Spinal Muscular Atrophy.' *Human Molecular Genetics*, 25(21) pp. 4703-4716.

Lorenzon, P., Bandi, E., de Guarrini, F., Pietrangelo, T., Schafer, R., Zweyer, M., Wernig, A. and Ruzzier, F. (2004) 'Ageing affects the differentiation potential of human myoblasts.' *Exp Gerontol*, 39(10), Oct, pp. 1545-1554.

Low, L. K. and Cheng, H.-J. (2006) 'Axon pruning: an essential step underlying the developmental plasticity of neuronal connections.' *Philosophical Transactions of the Royal Society B: Biological Sciences*, 361(1473), 07/28, pp. 1531-1544.

Luo, Z., Wang, Q., Dobbins, G. C., Levy, S., Xiong, W. C. and Mei, L. (2003) 'Signaling complexes for postsynaptic differentiation.' *J Neurocytol*, 32(5-8), Jun-Sep, pp. 697-708.

Machida, S. and Booth, F. W. (2004) 'Insulin-like growth factor 1 and muscle growth: implication for satellite cell proliferation.' *Proc Nutr Soc*, 63(2), May, pp. 337-340.

Maeda, M., Ohba, N., Nakagomi, S., Suzuki, Y., Kiryu-Seo, S., Namikawa, K., Kondoh, W., Tanaka, A. and Kiyama, H. (2004) 'Vesicular acetylcholine transporter can be a morphological marker for the reinnervation to muscle of regenerating motor axons.' *Neurosci Res*, 48(3), Mar, pp. 305-314.

Malomouzh, A. I., Nurullin, L. F. and Nikolsky, E. E. (2015) 'Immunohistochemical evidence of the presence of metabotropic receptors for γ-aminobutyric acid at the rat neuromuscular junctions.' *Doklady Biochemistry and Biophysics*, 463(1), July 01, pp. 236-238.

Malomouzh, A. I., Petrov, K. A., Nurullin, L. F. and Nikolsky, E. E. (2015) 'Metabotropic GABAB receptors mediate GABA inhibition of acetylcholine release in the rat neuromuscular junction.' *J Neurochem*, 135(6), Dec, pp. 1149-1160.

Mamchaoui, K., Trollet, C., Bigot, A., Negroni, E., Chaouch, S., Wolff, A., Kandalla, P. K., Marie, S., Di Santo, J., St Guily, J. L., Muntoni, F., Kim, J., Philippi, S., Spuler, S., Levy, N., Blumen, S. C., Voit, T., Wright, W. E., Aamiri, A., Butler-Browne, G. and Mouly, V. (2011) 'Immortalized pathological human myoblasts: towards a universal tool for the study of neuromuscular disorders.' *Skelet Muscle*, 1 p. 34.

Manabe, Y., Miyatake, S., Takagi, M., Nakamura, M., Okeda, A., Nakano, T., Hirshman, M. F., Goodyear, L. J. and Fujii, N. L. (2012) 'Characterization of an acute muscle contraction model using cultured C2C12 myotubes.' *PloS one*, 7(12) pp. e52592-e52592.

Manske, R. H. F. (1932) 'THE ALKALOIDS OF FUMARACEOUS PLANTS: II. DICENTRA CUCULLARIA (L.) BERNH.' *Canadian Journal of Research*, 7(3), 1932/09/01, pp. 265-269.

Mantilla, C. B., Zhan, W. Z. and Sieck, G. C. (2004) 'Neurotrophins improve neuromuscular transmission in the adult rat diaphragm.' *Muscle Nerve*, 29(3), Mar, pp. 381-386.

Manuel, M. and Zytnicki, D. (2011) 'Alpha, beta and gamma motoneurons: functional diversity in the motor system's final pathway.' *J Integr Neurosci*, 10(3), Sep, pp. 243-276.

Marangi, P. A., Forsayeth, J. R., Mittaud, P., Erb-Vogtli, S., Blake, D. J., Moransard, M., Sander, A. and Fuhrer, C. (2001) 'Acetylcholine receptors are required for agrin-induced clustering of postsynaptic proteins.' *Embo j*, 20(24), Dec 17, pp. 7060-7073.

Marchand, S., Devillers-Thiery, A., Pons, S., Changeux, J. P. and Cartaud, J. (2002) 'Rapsyn escorts the nicotinic acetylcholine receptor along the exocytic pathway via association with lipid rafts.' *J Neurosci*, 22(20), Oct 15, pp. 8891-8901.

Marty, I., Robert, M., Villaz, M., Dejongh, K. S., Lai, Y., Catterall, W. A. and Ronjat, M. (1994) 'BIOCHEMICAL-EVIDENCE FOR A COMPLEX INVOLVING DIHYDROPYRIDINE RECEPTOR AND RYANODINE RECEPTOR IN TRIAD JUNCTIONS OF SKELETAL-MUSCLE.' *Proceedings of the National Academy of Sciences of the United States of America*, 91(6), Mar, pp. 2270-2274.

Maselli, R. A., Arredondo, J., Cagney, O., Ng, J. J., Anderson, J. A., Williams, C., Gerke, B. J., Soliven, B. and Wollmann, R. L. (2010) 'Mutations in MUSK causing congenital myasthenic syndrome impair MuSK-Dok-7 interaction.' *Hum Mol Genet*, 19(12), Jun 15, pp. 2370-2379.

Matthews, V. B., Astrom, M. B., Chan, M. H., Bruce, C. R., Krabbe, K. S., Prelovsek, O., Akerstrom, T., Yfanti, C., Broholm, C., Mortensen, O. H., Penkowa, M., Hojman, P., Zankari, A., Watt, M. J., Bruunsgaard, H., Pedersen, B. K. and Febbraio, M. A. (2009) 'Brain-derived neurotrophic factor is produced by skeletal muscle cells in response to contraction and enhances fat oxidation via activation of AMP-activated protein kinase.' *Diabetologia*, 52(7), Jul, pp. 1409-1418.

McComas, A. J., Fawcett, P. R. W., Campbell, M. J. and Sica, R. E. P. (1971) 'ELECTROPHYSIOLOGICAL ESTIMATION OF NUMBER OF MOTOR UNITS WITHIN A HUMAN MUSCLE.' *Journal of Neurology Neurosurgery and Psychiatry*, 34(2) pp. 121-&.

McPhee, J. S., Hogrel, J. Y., Maier, A. B., Seppet, E., Seynnes, O. R., Sipila, S., Bottinelli, R., Barnouin, Y., Bijlsma, A. Y., Gapeyeva, H., Maden-Wilkinson, T. M., Meskers, C. G., Paasuke, M., Sillanpaa, E., Stenroth, L., Butler-Browne, G., Narici, M. V. and Jones, D. A. (2013) 'Physiological and functional evaluation of healthy young and older men and women: design of the European MyoAge study.' *Biogerontology*, 14(3), Jun, pp. 325-337.

Mears, S. C. and Frank, E. (1997) 'Formation of specific monosynaptic connections between muscle spindle afferents and motoneurons in the mouse.' *J Neurosci*, 17(9), May 1, pp. 3128-3135.

Miles, G. B., Yohn, D. C., Wichterle, H., Jessell, T. M., Rafuse, V. F. and Brownstone, R. M. (2004) 'Functional Properties of Motoneurons Derived from Mouse Embryonic Stem Cells.' *The Journal of Neuroscience*, 24(36) pp. 7848-7858.

Milner, L. D. and Landmesser, L. T. (1999) 'Cholinergic and GABAergic inputs drive patterned spontaneous motoneuron activity before target contact.' *J Neurosci*, 19(8), Apr 15, pp. 3007-3022.

Mis, K., Grubic, Z., Lorenzon, P., Sciancalepore, M., Mars, T. and Pirkmajer, S. (2017) 'In Vitro Innervation as an Experimental Model to Study the Expression and Functions of Acetylcholinesterase and Agrin in Human Skeletal Muscle.' *Molecules (Basel, Switzerland)*, 22(9) p. 1418.

Misgeld, T., Burgess, R. W., Lewis, R. M., Cunningham, J. M., Lichtman, J. W. and Sanes, J. R. (2002) 'Roles of neurotransmitter in synapse formation: development of neuromuscular junctions lacking choline acetyltransferase.' *Neuron*, 36(4), Nov 14, pp. 635-648.

Modlin, I. M., Moss, S. F., Chung, D. C., Jensen, R. T. and Snyderwine, E. (2008) 'Priorities for improving the management of gastroenteropancreatic neuroendocrine tumors.' *J Natl Cancer Inst*, 100(18), Sep 17, pp. 1282-1289.

Monaco, C. M. F., Perry, C. G. R. and Hawke, T. J. (2017) 'Diabetic Myopathy: current molecular understanding of this novel neuromuscular disorder.' *Curr Opin Neurol*, 30(5), Oct, pp. 545-552.

Monani, U. R., Sendtner, M., Coovert, D. D., Parsons, D. W., Andreassi, C., Le, T. T., Jablonka, S., Schrank, B., Rossoll, W., Prior, T. W., Morris, G. E. and Burghes, A. H. (2000) 'The human centromeric survival motor neuron gene (SMN2) rescues embryonic lethality in Smn(-/-) mice and results in a mouse with spinal muscular atrophy.' *Hum Mol Genet*, 9(3), Feb 12, pp. 333-339.

Moore, C., Leu, M., Muller, U. and Brenner, H. R. (2001) 'Induction of multiple signaling loops by MuSK during neuromuscular synapse formation.' *Proc Natl Acad Sci U S A*, 98(25), Dec 4, pp. 14655-14660.

Moransard, M., Borges, L. S., Willmann, R., Marangi, P. A., Brenner, H. R., Ferns, M. J. and Fuhrer, C. (2003) 'Agrin regulates rapsyn interaction with surface acetylcholine receptors, and this underlies cytoskeletal anchoring and clustering.' *J Biol Chem*, 278(9), Feb 28, pp. 7350-7359.

Morimoto, Y., Kato-Negishi, M., Onoe, H. and Takeuchi, S. (2013) 'Three-dimensional neuron-muscle constructs with neuromuscular junctions.' *Biomaterials*, 34(37), Dec, pp. 9413-9419.

Morris, J. K., Lin, W., Hauser, C., Marchuk, Y., Getman, D. and Lee, K. F. (1999) 'Rescue of the cardiac defect in ErbB2 mutant mice reveals essential roles of ErbB2 in peripheral nervous system development.' *Neuron*, 23(2), Jun, pp. 273-283.

Mouly, V., Aamiri, A., Perie, S., Mamchaoui, K., Barani, A., Bigot, A., Bouazza, B., Francois, V., Furling, D., Jacquemin, V., Negroni, E., Riederer, I., Vignaud, A., St Guily, J. L. and Butler-Browne, G. S. (2005) 'Myoblast transfer therapy: is there any light at the end of the tunnel?' *Acta Myol*, 24(2), Oct, pp. 128-133.

Murray, L. M., Comley, L. H., Thomson, D., Parkinson, N., Talbot, K. and Gillingwater, T. H. (2008) 'Selective vulnerability of motor neurons and dissociation of pre- and post-synaptic pathology at the neuromuscular junction in mouse models of spinal muscular atrophy.' *Hum Mol Genet*, 17(7), Apr 1, pp. 949-962.

Nelson, P. G., Fields, R. D., Yu, C. and Liu, Y. (1993) 'Synapse elimination from the mouse neuromuscular junction in vitro: a non-Hebbian activity-dependent process.' *J Neurobiol*, 24(11), Nov, pp. 1517-1530.

Nguyen, Q. T., Parsadanian, A. S., Snider, W. D. and Lichtman, J. W. (1998) 'Hyperinnervation of neuromuscular junctions caused by GDNF overexpression in muscle.' *Science*, 279(5357), Mar 13, pp. 1725-1729.

Nilwik, R., Snijders, T., Leenders, M., Groen, B. B., van Kranenburg, J., Verdijk, L. B. and van Loon, L. J. (2013) 'The decline in skeletal muscle mass with aging is mainly attributed to a reduction in type II muscle fiber size.' *Exp Gerontol*, 48(5), May, pp. 492-498.

Nixon, R. A., Yang, D. S. and Lee, J. H. (2008) 'Neurodegenerative lysosomal disorders: a continuum from development to late age.' *Autophagy*, 4(5), Jul, pp. 590-599.

Nurullin, L. F., Nikolsky, E. E. and Malomouzh, A. I. (2018) 'Elements of molecular machinery of GABAergic signaling in the vertebrate cholinergic neuromuscular junction.' *Acta Histochemica*, 120(3), 2018/04/01/, pp. 298-301.

Obata, K. (2013) 'Synaptic inhibition and γ-aminobutyric acid in the mammalian central nervous system.' *Proceedings of the Japan Academy, Series B*, 89(4) pp. 139-156.

Oda, Y. (1999) 'Choline acetyltransferase: the structure, distribution and pathologic changes in the central nervous system.' *Pathol Int*, 49(11), Nov, pp. 921-937.

Okada, K., Inoue, A., Okada, M., Murata, Y., Kakuta, S., Jigami, T., Kubo, S., Shiraishi, H., Eguchi, K., Motomura, M., Akiyama, T., Iwakura, Y., Higuchi, O. and Yamanashi, Y. (2006) 'The muscle protein Dok-7 is essential for neuromuscular synaptogenesis.' *Science*, 312(5781), Jun 23, pp. 1802-1805.

Olsen, R. W. and Sieghart, W. (2008) 'International Union of Pharmacology. LXX. Subtypes of gamma-aminobutyric acid(A) receptors: classification on the basis of subunit composition, pharmacology, and function. Update.' *Pharmacol Rev*, 60(3), Sep, pp. 243-260.

Oppenheim, R. W. (1991) 'Cell death during development of the nervous system.' *Annu Rev Neurosci*, 14 pp. 453-501.

Oppenheim, R. W., Houenou, L. J., Johnson, J. E., Lin, L. F., Li, L., Lo, A. C., Newsome, A. L., Prevette, D. M. and Wang, S. (1995) 'Developing motor neurons rescued from programmed and axotomy-induced cell death by GDNF.' *Nature*, 373(6512), Jan 26, pp. 344-346.

Ordahl, C. P., Berdougo, E., Venters, S. J. and Denetclaw, W. F., Jr. (2001) 'The dermomyotome dorsomedial lip drives growth and morphogenesis of both the primary myotome and dermomyotome epithelium.' *Development*, 128(10), May, pp. 1731-1744.

Paliwal, P., Pishesha, N., Wijaya, D. and Conboy, I. M. (2012) 'Age dependent increase in the levels of osteopontin inhibits skeletal muscle regeneration.' *Aging (Albany NY)*, 4(8), Aug, pp. 553-566.

Park, J. C., Song, D. Y., Lee, J. S., Kong, I. D., Jeong, S.-W., Lee, B. H., Kang, H. S. and Cho, B. P. (2006) 'Expression of GABAA receptor β2/3 subunits in the rat major pelvic ganglion.' *Neuroscience Letters*, 403(1), 2006/07/31/, pp. 35-39.

Patton, B. L., Miner, J. H., Chiu, A. Y. and Sanes, J. R. (1997) 'Distribution and function of laminins in the neuromuscular system of developing, adult, and mutant mice.' *J Cell Biol*, 139(6), Dec 15, pp. 1507-1521.

Pavlath, G. K., Dominov, J. A., Kegley, K. M. and Miller, J. B. (2003) 'Regeneration of transgenic skeletal muscles with altered timing of expression of the basic helix-loop-helix muscle regulatory factor MRF4.' *Am J Pathol*, 162(5), May, pp. 1685-1691.

Payne, A. M., Zheng, Z., Messi, M. L., Milligan, C. E., Gonzalez, E. and Delbono, O. (2006) 'Motor neurone targeting of IGF-1 prevents specific force decline in ageing mouse muscle.' *J Physiol*, 570(Pt 2), Jan 15, pp. 283-294.

Pedersen, B. K. (2011) 'Muscles and their myokines.' *J Exp Biol*, 214(Pt 2), Jan 15, pp. 337-346.

Pedersen, B. K. and Febbraio, M. A. (2008) 'Muscle as an endocrine organ: focus on muscle-derived interleukin-6.' *Physiol Rev*, 88(4), Oct, pp. 1379-1406.

Peng, H. B., Yang, J. F., Dai, Z., Lee, C. W., Hung, H. W., Feng, Z. H. and Ko, C. P. (2003) 'Differential effects of neurotrophins and schwann cell-derived signals on neuronal survival/growth and synaptogenesis.' *J Neurosci*, 23(12), Jun 15, pp. 5050-5060.

Pette, D. and Staron, R. S. (2000) 'Myosin isoforms, muscle fiber types, and transitions.' *Microsc Res Tech*, 50(6), Sep 15, pp. 500-509.

Phelan, M. C. and Lawler, G. (2001) 'Cell counting.' *Curr Protoc Cytom*, Appendix 3, May, p. Appendix 3A.

Philippidou, P., Walsh, C. M., Aubin, J., Jeannotte, L. and Dasen, J. S. (2012) 'Sustained Hox5 gene activity is required for respiratory motor neuron development.' *Nature neuroscience*, 15(12) pp. 1636-1644.

Pietrangelo, T., Puglielli, C., Mancinelli, R., Beccafico, S., Fano, G. and Fulle, S. (2009) 'Molecular basis of the myogenic profile of aged human skeletal muscle satellite cells during differentiation.' *Exp Gerontol*, 44(8), Aug, pp. 523-531.

Pourquie, O. (2001) 'Vertebrate somitogenesis.' *Annual Review of Cell and Developmental Biology*, 17 pp. 311-350.

Prasad, A. and Hollyday, M. (1991) 'Development and migration of avian sympathetic preganglionic neurons.' *J Comp Neurol*, 307(2), May 8, pp. 237-258.

Prather, R. S., Lorson, M., Ross, J. W., Whyte, J. J. and Walters, E. (2013) 'Genetically Engineered Pig Models for Human Diseases.' *Annual review of animal biosciences*, 1, 01/03, pp. 203-219.

Pronsato, L., La Colla, A., Ronda, A. C., Milanesi, L., Boland, R. and Vasconsuelo, A. (2013) 'High passage numbers induce resistance to apoptosis in C2C12 muscle cells.' *Biocell*, 37(1), Apr, pp. 1-9.

Proske, U. and Gandevia, S. C. (2009) 'The kinaesthetic senses.' *The Journal of physiology*, 587(Pt 17) pp. 4139-4146.

Punga, A. R. and Ruegg, M. A. (2012) 'Signaling and aging at the neuromuscular synapse: lessons learnt from neuromuscular diseases.' *Curr Opin Pharmacol*, 12(3), Jun, pp. 340-346.

Punga, A. R., Maj, M., Lin, S., Meinen, S. and Ruegg, M. A. (2011) 'MuSK levels differ between adult skeletal muscles and influence postsynaptic plasticity.' *Eur J Neurosci*, 33(5), Mar, pp. 890-898.

Purves, D., Augustine, G. J. and Fitzpatrick, D. (2001) *Neuroscience.* 2nd edition. ed., Vol. 2nd edition. Sunderland (MA): Sinauer Associates.

Puttonen, K. A., Ruponen, M., Naumenko, N., Hovatta, O. H., Tavi, P. and Koistinaho, J. (2015) 'Generation of Functional Neuromuscular Junctions from Human Pluripotent Stem Cell Lines.' *Frontiers in cellular neuroscience*, 9 pp. 473-473.

Rayment, I., Holden, H. M., Whittaker, M., Yohn, C. B., Lorenz, M., Holmes, K. C. and Milligan, R. A. (1993) 'STRUCTURE OF THE ACTIN-MYOSIN COMPLEX AND ITS IMPLICATIONS FOR MUSCLE-CONTRACTION.' *Science*, 261(5117), Jul, pp. 58-65.

Reichardt, L. F. (2006) 'Neurotrophin-regulated signalling pathways.' *Philosophical transactions of the Royal Society of London. Series B, Biological sciences*, 361(1473) pp. 1545-1564.

Relaix, F. and Zammit, P. S. (2012) 'Satellite cells are essential for skeletal muscle regeneration: the cell on the edge returns centre stage.' *Development*, 139(16), Aug, pp. 2845-2856.

Ren, K., Crouzier, T., Roy, C. and Picart, C. (2008) 'Polyelectrolyte multilayer films of controlled stiffness modulate myoblast cells differentiation.' *Adv Funct Mater*, 18(9) pp. 1378-1389.

Rhodes, S. J. and Konieczny, S. F. (1989) 'Identification of MRF4: a new member of the muscle regulatory factor gene family.' *Genes Dev*, 3(12b), Dec, pp. 2050-2061.

Ricotti, L., Taccola, S., Bernardeschi, I., Pensabene, V., Dario, P. and Menciassi, A. (2011) 'Quantification of growth and differentiation of C2C12 skeletal muscle cells on PSS-PAH-based polyelectrolyte layer-by-layer nanofilms.' *Biomed Mater*, 6(3), Jun, p. 031001.

Riethmacher, D., Sonnenberg-Riethmacher, E., Brinkmann, V., Yamaai, T., Lewin, G. R. and Birchmeier, C. (1997) 'Severe neuropathies in mice with targeted mutations in the ErbB3 receptor.' *Nature*, 389(6652), Oct 16, pp. 725-730.

Rios, E. and Brum, G. (1987) 'Involvement of dihydropyridine receptors in excitation-contraction coupling in skeletal muscle.' *Nature*, 325(6106), Feb 19-25, pp. 717-720.

Rockl, K. S. C., Hirshman, M. F., Brandauer, J., Fujii, N., Witters, L. A. and Goodyear, L. J. (2007) 'Skeletal muscle adaptation to exercise training - AMP-activated protein kinase mediates muscle fiber type shift.' *Diabetes*, 56(8), Aug, pp. 2062-2069.

Rojas Vega, S., Struder, H. K., Vera Wahrmann, B., Schmidt, A., Bloch, W. and Hollmann, W. (2006) 'Acute BDNF and cortisol response to low intensity exercise and following ramp incremental exercise to exhaustion in humans.' *Brain Res*, 1121(1), Nov 22, pp. 59-65.

Rosen, D. R., Siddique, T., Patterson, D., Figlewicz, D. A., Sapp, P., Hentati, A., Donaldson, D., Goto, J., Oregan, J. P., Deng, H. X., Rahmani, Z., Krizus, A., McKennayasek, D., Cayabyab, A., Gaston, S. M., Berger, R., Tanzi, R. E., Halperin, J. J., Herzfeldt, B., Vandenbergh, R., Hung, W. Y., Bird, T., Deng, G., Mulder, D. W., Smyth, C., Laing, N. G., Soriano, E., Pericakvance, M. A., Haines, J., Rouleau, G. A., Gusella, J. S., Horvitz, H. R. and Brown, R. H. (1993) 'MUTATIONS IN CU/ZN SUPEROXIDE-DISMUTASE GENE ARE ASSOCIATED WITH FAMILIAL AMYOTROPHIC-LATERAL-SCLEROSIS.' *Nature*, 362(6415), Mar, pp. 59-62.

Rosenstein, J. M., Krum, J. M. and Ruhrberg, C. (2010) 'VEGF in the nervous system.' *Organogenesis*, 6(2), Apr-Jun, pp. 107-114.

Rudnicki, M. A. and Jaenisch, R. (1995) 'The MyoD family of transcription factors and skeletal myogenesis.' *Bioessays*, 17(3), Mar, pp. 203-209.

Rudolf, R., Deschenes, M. R. and Sandri, M. (2016) 'Neuromuscular junction degeneration in muscle wasting.' *Current opinion in clinical nutrition and metabolic care*, 19(3) pp. 177-181.

Ruiz de Almodovar, C., Lambrechts, D., Mazzone, M. and Carmeliet, P. (2009) 'Role and therapeutic potential of VEGF in the nervous system.' *Physiol Rev*, 89(2), Apr, pp. 607-648.

Rumsey, J. W., Das, M., Bhalkikar, A., Stancescu, M. and Hickman, J. J. (2010) 'Tissue engineering the mechanosensory circuit of the stretch reflex arc: Sensory neuron innervation of intrafusal muscle fibers.' *Biomaterials*, 31(32), 2010/11/01/, pp. 8218-8227.

Rumsey, J. W., Das, M., Stancescu, M., Bott, M., Fernandez-Valle, C. and Hickman, J. J. (2009) 'Node of Ranvier Formation on Motoneurons In Vitro.' *Biomaterials*, 30(21), 04/10, pp. 3567-3572.

Rundell, V. L., Geenen, D. L., Buttrick, P. M. and de Tombe, P. P. (2004) 'Depressed cardiac tension cost in experimental diabetes is due to altered myosin heavy chain isoform expression.' *Am J Physiol Heart Circ Physiol*, 287(1), Jul, pp. H408-413.

Sachidanandan, C. and Dhawan, J. (2003) *Skeletal Muscle Progenitor Cells in Development and Regeneration.* Vol. 5.

Sahashi, K., Hua, Y., Ling, K. K. Y., Hung, G., Rigo, F., Horev, G., Katsuno, M., Sobue, G., Ko, C.-P., Bennett, C. F. and Krainer, A. R. (2012) 'TSUNAMI: an antisense method to phenocopy splicing-associated diseases in animals.' *Genes & development*, 26(16) pp. 1874-1884.

Saini, J., McPhee, J. S., Al-Dabbagh, S., Stewart, C. E. and Al-Shanti, N. (2016) 'Regenerative function of immune system: Modulation of muscle stem cells.' *Ageing Res Rev*, 27, May, pp. 67-76.

Saini, J., Faroni, A., Abd Al Samid, M., Reid, A. J., Lightfoot, A. P., Mamchaoui, K., Mouly, V., Butler-Browne, G., McPhee, J. S., Degens, H. and Al-Shanti, N. (2019) 'Simplified in vitro engineering of neuromuscular junctions between rat embryonic motoneurons and immortalized human skeletal muscle cells.' *Stem Cells Cloning*, 12 pp. 1-9.

Sander, A., Hesser, B. A. and Witzemann, V. (2001) 'MuSK induces in vivo acetylcholine receptor clusters in a ligand-independent manner.' *J Cell Biol*, 155(7), Dec 24, pp. 1287-1296.

Sandstrom, C. E., Miller, W. M. and Papoutsakis, E. T. (1994) 'Serum-free media for cultures of primitive and mature hematopoietic cells.' *Biotechnol Bioeng*, 43(8), Apr 5, pp. 706-733.

Sanes, J. R. and Lichtman, J. W. (1999) 'Development of the vertebrate neuromuscular junction.' *Annu Rev Neurosci*, 22 pp. 389-442.

Sanes, J. R. and Lichtman, J. W. (2001) 'Induction, assembly, maturation and maintenance of a postsynaptic apparatus.' *Nat Rev Neurosci*, 2(11), Nov, pp. 791-805.

Schafer, R., Knauf, U., Zweyer, M., Hogemeier, O., de Guarrini, F., Liu, X., Eichhorn, H. J., Koch, F. W., Mundegar, R. R., Erzen, I. and Wernig, A. (2006) 'Age dependence of the human skeletal muscle stem cell in forming muscle tissue.' *Artif Organs*, 30(3), Mar, pp. 130-140.

Schiaffino, S. and Reggiani, C. (2011) 'FIBER TYPES IN MAMMALIAN SKELETAL MUSCLES.' *Physiological Reviews*, 91(4), Oct, pp. 1447-1531.

Schiaffino, S., Gorza, L., Sartore, S., Saggin, L. and Carli, M. (1986) 'Embryonic myosin heavy chain as a differentiation marker of developing human skeletal muscle and rhabdomyosarcoma. A monoclonal antibody study.' *Exp Cell Res*, 163(1), Mar, pp. 211-220.

Schnabel, J. (2008) 'Neuroscience: Standard model.' *Nature*, 454(7205), Aug 7, pp. 682-685.

Schneider, C. A., Rasband, W. S. and Eliceiri, K. W. (2012) 'NIH Image to ImageJ: 25 years of image analysis.' *Nature Methods*, 9, 06/28/online, p. 671.

Scholzen, T. and Gerdes, J. (2000) 'The Ki-67 protein: from the known and the unknown.' *J Cell Physiol*, 182(3), Mar, pp. 311-322.

Schonk, D. M., Kuijpers, H. J. H., van Drunen, E., van Dalen, C. H., Geurts van Kessel, A. H. M., Verheijen, R. and Ramaekers, F. C. S. (1989) 'Assignment of the gene(s) involved in the expression of

the proliferation-related Ki-67 antigen to human chromosome 10.' *Human Genetics*, 83(3), October 01, pp. 297-299.

Schrank, B., Gotz, R., Gunnersen, J. M., Ure, J. M., Toyka, K. V., Smith, A. G. and Sendtner, M. (1997) 'Inactivation of the survival motor neuron gene, a candidate gene for human spinal muscular atrophy, leads to massive cell death in early mouse embryos.' *Proc Natl Acad Sci U S A*, 94(18), Sep 2, pp. 9920-9925.

Seale, P., Sabourin, L. A., Girgis-Gabardo, A., Mansouri, A., Gruss, P. and Rudnicki, M. A. (2000) 'Pax7 is required for the specification of myogenic satellite cells.' *Cell*, 102(6), Sep 15, pp. 777-786.

Shadrin, I. Y., Khodabukus, A. and Bursac, N. (2016) 'Striated Muscle Function, Regeneration, and Repair.' *Cellular and molecular life sciences : CMLS*, 73(22), 06/06, pp. 4175-4202.

Shavlakadze, T., McGeachie, J. and Grounds, M. D. (2010) 'Delayed but excellent myogenic stem cell response of regenerating geriatric skeletal muscles in mice.' *Biogerontology*, 11(3), Jun, pp. 363-376.

Sheard, P. W., Bewick, G. S., Woolley, A. G., Shaw, J., Fisher, L., Fong, S. W. and Duxson, M. J. (2010) 'Investigation of neuromuscular abnormalities in neurotrophin-3-deficient mice.' *European Journal of Neuroscience*, 31(1), Jan, pp. 29-41.

Sherrington, C. S. (1925) 'Remarks on some Aspects of Reflex Inhibition.' *Proceedings of the Royal Society of London. Series B, Containing Papers of a Biological Character*, 97(686) pp. 519-545.

Shirendeb, U., Hishikawa, Y., Moriyama, S., Win, N., Minn Myint Thu, M., Swe Mar, K., Khatanbaatar, G., Masuzaki, H. and Koji, T. (2009) 'Human Papillomavirus Infection and Its Possible Correlation with p63 Expression in Cervical Cancer in Japan, Mongolia, and Myanmar.' *ACTA HISTOCHEMICA ET CYTOCHEMICA*, 42(6) pp. 181-190.

Shklover, J., Etzioni, S., Weisman-Shomer, P., Yafe, A., Bengal, E. and Fry, M. (2007) 'MyoD uses overlapping but distinct elements to bind E-box and tetraplex structures of regulatory sequences of muscle-specific genes.' *Nucleic acids research*, 35(21) pp. 7087-7095.

Shvartsman, D., Storrie-White, H., Lee, K., Kearney, C., Brudno, Y., Ho, N., Cezar, C., McCann, C., Anderson, E., Koullias, J., Tapia, J. C., Vandenburgh, H., Lichtman, J. W. and Mooney, D. J. (2014) 'Sustained delivery of VEGF maintains innervation and promotes reperfusion in ischemic skeletal muscles via NGF/GDNF signaling.' *Molecular therapy : the journal of the American Society of Gene Therapy*, 22(7) pp. 1243-1253.

Siegel, A. L., Kuhlmann, P. K. and Cornelison, D. D. (2011) 'Muscle satellite cell proliferation and association: new insights from myofiber time-lapse imaging.' *Skelet Muscle*, 1(1), Feb 2, p. 7.

Siegel, A. L., Atchison, K., Fisher, K. E., Davis, G. E. and Cornelison, D. D. (2009) '3D timelapse analysis of muscle satellite cell motility.' *Stem Cells*, 27(10), Oct, pp. 2527-2538.

Siller, R., Greenhough, S., Park, I. H. and Sullivan, G. J. (2013) 'Modelling human disease with pluripotent stem cells.' *Curr Gene Ther*, 13(2), Apr, pp. 99-110.

Simionescu, A. and Pavlath, G. K. (2011) 'Molecular mechanisms of myoblast fusion across species.' *Adv Exp Med Biol*, 713 pp. 113-135.

Sinha, M., Jang, Y. C., Oh, J., Khong, D., Wu, E. Y., Manohar, R., Miller, C., Regalado, S. G., Loffredo, F. S., Pancoast, J. R., Hirshman, M. F., Lebowitz, J., Shadrach, J. L., Cerletti, M., Kim, M. J., Serwold, T., Goodyear, L. J., Rosner, B., Lee, R. T. and Wagers, A. J. (2014) 'Restoring systemic GDF11 levels reverses age-related dysfunction in mouse skeletal muscle.' *Science*, 344(6184), May 9, pp. 649-652.

Slater, C. R. (2008) 'Reliability of neuromuscular transmission and how it is maintained.' *Handb Clin Neurol*, 91 pp. 27-101.

Sleigh, J. N., Gillingwater, T. H. and Talbot, K. (2011) 'The contribution of mouse models to understanding the pathogenesis of spinal muscular atrophy.' *Dis Model Mech*, 4(4), Jul, pp. 457-467.

Smith, A. S., Passey, S. L., Martin, N. R., Player, D. J., Mudera, V., Greensmith, L. and Lewis, M. P. (2016) 'Creating Interactions between Tissue-Engineered Skeletal Muscle and the Peripheral Nervous System.' *Cells Tissues Organs*, 202(3-4) pp. 143-158.

Smythe, G. M., Shavlakadze, T., Roberts, P., Davies, M. J., McGeachie, J. K. and Grounds, M. D. (2008) 'Age influences the early events of skeletal muscle regeneration: studies of whole muscle grafts transplanted between young (8 weeks) and old (13-21 months) mice.' *Exp Gerontol*, 43(6), Jun, pp. 550-562.

Son, Y. J., Trachtenberg, J. T. and Thompson, W. J. (1996) 'Schwann cells induce and guide sprouting and reinnervation of neuromuscular junctions.' *Trends Neurosci*, 19(7), Jul, pp. 280-285.

Song, J. H. (2014) *Mysteries of NMJ revealed!*: ThingLink. [Online] [Accessed on 01/03/2019] https://www.thinglink.com/scene/466990689142439938

Song, W. and Jin, X. A. (2015) 'Brain-derived neurotrophic factor inhibits neuromuscular junction maturation in a cAMP-PKA-dependent way.' *Neurosci Lett*, 591, Mar 30, pp. 8-12.

Sousa-Victor, P., Garcia-Prat, L., Serrano, A. L., Perdiguero, E. and Munoz-Canoves, P. (2015) 'Muscle stem cell aging: regulation and rejuvenation.' *Trends Endocrinol Metab*, 26(6), Jun, pp. 287-296.

Sousa-Victor, P., Gutarra, S., Garcia-Prat, L., Rodriguez-Ubreva, J., Ortet, L., Ruiz-Bonilla, V., Jardi, M., Ballestar, E., Gonzalez, S., Serrano, A. L., Perdiguero, E. and Munoz-Canoves, P. (2014) 'Geriatric muscle stem cells switch reversible quiescence into senescence.' *Nature*, 506(7488), Feb 20, pp. 316-321.

Southam, K. A., King, A. E., Blizzard, C. A., McCormack, G. H. and Dickson, T. C. (2013) 'Microfluidic primary culture model of the lower motor neuron–neuromuscular junction circuit.' *Journal of Neuroscience Methods*, 218(2), 2013/09/15/, pp. 164-169.

Staron, R. S. (1997) 'Human skeletal muscle fiber types: delineation, development, and distribution.' *Can J Appl Physiol*, 22(4), Aug, pp. 307-327.

Steinbeck, J. A., Jaiswal, M. K., Calder, E. L., Kishinevsky, S., Weishaupt, A., Toyka, K. V., Goldstein, P. A. and Studer, L. (2016) 'Functional Connectivity under Optogenetic Control Allows Modeling of Human Neuromuscular Disease.' *Cell Stem Cell*, 18(1), Jan 7, pp. 134-143.

Stephenson, G. M. (2001) 'Hybrid skeletal muscle fibres: a rare or common phenomenon?' *Clin Exp Pharmacol Physiol*, 28(8), Aug, pp. 692-702.

Stewart, C. E., Bates, P. C., Calder, T. A., Woodall, S. M. and Pell, J. M. (1993) 'Potentiation of insulin-like growth factor-I (IGF-I) activity by an antibody: supportive evidence for enhancement of IGF-I bioavailability in vivo by IGF binding proteins.' *Endocrinology*, 133(3), Sep, pp. 1462-1465.

Stifani, N. (2014) 'Motor neurons and the generation of spinal motor neuron diversity.' *Frontiers in cellular neuroscience*, 8 pp. 293-293.

Stockmann, M., Linta, L., Fohr, K. J., Boeckers, A., Ludolph, A. C., Kuh, G. F., Udvardi, P. T., Proepper, C., Storch, A., Kleger, A., Liebau, S. and Boeckers, T. M. (2013) 'Developmental and functional nature of human iPSC derived motoneurons.' *Stem Cell Rev*, 9(4), Aug, pp. 475-492.

Sullivan, K. F. and Cleveland, D. W. (1986) 'Identification of conserved isotype-defining variable region sequences for four vertebrate beta tubulin polypeptide classes.' *Proceedings of the National Academy of Sciences of the United States of America*, 83(12) pp. 4327-4331.

Suuronen, E. J., McLaughlin, C. R., Stys, P. K., Nakamura, M., Munger, R. and Griffith, M. (2004) 'Functional Innervation in Tissue Engineered Models for In Vitro Study and Testing Purposes.' *Toxicological Sciences*, 82(2) pp. 525-533.

Syverud, B. C., VanDusen, K. W. and Larkin, L. M. (2016) 'Growth Factors for Skeletal Muscle Tissue Engineering.' *Cells, tissues, organs*, 202(3-4) pp. 169-179.

Tajbakhsh, S. (2009) 'Skeletal muscle stem cells in developmental versus regenerative myogenesis.' *J Intern Med*, 266(4), Oct, pp. 372-389.

Tajbakhsh, S., Rocancourt, D., Cossu, G. and Buckingham, M. (1997) 'Redefining the genetic hierarchies controlling skeletal myogenesis: Pax-3 and Myf-5 act upstream of MyoD.' *Cell*, 89(1), Apr, pp. 127-138.

Tanaka, A., Woltjen, K., Miyake, K., Hotta, A., Ikeya, M., Yamamoto, T., Nishino, T., Shoji, E., Sehara-Fujisawa, A., Manabe, Y., Fujii, N., Hanaoka, K., Era, T., Yamashita, S., Isobe, K., Kimura, E. and Sakurai, H. (2013) 'Efficient and reproducible myogenic differentiation from human iPS cells: prospects for modeling Miyoshi Myopathy in vitro.' *PLoS One*, 8(4) p. e61540.

ter Keurs, H. E., Deis, N., Landesberg, A., Nguyen, T. T., Livshitz, L., Stuyvers, B. and Zhang, M. L. (2003) 'Force, sarcomere shortening velocity and ATPase activity.' *Adv Exp Med Biol*, 538 pp. 583-602; discussion 602.

Thomson, S. R., Wishart, T. M., Patani, R., Chandran, S. and Gillingwater, T. H. (2012) 'Using induced pluripotent stem cells (iPSC) to model human neuromuscular connectivity: promise or reality?' *Journal of Anatomy*, 220(2) pp. 122-130.

Tidball, J. G. (2005) 'Inflammatory processes in muscle injury and repair.' *Am J Physiol Regul Integr Comp Physiol*, 288(2), Feb, pp. R345-353.

Tintignac, L. A., Brenner, H. R. and Ruegg, M. A. (2015) 'Mechanisms Regulating Neuromuscular Junction Development and Function and Causes of Muscle Wasting.' *Physiol Rev*, 95(3), Jul, pp. 809-852.

Tosney, K. W. and Landmesser, L. T. (1985) 'Growth cone morphology and trajectory in the lumbosacral region of the chick embryo.' *J Neurosci*, 5(9), Sep, pp. 2345-2358.

Ulfhake, B., Bergman, E., Edstrom, E., Fundin, B. T., Johnson, H., Kullberg, S. and Ming, Y. (2000) 'Regulation of neurotrophin signaling in aging sensory and motoneurons: dissipation of target support?' *Mol Neurobiol*, 21(3), Jun, pp. 109-135.

Ulreich, J. B. and Chvapil, M. (1982) 'Altered activity in cultured cells caused by contaminants in tubes widely used for blood collection and serum preparation.' *In Vitro*, 18(2), Feb, pp. 117-121.

Umbach, J. A., Adams, K. L., Gundersen, C. B. and Novitch, B. G. (2012) 'Functional Neuromuscular Junctions Formed by Embryonic Stem Cell-Derived Motor Neurons.' *PLoS ONE*, 7(5), 05/04, p. e36049.

Umemori, H., Linhoff, M. W., Ornitz, D. M. and Sanes, J. R. (2004) 'FGF22 and its close relatives are presynaptic organizing molecules in the mammalian brain.' *Cell*, 118(2), Jul 23, pp. 257-270.

Unwin, N. (2013) 'Nicotinic acetylcholine receptor and the structural basis of neuromuscular transmission: insights from Torpedo postsynaptic membranes.' *Q Rev Biophys*, 46(4), Nov, pp. 283-322.

Urazaev, A. K., Magsumov, S. T., Poletayev, G. I., Nikolsky, E. E. and Vyskocil, F. (1995) 'Muscle NMDA receptors regulate the resting membrane potential through NO-synthase.' *Physiol Res*, 44(3) pp. 205-208.

Valdez, G., Tapia, J. C., Kang, H., Clemenson, G. D., Jr., Gage, F. H., Lichtman, J. W. and Sanes, J. R. (2010) 'Attenuation of age-related changes in mouse neuromuscular synapses by caloric restriction

and exercise.' *Proceedings of the National Academy of Sciences of the United States of America*, 107(33) pp. 14863-14868.

van der Worp, H. B., Howells, D. W., Sena, E. S., Porritt, M. J., Rewell, S., O'Collins, V. and Macleod, M. R. (2010) 'Can animal models of disease reliably inform human studies?' *PLoS Med*, 7(3), Mar 30, p. e1000245.

Velloso, C. P. (2008) 'Regulation of muscle mass by growth hormone and IGF-I.' *British journal of pharmacology*, 154(3) pp. 557-568.

Venuti, J. M., Morris, J. H., Vivian, J. L., Olson, E. N. and Klein, W. H. (1995) 'Myogenin is required for late but not early aspects of myogenesis during mouse development.' *J Cell Biol*, 128(4), Feb, pp. 563-576.

Vilmont, V., Cadot, B., Ouanounou, G. and Gomes, E. R. (2016) 'A system for studying mechanisms of neuromuscular junction development and maintenance.' *Development*, 143(13), Jul 1, pp. 2464-2477.

Vincent, A., Lang, B. and Newsomdavis, J. (1989) 'AUTOIMMUNITY TO THE VOLTAGE-GATED CALCIUM-CHANNEL UNDERLIES THE LAMBERT-EATON MYASTHENIC SYNDROME, A PARA-NEOPLASTIC DISORDER.' *Trends in Neurosciences*, 12(12), Dec, pp. 496-502.

von Maltzahn, J., Jones, A. E., Parks, R. J. and Rudnicki, M. A. (2013) 'Pax7 is critical for the normal function of satellite cells in adult skeletal muscle.' *Proc Natl Acad Sci U S A*, 110(41), Oct 8, pp. 16474-16479.

Wang, C. Y., Yang, F., He, X. P., Je, H. S., Zhou, J. Z., Eckermann, K., Kawamura, D., Feng, L., Shen, L. and Lu, B. (2002) 'Regulation of neuromuscular synapse development by glial cell line-derived neurotrophic factor and neurturin.' *J Biol Chem*, 277(12), Mar 22, pp. 10614-10625.

Watanabe, M., Maemura, K., Kanbara, K., Tamayama, T. and Hayasaki, H. (2002) 'GABA and GABA Receptors in the Central Nervous System and Other Organs.' *In* Jeon, K. W. (ed.) *International Review of Cytology*. Vol. 213. Academic Press, pp. 1-47.

Watt, D. J., Morgan, J. E., Clifford, M. A. and Partridge, T. A. (1987) 'The movement of muscle precursor cells between adjacent regenerating muscles in the mouse.' *Anat Embryol (Berl)*, 175(4) pp. 527-536.

Weatherbee, S. D., Anderson, K. V. and Niswander, L. A. (2006) 'LDL-receptor-related protein 4 is crucial for formation of the neuromuscular junction.' *Development*, 133(24), Dec, pp. 4993-5000.

Webster, C. and Blau, H. M. (1990) 'Accelerated age-related decline in replicative life-span of Duchenne muscular dystrophy myoblasts: implications for cell and gene therapy.' *Somat Cell Mol Genet*, 16(6), Nov, pp. 557-565.

White, J. D., Scaffidi, A., Davies, M., McGeachie, J., Rudnicki, M. A. and Grounds, M. D. (2000) 'Myotube formation is delayed but not prevented in MyoD-deficient skeletal muscle: studies in regenerating whole muscle grafts of adult mice.' *J Histochem Cytochem*, 48(11), Nov, pp. 1531-1544.

Wilson, S. J. and Harris, A. J. (1993) 'Formation of myotubes in aneural rat muscles.' *Dev Biol*, 156(2), Apr, pp. 509-518.

Woldeyesus, M. T., Britsch, S., Riethmacher, D., Xu, L., Sonnenberg-Riethmacher, E., Abou-Rebyeh, F., Harvey, R., Caroni, P. and Birchmeier, C. (1999) 'Peripheral nervous system defects in erbB2 mutants following genetic rescue of heart development.' *Genes Dev*, 13(19), Oct 1, pp. 2538-2548.

Wolpowitz, D., Mason, T. B., Dietrich, P., Mendelsohn, M., Talmage, D. A. and Role, L. W. (2000) 'Cysteine-rich domain isoforms of the neuregulin-1 gene are required for maintenance of peripheral synapses.' *Neuron*, 25(1), Jan, pp. 79-91.

Wood, S. J. and Slater, C. R. (2001) 'Safety factor at the neuromuscular junction.' *Prog Neurobiol*, 64(4), Jul, pp. 393-429.

Woolley, A., Sheard, P., Dodds, K. and Duxson, M. (1999) 'Alpha motoneurons are present in normal numbers but with reduced soma size in neurotrophin-3 knockout mice.' *Neurosci Lett*, 272(2), Sep 10, pp. 107-110.

Woolley, A. G., Sheard, P. W. and Duxson, M. J. (2005) 'Neurotrophin-3 null mutant mice display a postnatal motor neuropathy.' *Eur J Neurosci*, 21(8), Apr, pp. 2100-2110.

Wu, H., Xiong, W. C. and Mei, L. (2010) 'To build a synapse: signaling pathways in neuromuscular junction assembly.' *Development*, 137(7), Apr, pp. 1017-1033.

Yan, Q., Elliott, J. L., Matheson, C., Sun, J., Zhang, L., Mu, X., Rex, K. L. and Snider, W. D. (1993) 'Influences of neurotrophins on mammalian motoneurons in vivo.' *J Neurobiol*, 24(12), Dec, pp. 1555-1577.

Yang, X., Arber, S., William, C., Li, L., Tanabe, Y., Jessell, T. M., Birchmeier, C. and Burden, S. J. (2001) 'Patterning of muscle acetylcholine receptor gene expression in the absence of motor innervation.' *Neuron*, 30(2), May, pp. 399-410.

Yin, H., Price, F. and Rudnicki, M. A. (2013) 'Satellite cells and the muscle stem cell niche.' *Physiol Rev*, 93(1), Jan, pp. 23-67.

Yoshiko, Y., Hirao, K. and Maeda, N. (2002) 'Differentiation in C2C12 myoblasts depends on the expression of endogenous IGFs and not serum depletion.' *American Journal of Physiology-Cell Physiology*, 283(4) pp. C1278-C1286.

Young, H. S., Herbette, L. G. and Skita, V. (2003) 'Alpha-bungarotoxin binding to acetylcholine receptor membranes studied by low angle X-ray diffraction.' *Biophys J*, 85(2), Aug, pp. 943-953.

Yousef, H., Conboy, M. J., Morgenthaler, A., Schlesinger, C., Bugaj, L., Paliwal, P., Greer, C., Conboy, I. M. and Schaffer, D. (2015) *Systemic attenuation of the TGF-β pathway by a single drug simultaneously rejuvenates hippocampal neurogenesis and myogenesis in the same old mammal.*

Yu, S.-C., Klosterman, S. M., Martin, A. A., Gracheva, E. O. and Richmond, J. E. (2013) 'Differential roles for snapin and synaptotagmin in the synaptic vesicle cycle.' *PloS one*, 8(2) pp. e57842-e57842.

Zhang, B., Luo, S., Wang, Q., Suzuki, T., Xiong, W. C. and Mei, L. (2008) 'LRP4 serves as a coreceptor of agrin.' *Neuron*, 60(2), Oct 23, pp. 285-297.

Zhang, X. and Poo, M. M. (2002) 'Localized synaptic potentiation by BDNF requires local protein synthesis in the developing axon.' *Neuron*, 36(4), Nov 14, pp. 675-688.

Zhao, S., Shetty, J., Hou, L., Delcher, A., Zhu, B., Osoegawa, K., de Jong, P., Nierman, W. C., Strausberg, R. L. and Fraser, C. M. (2004) 'Human, mouse, and rat genome large-scale rearrangements: stability versus speciation.' *Genome research*, 14(10A) pp. 1851-1860.

Zheng, C., Skold, M. K., Li, J., Nennesmo, I., Fadeel, B. and Henter, J. I. (2007) 'VEGF reduces astrogliosis and preserves neuromuscular junctions in ALS transgenic mice.' *Biochem Biophys Res Commun*, 363(4), Nov 30, pp. 989-993.

Appendix

Appendix A

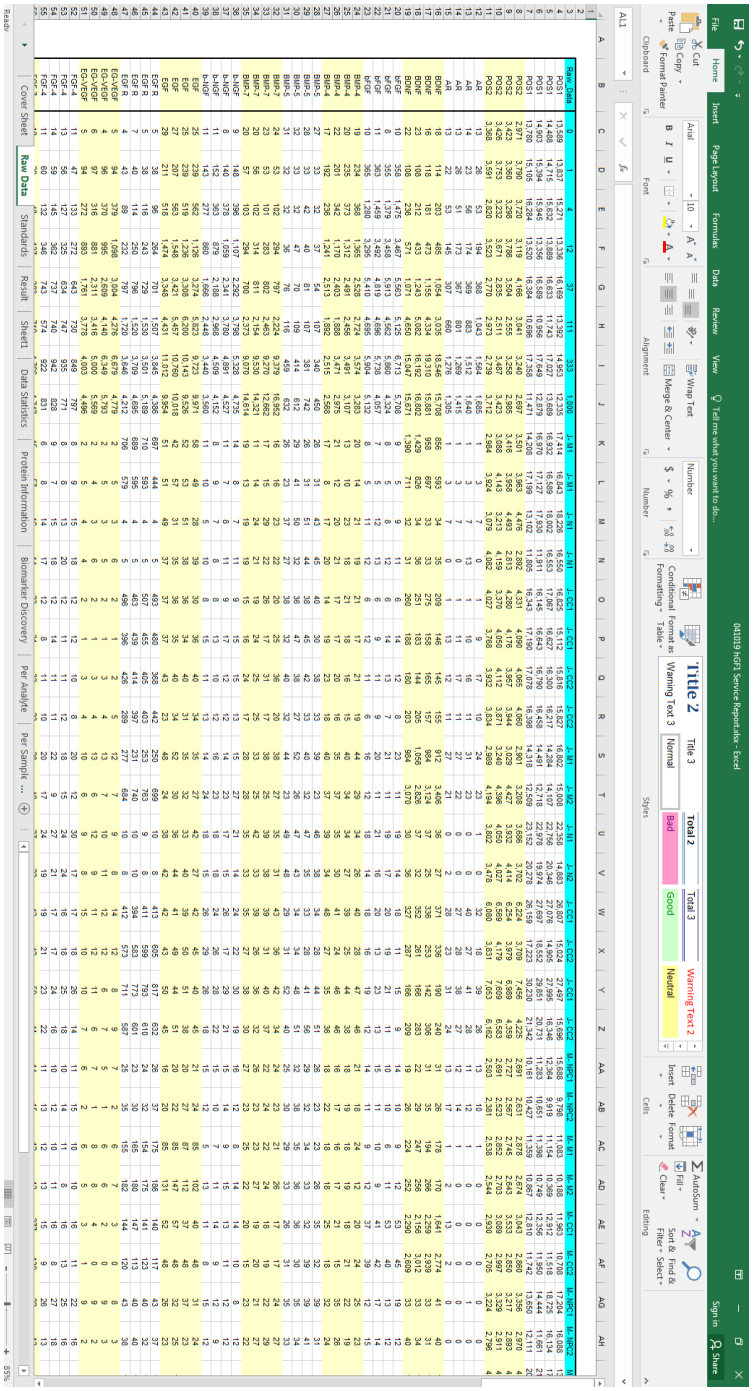

An example of raw data generated from ELISA-based microarray analysis of supernatant from spinal cord explants co-cultured with 25-year-old immortalised human myoblasts vs. supernatant from aneurally-cultured 25-year-old immortalised human myoblasts.

Appendix B

This appendix shows published papers that were produced using the research that was conducted throughout the duration of this thesis. The first publication details the NMJ model created during this project. The second publication is a review paper exploring how the immune system influences SkM repair and regeneration. The author of this thesis was also a contributing author for the final paper in this appendix. The final paper details a fully human NMJ model, which is an alternative system to the model detailed in this thesis.

Stem Cells and Cloning: Advances and Applications

Dovepress
open access to scientific and medical research

Open Access Full Text Article

ORIGINAL RESEARCH

Simplified in vitro engineering of neuromuscular junctions between rat embryonic motoneurons and immortalized human skeletal muscle cells

This article was published in the following Dove Medical Press journal:
Stem Cells and Cloning: Advances and Applications

Jasdeep Saini[1]
Alessandro Faroni[2,3]
Marwah Abd Al Samid[1]
Adam J Reid[2,3]
Adam P Lightfoot[1]
Kamel Mamchaoui[4]
Vincent Mouly[4]
Gillian Butler-Browne[4]
Jamie S McPhee[5]
Hans Degens[1,6,7]
Nasser Al-Shanti[1]

[1]Musculoskeletal Science & Sports Medicine Research Centre, School of Healthcare Science, Manchester Metropolitan University, Manchester, UK; [2]Blond McIndoe Laboratories, Division of Cell Matrix Biology and Regenerative Medicine, School of Biological Sciences, Faculty of Biology Medicine and Health, University of Manchester, Manchester Academic Health Science Centre, Manchester, UK; [3]Department of Plastic Surgery & Burns, University Hospitals of South Manchester, Manchester Academic Health Science Centre, Manchester, UK; [4]Center for Research in Myology, Sorbonne Université–INSERM, Paris, France; [5]Department of Sport and Exercise Science, Manchester Metropolitan University, Manchester, UK; [6]Institute of Sport Science and Innovations, Lithuanian Sports University, Kaunas, Lithuania; [7]University of Medicine and Pharmacy of Targu Mures, Targu Mures, Romania

Correspondence: Jasdeep Saini
School of Healthcare Science, Manchester Metropolitan University, John Dalton Building, E247, Oxford Road, Manchester, M1 5GD, UK
Tel +44 0161 247 5712
Email Jas.Saini2015@gmail.com

Background: Neuromuscular junctions (NMJs) consist of the presynaptic cholinergic motoneuron terminals and the corresponding postsynaptic motor endplates on skeletal muscle fibers. At the NMJ the action potential of the neuron leads, via release of acetylcholine, to muscle membrane depolarization that in turn is translated into muscle contraction and physical movement. Despite the fact that substantial NMJ research has been performed, the potential of in vivo NMJ investigations is inadequate and difficult to employ. A simple and reproducible in vitro NMJ model may provide a robust means to study the impact of neurotrophic factors, growth factors, and hormones on NMJ formation, structure, and function.

Methods: This report characterizes a novel in vitro NMJ model utilizing immortalized human skeletal muscle stem cells seeded on 35 mm glass-bottom dishes, cocultured and innervated with spinal cord explants from rat embryos at ED 13.5. The cocultures were fixed and stained on day 14 for analysis and assessment of NMJ formation and development.

Results: This unique serum- and trophic factor-free system permits the growth of cholinergic motoneurons, the formation of mature NMJs, and the development of highly differentiated contractile myotubes, which exhibit appropriate configuration of transversal triads, representative of in vivo conditions.

Conclusion: This coculture system provides a tool to study vital features of NMJ formation, regulation, maintenance, and repair, as well as a model platform to explore neuromuscular diseases and disorders affecting NMJs.

Keywords: neuromuscular junction, NMJ, coculture, myoblast, myotube, motor neuron, motoneuron

Introduction

Although the neuromuscular junction (NMJ) plays a central role in the pathology of neuromuscular (NM) disorders, current methods to study its role in NM pathology have severe limitations. For instance, most studies on NM diseases rely on in vivo animal models that do not entirely reflect disease in humans.[1] Shortcomings of in vitro models of NM disorders are that they are largely based on cells derived from animals,[2,3] or skeletal muscle cell (SkMC) culture systems that fail to mimic in vivo conditions, particularly due to the lack of functional innervation.[4] Thus, the development of new models to study and manipulate NMJs has the potential to provide significant insight into NM disease pathogenesis and detection, and to test the efficacy of innovative therapies.

To fill this gap, a small number of promising nerve–muscle coculture models have been developed using mouse, rat, primary human myoblasts, human embryonic

stem cell (hESC) and human induced pluripotent stem cell (hiPSC)-derived cells, and cross-species systems.[5–9] However, some previously established coculture systems suffer from poor experimental reproducibility due to the complexity of the culture system. For example, the use of serum in nerve–muscle coculture systems introduces unspecified variables that can distort the effects of experimental treatments on the system. Further research demonstrates diminished motoneuron myelination in vitro that can be attributed to the use of serum within the culture system.[10]

Coculture systems utilizing primary human skeletal muscle stem cells obtained from muscle biopsies present their own distinct complications as they have limited proliferative capacity and varied cell purity, and experience phenotypic changes when expanded. The phenotypic change is further compounded by progressive cellular senescence during primary cell expansion,[11,12] rendering primary myoblasts a problematic choice for a consistently reproducible coculture system. The use of hESC/hiPSC-derived cells to generate myoblasts[13] and motoneurons[14] may allow for the development of novel coculture systems. However, neuronal cells derived from stem cells are particularly challenging to culture, involving complex media with numerous neurotrophic factors that can have detrimental effects on SkMCs. In addition, cocultures of stem-cell-derived motoneurons and myoblasts result in poorly developed NMJs and have not been maintained for longer than 21 days,[15] which is inadequate for long-duration studies.

This work set out to establish a simplified and easily reproducible nerve–muscle coculture system generating the formation of NMJs. Thus, we developed a novel coculture model devoid of serum and growth/neurotrophic factors. Immortalized human myoblasts were differentiated to mature myotubes while simultaneously being innervated with motoneurons, emanating from neonatal rat spinal cord explants. We observed that this system resulted in the development of highly contractile myotubes that exhibited acetylcholine receptor (AChR) aggregation in the typical twisting knotted structure of mature NMJs that co-localized with motoneuron axon terminals. The success of this system thus offers an easy and reproducible bridge between animal and clinical studies of NM disease and may well serve as a platform to screen the efficacy of novel therapeutic agents.

Experimental procedures

Immortalized human SkMC culture

A non-commercial immortalized human skeletal muscle cell (SkMC) line was generated at the Institute of Myology (Paris, France). The cell line was established using primary human myoblasts obtained anonymously from Myobank, a tissue bank affiliated to Eurobiobank, which has an agreement from the French Ministry of Research (authorization number AC-2013-1868). The primary myoblasts originated from biopsies of the semitendinosus muscle of a 25-year-old man, free of genetic defects and disease. Myoblast immortalization was achieved using transduction with both telomerase-expressing and cyclin-dependent kinase 4-expressing vectors.[37] A 1-mL frozen vial containing a suspension of 1×10^6 SkMCs in 90% FBS and 10% dimethyl sulfoxide (DMSO) was thawed and resuspended in 10 mL of complete growth media (GM)[37] to induce SkMC proliferation.

Cells were incubated at 37°C with a 5% CO_2 atmosphere until 80% confluent. Subsequently, cells were washed twice with Dulbecco's phosphate-buffered saline (DPBS) (Lonza, Basel, Switzerland). Cells were disassociated using 2 mL of TrypLE™ Express Enzyme (Thermo Fisher Scientific, Waltham, MA, USA) and incubated at 37°C in 5% CO_2 for 5 minutes. The cells were counted and then seeded on a 35-mm glass-bottom µ-Dish (ibidi®, Martinsried, Germany) at a density of 350 cells/mm^2, and incubated at 37°C with a 5% CO_2 atmosphere for 24 hours.

Following incubation in GM, cells were washed twice with DPBS and switched to a simplified differentiation medium (DM) consisting of 99% (v/v) DMEM, 1% (v/v) L-glutamine, 10 µg/mL recombinant human insulin, and 10 µg/mL gentamicin. The cells were incubated for 24 hours in DM at 37°C with a 5% CO_2 atmosphere before plating the rat embryo spinal cord explants.

Isolation of rat embryonic spinal cord explants

Ethical approval for the animal work was obtained from the animal facility under a general S1 Home Office license at the University of Manchester. Animal welfare was in accordance with the guidelines detailed in the Animals Scientific Procedures Act 1986, which regulates the use of living vertebrates and cephalopods in scientific procedures within the UK. Time-mated Sprague–Dawley rats from Charles River (Oxford, UK) were killed with CO_2 when embryos were between embryonic development day 13 and 14. Embryo dissection was performed in a 100-mm dish under a binocular microscope using 21-gage needles. The spinal cord was dissected in one piece from the embryo and surrounding connective tissue removed, ensuring that the dorsal root ganglia (DRGs) remained attached to the spinal cord. The spinal cord was sliced transversally into ~1–2 mm^3 explants.

Coculture

DM was removed from the dishes and the cells were washed twice with DPBS; 500 µL DM was added to each dish. Five evenly spaced explants were placed in each dish and incubated for 3 hours at 37°C with a 5% CO_2 atmosphere. Once explants were slightly attached to the SkMCs, an additional 500 µL DM was added to each dish and then incubated for 24 hours. After 24 hours of incubation, a further 1 mL of DM was added to each dish. As the myocytes fuse into immature myotube between 24 and 48 hours, sprouting neurites from the explants innervate the cells at this stage of development. Cocultures were maintained by changing half the DM every 48 hours. Live cells were visualized using a Leica DMI6000 B inverted microscope (Leica Microsystems, Milton Keynes, UK). In addition, real-time myotube contractions were video-captured with phase-contrast microscopy on day 7 at 24 frames per second. Cell fixation for immunocytochemistry was performed on day 14.

Immunocytochemistry

Cells were washed twice with DPBS and fixed in 4% paraformaldehyde for 10 minutes at 21°C. Fixed cells were washed thrice with DPBS and permeabilized with 1× perm/wash buffer (BD Biosciences, Franklin Lakes, NJ, USA), and incubated for 30 minutes at 21°C, followed by a final wash with DPBS. Cells were then incubated for 1 hour in a blocking solution of 0.2% Triton X-100 with 10% normal goat serum (GS) or 10% normal donkey serum (DS) (all from Sigma-Aldrich, St Louis, MO, USA). Blocking solution was removed and cells were washed once with DPBS. The primary antibody in a diluent consisting of 3% GS or DS with 0.05% Tween-20 (Sigma-Aldrich, St Louis, MO, USA) was added to the cells and incubated for 18–24 hours at 4°C. Following primary antibody incubation, the cells were washed thrice with DPBS before incubation with the corresponding secondary antibodies for 1 hour at 21°C. Confirmation of myotube innervation and NMJ formation was assessed via confocal microscopy using the Leica TCS SP5 confocal microscope (Leica Microsystems, Wetzlar, Germany).

Quantification of NMJ morphologies

Innervated and aneural cultures were fixed and stained as described above. Various NMJ morphologies were quantified using previously established NMJ morphology development classifications (ie, mature, fragmented, faint, premature, denervated).[38-41] Twenty random fields of view were assessed at 20× magnification using the Leica TCS SP5 confocal microscope for each data set.

Triad quantification

Innervated and aneural cultures were fixed and stained as described above. Verification of triad formation was assessed using the Leica TCS SP5 confocal microscope. Thirty random fields of view were assessed at 40× magnification.

Results

Characterization of cholinergic motoneurons

An appropriate NMJ is characterized by the connection of cholinergic motoneurons via endplates with SkMCs.[16] In our coculture, motoneurons and myotubes were identified by their staining for choline acetyltransferase (ChAT) and myosin heavy chain (MHC), respectively. Indeed, they were often co-localized (Figure 1) and, together with the numerous motoneuron axon terminals in contact with differentiated myotubes, suggest innervation of the SkMCs. There were also some myotubes with multiple points of contact with

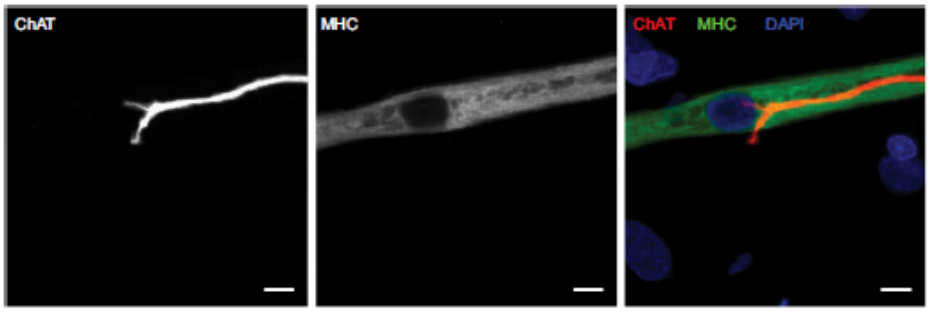

Figure 1 Cholinergic motoneurons co-localize with myotubes at day 14.
Notes: Representative images of human myotube cocultured with embryonic rat motoneuron stained for choline acetyltransferase (ChAT) (red), myosin heavy chain (MHC) (green), and DAPI (blue). Scale bars –7.5 µm.

axon terminals, similar to what is seen in early postnatal muscle development. During in vivo development, myotubes are innervated by multiple branching axons, which extend from many motoneurons. As development progresses, axon pruning occurs and hundreds of mature muscle fibers are innervated by single motoneurons, creating a functional motor unit.[17] Importantly, the development of the cocultures appeared similar to what is observed in vivo before axon pruning occurs.

NMJ formation

Having confirmed the co-localization of cholinergic motoneurons with differentiated myotubes, subsequent experiments were performed to verify that synaptic connections were indeed formed between the motoneurons and myotubes. NMJs are distinguishable by highly clustered AChRs on the myotube membrane in close proximity of motoneuron axons. Motoneurons were identified by staining for β-III-tubulin and AChR clusters were identified with fluorescently labeled α-bungarotoxin (α-BTX) (Figure 2). In the cocultures, numerous axon terminals co-localized with AChR aggregations on the myotube membrane. These clusters of AChRs had the typical twisting-knotted configuration, as seen in vivo, while sparse, unstructured and disjointed AChRs were observed on the membranes of myotubes that were aneurally cultured.

The efficacy of NMJ formation in the coculture system was much better than that in aneurally cultured myotubes, as reflected by a larger proportion of mature NMJs (Figure 3).

Spontaneous myotube contractions

The first spontaneous muscle contractions were detected in the myotubes ~3 days after co-culturing the SkMCs with rat embryo spinal cord explants. We believe this is the first time spontaneous contractions have been observed at this early stage of development in a nerve–muscle coculture system. Despite the fact that myotube contractions were observed as early as 72 hours, only individual arrhythmically contracting myotubes were observed at this time point, with the most vigorously contracting myotubes closest to the explant. The cocultures progressively displayed an increase in both the number of contracting myotubes and the frequency of contractions. By day 7 post coculture, networks of myotubes were contracting simultaneously in a rhythmic manner (Video S1), suggesting that the myotube network functioned as a single motor unit, receiving bursts of stimulation from the motoneurons. Contracting myotubes separated from the culture plate adopted the morphological characteristics of three-dimensional tubes. Conversely, aneurally cultured myotubes did not contract and maintained a flat two-dimensional morphology, firmly fixed to the culture plate surface. These observations indicate that the observed NMJs are in fact functional. However, even at this time point, multiple innervations were still visible on a large proportion (83.4±12.6%, n=20) of the innervated myotubes.

Characterization of innervated myotubes

Mature myotubes in vivo display triads that are arranged in a repetitive transversal manner. Triads consist of a T-tubule with terminal cisternae on each side.[18] T-tubules were identified by staining for the dihydropyridine receptor (DHPR), a voltage-dependent calcium channel located in the T-tubule membrane,[19] and the terminal cisternae were identified by staining for the ryanodine receptor (RyR), which is located on the membrane of the sarcoplasmic reticulum.[20] By day 14, about 32% of the cocultured myotubes had well-developed triads (Figure 4A), whereas none of the aneurally cultured SkMCs exhibited the triad structure (Figure 4B, C).

Discussion

We developed a serum-free coculture of immortalized human myoblasts and embryonic rat spinal cord explants

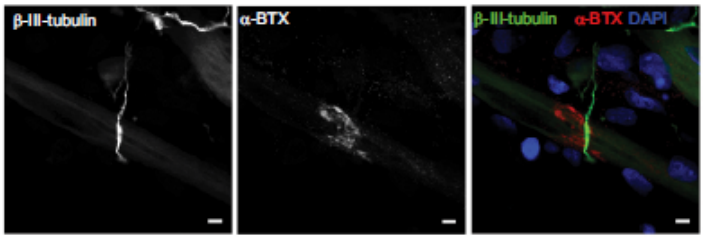

Figure 2 Characterization of neuromuscular junction formation at day 14.
Notes: Representative images of coculture stained for β-III-tubulin (green), α-bungarotoxin (α-BTX) (red), and DAPI (blue). Scale bars =5 μm.

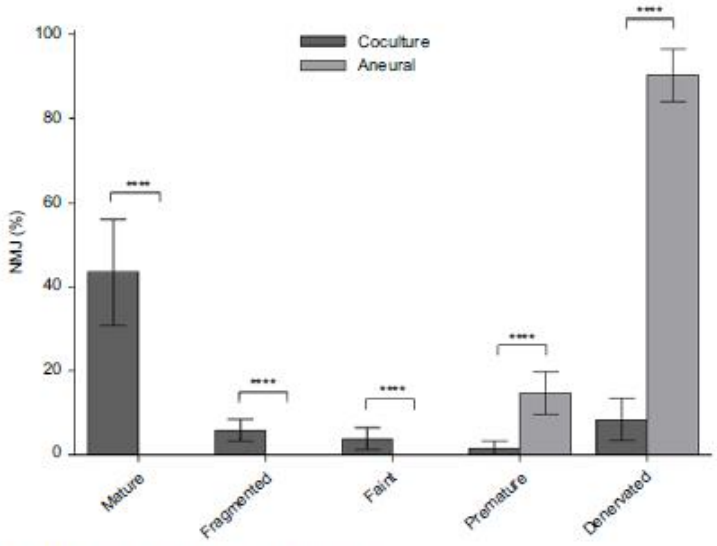

Figure 3 Percentage of various neuromuscular junction (NMJ) morphologies at day 14.
Notes: Cocultured and aneurally cultured myotubes. Results are expressed as mean ± SD, n=4, analyzed with unpaired *t*-test; ****P<0.0001.

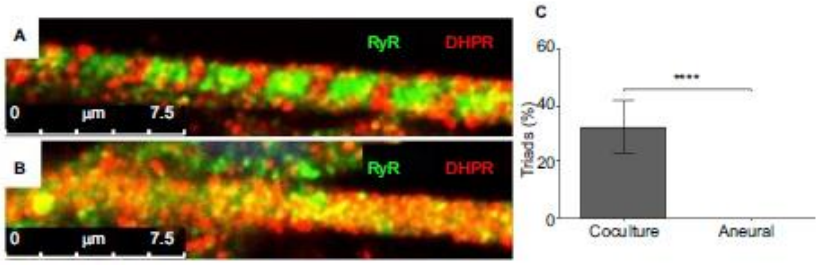

Figure 4 Characterization of myotubes at day 14.
Notes: Representative images of (**A**) a myotube cocultured with embryonic rat spinal cord and (**B**) an aneurally cultured myotube. Myotubes were stained for ryanodine receptor (RyR) (green) and dihydropyridine receptor (DHPR) (red); scale bars =7.5 µm. (**C**) The percentage of myotubes with triads from cocultured and aneurally cultured myotubes. Results are expressed as mean ± SD, n=10, analyzed with unpaired *t*-test; ****P<0.0001.

that successfully produced abundant functional NMJs, as reflected by the structural differentiation and coordinated contractions of myotubes. This coculture model can be used as a model platform to test the efficacy of agents to modulate NMJ structure and function. This may be particularly useful in studies on NM diseases.

Neurons generated in this coculture model were derived from ~1–2 mm transversally sliced spinal cord explants with intact DRGs.[9,21] Preliminary experiments with mechanically disassociated embryo spinal cords to create a neuronal cell suspension, or coculture of myoblasts with the ventral horn only without the DRGs, showed poorer results than the coculture with entire rat embryonic spinal cord explants. The poorer result was reflected by a delayed initiation of spontaneous myotube contractions, higher incidence of arrhythmic contractions, lower contraction frequency, and lower abundance of NMJs that were poorly developed or had a failed junction assembly in comparison to the myoblast plus complete embryonic spinal cord segment coculture (data not shown). While this suggests that both motor and sensory neurons[22] are required for correct innervation of myotubes and NMJ formation, it is more likely that the

progenitor and supporting cell types, such as glial cells, in the DRGs are crucial for correct innervation. Indeed, Schwann cells perform vital functions in motoneuron development, differentiation, and maintaining NMJ integrity.[23] Subsequently, we cocultured myoblasts with rat embryonic spinal cord explants.

In line with previous observations,[24] we found that innervated myotubes in our coculture system were in an advanced state of differentiation and exhibited endogenously stimulated contractility, something not seen in the aneurally cultured SkMCs. The innervation appears to be important, as while treatment of aneurally cultured human myotubes with the secretome of a rat-nerve/human-muscle coculture secretome did increase AChR clustering, it failed to induce advanced myotube differentiation and contractile activity.[25,26] In fact, early research found that myotubes that failed to become innervated within a nerve–muscle coculture system not only failed to differentiate, but eventually even deteriorated, despite nerve-derived secretions in the culture environment.[27]

In our coculture model, myotube contractions were observed as early as 72 hours post coculture, which we believe is the first time contractile functionality has been observed in any nerve–muscle coculture system. This indicates that functional NMJs were already present at this time point, as myotubes require nervous input to induce contraction.[28] Over time, the contraction frequency increased and the contractions occurred synchronously by day 7 (Video S1). At day 14, the cocultured innervated myotubes also displayed the regular appearance, every 2.4 µm, of transversal triads, peripherally located nuclei and actin–myosin striations, all morphological characteristics of advanced differentiation seen in vivo.[29,30] The advanced differentiation of innervated myotubes illustrates the strength of this coculture system over typical aneural in vitro SkMC cultures, which fail to achieve advanced stages of development. Our coculture model thus provides a promising tool to elucidate the significance of the integrity of the NMJ in conditions such as NM disorders.

Our coculture model not only resembled the in vivo skeletal muscle more than aneurally cultured SkMC, but was also simple and reproducibly generated large quantities of functional NMJs. In contrast to our simple model, which already has functional NMJs after 3 days of coculture, other nerve–muscle coculture models require various culture media formulations to separately differentiate myotubes and motoneurons for at least 10 days before co-culturing can even start,[31] and need another 21 days of co-culturing before NMJs form.[5] These lengthy protocols lead to avoidable postponements, possible unintended variation to experimental procedures, and a larger risk of contamination. In our model, however, coculture can start immediately, and after only 3 days, viable NMJs are already detectable.

In addition, other nerve–muscle coculture systems require serum or trophic factors, such as brain-derived neurotrophic factor or insulin-like growth factor-1, to induce spontaneous myotube contractions, myotube innervation, and functional NMJ formation.[5,31–33] Our coculture media were devoid of serum, neurotrophic factors, and growth factors, which will drastically reduce experimental variability. The simplicity of our system makes it ideal for high-throughput research of agents that may affect NMJ formation and myotube differentiation.

High throughput is also facilitated by the fact that a single pregnant rat can yield up to 100 embryo spinal cord explants. This also reduces between-experiment variation as the same spinal cord can be used for different experimental conditions and time points. Although our cocultures were characterized on day 14, preliminary viability experiments revealed that persistent myotube contractions continued to occur as late as day 30, with the potential for further extended viability. Even though the lack of extended viability of other nerve–muscle models[34] has been improved,[32] they still only generated immature NMJs with a speckled AChR morphology and myotubes without advanced differentiation. Clearly, our system is an improvement on these coculture systems as we did see advanced myotube differentiation and a large number of functional NMJs.

Another advantage of our heterologous coculture model is that antibodies specific for rat or human can be used to study both presynaptic and postsynaptic regions of the NMJ. One such application is illustrated by the exploitation of species-specific immunocytochemical staining against acetylcholinesterase (AChE) to differentiate between AChE originating from the human SkMCs and rat neuronal cells at the NMJ.[35] Alternative chimeric cocultures have demonstrated similar advantages. For instance, a coculture model consisting of chick SkMCs innervated by rat neurons was stained using species-specific antibodies to determine that agrin, which is a vital element in the development of the NMJ, is secreted from both SkMCs and motoneurons into the synaptic cleft of NMJs.[36] Fully human homologous hESC/hiPSC-derived SkMC and motoneuron coculture models would be of great interest. However, these systems are still in their infancy and require significant optimization before they parallel the formation of functional NMJs and express the level of differentiation demonstrated in our coculture model.

Conclusion

We have developed an easy and reproducible serum-free coculture of immortalized human myoblasts and embryonic rat spinal cord explants that induces a rapid formation of functional NMJs. The model can be a used as a high-throughput platform to assess the impact of interventions on NM integrity and drug testing.

Acknowledgments

This work was sponsored by the School of Healthcare Science, Faculty of Science and Engineering, Manchester Metropolitan University (Manchester, UK). Thank you to the Lumley Trust, which paid for the animal costs.

Author contributions

JS, AF, AJR, HD, and NAS developed the study concept. All the authors contributed to experimental procedures. JS, AF, and NAS carried out the investigation. AJR, JSM, HD, and NAS supervised the study. JS, HD, APL, and NAS wrote the original draft of the manuscript. JS, MAAS, JSM, HD, and NAS reviewed and edited the draft manuscript. All authors contributed to data analysis and drafting or revising the article, gave final approval of the version to be published, and agree to be accountable for all aspects of the work.

Disclosure

The authors report no conflicts of interest in this work.

References

1. van der Worp HB, Howells DW, Sena ES, et al. Can animal models of disease reliably inform human studies? *PLoS Med*. 2010;7(3):e1000245.
2. Haase G. Motor neuron diseases: cellular and animal models. In: Meyers RA, editor. *Reviews in Cell Biology and Molecular Medicine*. Weinheim: Wiley-VCH Verlag GmbH & Co. KGaA; 2006.
3. Prather RS, Lorson M, Ross JW, Whyte JJ, Walters E. Genetically engineered pig models for human diseases. *Annu Rev Anim Biosci*. 2013;1(1):203–219.
4. Suuronen EJ, Mclaughlin CR, Stys PK, Nakamura M, Munger R, Griffith M. Functional innervation in tissue engineered models for in vitro study and testing purposes. *Toxicol Sci*. 2004;82(2):525–533.
5. Demestre M, Orth M, Föhr KJ, et al. Formation and characterisation of neuromuscular junctions between hiPSC derived motoneurons and myotubes. *Stem Cell Res*. 2015;15(2):328–336.
6. Umbach JA, Adams KL, Gundersen CB, Novitch BG. Functional neuromuscular junctions formed by embryonic stem cell-derived motor neurons. *PLoS One*. 2012;7(5):e36049.
7. Harper JM, Krishnan C, Darman JS, et al. Axonal growth of embryonic stem cell-derived motoneurons in vitro and in motoneuron-injured adult rats. *Proc Natl Acad Sci USA*. 2004;101(18):7123–7128.
8. Guo X, Greene K, Akanda N, et al. In vitro differentiation of functional human skeletal myotubes in a defined system. *Biomater Sci*. 2014;2(1):131–138.
9. Arnold A-S, Christe M, Handschin C. A functional motor unit in the culture dish: co-culture of spinal cord explants and muscle cells. *J Vis Exp*. 2012;62(62):3616.
10. Rumsey JW, Das M, Stancescu M, Bott M, Fernandez-Valle C, Hickman JJ. Node of Ranvier formation on motoneurons in vitro. *Biomaterials*. 2009;30(21):3567–3572.
11. Mouly V, Aamiri A, Périé S, et al. Myoblast transfer therapy: is there any light at the end of the tunnel? *Acta Myol*. 2005;24(2):128–133.
12. Webster C, Blau HM. Accelerated age-related decline in replicative life-span of Duchenne muscular dystrophy myoblasts: implications for cell and gene therapy. *Somat Cell Mol Genet*. 1990;16(6):557–565.
13. Tanaka A, Woltjen K, Miyake K, et al. Efficient and reproducible myogenic differentiation from human iPS cells: prospects for modeling Miyoshi myopathy in vitro. *PLoS One*. 2013;8(4):e61540.
14. Stockmann M, Linta L, Föhr KJ, et al. Developmental and functional nature of human iPSC derived motoneurons. *Stem Cell Rev*. 2013;9(4):475–492.
15. Li XJ, Du ZW, Zarnowska ED, et al. Specification of motoneurons from human embryonic stem cells. *Nat Biotechnol*. 2005;23(2):215–221.
16. Sanes JR, Lichtman JW. Development of the vertebrate neuromuscular junction. *Annu Rev Neurosci*. 1999;22:389–442.
17. Low LK, Cheng HJ. Axon pruning: an essential step underlying the developmental plasticity of neuronal connections. *Philos Trans R Soc Lond B Biol Sci*. 2006;361(1473):1531–1544.
18. Marty I, Robert M, Villaz M, et al. Biochemical evidence for a complex involving dihydropyridine receptor and ryanodine receptor in triad junctions of skeletal muscle. *Proc Natl Acad Sci USA*. 1994;91(6):2270–2274.
19. Rios E, Brum G. Involvement of dihydropyridine receptors in excitation-contraction coupling in skeletal muscle. *Nature*. 1987;325(6106):717–720.
20. Coronado R, Morrissette J, Sukhareva M, Vaughan DM. Structure and function of ryanodine receptors. *Am J Physiol*. 1994;266(6 Pt 1):C1485–C1504.
21. Kobayashi T, Askanas V, Engel WK. Human muscle cultured in monolayer and cocultured with fetal rat spinal cord: importance of dorsal root ganglia for achieving successful functional innervation. *J Neurosci*. 1987;7(10):3131–3141.
22. Mears SC, Frank E. Formation of specific monosynaptic connections between muscle spindle afferents and motoneurons in the mouse. *J Neurosci*. 1997;17(9):3128–3135.
23. Riethmacher D, Sonnenberg-Riethmacher E, Brinkmann V, Yamaai T, Lewin GR, Birchmeier C. Severe neuropathies in mice with targeted mutations in the ErbB3 receptor. *Nature*. 1997;389(6652):725–730.
24. Feher J, editor. The neuromuscular junction and excitation–contraction coupling. In: *Quantitative Human Physiology*. 2nd ed. Boston: Academic Press; 2017:318–333.
25. Bandi E, Jevšek M, Mars T, et al. Neural agrin controls maturation of the excitation-contraction coupling mechanism in human myotubes developing in vitro. *Am J Physiol Cell Physiol*. 2008;294(1):C66–C73.
26. Arnold A-S, Gueye M, Guettier-Sigrist S, et al. Reduced expression of nicotinic AChRs in myotubes from spinal muscular atrophy I patients. *Lab Investig*. 2004;84(10):1271–1278.
27. Askanas V, Kwan H, Alvarez RB, et al. De novo neuromuscular junction formation on human muscle fibres cultured in monolayer and innervated by foetal rat spinal cord: ultrastructural and ultrastructural--cytochemical studies. *J Neurocytol*. 1987;16(4):523–537.
28. Hong IHK, Etherington SJ, editors. Neuromuscular junction. In: *eLS*. Vol. 1. Chichester: John Wiley & Sons; 2011.
29. Bruusgaard JC, Liestøl K, Ekmark M, Kollstad K, Gundersen K. Number and spatial distribution of nuclei in the muscle fibres of normal mice studied *in vivo*. *J Physiol*. 2003;551(2):467–478.
30. Shadrin IY, Khodabukus A, Bursac N. Striated muscle function, regeneration, and repair. *Cell Mol Life Sci*. 2016;73(22):4175–4202.
31. Guo X, Gonzalez M, Stancescu M, Vandenburgh HH, Hickman JJ. Neuromuscular junction formation between human stem cell-derived motoneurons and human skeletal muscle in a defined system. *Biomaterials*. 2011;32(36):9602–9611.

32. das M, Rumsey JW, Bhargava N, Stancescu M, Hickman JJ. A defined long-term in vitro tissue engineered model of neuromuscular junctions. *Biomaterials*. 2010;31(18):4880–4888.
33. Rumsey JW, das M, Bhalkikar A, Stancescu M, Hickman JJ. Tissue engineering the mechanosensory circuit of the stretch reflex arc: sensory neuron innervation of intrafusal muscle fibers. *Biomaterials*. 2010;31(32):8218–8227.
34. das M, Rumsey JW, Gregory CA, et al. Embryonic motoneuron-skeletal muscle co-culture in a defined system. *Neuroscience*. 2007;146(2):481–488.
35. Jevsek M, Mars T, Mis K, Grubic Z. Origin of acetylcholinesterase in the neuromuscular junction formed in the in vitro innervated human muscle. *Eur J Neurosci*. 2004;20(11):2865–2871.
36. Lieth E, Fallon JR. Muscle agrin: neural regulation and localization at nerve-induced acetylcholine receptor clusters. *J Neurosci*. 1993;13(6):2509–2514.
37. Mamchaoui K, Trollet C, Bigot A, et al. Immortalized pathological human myoblasts: towards a universal tool for the study of neuromuscular disorders. *Skelet Muscle*. 2011;1(1):34.
38. Valdez G, Tapia JC, Kang H, et al. Attenuation of age-related changes in mouse neuromuscular synapses by caloric restriction and exercise. *Proc Natl Acad Sci USA*. 2010;107(33):14863–14868.
39. Lee KY, Li M, Manchanda M, et al. Compound loss of muscleblind-like function in myotonic dystrophy. *EMBO Mol Med*. 2013;5(12):1887–1900.
40. Kummer TT, Misgeld T, Lichtman JW, Sanes JR. Nerve-independent formation of a topologically complex postsynaptic apparatus. *J Cell Biol*. 2004;164(7):1077–1087.
41. Sahashi K, Hua Y, Ling KK, et al. Tsunami: an antisense method to phenocopy splicing-associated diseases in animals. *Genes Dev*. 2012;26(16):1874–1884.

Supplementary material

Video S1 Phase-contrast video-micrograph of spontaneously contracting human myotubes that were cocultured with embryonic rat spinal cord explants at day 7. Representative video of innervated myotubes contracting within the coculture system without external stimulation. Scale bar =100 µm.

Ageing Research Reviews 27 (2016) 67–76

Contents lists available at ScienceDirect

Ageing Research Reviews

journal homepage: www.elsevier.com/locate/arr

Review

Regenerative function of immune system: Modulation of muscle stem cells

Jasdeep Saini[a], Jamie S. McPhee[a], Sarah Al-Dabbagh[a], Claire E. Stewart[b], Nasser Al-Shanti[a,*]

[a] Healthcare Science Research Institute, School of Healthcare Science Manchester Metropolitan University, John Dalton Building, Chester Street, M1 5GD Manchester, UK
[b] Research Institute for Sport & Exercise Sciences, School of Sport and Exercise Sciences, Tom Reilly Building, Byrom Street Campus, Liverpool John Moores University, Liverpool L3 3AF, UK

ARTICLE INFO

Article history:
Received 27 July 2015
Received in revised form 29 March 2016
Accepted 30 March 2016
Available online 31 March 2016

Keywords:
Muscle treg
Regeneration
Skeletal muscle
Immune system

ABSTRACT

Ageing is characterised by progressive deterioration of physiological systems and the loss of skeletal muscle mass is one of the most recognisable, leading to muscle weakness and mobility impairments. This review highlights interactions between the immune system and skeletal muscle stem cells (widely termed satellite cells or myoblasts) to influence satellite cell behaviour during muscle regeneration after injury, and outlines deficits associated with ageing. Resident neutrophils and macrophages in skeletal muscle become activated when muscle fibres are damaged via stimuli (e.g. contusions, strains, avulsions, hyperextensions, ruptures) and release high concentrations of cytokines, chemokines and growth factors into the microenvironment. These localised responses serve to attract additional immune cells which can reach in excess of 1×10^5 immune cell/mm^3 of skeletal muscle in order to orchestrate the repair process. T-cells have a delayed response, reaching peak activation roughly 4 days after the initial damage. The cytokines and growth factors released by activated T-cells play a key role in muscle satellite cell proliferation and migration, although the precise mechanisms of these interactions remain unclear. T-cells in older people display limited ability to activate satellite cell proliferation and migration which is likely to contribute to insufficient muscle repair and, consequently, muscle wasting and weakness. If the factors released by T-cells to activate satellite cells can be identified, it may be possible to develop therapeutic agents to enhance muscle regeneration and reduce the impact of muscle wasting during ageing and disease.

Contents

* Corresponding author at: School of Healthcare Science, John Dalton Building, Chester Street, M1 5GD Manchester, UK.
E-mail address: n.al-shanti@mmu.ac.uk (N. Al-Shanti).

http://dx.doi.org/10.1016/j.arr.2016.03.006
1568-1637/

1. Introduction

In older age, skeletal muscle atrophies considerably (Maden-Wilkinson et al., 2014; Lexell et al., 1988; Janssen et al., 2002; Lexell, 1995; Morley et al., 2001), which contributes to weakness and mobility impairments inherent to sarcopenia (Janssen, 2011; Cruz-Jentoft et al., 2010) and frailty (Fried et al., 2001). Loss of skeletal muscle mass and function with ageing are associated with altered immune, hormonal and metabolic factors directly impacting on muscle (Narici and Maffulli, 2010) and resulting in motor unit remodelling (Piasecki et al., 2015). This review will first outline the role of the immune system in myogenesis that occurs after injury and then discuss how changes in immune cells may contribute to ageing-related muscle impairments. Identification of the signalling molecules exchanged between immune and satellite cells may lead to novel therapeutic strategies to preserve muscle with advancing old age and muscle wasting conditions.

1.1. Myogenesis and satellite cell activation

Skeletal muscle is the most abundant tissue type in healthy humans (Yin et al., 2013). It powers movements and contributes to metabolism by storing amino acids, glucose and fatty acids as well as oxidising substrates to replenish adenosine triphosphate stores (Leto and Saltiel, 2012). Muscles also release cytokines and growth factors into the extra-cellular compartments to act locally or systemically (Pedersen, 2011). The production of skeletal muscle cells occurs during embryonic myogenesis and thereafter myofibres themselves are incapable of proliferation (Bentzinger et al., 2012). Hence, the number of skeletal muscle fibres is largely determined before birth. Postnatal muscle growth arises by adapting and remodelling pre-existing fibres and through recruitment of resident, non-fused, self-renewing satellite cells (Tedesco et al., 2010). Satellite cells reside beneath the basal lamina of mature fibres in a quiescent state, they neither undergo cell division nor differentiation unless they are specifically activated to do so (Kuang et al., 2007). Damage to the muscle through injury or very intense prolonged unaccustomed exercise training are examples of principal activators of quiescent satellite cells.

1.2. Young myogenesis

Increases in muscle mass (hypertrophy) and adapted metabolism after exercise training in adults improves athletic performance and health (Egan and Zierath, 2013). The training-induced hypertrophy can depend on satellite cell proliferation and differentiation (Joanisse et al., 2013; Yin et al., 2013). However, hypertrophy may not necessarily require activation of satellite cells, since a satellite cell deficient mouse model showed normal training-induced hypertrophy (McCarthy et al., 2011; Glass, 2003). Satellite cells are, however, centrally involved in muscle regeneration after damage (Lepper et al., 2011; Yin et al., 2013). Some minor muscle damage can be a feature of everyday living that goes largely unnoticed by the individual due to minimal muscle tenderness and no apparent effect on function. More painful and functionally impairing damage can occur after repeated intense or rapid muscular activations, especially following unaccustomed high-load eccentric contractions (lengthening under strain) performed across a large range of motion (Paulsen et al., 2012) or electrical stimulation protocols (Crameri et al., 2007; Mackey et al., 2008; Nosaka et al., 2011). External stressors such as heavy impact causing contusion, traumatic puncture wounds or pathogen invasion can also damage otherwise healthy muscle, and in animal models, damage can be induced through injection of substances such as cardiotoxin (Ctx) (Sousa-Victor et al., 2014). Once activated, satellite cells migrate to the damaged site and re-enter into the cell cycle (Tedesco et al., 2010; Siegel et al., 2009) to generate the required concentration of myoblasts through several cycles of proliferation to regenerate damaged fibres. Although the majority of activated satellite cells differentiate into myotubes, a population of satellite cells return to a quiescent state (self-renewal) to maintain their numbers for the next incidence of muscle injury (Relaix and Zammit, 2012; Yin et al., 2013). The differentiated myotubes either fuse with pre-existing damaged myofibers to provide additional myonuclei during muscle regeneration, or fuse with each other forming de novo myofibers to replace the damaged myofibres during muscle regeneration (Adams, 2006; Siegel et al., 2011).

Satellite cells do not function in an isolated environment, a number of non-myogenic cells also populate muscle and influence the regenerative actions of satellite cells (Cerletti et al., 2008). For example, mesenchymal interstitial cells (Farup et al., 2015; Uezumi et al., 2014) and infiltrating immune cells secrete numerous cytokines and growth factors into the localised microenvironment that orchestrate muscle regenerative mechanisms by clearing cellular debris and facilitating repair (Tedesco et al., 2010). These cytokines are not necessarily released into the general circulation to act systemically (Steensberg et al., 2002). Thus, effective muscle repair and regeneration relies not only on muscle satellite cells (known as the intrinsic niche) but also on other distinct cell types and their locally secreted cytokines (termed the extrinsic niche).

1.3. Aged myogenesis

Muscle from aged mice was estimated to contain around 65% fewer functioning satellite cells than muscle from young mice (Cosgrove et al., 2014) and the overall number of satellite cells was also lower in aged mouse muscle (Chakkalakal et al., 2012). However, this was not the main cause of sarcopenia, at least not in mice, where induced depletion of satellite cells in young adults had little impact on the rate of muscle ageing (Fry et al., 2015). It is interesting to note that healthy older people do maintain the ability to activate satellite cells after intense exercise (Verdijk et al., 2009). However, if the activation of satellite cells cannot keep pace with damage, then muscle wasting or atrophy will inevitably occur. The loss of muscle mass with ageing has been linked to the reduced regenerative actions of older satellite cells and altered immune response to damage (Peake et al., 2010; Degens, 2010). There are reports of intrinsic deficiencies within satellite cells that reduce their activity. For instance, two-thirds of satellite cells in older mice showed reduced capacity for muscle regeneration due to elevated activity of p38α and p38β mitogen-activated kinase signalling which was not overcome by transplantation into a young recipient (Cosgrove et al., 2014). However, the debate continues as to whether or not satellite cell intrinsic deficits can be overcome by exposure to a 'young' microenvironment (reviewed elsewhere: (Brack and Munoz-Canoves, 2015)). There is strong evidence implicating the aged microenvironment with reduced satellite cell responses (Chakkalakal et al., 2012; Barberi et al., 2013). Transplanted muscle from young into old mice fails to regenerate, but transplanted muscle from old into young regenerate (Carlson and Faulkner, 1989), but might have a delayed regenerative

response (Smythe et al., 2008). Moreover, 'rejuvenating' the microenvironment in older mice enhanced activation of satellite cells through increased Notch signalling, as shown in heterochronic parabiosis models (Conboy et al., 2005; Carlson et al., 2008).

Lower satellite cell function with ageing was linked to increased activity of the transforming growth factor beta (TGF-β) family of molecules within satellite cells that are negative regulators of growth and restrict the proliferative responses (Carlson et al., 2009; Sousa-Victor et al., 2014; Yousef et al., 2015). Elevated fibroblast growth factor (FGF) signalling from the aged microenvironment was associated with depletion of the stem cell population and impaired regenerative capacity, but was countered in the aged satellite cells that had higher levels of Sprouty1 (Spry1) to inhibit FGF signalling (Chakkalakal et al., 2012). By altering satellite cell signalling through Notch, Wnt and receptor tyrosine kinases/extracellular signal-regulated kinase (RTK/ERK) it has been possible to overcome deficits in aged satellite cell function (Brack and Rando, 2007; Carlson et al., 2008; Naito et al., 2012). Circulating soluble factors, such as hormones, or other molecules released locally into the microenvironment may influence the intracellular satellite cell signalling to regulate proliferative and differentiation responses. For example, elevating the circulating oxytocin had rejuvenating effects for satellite cells (Elabd et al., 2014); increasing circulating levels of growth differentiation factor 11 (GDF-11) also rejuvenated satellite cells (Sinha et al., 2014). However, alternative research investigating the effect of GDF-11 on myogenesis observed a significant inhibition of skeletal muscle regeneration (Brun and Rudnicki, 2015). Additionally, elevated levels of osteopontin in aged mice was associated with impaired satellite cell responses to damage and this was overcome by reducing osteopontin in vitro and in vivo (Paliwal et al., 2012). Thus, a key detail, which has not yet been fully understood, is how the satellite cells respond to the rapidly changing microenvironment occurring soon after muscle damage, which is heavily influenced by the infiltrating immune cells.

2. Innate immunity and muscle regeneration

Changes in immune cells with ageing have been well characterised and the observations of elevated systemic inflammation led to the term 'inflamm-ageing' (Franceschi et al., 2000). Human immunity is subdivided into two main areas, often described as *innate* and *adaptive* immunity. Innate immunity describes the primary capacity of the immune system to respond to pathophysiological triggers such as injury or pathogens and is mediated mainly through the myeloid progenitor cells (e.g. neutrophils, macrophages, dendritic cells, natural killer cells, mast cells, eosinophils, basophils) (Plackett et al., 2004). During normal physiological conditions, immune cells circulate within the blood and the lymphatic system, with considerable accumulations in lymphoid organs and most tissues of the body. Peripheral tissues also contain a population of resident immune cells, primarily consisting of macrophages and dendritic cells. However, during pathophysiological conditions supplementary leukocytes rapidly permeate tissues. During muscle regeneration, there can be in excess of 1×10^5 immune cell/mm^3 of skeletal muscle (Wehling et al., 2001). When activated, these immune cells secrete cytokines and growth factors which regulate the damaged muscle microenvironment (Merly et al., 1999; Warren et al., 2004; Smith et al., 2008).

2.1. Innate immune response to acute damage and repair

The regulation of infiltrating inflammatory cells is a dynamic process which varies depending on the extent of muscle damage and the time required to repair (Paulsen et al., 2012). Minor muscle damage, such as that which occurs after exercise, causes only a modest inflammatory response and may not cause substantial leukocyte cell infiltration, while more severe muscle damage occurring after very intense, unaccustomed exercise with high eccentric loads causes a considerably greater muscle tenderness, immune cell (e.g. neutrophil, macrophage and muscle T reg) infiltration (Fig. 1) of the damaged area and inflammatory responses consistent with rhabdomyolysis (reviewed in (Paulsen et al., 2012)).

The innate immune response to damage involves infiltration of inflammatory cells, but studies in aged mice have revealed a delayed inflammatory response (Shavlakadze et al., 2010). In healthy muscle, neutrophils show a transient response, infiltrating the extracellular space around the damaged fibres within 2 h before concentrations decline to negligible levels within 3 or 4 days. The mechanisms of neutrophil infiltration remain unclear, but the resulting perpetuation of inflammatory damage is believed to be important for initiating the reparative process (Dumont et al., 2008). Neutrophils release interleukin 1 (IL-1) and interleukin 8 (IL-8) which act as chemoattractants for macrophages, inducing the initial macrophage infiltration to the injury site (Fujishima et al., 1993; Cassatella, 1999). Resident macrophages within the endomysium and perimysium are also involved in phagocytosis and secrete enzymes, growth factors and cytokines/chemokines aiding the recruitment of additional immune cells (Wang et al., 2014).

Macrophages go through various stages of activation. *Classic activation* of macrophages is denoted as the M1 phenotype, where the increase in numbers and expression of proinflammatory mediators, cytokines and chemokines are observed from 24 h and reach peak activation around 2 or 3 days after damage (Rodriguez-Prados et al., 2010; Saclier et al., 2013) (Villalta et al., 2009). The M1 phenotype macrophages originating from the blood as monocytes are distinguishable by their expression of the glycoprotein lymphocyte antigen 6C (Ly6C) as well as receptors for the CX3C chemokine receptor 1 (CX3CR1) and C–C chemokine receptor type 2 (CCR2) (Geissmann et al., 2003). The chemokine CCR2 and its ligand CCL2 (or MCP-1) which are mainly produced by monocytes/macrophages coordinate the recruitment of macrophage Ly6C$^+$ to the site of injury supporting the proinflammatory response. Ly6C$^+$ monocytes differentiate into M1 macrophages in tissue and produce proinflammatory cytokines (Jetten et al., 2014). Ly6C$^-$ cells are recruited to the area by CX3CR1 and CCR2 chemokine receptor signalling and differentiate into M2 macrophages to perform anti-inflammatory and pro-myogenic functions that contribute to the later stages of regeneration (Forbes and Rosenthal, 2014). The M2 phenotype is known as *alternative activation* and peaks between 4 and 6 days (see Fig. 1) during the reparative process, where expression of anti-inflammatory mediators, cytokines and chemokines supports the regeneration through satellite cell activation (Tidball, 2005; Arnold et al., 2007). In cases of severe muscle damage causing fibre necrosis, macrophages can be found infiltrating the intracellular areas of fibres several days post-injury, and elevated macrophage concentrations are evident in muscle tissue up to 3 weeks later (Paulsen et al., 2010).

CCR2$^{-/-}$ mice show impaired monocyte recruitment to the site of injury, while neutrophil and other T-cells remain unaffected (Abbadie et al., 2003). The CCR2$^{-/-}$ mice also show impaired muscle regeneration, arrested angiogenesis along with increased fibrosis and excess adipocyte accumulation at the injury site (Martinez et al., 2010). Bone marrow transplants from wild-type mice into CCR2$^{-/-}$ mice recovered the regenerative capacity of skeletal muscle of the CCR2$^{-/-}$ mice. These results show that CCR2, released by proliferating myocytes and resident immune cells, recruits bone marrow derived monocytes (Sun et al., 2009). However, the same results are not observed in studies involving CCL2$^{-/-}$ mice. The

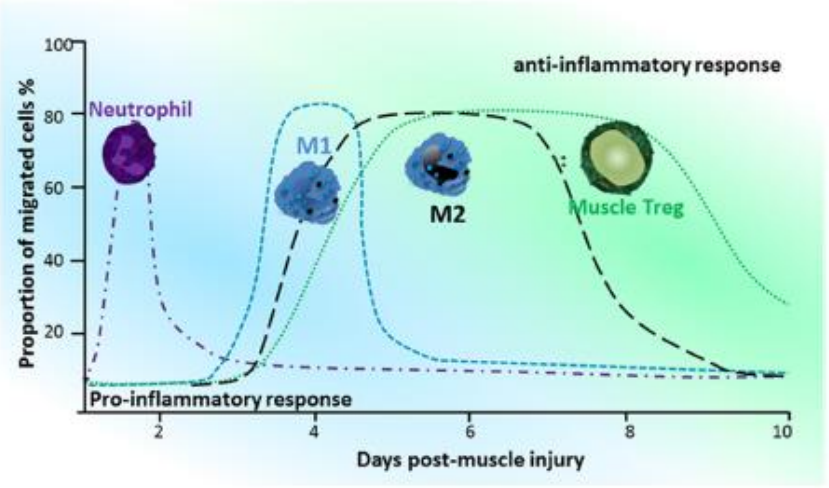

Fig. 1. Timeline of inflammatory responses and immune cell during muscle. The immune system responds to muscle damage by recruiting a precise sequence of pro and anti-inflammatory immune cells to the site of injury. Immune cells are observed from the initial pro-inflammatory phase required for removal of cellular debris through to the final repair of the damaged muscle fibres. Neutrophils rapidly infiltrate the extracellular space around the damaged fibres within 2 h and peak in number between 6 and 24 h followed by rapid decline of neutrophils to negligible levels within 72–96 h. This initial infiltration of neutrophils further contributes to the inflammatory damage to the injured muscle fibres. Subsequently, M1 macrophage concentrations rapidly being to increase at the site of injury and initiate the pro-inflammatory functions of muscle repair through secretion of several cytokines and mediators. The number of M1 macrophages will continue to increase until peak concentrations at 72–96 h after injury and then begin to decline sharply. This is followed by the increase in numbers of anti-inflammatory and pro-myogenic M2 macrophages, which reach peak concentrations in the regenerating muscle at roughly 120–144 h post injury, remaining significantly elevated for several days following. Finally activated T-cells are recruited to the regenerating muscle damage site, with concentrations beginning to peak as M2 macrophage number being to decline. Populations of T cells, specify mTreg remain significantly elevated for 30 following the initial injury causing muscle damage. (Modified from Tidball and Villalta, 2010; Forbes and Rosenthal, 2014).

CCL2$^{-/-}$ mice have only a mild deficiency in regeneration, which may indicate that alternative chemokine (C–C motif) ligands can bind with the CCR2 receptor and support the recruitment of monocytes and ultimately improve regenerative capacity (Lu et al., 2011a).

2.2. *Regulation of skeletal muscle regeneration via innate immune cell signalling*

In response to muscle injury, the innate immune system is activated, to enhance repair damaged tissue by secreting several cytokines (summarised in Fig. 2) (Madaro and Bouche, 2014). The cytokine interleukin 6 (IL-6) is involved in the initial infiltration of monocytes and macrophages during the inflammatory response shortly after muscle damage. Studies involving IL-6$^{-/-}$ mice revealed a significant decrease in the early infiltration of monocytes and macrophages to the injury site, resulting in diminished myofibre mass and more fibrosis of the muscle (Zhang et al., 2013). In the wild-type mice, much of the IL-6 produced soon after injury comes from the early monocyte and macrophage infiltration (Zhang et al., 2013). IL-6 also stimulates macrophage expression of another important molecule, granulocyte colony-stimulating factor (G-CSF), which is involved in normal myoblast proliferation and myofibre differentiation throughout the muscle regeneration process (Zhang et al., 2013; Wright et al., 2015). IL-6$^{-/-}$ mice show slower rates of hypertrophic muscle growth than wild-type animals (Serrano et al., 2008). This study also found that IL-6$^{-/-}$ animals have considerably lower levels of myogenin expression, but MyoD expression was unaffected, which helps to explain why myofibre differentiation was lower in IL-6$^{-/-}$ animals compared with wild-type.

Supplementary to IL-6 a rapid expression of tumour necrosis factor alpha (TNFα) after injury serves to intensify inflammation in the early stages following muscle damage and is linked to the innate immune response (Warren et al., 2002). TNFα is released by the resident neutrophils, along with interferon gamma (IFNγ) and Interleukin-1 beta (IL-1β), which can promote monocyte differentiation to M1 phenotype macrophages (Arango Duque and Descoteaux, 2014). Interestingly, as neutrophils and TNFα concentrations peak after 2 days post-injury, the quick tapering of neutrophils (3–4 days) is not paralleled by reductions in TNFα levels, which remain elevated for approximately 14 days after injury (Novak et al., 2014). This indicates that TNFα is not only involved with the early inflammatory process, but potentially has functions throughout muscle regeneration. Together, IL-6 and TNFα can enhance the proliferation of myoblasts, function as chemoattractants aimed at myoblasts and immune cells, hinder the fusion of myocytes and affect development of stimulated satellite cells to the early phases of differentiation.

As mentioned earlier macrophages undergo various phases of activation. Specific cytokines such as the ones described (i.e. CCL2, IL- 6, and TNFα) are observed to be critically linked with classically activated M1 macrophage infiltration to the site of muscle damage through the initial inflammatory response. However, the differentiation of M2 phenotype macrophages is more complex than that of M1 (Mantovani et al., 2004). The Sub-phenotype M2a macrophages emerge from the exposure to cytokines secreted by adaptive immune responses, including interleukin 4 (IL-4) and interleukin 13 (IL-13), which stimulate the complex phases of tissue restoration and injury healing. The arrival of M2b macrophage are believed to begin with the provocation of Toll-like receptor immune complexes, leading to the release of anti-inflammatory chemokines such as IL-10 and the inflammatory cytokines TNFα and IFNγ (Tidball et al., 2014). TNFα can activate NF-κB within macrophages, which then induce the production and upregulation of additional proinflam-

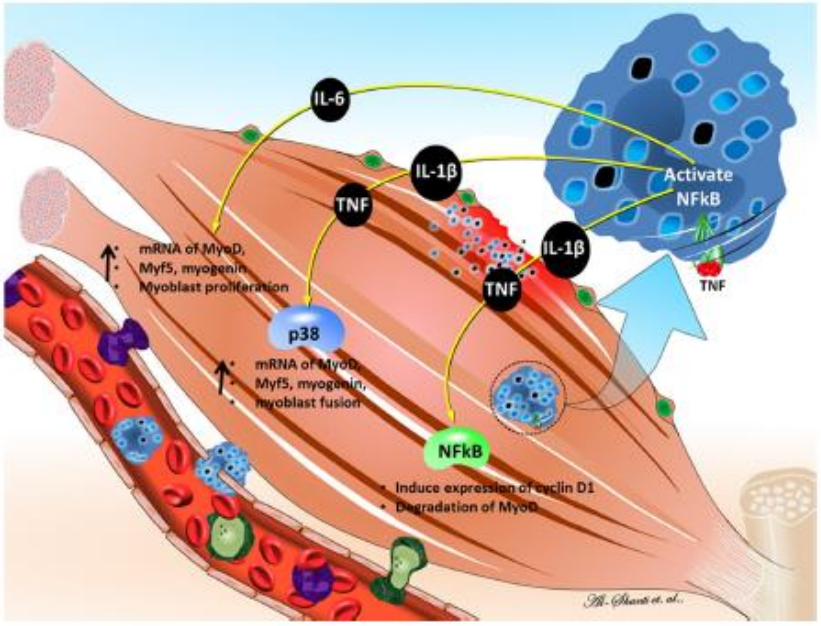

Fig. 2. Innate immune signalling pathways in skeletal muscle regeneration. The activation of NF-κB in either muscle cells or macrophages can affect muscle cell proliferation and differentiation. Cytokines (Il.1β, TNFα and IFNγ) can increase NF-κB activation in both muscle and/or macrophages. The cytokines contribute to further activation of NF-κB in macrophages and muscle cells or they can act on the muscle cells themselves to affect their proliferation or differentiation. TNFα can activate NF-κB within macrophages, which then induces the production of additional proinflammatory mediators. NF-κB activation can promote proliferation of muscle cells through the up regulation of transcripts needed for cell cycle progression (cyclin D1), while suppressing differentiation by decreasing the expression or destabilizing transcripts needed for muscle to experience early and terminal differentiation (MyoD and myogenin). Along with TNFα promoting proliferation and inhibiting differentiation through the NF-κB signalling pathway, it can also promote later stages of differentiation through the activation of p38 kinase. Nuclear factor-kappa B (NF- κB), interferon gamma (IFNγ), Interleukin-1 beta (IL-1β), Tumour necrosis factor (TNFα), (Modified from Tidball and Villalta, 2010; Forbes and Rosenthal, 2014).

matory mediators, including TNFα, which are then subsequently secreted by the macrophages into the microenvironment of the regenerating muscle. Research using TNFα$^{-/-}$ mouse models showed a reduction in myogenic differentiation when compared to wild-type mice, this suggests that TNFα signalling within the immuno-muscular microenvironment performs a regulatory role in muscle regeneration. (Chen et al., 2005). Alternatively, in vitro models using C2C12 murine myoblasts indicated that elevated TNFα hindered the myoblast capability to exit the cell cycle, indicating that TNFα prolonged myoblast proliferation while inhibiting myogenic differentiation.

TNFα can also activate NF-κB within myoblasts, resulting in myoblast proliferation through the up-regulation of cyclin D1 while suppressing differentiation, as well as inhibiting MyoD expression, further suppressing differentiation (Langen et al., 2004). Along with TNFα increasing proliferation and inhibiting differentiation through the NF-κB signalling pathway, NF-κB activation in myoblasts promotes the activation of p38 kinase. Animal studies have demonstrated that suppressing p38 leads to reductions in myotube formation along with lower levels of myogenin (Liu et al., 2012). When NF-κB signalling is activated within myoblasts via stimulation from TNFα secreted within the immuno-muscular microenvironment, an increase of IL-6 is also observed, delivering a supplementary route to enhancing the effects that NF-κB has on proliferation and increasing its suppression of differentiation. In vitro cell culture experiments where mouse myoblasts were treated with IL-6 displayed increases in myoblast proliferation, but not cell fusion (Pelosi et al., 2014). Likewise, in vitro cell culture experiments have shown that TNFα increase the migration capacity of myoblasts, demonstrating its role as a chemoattractant (Torrente et al., 2003). Providing further evidence that TNFα production by neutrophils and M1 phenotype macrophages following muscle damage promotes muscle regeneration via the attraction of satellite cells to the site of damage. Fig. 2 shows the interaction of TNFα and the NF-κB signalling pathway and its influence on skeletal muscle regeneration. The release of IL-10 by M2b macrophages also supports the recruitment of M2c macrophages, which release cytokines that are essential for the cessation of M1 macrophage infiltration and activity (Tidball et al., 2014). The IL-10 released by both M2b and M2c macrophages stimulates the proliferation of myoblasts needed for muscle growth and regeneration (Deng et al., 2012). Sub-phenotypes of M2b macrophages are observed throughout the repair process since their production of IL-10 is needed to promote anti-inflammatory actions during muscle regeneration (Bosurgi et al., 2012). IL-10$^{-/-}$ mice show impaired transition of macrophages from the M1 to M2 phenotypes, resulting in a corresponding impairment to muscle regeneration. It is interesting to note that IL-10$^{-/-}$ mice are also used as an animal model of early-onset frailty with poor muscle mass and function in older age (Walston et al., 2008). Furthermore, mouse myoblast cell cultures supplemented with IL-10 and M2 macrophages resulted in enhanced myoblast proliferation (Deng et al., 2012). Therefore, IL-10 can mediate the transition of M1 to M2 macrophages after muscle damage occurs and encourages the proliferation of myoblasts and maturation of myofibers.

As myoblasts switch from proliferation to differentiation, a shift from M1 macrophages and proinflammatory cytokines to M2 macrophages and anti-inflammatory cytokines occurs

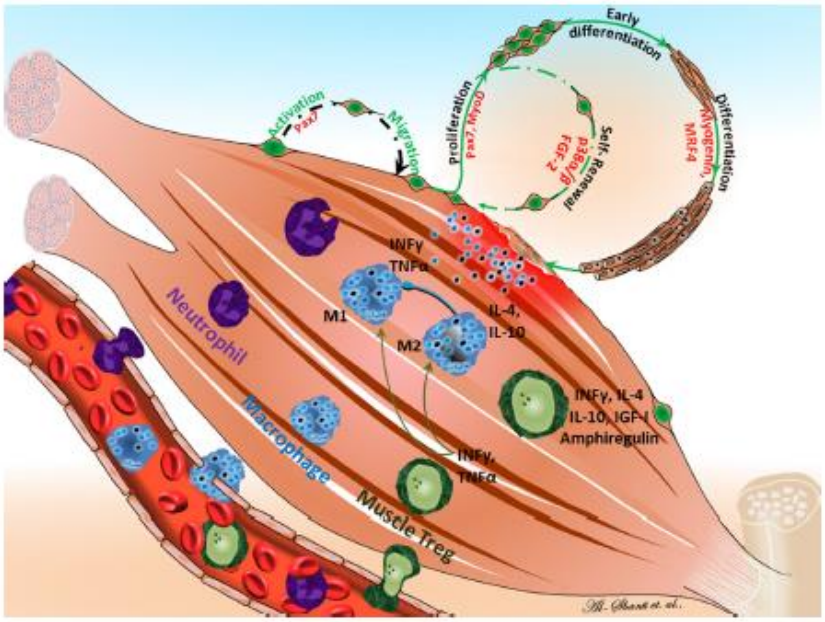

Fig. 3. Summary of general interactions between immune and muscle cells following acute muscle injury. Following muscle damage quiescent satellite cells become activated and begin to migrate to the site of injury. The satellite cells re-enter the cell cycle and begin to proliferate until a proliferative threshold is met. A required quantity of the proliferating satellite cells will self-renew to replenish the pool of quiescent cells while the remaining proliferating cells will continue to differentiate to repair the damaged muscle fibres. Importantly, the phases of satellite cell activation, migration, proliferation and differentiation are regulated by immune cells. The immune system responds to muscle damage with a complex sequence of reactions, which ultimately lead to inflammation followed by muscle regeneration. The initial infiltration of transient neutrophils contain and localize the damage in the muscle and clean up cellular debris. M1 macrophages secrete cytokines that induce satellite cell activation and proliferation. M2 macrophages that then promote muscle repair, differentiation and recruit T-cells to the injured muscle site. T-cells such as mTreg cells secreting numerous growth factors (e.g. IGF-I, amphiregulin) and cytokines, which may contribute to facilitating muscle regeneration. Insulin-like growth factor I (IGF-I), Interferon gamma (IFNγ), Interleukin-1 beta (IL-1β), Tumour necrosis factor (TNFα), fibroblast growth factor (FGF-2), muscle regulatory factors 4 (MRF4), Interleukin-4 (IL-4), Interleukin-10 (IL-10) (Modified from Siegel et al., 2009; Tidball and Villalta, 2010; Forbes and Rosenthal, 2014).

concurrently. This cytokine transference diminishes the proinflammatory response and supports the differentiation of myofibres (Deng et al., 2012), thereby positively influencing the regenerative process (Tidball, 2005; Arnold et al., 2007). This is in part linked to insulin-like growth factor I (IGF-I), a protein known for its growth-promoting properties and anabolic-inducing effects through the up-regulation of myogenic regulatory factors (MRFs) (Chakravarthy et al., 2000; Mourkioti and Rosenthal, 2005; Xu and Wu, 2000). Importantly, IGF-I is also secreted by M2 macrophages during muscle regeneration (Tonkin et al., 2015; Tidball and Welc, 2015). When observing the infiltration of monocytes and macrophages into the muscle injury site of $CCR2^{-/-}$ mice a considerable reduction of infiltrating cells is observed when compared to the controls. Interestingly, a reduction of circulating IGF-1 is also observed in conjunction with the reduced number of infiltrating immune cells. (Lu et al., 2011b). This fascinating discovery indicates that macrophages provide growth factors that aid in the repair of muscle tissue damage by encouraging IGF-I stimulated satellite cell proliferation.

Overall, the regeneration of healthy young muscle occurs by rapid recruitment of immune cells to the damaged site in order to orchestrate the regenerative process by removing necrotic cellular debris, coordinating pro/anti-inflammatory events and activating satellite cells through strictly regulated signalling and chemo-attractant molecules (i.e. cytokines, chemokines). Although damaged muscle fibres secrete a number of cytokines, chemokines and growth factors, it is the resident and infiltrating immune cells that are the main producers of these regenerating mediators. Consequently, any alterations to the numbers or types of cytokines, chemokines, or growth factors as a result of age related immune dysfunction has a considerable potential to disrupt the ability of satellite cells in elderly muscle to become activated, migrate to the site of injury, proliferate in adequate quantities and/or differentiate appropriately, resulting in an age linked decline of muscle size and function. Investigations regarding age associated changes to innate immune cell signalling molecules have discovered substantial difference when compared to young counterparts. Specifically, an increase in proinflammatory cytokines (i.e. IL-6, TNFα, IL-1β) is observed, leading to the chronic inflammatory state often observed in the elderly (Bruunsgaard et al., 2003; Ershler and Keller, 2000; O'Mahony et al., 1998). Increases in proinflammatory cytokines have been identified in the advancement of many geriatric disorders (Franceschi and Campisi, 2014). Thus, it can be appreciated that inflamm-ageing is also having a detrimental effect on the innate immune cells ability to properly coordinate the precisely programed stages of muscle regeneration, due to their inability to appropriately regulate the signalling molecules circulating within the immuno-muscular microenvironment during skeletal muscle regeneration.

3. Adaptive immunity and muscle regeneration

Adaptive immunity is observed as a secondary onset response to a pathophysiological incident, which is primarily mediated through

lymphoid stem cells such as the T-cells and B-cells (Kim et al., 2007). There has been a remarkable increase in the number of descriptive studies detailing the interactions between innate immune responses and muscle regeneration. However, understanding of the role of the adaptive immune system in muscle regeneration is limited. Just as macrophages and cells involved with innate immunity are detected during acute muscle injury, adaptive immune cells such as T-cells are also present during the regeneration process (Cheng et al., 2008).

3.1. Adaptive immune response to muscle damage

T-cell infiltration to the site of injury is apparent approximately 3 days after injury and remains elevated for at least 10 days (Cheng et al., 2008). The satellite cells begin to migrate in damaged muscle in the initial 24 h and begin to proliferate rapidly thereafter. These initial activities are likely regulated via cytokines secreted by innate immune cells (e.g. macrophages). However, adaptive immune responses to damaged muscle via the delayed release of cytokines by T-cells will promote continued satellite cell proliferation. The sustained T-cell presence throughout the regenerative process suggests that T-cells are fundamentally involved with skeletal muscle repair, but the mechanisms of these interactions are not well understood.

Experiments conducted with T-cell deficient mice resulted in a significant reduction in the early growth and development of muscle (Morrison et al., 2005). Cell culture investigations observing the impact of activated murine splenic T-cell cytokine secretions (secretome) on satellite cell function presented a ~24% increase in the proliferation of satellite cells isolated from young (3 months old) mouse muscle, compared to non-secretome treated satellite cell cultures (Dumke and Lees, 2011). Conversely, there was no significant effect on the proliferation of aged (32 months old) mouse muscle satellite cells when exposed to the same T-cell secretome. Furthermore, T-cells signalling (i.e. chemokines) also increased the rate of migration of young satellite cells but not old. However, T-cell secretome significantly reduced the ability of aged satellite cells to differentiate when compared to young satellite cells (Dumke and Lees, 2011). Additionally, recent research employing a mouse model observed that adding the secretome from human T-cells onto a punch-biopsy muscle wound accelerated healing (Mildner et al., 2013).

These findings reveal T-cell regulation of muscle repair, as well as the possibility that ageing may diminish T-cell regulated satellite cell function. Further research has explored the impact of T-cell secretome from activated and non-activated T-cells isolated from young (20–25 years old) human blood on immortalized murine satellite cells. The young activated-T-cell secretome enhanced proliferation of the satellite cells and reduced differentiation (Al-Shanti et al., 2014). Demonstrating that regenerating muscle is influenced by, and responds to, a typical 'young' adaptive immune response. Follow-on work showed that the secretome from young (18–25 years old) activated T-cells enhances both proliferation and migration in immortalized murine satellite cell, however, the secretome from old (78–85 years old) activated T-cells induced premature differentiation similar to control conditions, with no effects on proliferation or migration of the satellite cells (Al-Dabbagh et al., 2015). This outcome implies that proteins secreted by the adaptive immune cells in young people enhance satellite cell proliferation and migration, whereas secreted proteins by the adaptive immune cells of old people attenuates satellite cell proliferation and migration by prematurely stimulating differentiation. These studies indicate that impairments in the ability of satellite cells in elderly people to appropriately proliferate and migrate to the site of muscle injury are related to age-associated T-cell deficiencies, promoting age-related reductions in skeletal muscle size and function.

Various studies have established that T-cells secrete growth factors and cytokines, some of which can influence satellite cell function (e.g. FGF2, IFNγ, TGFβ, TNFα, and IL4) (Blotnick et al., 1994; De Rosa et al., 2004; Levings et al., 2002). The challenge for future studies will be to determine how advanced ageing alters the specific types and concentrations of proteins secreted by old T-cells when compared to young T-cells. This will identify the up- and/or down- regulated immune factors responsible for altering satellite cell function during muscular regeneration in elderly people. Conceivably, these discoveries could lead to the manipulation of immune factors in the immuno-muscular microenvironment of elderly people, possibly replicating a young immuno-muscular microenvironment and overcoming the age associated defects in aged satellite cell function.

3.2. Regulation of skeletal muscle regeneration via regulatory T-cells

Much of the early research beginning to expose the role of adaptive immunity on muscle regeneration has focused on investigating all T-cells as a single component of immunity interacting with satellite cells (Fig. 3). However, there are several different sub-phenotypes of T-cells and distinguishing between them during regeneration may be crucial for identifying which T-cell subphenotypes are up and/or down regulating cytokines and growth factors that influence satellite cell function. Attention has been drawn to a specific population of immune response regulatory T-cells (Treg), denoted as the $CD4^+Foxp3^+$ sub-phenotype. Not only are these Treg cells involved with immune response regulation (Josefowicz et al., 2012), they have also been detected at concentrations of $1.05 \pm 0.38 \times 10^4$ cells/g of muscle 28 days after injury. However, alternate T-cell sub-phenotype populations decrease to pre-injury levels of $0.13 \pm 0.06 \times 10^4$ cells/g of muscle by the same time point of the repair process (Burzyn et al., 2013a). This finding indicates that Treg cells may be a vital immune cell type influencing muscle regeneration.

Using mouse models with muscular injury induced via Ctx, it was shown that the Treg cell concentrations increased within the injured muscle as the innate immune cells shifted from a pro- inflammatory to anti-inflammatory phenotype (i.e. M1 to M2) (Burzyn et al., 2013a). It was also discovered that Treg cells found specifically in muscle (mTreg) produce distinctive proteins from their counterparts found in other tissues. These proteins include the anti-inflammatory cytokine IL-10 and the growth factors amphiregulin and platelet-derived growth factor (PDGF), all of which have been shown to influence typical muscle regeneration (Burzyn et al., 2013a; Huey et al., 2008; Yablonkareuveni et al., 1990). Furthermore, experiments where Treg cells were prevented from entering the Ctx injured mouse muscle resulted in innate immune cells failing to switch from pro-inflammatory M1 phenotype to the anti-inflammatory M2 phenotype. Treg ablation from damaged muscle also caused and abnormal inflamed morphology of the regenerating muscle fibres with fibrosis (Castiglioni et al., 2015). Treg-stimulated satellite cells showed sustained proliferation and delayed differentiation (Castiglioni et al., 2015).

Although evidence has been presented outlining the role Treg cells perform during muscle regeneration, further research is required to fully understand how Treg cells are recruited and expanded within damaged muscle. It is also interesting to consider that Treg cells are able to influence muscle repair via interaction with innate immune cells (i.e. macrophages) as well as activating satellite cells (Burzyn et al., 2013b). These observations may help to serve as a foundation for future studies looking at the impact ageing has on Treg cells and whether ageing causes a reduction or increase

in the number of Treg cells infiltrating the site of muscle damage. These studies may also help to determine if ageing impacts Treg cells' ability to produce the appropriate types and concentrations of cytokines and growth factors needed for normal muscle repair and regeneration.

4. Conclusions

Immune cell infiltration into the site of muscle damage and subsequent release of signalling molecules (i.e. cytokines and growth factors) into the microenvironment regulate muscle repair and regeneration through direct interaction with satellite cells (see Fig. 3). Immune factors released within an aged immuno-muscular microenvironment differ from those of young. Investigating specific populations and sub-phenotypes of both innate and adaptive immune cells, in both young and elderly people, will provide insight into the mechanisms of age-associated muscle wasting. Developing novel therapies to treat sarcopenia by manipulating the aged immuno-muscular microenvironment during regeneration may enhanced muscle size and restore muscle function in the elderly. Current strategies to promote muscle regeneration and maintenance in elderly people are primarily focused on nutrition and physical activity (English and Paddon-Jones, 2010; Moore, 2014). These approaches may alleviate the progression and trajectory of sarcopenia, but only to a relatively minor degree. These therapies are only able to delay the inevitable loss of skeletal muscle mass, function and regenerative capacity associated with progressive ageing. A number of pharmacological strategies to tackle muscle wasting have been proposed, although no treatments are currently in clinical use that block or reverse the loss of muscle in the elderly (Glass and Roubenoff, 2010). Therefore, developing a novel approach to prevent sarcopenia is essential and elucidating the role of the immune system in muscle regeneration will help to identify regulatory processes that are candidates for intervention.

References

Abbadie, C., Lindia, J.A., Cumiskey, A.M., Peterson, L.B., Mudgett, J.S., Bayne, E.K., DeMartino, J.A., MacIntyre, D.E., Forrest, M.J., 2003. Impaired neuropathic pain responses in mice lacking the chemokine receptor CCR2. Proc. Natl. Acad. Sci. U. S. A. 100 (June (13)), 7947–7952.

Adams, G.R., 2006. Satellite cell proliferation and skeletal muscle hypertrophy. Appl. Physiol. Nutr. Metab. 31 (December (6)), 782–790.

Al-Dabbagh, S., McPhee, J.S., Murgatroyd, C., Butler-Browne, G., Stewart, C.E., Al-Shanti, N., 2015. The lymphocyte secretome from young adults enhances skeletal muscle proliferation and migration, but effects are attenuated in the secretome of older adults. Physiol. Rep. 3 (November (11)).

Al-Shanti, N., Durcan, P., Al-Dabbagh, S., Dimchev, G.A., Stewart, C.E., 2014. Activated lymphocytes secretome inhibits differentiation and induces proliferation of C2C12 myoblasts. Cell. Physiol. Biochem. 33 (1), 117–128.

Arango Duque, G., Descoteaux, A., 2014. Macrophage cytokines: involvement in immunity and infectious diseases. Front. Immunol. 5, 491.

Arnold, L., Henry, A., Poron, F., Baba-Amer, Y., van Rooijen, N., Plonquet, A., Gherardi, R.K., Chazaud, B., 2007. Inflammatory monocytes recruited after skeletal muscle injury switch into antiinflammatory macrophages to support myogenesis. J. Exp. Med. 204 (May (5)), 1057–1069.

Barberi, L., Scicchitano, B.M., De Rossi, M., Bigot, A., Duguez, S., Wielgosik, A., Stewart, C., McPhee, J., Conte, M., Narici, M., Franceschi, C., Mouly, V., Butler-Browne, G., Musarò, A., 2013. Age-dependent alteration in muscle regeneration: the critical role of tissue niche. Biogerontology 14 (June (3)), 273–292.

Bentzinger, C.F., Wang, Y.X., Rudnicki, M.A., 2012. Building muscle: molecular regulation of myogenesis. Cold Spring Harb. Perspect. Biol. 4 (February (2)).

Blotnick, S., Peoples, G.E., Freeman, M.R., Eberlein, T.J., Klagsbrun, M., 1994. T lymphocytes synthesize and export heparin-binding epidermal growth factor-like growth factor and basic fibroblast growth factor mitogens for vascular cells and fibroblasts: differential production and release by CD4+ and CD8+ T cells. Proc. Natl. Acad. Sci. U. S. A. 91 (April (8)), 2890–2894.

Bosurgi, L., Corna, G., Vezzoli, M., Touvier, T., Cossu, G., Manfredi, A.A., Brunelli, S., Rovere-Querini, P., 2012. Transplanted mesoangioblasts require macrophage IL-10 for survival in a mouse model of muscle injury. J. Immunol. 188 (June (12)), 6267–6277.

Brack, A.S., Rando, T.A., 2007. Intrinsic changes and extrinsic influences of myogenic stem cell function during aging. Stem Cell Rev. 3 (Fall (3)), 226–237.

Brack, A.S., Munoz-Canoves, P., 2015. The ins and outs of muscle stem cell aging. Skelet. Muscle 6, 1.

Brun, Caroline E., Rudnicki, Michael A., 2015. GDF11 and the mythical fountain of youth. Cell Metab. 22 (1), 54–56.

Bruunsgaard, H., Andersen-Ranberg, K., Hjelmborg, J., Pedersen, B.K., Jeune, B., 2003. Elevated levels of tumor necrosis factor alpha and mortality in centenarians. Am. J. Med. 115 (September (4)), 278–283.

Burzyn, D., Benoist, C., Mathis, D., 2013a. Regulatory T cells in nonlymphoid tissues. Nat. Immunol. 14 (October (10)), 1007–1013.

Burzyn, D., Kuswanto, W., Kolodin, D., Shadrach Jennifer, L., Cerletti, M., Jang, Y., Sefik, E., Tan Tze, G., Wagers Amy, J., Benoist, C., Mathis, D., 2013b. A special population of regulatory T cells potentiates muscle repair. Cell 155 (6), 1282–1295 (12/5/).

Carlson, B.M., Faulkner, J.A., 1989. Muscle transplantation between young and old rats: age of host determines recovery. Am. J. Physiol. 256 (June (6 Pt. 1)), C1262–C1266.

Carlson, M.E., Hsu, M., Conboy, I.M., 2008. Imbalance between pSmad3 and Notch induces CDK inhibitors in old muscle stem cells. Nature 454 (7203), 528–532, 07/24/print.

Carlson, M.E., Suetta, C., Conboy, M.J., Aagaard, P., Mackey, A., Kjaer, M., Conboy, I., 2009. Molecular aging and rejuvenation of human muscle stem cells. EMBO Mol. Med. 1 (November (8–9)), 381–391.

Cassatella, M.A., 1999. Neutrophil-derived proteins: selling cytokines by the pound. Adv. Immunol. 73, 369–509.

Castiglioni, A., Corna, G., Rigamonti, E., Basso, V., Vezzoli, M., Monno, A., Almada, A.E., Mondino, A., Wagers, A.J., Manfredi, A.A., Rovere-Querini, P., 2015. FOXP3+ T cells recruited to sites of sterile skeletal muscle injury regulate the fate of satellite cells and guide effective tissue regeneration. PLoS One 10 (6), e0128094.

Cerletti, M., Shadrach, J.L., Jurga, S., Sherwood, R., Wagers, A.J., 2008. Regulation and function of skeletal muscle stem cells. Cold Spring Harb. Symp. Quant. Biol. 73, 317–322.

Chakkalakal, J.V., Jones, K.M., Basson, M.A., Brack, A.S., 2012. The aged niche disrupts muscle stem cell quiescence. Nature 490 (October (7420)), 355–360.

Chakravarthy, M.V., Abraha, T.W., Schwartz, R.J., Fiorotto, M.L., Booth, F.W., 2000. Insulin-like growth factor-i extends in vitro replicative life span of skeletal muscle satellite cells by enhancing G1/S cell cycle progression via the activation of phosphatidylinositol 3'-kinase/Akt signaling pathway. J. Biol. Chem. 275 (November (46)), 35942–35952.

Chen, S.E., Gerken, E., Zhang, Y., Zhan, M., Mohan, R.K., Li, A.S., Reid, M.B., Li, Y.P., 2005. Role of TNF-{alpha} signaling in regeneration of cardiotoxin-injured muscle. Am. J. Physiol. Cell Physiol. 289 (November (5)), C1179–1187.

Cheng, M., Nguyen, M.H., Fantuzzi, G., Koh, T.J., 2008. Endogenous interferon-gamma is required for efficient skeletal muscle regeneration. Am. J. Physiol. Cell Physiol. 294 (May (5)), C1183–1191.

Conboy, I.M., Conboy, M.J., Wagers, A.J., Girma, E.R., Weissman, I.L., Rando, T.A., 2005. Rejuvenation of aged progenitor cells by exposure to a young systemic environment. Nature 433 (7027), 760–764 (02/17/print).

Cosgrove, B.D., Gilbert, P.M., Porpiglia, E., Mourkioti, F., Lee, S.P., Corbel, S.Y., Llewellyn, M.E., Delp, S.L., Blau, H.M., 2014. Rejuvenation of the muscle stem cell population restores strength to injured aged muscles. Nat. Med. 20 (3), 255–264, 03//print.

Crameri, R.M., Aagaard, P., Qvortrup, K., Langberg, H., Olesen, J., Kjaer, M., 2007. Myofibre damage in human skeletal muscle: effects of electrical stimulation versus voluntary contraction. J. Physiol. 583 (August (Pt. 1)), 365–380.

Cruz-Jentoft, A.J., Baeyens, J.P., Bauer, J.M., Boirie, Y., Cederholm, T., Landi, F., Martin, F.C., Michel, J.P., Rolland, Y., Schneider, S.M., Topinkova, E., Vandewoude, M., Zamboni, M., 2010. Sarcopenia: european consensus on definition and diagnosis: report of the european working group on sarcopenia in older people. Age Ageing 39 (July (4)), 412–423.

De Rosa, S.C., Lu, F.X., Yu, J., Perfetto, S.P., Falloon, J., Moser, S., Evans, T.G., Koup, R., Miller, C.J., Roederer, M., 2004. Vaccination in humans generates broad T cell cytokine responses. J. Immunol. 173 (November (9)), 5372–5380.

Degens, H., 2010. The role of systemic inflammation in age-related muscle weakness and wasting. Scand. J. Med. Sci. Sports 20 (February (1)), 28–38.

Deng, B., Wehling-Henricks, M., Villalta, S.A., Wang, Y., Tidball, J.G., 2012. IL-10 triggers changes in macrophage phenotype that promote muscle growth and regeneration. J. Immunol. 189 (October (7)), 3669–3680.

Dumke, B.R., Lees, S.J., 2011. Age-related impairment of T cell-induced skeletal muscle precursor cell function. Am. J. Physiol. Cell Physiol. 300 (June (6)), C1226–1233.

Dumont, N., Bouchard, P., Frenette, J., 2008. Neutrophil-induced skeletal muscle damage: a calculated and controlled response following hindlimb unloading and reloading. Am. J. Physiol. Regul. Integr. Comp. Physiol. 295 (December (6)), R1831–R1838.

Egan, B., Zierath, J.R., 2013. Exercise metabolism and the molecular regulation of skeletal muscle adaptation. Cell Metab. 17 (February (2)), 162–184.

Elabd, C., Cousin, W., Upadhyayula, P., Chen, R.Y., Chooljian, M.S., Li, J., Kung, S., Jiang, K.P., Conboy, I.M., 2014. Oxytocin is an age-specific circulating hormone that is necessary for muscle maintenance and regeneration. Nat. Commun. 5, 06/10/online.

English, K.L., Paddon-Jones, D., 2010. Protecting muscle mass and function in older adults during bed rest. Curr. Opin. Clin. Nutr. Metab. Care 13 (January (1)), 34–39.

Ershler, W.B., Keller, E.T., 2000. Age-associated increased interleukin-6 gene expression, late-life diseases and frailty. Annu. Rev. Med. 51, 245–270.

Farup, J., Madaro, L., Puri, P.L., Mikkelsen, U.R., 2015. Interactions between muscle stem cells, mesenchymal-derived cells and immune cells in muscle homeostasis, regeneration and disease. Cell Death Dis. 6, e1830.
Forbes, S.J., Rosenthal, N., 2014. Preparing the ground for tissue regeneration: from mechanism to therapy. Nat. Med. 20 (August (8)), 857–869.
Franceschi, C., Campisi, J., 2014. Chronic inflammation (inflammaging) and its potential contribution to age-associated diseases. J. Gerontol. A Biol. Sci. Med. Sci. 69 (June (Suppl. 1)), S4–S9.
Franceschi, C., Bonafe, M., Valensin, S., Olivieri, F., De Luca, M., Ottaviani, E., De Benedictis, G., 2000. Inflamm-aging. An evolutionary perspective on immunosenescence. Ann. N. Y. Acad. Sci. 908 (June), 244–254.
Fried, L.P., Tangen, C.M., Walston, J., Newman, A.B., Hirsch, C., Gottdiener, J., Seeman, T., Tracy, R., Kop, W.J., Burke, G., McBurnie, M.A., 2001. Frailty in older adults: evidence for a phenotype. J. Gerontol. A Biol. Sci. Med. Sci. 56 (March (3)), M146–M156.
Fry, C.S., Lee, J.D., Mula, J., Kirby, T.J., Jackson, J.R., Liu, F., Yang, L., Mendias, C.L., Dupont-Versteegden, E.E., McCarthy, J.J., Peterson, C.A., 2015. Inducible depletion of satellite cells in adult, sedentary mice impairs muscle regenerative capacity without affecting sarcopenia. Nat. Med. 21 (1), 76–80, 01//print.
Fujishima, S., Hoffman, A.R., Vu, T., Kim, K.J., Zheng, H., Daniel, D., Kim, Y., Wallace, E.F., Larrick, J.W., Raffin, T.A., 1993. Regulation of neutrophil interleukin 8 gene expression and protein secretion by LPS, TNF-alpha, and IL-1 beta. J. Cell. Physiol. 154 (March (3)), 478–485.
Geissmann, F., Jung, S., Littman, D.R., 2003. Blood monocytes consist of two principal subsets with distinct migratory properties. Immunity 19 (July (1)), 71–82.
Glass, D., Roubenoff, R., 2010. Recent advances in the biology and therapy of muscle wasting. Ann. N. Y. Acad. Sci. 1211 (November), 25–36.
Glass, D.J., 2003. Molecular mechanisms modulating muscle mass. Trends Mol. Med. 9 (August (8)), 344–350.
Huey, K.A., Meador, B.M., Krzyszton, C.P., Johnson, R.W., 2008. Effects of IL-10 and age on IL-6 IL-1 beta, and TNF alpha responses to an acute inflammatory insult in mouse skeletal muscle. Faseb J. 22 (April), p1.
Janssen, I., 2011. The epidemiology of sarcopenia. Clin. Geriatr. Med. 27 (August (3)), 355.
Janssen, I., Heymsfield, S.B., Ross, R., 2002. Low relative skeletal muscle mass (sarcopenia) in older persons is associated with functional impairment and physical disability. J. Am. Geriatr. Soc. 50 (May (5)), 889–896.
Jetten, N., Verbruggen, S., Gijbels, M.J., Post, M.J., De Winther, M.P.J., Donners, M., 2014. Anti-inflammatory M2, but not pro-inflammatory M1 macrophages promote angiogenesis in vivo. Angiogenesis 17 (January (1)), 109–118.
Joanisse, S., Gillen, J.B., Bellamy, L.M., McKay, B.R., Tarnopolsky, M.A., Gibala, M.J., Parise, G., 2013. Evidence for the contribution of muscle stem cells to nonhypertrophic skeletal muscle remodeling in humans. FASEB J. 27 (November (11)), 4596–4605.
Josefowicz, S.Z., Lu, L.F., Rudensky, A.Y., 2012. Regulatory T cells: mechanisms of differentiation and function. Annu. Rev. Immunol. 30, 531–564.
Kim, K.D., Zhao, J., Auh, S., Yang, X.M., Du, P.S., Tang, H., Fu, Y.X., 2007. Adaptive immune cells temper initial innate responses. Nat. Med. 13 (October (10)), 1248–1252.
Kuang, S., Kuroda, K., Le Grand, F., Rudnicki, M.A., 2007. Asymmetric self-renewal and commitment of satellite stem cells in muscle. Cell 129 (June (5)), 999–1010.
Langen, R.C., Van Der Velden, J.L., Schols, A.M., Kelders, M.C., Wouters, E.F., Janssen-Heininger, Y.M., 2004. Tumor necrosis factor-alpha inhibits myogenic differentiation through MyoD protein destabilization. FASEB J. 18 (February (2)), 227–237.
Lepper, C., Partridge, T.A., Fan, C.M., 2011. An absolute requirement for Pax7-positive satellite cells in acute injury-induced skeletal muscle regeneration. Development 138 (September (17)), 3639–3646.
Leto, D., Saltiel, A.R., 2012. Regulation of glucose transport by insulin: traffic control of GLUT4. Nat. Rev. Mol. Cell Biol. 13 (June (6)), 383–396.
Levings, M.K., Bacchetta, R., Schulz, U., Roncarolo, M.G., 2002. The role of IL-10 and TGF-beta in the differentiation and effector function of T regulatory cells. Int. Arch. Allergy Immunol. 129 (December (4)), 263–276.
Lexell, J., 1995. Human aging, muscle mass and fiber-type composition. J. Gerontol. A Biol. Sci. Med. Sci. 50 (November), 11–16.
Lexell, J., Taylor, C.C., Sjostrom, M., 1988. What is the cause of the aging atrophy—total number, size and proportion of different fiber types studied in whole vastus lateralis muscle from 15-year-old to 83-year-old men. J. Neurol. Sci. 84 (April (2–3)), 275–294.
Liu, Q.C., Zha, X.H., Faralli, H., Yin, H., Louis-Jeune, C., Perdiguero, E., Pranckeviciene, E., Munoz-Canoves, P., Rudnicki, M.A., Brand, M., Perez-Iratxeta, C., Dilworth, F.J., 2012. Comparative expression profiling identifies differential roles for Myogenin and p38 alpha MAPK signaling in myogenesis. J. Mol. Cell Biol. 4 (December (6)), 386–397.
Lu, H., Huang, D., Ransohoff, R.M., Zhou, L., 2011a. Acute skeletal muscle injury: CCL2 expression by both monocytes and injured muscle is required for repair. FASEB J. 25 (October (10)), 3344–3355.
Lu, H., Huang, D., Saederup, N., Charo, I.F., Ransohoff, R.M., Zhou, L., 2011b. Macrophages recruited via CCR2 produce insulin-like growth factor-1 to repair acute skeletal muscle injury. FASEB J. 25 (January (1)), 358–369.
Mackey, A.L., Bojsen-Moller, J., Qvortrup, K., Langberg, H., Suetta, C., Kalliokoski, K.K., Kjaer, M., Magnusson, S.P., 2008. Evidence of skeletal muscle damage following electrically stimulated isometric muscle contractions in humans. J. Appl. Physiol. (1985) 105 (November (5)), 1620–1627.
Madaro, L., Bouche, M., 2014. From innate to adaptive immune response in muscular dystrophies and skeletal muscle regeneration: the role of lymphocytes. Biomed. Res. Int. 2014, 438675.
Maden-Wilkinson, T.M., McPhee, J.S., Rittweger, J., Jones, D.A., Degens, H., 2014. Thigh muscle volume in relation to age, sex and femur volume age, sex and femur volume. Age (Dordr) 36 (February (1)), 383–393.
Mantovani, A., Sica, A., Sozzani, S., Allavena, P., Vecchi, A., Locati, M., 2004. The chemokine system in diverse forms of macrophage activation and polarization. Trends Immunol. 25 (December (12)), 677–686.
Martinez, C.O., McHale, M.J., Wells, J.T., Ochoa, O., Michalek, J.E., McManus, L.M., Shireman, P.K., 2010. Regulation of skeletal muscle regeneration by CCR2-activating chemokines is directly related to macrophage recruitment. Am. J. Physiol. Regul. Integr. Comp. Physiol. 299 (September (3)), R832–842.
McCarthy, J.J., Mula, J., Miyazaki, M., Erfani, R., Garrison, K., Farooqui, A.B., Srikuea, R., Lawson, B.A., Grimes, B., Keller, C., Van Zant, G., Campbell, K.S., Esser, K.A., Dupont-Versteegden, E.E., Peterson, C.A., 2011. Effective fiber hypertrophy in satellite cell-depleted skeletal muscle. Development 138 (September (17)), 3657–3666.
Merly, F., Lescaudron, L., Rouaud, T., Crossin, F., Gardahaut, M.F., 1999. Macrophages enhance muscle satellite cell proliferation and delay their differentiation. Muscle Nerve 22 (June (6)), 724–732.
Mildner, M., Hacker, S., Haider, T., Gschwandtner, M., Werba, G., Barresi, C., Zimmermann, M., Golabi, B., Tschachler, E., Ankersmit, H.J., 2013. Secretome of peripheral blood mononuclear cells enhances wound healing. PLoS One 8 (3), e60103.
Moore, D.R., 2014. Keeping older muscle young through dietary protein and physical activity12. Adv. Nutr. 5 (September (5)), 599s–607s.
Morley, J.E., Baumgartner, R.N., Roubenoff, R., Mayer, J., Nair, K.S., 2001. Sarcopenia. J. Lab. Clin. Med. 137 (April (4)), 231–243.
Morrison, J., Partridge, T., Bou-Gharios, G., 2005. Nude mutation influences limb skeletal muscle development. Matrix Biol. 23 (January (8)), 535–542.
Mourkioti, F., Rosenthal, N., 2005. IGF-1, inflammation and stem cells: interactions during muscle regeneration. Trends Immunol. 26 (October (10)), 535–542.
Naito, A.T., Sumida, T., Nomura, S., Liu, M.L., Higo, T., Nakagawa, A., Okada, K., Sakai, T., Hashimoto, A., Hara, Y., Shimizu, I., Zhu, W., Toko, H., Katada, A., Akazawa, H., Oka, T., Lee, J.K., Minamino, T., Nagai, T., Walsh, K., Kikuchi, A., Matsumoto, M., Botto, M., Shiojima, I., Komuro, I., 2012. Complement C1q activates canonical Wnt signaling and promotes aging-related phenotypes. Cell 149 (June (6)), 1298–1313.
Narici, M.V., Maffulli, N., 2010. Sarcopenia: characteristics mechanisms and functional significance. Br. Med. Bull. 95, 139–159.
Nosaka, K., Aldayel, A., Jubeau, M., Chen, T.C., 2011. Muscle damage induced by electrical stimulation. Eur. J. Appl. Physiol. 111 (October (10)), 2427–2437.
Novak, M.L., Weinheimer-Haus, E.M., Koh, T.J., 2014. Macrophage activation and skeletal muscle healing following traumatic injury. J. Pathol. 232 (February (3)), 344–355.
O'Mahony, L., Holland, J., Jackson, J., Feighery, C., Hennessy, T.P., Mealy, K., 1998. Quantitative intracellular cytokine measurement: age-related changes in proinflammatory cytokine production. Clin. Exp. Immunol. 113 (August (2)), 213–219.
Paliwal, P., Pishesha, N., Wijaya, D., Conboy, I.M., 2012. Age dependent increase in the levels of osteopontin inhibits skeletal muscle regeneration. Aging (Albany NY) 4 (August (8)), 553–566.
Paulsen, G., Mikkelsen, U.R., Raastad, T., Peake, J.M., 2012. Leucocytes, cytokines and satellite cells: what role do they play in muscle damage and regeneration following eccentric exercise. Exerc. Immunol. Rev. 18, 42–97.
Paulsen, G., Crameri, R., Benestad, H.B., Fjeld, J.G., Morkrid, L., Hallen, J., Raastad, T., 2010. Time course of leukocyte accumulation in human muscle after eccentric exercise. Med. Sci. Sports Exerc. 42 (January (1)), 75–85.
Peake, J., Della Gatta, P., Cameron-Smith, D., 2010. Aging and its effects on inflammation in skeletal muscle at rest and following exercise-induced muscle injury. Am. J. Physiol. Regul. Integr. Comp. Physiol. 298 (June (6)), R1485–R1495.
Pedersen, B.K., 2011. Muscles and their myokines. J. Exp. Biol. 214 (January (Pt. 2)), 337–346.
Pelosi, M., De Rossi, M., Barberi, L., Musarò, A., 2014. IL-6 impairs myogenic differentiation by downmodulation of p90RSK/eEF2 and mTOR/p70S6K axes without affecting AKT activity. BioMed. Res. Int., 12.
Piasecki, M., Ireland, A., Stashuk, D., Hamilton-Wright, A., Jones, D.A., McPhee, J.S., 2015. Age-related neuromuscular changes affecting human vastus lateralis. J. Physiol., 1–12, http://dx.doi.org/10.1113/JP271087.
Plackett, T.P., Boehmer, E.D., Faunce, D.E., Kovacs, E.J., 2004. Aging and innate immune cells. J. Leukoc. Biol. 76 (August (2)), 291–299.
Relaix, F., Zammit, P.S., 2012. Satellite cells are essential for skeletal muscle regeneration: the cell on the edge returns centre stage. Development 139 (August (16)), 2845–2856.
Rodriguez-Prados, J.C., Traves, P.G., Cuenca, J., Rico, D., Aragones, J., Martin-Sanz, P., Cascante, M., Bosca, L., 2010. Substrate fate in activated macrophages: a comparison between innate, classic, and alternative activation trate fate in activated macrophages. J. Immunol. 185 (July (1)), 605–614.
Saclier, M., Cuvellier, S., Magnan, M., Mounier, R., Chazaud, B., 2013. Monocyte/macrophage interactions with myogenic precursor cells during skeletal muscle regeneration. FEBS J. 280 (September (17)), 4118–4130.
Serrano, A.L., Baeza-Raja, B., Perdiguero, E., Jardi, M., Munoz-Canoves, P., 2008. Interleukin-6 is an essential regulator of satellite cell-mediated skeletal muscle hypertrophy. Cell Metab. 7 (January (1)), 33–44.

Shavlakadze, T., McGeachie, J., Grounds, M.D., 2010. Delayed but excellent myogenic stem cell response of regenerating geriatric skeletal muscles in mice. Biogerontology 11 (June (3)), 363–376.
Siegel, A.L., Kuhlmann, P.K., Cornelison, D.D., 2011. Muscle satellite cell proliferation and association: new insights from myofiber time-lapse imaging le satellite cell proliferation and association: new insights from myofiber time-lapse imaging. Skelet. Muscle 1 (1), 7.
Siegel, A.L., Atchison, K., Fisher, K.E., Davis, G.E., Cornelison, D.D., 2009. 3D timelapse analysis of muscle satellite cell motility. Stem Cells 27 (October (10)), 2527–2538.
Sinha, M., Jang, Y.C., Oh, J., Khong, D., Wu, E.Y., Manohar, R., Miller, C., Regalado, S.G., Loffredo, F.S., Pancoast, J.R., Hirshman, M.F., Lebowitz, J., Shadrach, J.L., Cerletti, M., Kim, M.J., Serwold, T., Goodyear, L.J., Rosner, B., Lee, R.T., Wagers, A.J., 2014. Restoring systemic GDF11 levels reverses age-related dysfunction in mouse skeletal muscle. Science 344 (May (6184)), 649–652.
Smith, C., Kruger, M.J., Smith, R.M., Myburgh, K.H., 2008. The inflammatory response to skeletal muscle injury. Sports Med. 38 (11), 947–969.
Smythe, G.M., Shavlakadze, T., Roberts, P., Davies, M.J., McGeachie, J.K., Grounds, M.D., 2008. Age influences the early events of skeletal muscle regeneration: studies of whole muscle grafts transplanted between young (8 weeks) and old (13–21 months) mice. Exp. Gerontol. 43 (June (6)), 550–562.
Sousa-Victor, P., Gutarra, S., Garcia-Prat, L., Rodriguez-Ubreva, J., Ortet, L., Ruiz-Bonilla, V., Jardi, M., Ballestar, E., Gonzalez, S., Serrano, A.L., Perdiguero, E., Munoz-Canoves, P., 2014. Geriatric muscle stem cells switch reversible quiescence into senescence. Nature 506 (February (7488)), 316–321.
Steensberg, A., Keller, C., Starkie, R.L., Osada, T., Febbraio, M.A., Pedersen, B.K., 2002. IL-6 and TNF-alpha expression in, and release from, contracting human skeletal muscle. Am. J. Physiol. Endocrinol. Metab. 283 (December (6)), E1272–E1278.
Sun, D., Martinez, C.O., Ochoa, O., Ruiz-Willhite, L., Bonilla, J.R., Centonze, V.E., Waite, L.L., Michalek, J.E., McManus, L.M., Shireman, P.K., 2009. Bone marrow-derived cell regulation of skeletal muscle regeneration. FASEB J. 23 (February (2)), 382–395.
Tedesco, F.S., Dellavalle, A., Diaz-Manera, J., Messina, G., Cossu, G., 2010. Repairing skeletal muscle: regenerative potential of skeletal muscle stem cells. J. Clin. Invest. 120 (January (1)), 11–19.
Tidball, J.G., 2005. Inflammatory processes in muscle injury and repair. Am. J. Physiol. Regul. Integr. Comp. Physiol. 288 (February (2)), R345–R353.
Tidball, J.G., Welc, S.S., 2015. Macrophage-derived IGF-1 is a potent coordinator of myogenesis and inflammation in regenerating muscle. Mol. Ther. 23 (7), 1134–1135, 07//print.
Tidball, J.G., Dorshkind, K., Wehling-Henricks, M., 2014. Shared signaling systems in myeloid cell-mediated muscle regeneration. Development 141 (March (6)), 1184–1196.
Tonkin, J., Temmerman, L., Sampson, R.D., Gallego-Colon, E., Barberi, L., Bilbao, D., Schneider, M.D., Musaro, A., Rosenthal, N., 2015. Monocyte/macrophage-derived IGF-1 orchestrates murine skeletal muscle regeneration and modulates autocrine polarization. Mol. Ther. 23 (July (7)), 1189–1200.
Torrente, Y., El Fahime, E., Caron, N.J., Del Bo, R., Belicchi, M., Pisati, F., Tremblay, J.P., Bresolin, N., 2003. Tumor necrosis factor-alpha (TNF-alpha) stimulates chemotactic response in mouse myogenic cells. Cell Transplant. 12 (1), 91–100.
Uezumi, A., Ikemoto-Uezumi, M., Tsuchida, K., 2014. Roles of nonmyogenic mesenchymal progenitors in pathogenesis and regeneration of skeletal muscles of nonmyogenic mesenchymal progenitors in pathogenesis and regeneration of skeletal muscle. Front. Physiol. 5.
Verdijk, L.B., Gleeson, B.G., Jonkers, R.A., Meijer, K., Savelberg, H.H., Dendale, P., van Loon, L.J., 2009. Skeletal muscle hypertrophy following resistance training is accompanied by a fiber type-specific increase in satellite cell content in elderly men. J. Gerontol. A Biol. Sci. Med. Sci. 64 (March (3)), 332–339.
Villalta, S.A., Nguyen, H.X., Deng, B., Gotoh, T., Tidball, J.G., 2009. Shifts in macrophage phenotypes and macrophage competition for arginine metabolism affect the severity of muscle pathology in muscular dystrophy. Hum. Mol. Genet. 18 (February (3)), 482–496.
Walston, J., Fedarko, N., Yang, H., Leng, S., Beamer, B., Espinoza, S., Lipton, A., Zheng, H., Becker, K., 2008. The physical and biological characterization of a frail mouse model. J. Gerontol. A Biol. Sci. Med. Sci. 63 (April (4)), 391–398.
Wang, H., Melton, D.W., Porter, L., Sarwar, Z.U., McManus, L.M., Shireman, P.K., 2014. Altered macrophage phenotype transition impairs skeletal muscle regeneration. Am. J. Pathol. 184 (4), 1167–1184.
Warren, G.L., Hulderman, T., Jensen, N., McKinstry, M., Mishra, M., Luster, M.I., Simeonova, P.P., 2002. Physiological role of tumor necrosis factor alpha in traumatic muscle injury. FASEB J. 16 (October (12)), 1630–1632.
Warren, G.L., O'Farrell, L., Summan, M., Hulderman, T., Mishra, D., Luster, M.I., Kuziel, W.A., Simeonova, P.P., 2004. Role of CC chemokines in skeletal muscle functional restoration after injury. Am. J. Physiol. Cell Physiol. 286 (May (5)), C1031–1036.
Wehling, M., Spencer, M.J., Tidball, J.G., 2001. A nitric oxide synthase transgene ameliorates muscular dystrophy in mdx mice. J. Cell Biol. 155 (October (1)), 123–131.
Wright, C.R., Brown, E.L., Della Gatta, P.A., Fatouros, I.G., Karagounis, L.G., Terzis, G., Mastorakos, G., Michailidis, Y., Mandalidis, D., Spengos, K., Chatzinikolaou, A., Methenitis, S., Draganidis, D., Jamurtas, A.Z., Russell, A.P., 2015. Regulation of granulocyte colony-stimulating factor and its receptor in skeletal muscle is dependent upon the type of inflammatory stimulus. J. Interferon Cytokine Res. 35 (September (9)), 710–719.
Xu, Q., Wu, Z., 2000. The insulin-like growth factor-phosphatidylinositol 3-kinase-akt signaling pathway regulates myogenin expression in normal myogenic cells but not in rhabdomyosarcoma-derived RD cells. J. Biol. Chem. 275 (November (47)), 36750–36757.
Yablonkareuveni, Z., Balestreri, T.M., Bowenpope, D.F., 1990. Regulation of proliferation and differentiation of myoblasts derived from adult-mouse skeletal-muscle by specific isoforms of PDGF. J. Cell Biol. 111 (October (4)), 1623–1629.
Yin, H., Price, F., Rudnicki, M.A., 2013. Satellite cells and the muscle stem cell niche. Physiol. Rev. 93 (January (1)), 23–67.
Yousef, H., Conboy, M.J., Morgenthaler, A., Schlesinger, C., Bugaj, L., Paliwal, P., Greer, C., Conboy, I.M., Schaffer, D., 2015. Systemic attenuation of the TGF-β pathway by a single drug simultaneously rejuvenates hippocampal neurogenesis and myogenesis in the same old mammal. Oncotarget 6 (May (14)), 11959–11978.
Zhang, C., Li, Y., Wu, Y., Wang, L., Wang, X., Du, J., 2013. Interleukin-6/signal transducer and activator of transcription 3 (STAT3) pathway is essential for macrophage infiltration and myoblast proliferation during muscle regeneration. J. Biol. Chem. 288 (January (3)), 1489–1499.

Stem Cells and Cloning: Advances and Applications

Dovepress
open access to scientific and medical research

Open Access Full Text Article

ORIGINAL RESEARCH

A functional human motor unit platform engineered from human embryonic stem cells and immortalized skeletal myoblasts

This article was published in the following Dove Press journal:
Stem Cells and Cloning: Advances and Applications

Marwah Abd Al Samid[1]
Jamie S McPhee[2]
Jasdeep Saini[1]
Tristan R McKay[1]
Lorna M Fitzpatrick[1]
Kamel Mamchaoui[3]
Anne Bigot[3]
Vincent Mouly[3]
Gillian Butler-Browne[3]
Nasser Al-Shanti[1]

[1]Healthcare Science Research Institute, School of Healthcare Science, Manchester Metropolitan University, Manchester, UK; [2]Department of Sport and Exercise Science, Manchester Metropolitan University, Manchester, UK; [3]Center for Research in Myology, Sorbonne Université-INSERM, Paris, France

Background: Although considerable research on neuromuscular junctions (NMJs) has been conducted, the prospect of in vivo NMJ studies is limited and these studies are challenging to implement. Therefore, there is a clear unmet need to develop a feasible, robust, and physiologically relevant in vitro NMJ model.

Objective: We aimed to establish a novel functional human NMJs platform, which is serum and neural complex media/neural growth factor-free, using human immortalized myoblasts and human embryonic stem cells (hESCs)-derived neural progenitor cells (NPCs) that can be used to understand the mechanisms of NMJ development and degeneration.

Methods: Immortalized human myoblasts were co-cultured with hESCs derived committed NPCs. Over the course of the 7 days myoblasts differentiated into myotubes and NPCs differentiated into motor neurons.

Results: Neuronal axon sprouting branched to form multiple NMJ innervation sites along the myotubes and the myotubes showed extensive, spontaneous contractile activity. Choline acetyltransferase and βIII-tubulin immunostaining confirmed that the NPCs had matured into cholinergic motor neurons. Postsynaptic site of NMJs was further characterized by staining dihydropyridine receptors, ryanodine receptors, and acetylcholine receptors by α-bungarotoxin.

Conclusion: We established a functional human motor unit platform for in vitro investigations. Thus, this co-culture system can be used as a novel platform for 1) drug discovery in the treatment of neuromuscular disorders, 2) deciphering vital features of NMJ formation, regulation, maintenance, and repair, and 3) exploring neuromuscular diseases, age-associated degeneration of the NMJ, muscle aging, and diabetic neuropathy and myopathy.

Keywords: motor unit, neuromuscular junctions, human embryonic stem cells, neuronal progenitor cells, human myoblasts

Introduction

Neuromuscular junctions (NMJs) serve as the interface between nerves and skeletal muscles. Maintenance, structure, and formation of NMJs depend on the bidirectional molecular interaction between the muscle and motor neuron.[1] The NMJ consists of a presynaptic motor neuron terminal, a postsynaptic motor end plate and a synaptic cleft. If chemical or molecular communication is disrupted, NMJ deterioration can follow. This involves axon degeneration, synapse disruption, impaired NMJ transmission, and muscle fiber degradation[2] which are the features of neuromuscular diseases, myopathies, and age-associated neuromuscular impairments.[3]

Despite decades of intensive research to characterize the structure and function of NMJs by utilizing animals and ex vivo models,[4] effective treatment of neuromuscular

Correspondence: Nasser Al-Shanti
School of Healthcare Science, Faculty of Science and Engineering, Manchester Metropolitan University, John Dalton Building, Chester Street, M1 5GD Manchester, UK
Tel +44 161 247 5712
Fax +44 161 247 6831
Email n.al-shanti@mmu.ac.uk

http://dx.doi.org/10.2147/SCCAA.S178562

and neurodegenerative diseases remains a significant unmet clinical need. This is mainly due to the failure of experimental animal models to reflect complex processes of human aging and disease progression.[5] In order to advance this field, novel, alternative, experimental models are needed.

There has been recent progress toward the development of in vitro co-culture models using human induced pluripotent stem cells (iPSCs);[6,7] mouse,[8] rat,[9] and human primary myoblasts;[10,11] and human embryonic stem cells (hESCs)[12–14] and cross-species models.[15,16] However, existing in vitro motor neuron and skeletal muscle co-culture systems typically require a complex neural growth medium that contains serum and cocktails of around 15 neural growth factors (some of which are derived from animals).[11,12,17] This further complicates drug discovery and toxicology studies due to possible cross-communication of the novel compound with factors contained within the added media, possibly explaining why many promising therapies do not translate to clinics. Another issue with existing models is that muscle contraction is induced by applied electrical or chemical stimulation, which does not replicate the native physiological stimulation required for muscle contractions.[8,17–19] Recent innovation in the use of iPSCs offers the potential to derive myoblasts and motor neurons for use with in vitro NMJ models. However, cells derived from iPSCs may exhibit genetic inconsistency and genetic modification, which limit their use.[20] Recent human iPSC-based studies have failed to recapitulate the severe neuronal loss observed in human neurodegenerative diseases.[21–23] Human skeletal myoblasts which were used in some of the abovementioned models[10,11] were obtained from primary cells (eg, muscle biopsy or surgical samples), but their life span is limited to just a few passages which restricts experimentation and necessitates repeated supply of the primary cells.[24,25] Furthermore, primary cells have varied cell purity[26] and experience phenotypic changes when expanded, rendering primary myoblasts a problematic choice for a consistently reproducible co-culture system.[24,25] Therefore, there is a clear need for a more relevant human experimental model to study motor units and NMJs to overcome the limitations of existing models.

Methods

Human immortalized myoblast cultures

The human immortalized myoblasts cell line ("C25") was obtained from the Institute of Myology.[27] This cell line was established using a biopsy of semi-tendinosis from a 25-year-old male (obtained anonymously from Myobank, a tissue bank affiliated to EuroBioBank which is authorized by the French Ministry of Research [authorization AC-2013-1868]). After attaining 80% confluence, cells were seeded in six-well plates recoated with gelatin (0.5%) at a concentration of 1.5×10^5 cells/mL in growth media. The growth media was supplemented with DMEM from Lonza (Basel, Switzerland), 60% (v/v) Medium 199 with Earle's Balanced Salt Solution from Lonza, 20% (v/v) heat-inactivated FBS from Thermo Fisher Scientific (Waltham, MA, USA), 20% (v/v) L-glutamine from Lonza, 1% (v/v) fetuin from FBS from Sigma-Aldrich (St Louis, MO, USA) 25 µg/mL, recombinant human basic fibroblast growth factor from Thermo Fisher Scientific 0.5 ng/mL, recombinant human EGF from Thermo Fisher Scientific 5 ng/mL, recombinant human hepatocyte growth factor from Sino Biological Inc. (Beijing, China) 2.5 ng/mL, recombinant human insulin from Sigma-Aldrich 5 µg/mL, dexamethasone from Sigma-Aldrich 0.2 µg/mL and gentamicin from Thermo Fisher Scientific.

Neural differentiation of hESCs

Induction of neuroepithelial clusters (NECs)

Mouse embryonic fibroblasts (MEFs; Cell Biolabs, San Diego, CA, USA) were cultured within MEF growth media (summarized in Table 1) and were passaged at a 1:4 ratio. At passage 4 (p4), MEFs were inactivated mitotically using 0.1 µg/mL mitomycin C (Sigma-Aldrich). The Shef3 hESC line was obtained from the UK StemCell Bank under the project SCSC10-48 and maintained on mitotically inactivated MEFs

Table 1 MEF growth media

MEF growth media components	Volume
DMEM from Lonza (Basel, Switzerland)	500 mL
L-glutamine from Lonza	1% (v/v)
Penicillin/streptomycin (Sigma-Aldrich, St Louis, MO, USA)	5 mL (2 mM)
Heat-inactivated FBS from Thermo Fisher Scientific (Waltham, MA, USA)	10% (v/v)

Abbreviation: MEF, mouse embryonic fibroblast.

Table 2 hESC media for cells on MEFs

hESC/MEF cell medium components	Volume
DMEM-F12 (1:1) from Lonza (Basel, Switzerland)	38.5 mL
MEM nonessential amino acids (Thermo Fisher Scientific, Waltham, MA, USA)	0.5 mL (1X)
Penicillin/streptomycin (Sigma-Aldrich, St Louis, MO, USA)	0.5 mL (1X)
bFGF (R&D Systems, Minneapolis, MN, USA) (100 µg/mL)	5 µL (10 ng/mL)
Knockout serum replacement (Thermo Fisher Scientific)	10 mL (20%)

Abbreviations: bFGF, basic fibroblast growth factor; hESC, human embryonic stem cell; MEF, mouse embryonic fibroblast; MEM, Minimum Essential Medium.

in hESC medium (summarized in Table 2) in 96-well plates. hESCs were mechanically passaged every 5–7 days and then conditioned to feeder-free culture by TrypLE Express (Thermo Fisher Scientific) enzyme dissociation and plated at a high density (1:1) onto hESC-qualified Matrigel® (Corning)-coated flasks in mTESR (STEMCELL Technologies). For neural induction, feeder-free hESCs were dissociated with TrypLE and replated in neural induction medium (NIM; summarized in Table 3) in uncoated, V-shaped 96-well plates at a density of 1×10^4 cells/well. Within 24 hours, NECs formed.

Generation of neural rosette-forming progenitor cells (NRPCs)

Medium was replaced daily for 5 days. On day 6, aggregates were replated in 96-well plates in NIM onto 20 µg/mL laminin (Millipore)-coated dishes to allow neural rosette formation (2–3 days).

Expansion of neural progenitor cells

Neural rosette clusters were mechanically isolated and replated in 96-well plates onto laminin-coated dishes in neural expansion medium (NIM plus 1X B27 supplement; Thermo Fisher Scientific). Early- and late-passage neural progenitor cells (NPCs) were cultured in the same conditions and passaged at a 1:3 ratio using TrypLE. To monitor NPCs differentiation into motor neurons, some of the NPCs were transfected with a GFP-reporter lentivirus system.

Immunohistochemistry of NECs, NRPCs, and NPCs

For immunostaining, at each stage of neural differentiation (NECs and NRPCs), cells were sectioned onto glass slides. Sectioned NECs and NRPCs and cultured NPCs in six-well plates were fixed with 4% paraformaldehyde. Fixed sections and NPCs were permeabilized with 0.3% Triton X in PBS and then subsequently blocked with 2% BSA in PBS/Tween 20. The slides were then incubated overnight at 4°C with a primary antibody (MAB2736; R&D Systems). The following day, sections and NPCs were washed with PBS and incubated for 1 hour at room temperature (RT) with goat anti-mouse secondary antibody (Alexa Flour 568-red for NECs, NRPCs and NPCs; Thermo Fisher Scientific) and imaged under a fluorescent microscope (Leica CTR 6000; Leica Microsystems, Wetzlar, Germany).

Table 3 Neural induction medium

NIM components	Volume
DMEM-F12 (1:1) from Lonza (Basel, Switzerland)	48.5 mL
MEM nonessential amino acids (Thermo Fisher Scientific, Waltham, MA, USA)	0.5 mL (1X)
Penicillin/streptomycin (Sigma-Aldrich, St Louis, MO, USA)	0.5 mL (1X)
bFGF (R&D Systems, Minneapolis, MN, USA) (100 µg/mL)	10 µL (20 ng/mL)
N2 supplement (Thermo Fisher Scientific)	0.5 mL (1X)
Heparin (Sigma-Aldrich) (2 mg/mL)	50 µL (2 µg/mL)
Poly (vinyl alcohol) (Sigma-Aldrich)	4 mg/mL

Abbreviations: bFGF, basic fibroblast growth factor; MEM, Minimum Essential Medium; NIM, neural induction medium.

Co-culture of NPCs and human myoblasts

Human myoblasts were incubated over 24 hours at 37°C within a 5% CO_2 environment in six-well plates. Then, the growth media was replaced with co-culture media supplemented with DMEM (500 mL), 10 µg/mL recombinant human insulin, and 10 µg/mL gentamicin. NPCs were present at a concentration of 25×10^3 cells/mL and incubated at 37°C with 5% CO_2 for up to 7 days. At day 7, myotube contractions were observed.

Immunohistochemistry

At day 7, cells were stained with α-Bungarotoxin (α-BTX) (T0195, 1/200; Sigma-Aldrich), and then fixed with 4% paraformaldehyde for 10 minutes at RT. Co-cultures were washed twice with PBS (Thermo Fisher Scientific). After α-BTX staining, cells were washed twice with PBS and permeabilized with 1X perm/wash buffer (BD, Franklin Lakes, NJ, USA) for 30 minutes at RT. Cells were washed twice with PBS and then blocked with PBS containing 1% BSA and 10% goat serum (Thermo Fisher Scientific) for 1 hour at RT. The following antibodies were used: mouse anti-βIII-tubulin (MAB1195, clone #TuJ1, 1/400; R&D Systems), rabbit anti-ryanodine receptor (anti-RyR; AB9078, 1/200; Millipore), goat anti-choline acetyltransferase (anti-ChAT; ABN100, 1/200; Millipore), goat anti-ChAT (AB144, 1/200; Millipore), and mouse anti-dihydropyridine receptor (anti-DHPR; Ab2864, 1/400; Abcam). These antibodies were incubated overnight at 4°C in 1X perm/wash buffer. Co-cultures were washed with PBS and stained with the corresponding secondary antibodies supplemented with DAPI (1/10,000; Sigma-Aldrich) for 1 hour at RT. Stained co-culture cells were visualized using a Leica SP5 confocal microscope sourced by Leica Microsystems for fluorescent microscopy.

Results

A functional human motor unit platform

The present work describes a functional human motor unit platform established using immortalized skeletal myoblasts

and hESCs-derived NPCs that develop into motor neurons in muscle differentiation media (co-culture media) devoid of any complex neural growth factors or serum.

To validate the platform, two monoculture controls were included, one of NPCs and the other of immortalized human myoblasts[27] with co-culture media for 7 days. Cultured GFP-transfected NPCs did not show any morphological changes or motor neuron differentiation, but instead they deteriorated and died (Figure 1A). The human myoblasts stained with phalloidin-DAPI showed normal morphology and differentiation features with centrally and peripherally located nuclei, but the myotubes did not spontaneously contract (Figure 1B).

Derivation of NPCs from hESCs and establishment of the NMJs model

The NPCs were derived from hESCs, as described previously.[28] Neural differentiation of hESCs progressed through three stages of differentiation to NECs (Figure 2A) and NRPCs (Figure 2B) which were stained with Nestin red color. To confirm that differentiated NPCs were homogeneous committed neural lineage, cells were stained with DAPI, anti-GFAP (a specific marker for glial cells) and anti-Nestin. Double-positive staining (DAPI blue and Nestin red) confirmed the formation of NPCs while single DAPI staining was not observed, which confirmed that the differentiated cells were NPCs (Figure 2C). Staining of GFAP was not present, confirming again that all of the cells were NPCs (Figure 2C).

The NPCs were co-cultured with human immortalized myoblasts for 7 days in co-culture media. After myogenic differentiation was initiated, the characteristics of functional motor units began to develop. This included myotube formation and axonal sprouting from the NPCs which subsequently formed NMJs along the myotubes (Figure 2D). The myotubes showed spontaneous muscle contractions from approximately day 7 onwards in the absence of any exogenous electrical and chemical stimuli (Video S1). Due to the force of contractions, some myotubes were detached from the culture plate, causing large spaces within the co-culture. Since the myotubes cultured without NPCs did not contract, they did not detach from the culture plate and did not open up large spaces (Figure 1B).

Characterization of co-cultures

On day 7, the motor neuron formation was assessed using the specific marker for motor neuron differentiation, βIII-tubulin. Figure 3A shows a typical shape of mature motor neurons with axons terminating on myotubes. To further confirm the formation of cholinergic motor neurons, acetyltransferase antibodies (ChAT, a key enzyme for acetylcholine biosynthesis) were used and are shown in green in Figure 3B.

Neurally and aneurally cultured myotubes were characterized by antibody staining against DHPRs and RyRs voltage-gated channels which are located at muscle fiber T-tubules and the sarcoplasmic reticulum, respectively. The DHPR- and RYR-stained images showed transversal triad structures (Figure 3C). These images illustrated mature differentiated myotubes within the co-culture platform with peripherally located nuclei (Figure 3A and B). The aneurally cultured myotubes (control image) differentiated as expected, but did not exhibit appropriate transversal triad structures (Figure 3D).

NMJs display acetylcholine receptor (AChR) clusters along myotubes, and these were assessed by staining for α-BTX, as shown in Figure 3B and E where AChRs are marked by red clusters. As shown in Figure 3A and E, motor neuron axons extend to innervate myotubes and AChR clusters at this same location, marked with α-BTX (red),

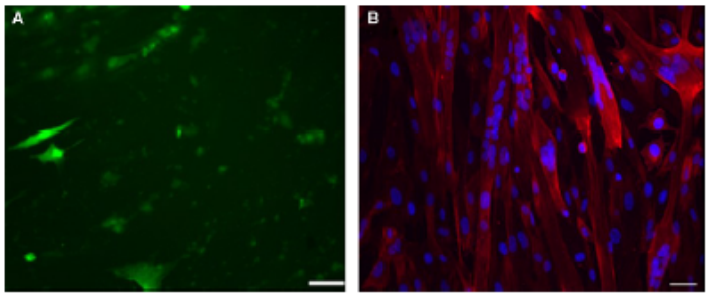

Figure 1 Monoculture of NPCs (**A**) and myoblasts (**B**).
Notes: NPCs and myoblasts were separately cultured for 7 days. The same growth media was used for monocultures and co-cultures. (**A**) A representative image of GFP-transfected NPCs. The NPCs did not exhibit any morphological changes or motor neuron differentiation; instead, they deteriorated and died. (**B**) A representative image of phalloidin-DAPI-stained human myoblasts showed normal morphology and differentiation features with centrally and peripherally located nuclei. Scale bar: 50 μM.
Abbreviation: NPC, neural progenitor cell.

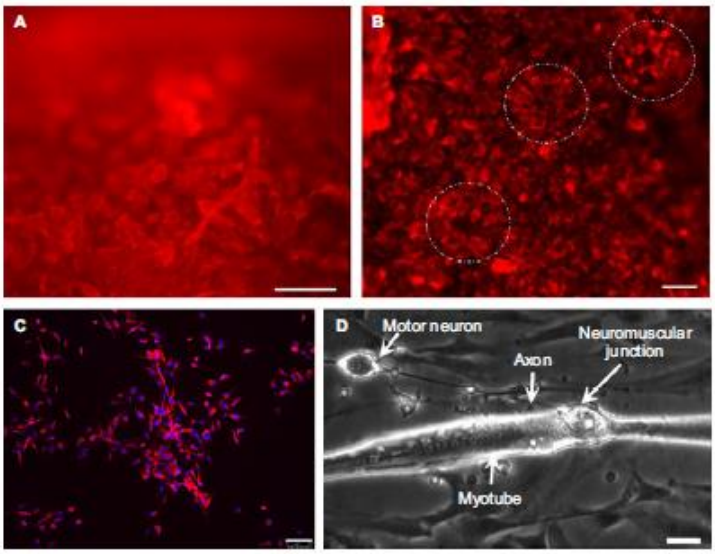

Figure 2 Neural differentiation of hESCs.
Notes: Identification of NPCs from hESCs using Nestin red color as a specific neural differentiation marker. (**A**) NECs. (**B**) NRPCs. (**C**) Nestin-red color for NPCs. (**D**) A representative phase-contrast image of NMJ formation showing an axon extended to contact a myotube. White dotted circle indicates a rosette shape. Scale bars are 100 μM for images (**A**)–(**C**) and 25 μM for image (**D**).
Abbreviations: hESC, human embryonic stem cell; NEC, neuroepithelial cluster; NMJ, neuromuscular junction; NPC, neural progenitor cell; NRPC, neural rosette-forming progenitor cell.

indicating NMJ formation. Spontaneous myotube contractile activity was determined on day 7. The myotubes co-cultured with motor neurons showed high levels of spontaneous contractile activity (Video S1). Muscle contractions were absent from aneural myoblast cultures.

Discussion

Implications and future uses

This report describes a novel functional human motor unit platform engineered from immortalized skeletal myoblasts and NPCs derived from hESCs. This unique platform was established for investigation of human NMJs and motor unit formation, maintenance, and disease, as well as for drug discovery and toxicity research.

The motor neuron and skeletal muscle co-cultures matured without adding complex cocktails of serum or neural growth factors. NMJ formation was observed and spontaneous myotube contractions were recorded (Video S1) over a period as short as 6–7 days, which is very early compared with the 14 days needed in previous studies[16] or where NMJs formed after 20–25 days.[29] These are crucial advances for studying the basic aspects of development and for recognizing pathophysiological systems of NMJ disorders associated with disease or aging. It is important that this type of work is carried out with relevant human cultures to increase the possibility for translation to clinical practice. Most previous cell culture model systems used cross-species cell types[15,19] and required cocktails of serum[30,31] and growth factors.[10,17,19,29] These were absent from the present model without any adverse effects, which suggests that nerve and muscle cells release all of the necessary factors needed to stimulate nerve axonal sprouting and formation of NMJs with myotubes. Moreover, eliminating serum, which contains unknown factors that may affect assay reproducibility, simplifies the interpretation of pharmacology and toxicity studies.[32] Functional NMJ formation is strongly supported by bidirectional communication[1] between nerve and muscle as well as by neural growth factors (such as brain-derived neurotrophic factor, glial cell line-derived neurotrophic factor and neurotrophin-3/4) secreted by muscle to support NMJ formation, maturation and maintenance.[33,34] Future investigations using this model will identify key factors released from nerve and muscle to orchestrate axonal sprouting, localization, and NMJ maintenance.

Although animal models can represent essential parts of physiological changes in a human disease,[35] in vitro human cell cultures offer many advantages because they are formed

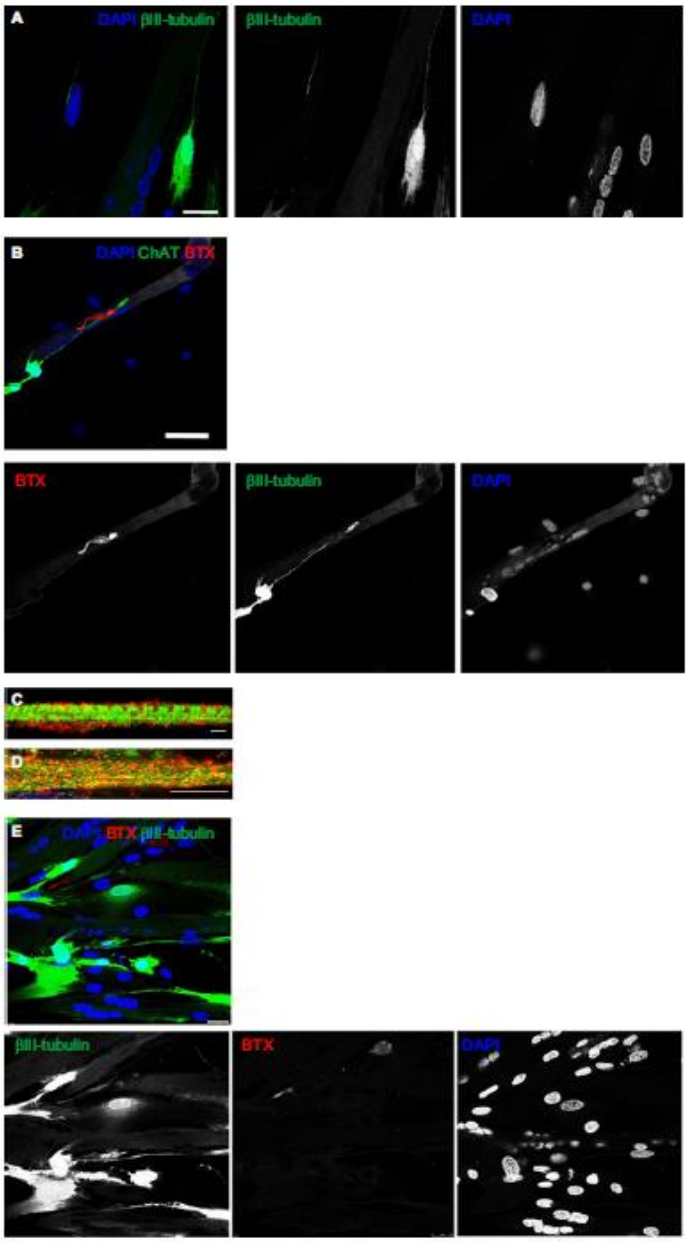

Figure 3 Characterization of muscle–nerve co-cultures.

Notes: (**A** and **B**) Characterization of motor neuron formation. (**A**) A representative image of the co-culture cells stained for βIII-tubulin (green) and DAPI (blue); scale bars: 25 μm. (**B**) A representative image of the co-culture cells stained for ChAT (green), α-BTX (red), and DAPI (blue); scale bars: 75 μm. (**C** and **D**) Characterization of advanced differentiated myotubes. (**C**) A representative image of the co-culture cells stained for DHPR (red), RyR (green), and DAPI (blue); scale bars: 2.5 μm. (**D**) A representative image of the co-culture cells stained for DHPR (red), RyR (green), and DAPI (blue); scale bars: 7.5 μm. (**E**) Characterization of functional NMJs formation. A representative image of the co-culture cells stained for βIII-tubulin (Tuj1; green), α-BTX (red), and DAPI (blue); scale bars: 25 μm.

Abbreviations: α-BTX, α-bungarotoxin; ChAT, choline acetyltransferase; DHPR, dihydropyridine receptor; NMJ, neuromuscular junction; RyR, ryanodine receptor.

of relevant cell types, they can be produced quickly for high-throughput screening, and they are more cost-effective in comparison to animal models.[10,17]

Conclusion

In summary, human immortalized myoblasts were co-cultured with hESCs-derived NPCs. Over the course of 7 days, myoblasts differentiated into myotubes and NPCs sprouted axons that branched to form multiple NMJ innervation sites along myotubes, and myotubes showed extensive, spontaneous contractile activity. This cell culture platform may be used to study human NMJ growth and disease and may reduce the use of animal models in future related research.

Acknowledgment

This work was sponsored by the School of Healthcare Science, Faculty of Science and Engineering, Manchester Metropolitan University (Manchester, UK).

Author contributions

MAS, JSM, and NAS developed the study concept. All the authors contributed to methodology. MAS, JSM, and NAS carried out the investigation. JSM, TRM, and NAS supervised the study. MAS, JSM, and NAS wrote the original draft of the manuscript. MAS, JSM, VM, and NAS reviewed and edited the draft manuscript. All authors contributed to data analysis, drafting or revising the article, gave final approval of the version to be published, and agree to be accountable for all aspects of the work.

Disclosure

The authors report no conflicts of interest in this work.

References

1. Zahavi EE, Ionescu A, Gluska S, Gradus T, Ben-Yaakov K, Perlson E. A compartmentalized microfluidic neuromuscular co-culture system reveals spatial aspects of GDNF functions. *J Cell Sci*. 2015;128(6):1241–1252.
2. Gonzalez-Freire M, de Cabo R, Studenski SA, Ferrucci L. The Neuromuscular Junction: Aging at the Crossroad between Nerves and Muscle. *Front Aging Neurosci*. 2014;6:208.
3. Zhou C, Wu L, Ni F, Ji W, Wu J, Zhang H. Critical illness polyneuropathy and myopathy: a systematic review. *Neural Regen Res*. 2014;9(1):101–110.
4. Wu H, Xiong WC, Mei L. To build a synapse: signaling pathways in neuromuscular junction assembly. *Development*. 2010;137(7):1017–1033.
5. van der Worp HB, Howells DW, Sena ES, et al. Can animal models of disease reliably inform human studies? *PLoS Med*. 2010;7(3):e1000245.
6. Thomson SR, Wishart TM, Patani R, Chandran S, Gillingwater TH. Using induced pluripotent stem cells (iPSC) to model human neuromuscular connectivity: promise or reality? *J Anat*. 2012;220(2):122–130.
7. Berry BJ, Akanda N, Smith AS, et al. Morphological and functional characterization of human induced pluripotent stem cell-derived neurons (iCell Neurons) in defined culture systems. *Biotechnol Prog*. 2015;31(6):1613–1622.
8. Umbach JA, Adams KL, Gundersen CB, Novitch BG. Functional neuromuscular junctions formed by embryonic stem cell-derived motor neurons. *PLoS One*. 2012;7(5):e36049.
9. Smith AS, Long CJ, Pirozzi K, Hickman JJ. A functional system for high-content screening of neuromuscular junctions *in vitro*. *Technology*. 2013;1(1):37–48.
10. Demestre M, Orth M, Föhr KJ, et al. Formation and characterisation of neuromuscular junctions between hiPSC derived motoneurons and myotubes. *Stem Cell Res*. 2015;15(2):328–336.
11. Guo X, Colon A, Akanda N, et al. Tissue engineering the mechanosensory circuit of the stretch reflex arc with human stem cells: Sensory neuron innervation of intrafusal muscle fibers. *Biomaterials*. 2017;122:179–187.
12. Guo X, Greene K, Akanda N, et al. In vitro Differentiation of Functional Human Skeletal Myotubes in a Defined System. *Biomater Sci*. 2014;2(1):131–138.
13. Santhanam N, Kumanchik L, Guo X, et al. Stem cell derived phenotypic human neuromuscular junction model for dose response evaluation of therapeutics. *Biomaterials*. 2018;166:64–78.
14. Happe CL, Tenerelli KP, Gromova AK, Kolb F, Engler AJ. Mechanically patterned neuromuscular junctions-in-a-dish have improved functional maturation. *Mol Biol Cell*. 2017;28(14):1950–1958.
15. Arnold AS, Christe M, Handschin C. A functional motor unit in the culture dish: co-culture of spinal cord explants and muscle cells. *J Vis Exp*. 2012 (62):3616.
16. Vilmont V, Cadot B, Ouanounou G, Gomes ER. A system for studying mechanisms of neuromuscular junction development and maintenance. *Development*. 2016;143(13):2464–2477.
17. Guo X, Gonzalez M, Stancescu M, Vandenburgh HH, Hickman JJ. Neuromuscular junction formation between human stem cell-derived motoneurons and human skeletal muscle in a defined system. *Biomaterials*. 2011;32(36):9602–9611.
18. Miles GB, Yohn DC, Wichterle H, Jessell TM, Rafuse VF, Brownstone RM. Functional properties of motoneurons derived from mouse embryonic stem cells. *J Neurosci*. 2004;24(36):7848–7858.
19. Guo X, das M, Rumsey J, Gonzalez M, Stancescu M, Hickman J. Neuromuscular junction formation between human stem-cell-derived motoneurons and rat skeletal muscle in a defined system. *Tissue Eng Part C Methods*. 2010;16(6):1347–1355.
20. Chin MH, Mason MJ, Xie W, et al. Induced pluripotent stem cells and embryonic stem cells are distinguished by gene expression signatures. *Cell Stem Cell*. 2009;5(1):111–123.
21. Chung CY, Khurana V, Auluck PK, et al. Identification and rescue of α-synuclein toxicity in Parkinson patient-derived neurons. *Science*. 2013;342(6161):983–987.
22. Kondo T, Asai M, Tsukita K, et al. Modeling Alzheimer's disease with iPSCs reveals stress phenotypes associated with intracellular Aβ and differential drug responsiveness. *Cell Stem Cell*. 2013;12(4):487–496.
23. Sareen D, O'Rourke JG, Meera P, et al. Targeting RNA foci in iPSC-derived motor neurons from ALS patients with a C9ORF72 repeat expansion. *Sci Transl Med*. 2013;5(208):ra149.
24. Mouly V, Aamiri A, Périé S, et al. Myoblast transfer therapy: is there any light at the end of the tunnel? *Acta Myol*. 2005;24(2):128–133.
25. Webster C, Blau HM. Accelerated age-related decline in replicative life-span of Duchenne muscular dystrophy myoblasts: implications for cell and gene therapy. *Somat Cell Mol Genet*. 1990;16(6):557–565.
26. Kaur G, Dufour JM. Cell lines: Valuable tools or useless artifacts. *Spermatogenesis*. 2012;2(1):1–5.
27. Mamchaoui K, Trollet C, Bigot A, et al. Immortalized pathological human myoblasts: towards a universal tool for the study of neuromuscular disorders. *Skelet Muscle*. 2011;1:34.
28. Fitzpatrick LM, Hawkins KE, Delhove J, et al. NF-κB Activity Initiates Human ESC-Derived Neural Progenitor Cell Differentiation by Inducing a Metabolic Maturation Program. *Stem Cell Reports*. 2018;10(6):1766–1781.

29. das M, Rumsey JW, Bhargava N, Stancescu M, Hickman JJ. A defined long-term in vitro tissue engineered model of neuromuscular junctions. *Biomaterials*. 2010;31(18):4880–4888.
30. Zhou FM, Hablitz JJ. Layer I neurons of rat neocortex. I. Action potential and repetitive firing properties. *J Neurophysiol*. 1996;76(2):651–667.
31. Walsh K, Megyesi J, Hammond R. Human central nervous system tissue culture: a historical review and examination of recent advances. *Neurobiol Dis*. 2005;18(1):2–18.
32. Rumsey JW, das M, Stancescu M, Bott M, Fernandez-Valle C, Hickman JJ. Node of Ranvier formation on motoneurons in vitro. *Biomaterials*. 2009;30(21):3567–3572.
33. Funakoshi H, Belluardo N, Arenas E, et al. Muscle-derived neurotrophin-4 as an activity-dependent trophic signal for adult motor neurons. *Science*. 1995;268(5216):1495–1499.
34. Henderson CE, Camu W, Mettling C, et al. Neurotrophins promote motor neuron survival and are present in embryonic limb bud. *Nature*. 1993;363(6426):266–270.
35. Jensen J, Hyllner J, Björquist P. Human embryonic stem cell technologies and drug discovery. *J Cell Physiol*. 2009;219(3):513–519.

Supplementary material

Video S1 Phase contrast video micrograph of innervated human myotube contractions at Day 7.